



Title Development of new methods to assess the
 quality of zebrafish (*Danio rerio*) ovarian
 follicles

Name Tizianna Zampolla

This is a digitised version of a dissertation submitted to the University of Bedfordshire.

It is available to view only.

This item is subject to copyright.

**DEVELOPMENT OF NEW METHODS TO ASSESS THE QUALITY OF
ZEBRAFISH (*Danio rerio*) OVARIAN FOLLICLES**

by

TIZIANA ZAMPOLLA

**A thesis submitted for the degree of Doctor of Philosophy of the University of
Bedfordshire**

LIRANS

Institute of Research in the Applied Natural Sciences

University of Bedfordshire

250 Butterfield

Great Marlings

Luton LU2 8DL

March, 2009

DEVELOPMENT OF NEW METHODS TO ASSESS THE QUALITY OF ZEBRAFISH (*Danio rerio*) OVARIAN FOLLICLES

TIZIANA ZAMPOLLA

ABSTRACT

High quality fish oocytes are essential for *in vitro* maturation (IVM), *in vitro* fertilization (IVF) protocols, and for use in cryopreservation. It is important to develop methods for assessing oocyte quality for applications in aquaculture, the preservation of endangered species and managing fish models used in biomedical research. The lack of reliable methods of evaluating oocyte quality limits progress in these areas.

The present study was undertaken to develop new methods to assess ovarian follicle viability and quality of stage III zebrafish (*Danio rerio*) ovarian follicles. The methods developed were then applied to study the impact of cryoprotectant and/or cryopreservation procedures.

A vital staining procedure, not previously used with zebrafish oocytes, has been investigated. FDA-PI (Fluorescein diacetate-Propidium Iodide) staining was found to be a more sensitive than currently used viability tests and it could also be applied to all ovarian follicles developmental stages. Mitochondrial activity and distribution as biological markers was investigated with the mitochondrial membrane potential-sensitive dye JC-1 (5,5',6,6'-tetrachloro-1,1',3,3'-tetraethylbenzimidazolyl-carbocyanine iodide). Confocal microscopy, Cryo-scanning and electron microscopy studies were undertaken to determine mitochondria distributional arrangement within the ovarian follicle. This provided new information on zebrafish ovarian follicle structure, and showed that mitochondria exhibited a contiguous distribution at the margin of the granulosa cell layer surrounding stage III zebrafish oocytes. Cryo-scanning results showed a polygonal structure of the vitelline envelope, which is

reported here for the first time with the mitochondrial distributional arrangement in the granulosa cell layer.

Mitochondrial distribution and the evaluation of mitochondrial activity proved to be sensitive markers for ovarian follicle quality, providing more detailed information on cryoprotectant impact. The measurement of ATP levels, ADP/ATP ratio and mtDNA copy number were also undertaken following cryoprotectant exposure. These findings, together with the observation of mitochondrial distribution, suggested that even cryoprotectant treatments that are considered to have little or no toxicity can have a deleterious effect on mitochondrial activity, potentially compromising oocyte growth and embryo development. Therefore, a further optimization of the currently used protocol may need to be considered.

The study of organelle distribution and organisation would support *in vitro* maturation and oocyte development fields, as well as their use as biological markers for quality determination. These findings will contribute to a better understanding of oogenesis/folliculogenesis processes in fish.

ACKNOWLEDGEMENTS

It is a pleasure to thank the many people who made this thesis possible.

Above all, I would like to express my deep and sincere gratitude to my two supervisors, Professor David Rawson and Professor Tiantian Zhang for their important support and guidance throughout this work.

I am deeply grateful to my external supervisor, Professor William V. Holt, for his support with his detailed and constructive comments, and for giving me the opportunity to come to England and take up this PhD.

I warmly thank Dr Emma Spiking, for her friendly help and valuable advice. Her support and interest has been very helpful for this study.

My warm thanks are due to Dr Allison Van de Meen and Mrs Jean Devonshire, at Rothamsted Research centre, who helped me during my microscopy studies. Their kind support and guidance have been of great value in this study.

I would like to thank Dr Fataneh Ghafari, for stimulating discussions and advice.

I especially thank my lab-mates and friends Yurong Ding, Mo Guan, Sujune Tsai and Chiahsin Lin for providing a nice and fun environment where to learn and work.

I also would like to thank Dr Barry Haggett, laboratory manager at LIRANS, for his assistance with all types of technical problems and for keeping me safe throughout my studies.

I wish to extend my warmest thanks to all those who have helped me throughout this fantastic experience of my life.

Finally, I would like to thank my parents for their love and their support throughout the past twenty-nine years. I dedicate this work to them.

DECLARATION

I declare that this thesis is my own unaided work. It is being submitted for the degree of Doctor of Philosophy at the University of Bedfordshire. It has not been submitted before to any degree or examination in any other University.

_____ day of 2009

LIST OF CONTENTS

Abstract	2
Acknowledgements	4
Author's declaration	5
List of contents	6
List of Tables	13
List of Figures	14
<u>Chapter 1: Introduction</u>	21
1.1 Quality of fish oocyte.....	21
1.2 Viability assay.....	25
1.3 Using zebrafish as a model system.....	27
1.4 Structure of zebrafish ovary.....	28
1.4.1 Stage I.....	29
1.4.2 Stage II.....	30
1.4.3 Stage III.....	31
1.4.3.1 The Vitelline Envelope.....	32
1.4.3.2 Vitellogenesis and vitellogenin uptake.....	34
1.4.3.3 Cortical alveoli.....	35
1.4.3.4 Maturation competence.....	35
1.4.4 Stage IV.....	37
1.4.5 Stage V.....	38
1.5 Mitochondria.....	38
1.5.1 Structure of mitochondria.....	38
1.5.2 Mitochondrial distribution in oocyte and role in reproduction.....	39
1.5.3 Mitochondrial DNA (mtDNA).....	40
1.5.3.1 MtDNA copy number.....	42

1.5.3.2 Mechanism of mtDNA damage.....	43
1.5.3.3 MtDNA repair.....	44
1.5.4 Role of mitochondria.....	44
1.5.4.1 The respiratory chain.....	45
1.5.4.2 ATP.....	45
1.5.4.3 ADP:ATP ratio.....	46
1.5.5 Uncoupling and inhibition of oxidative phosphorylation.....	47
1.5.6 Evaluation of mitochondria distribution and activity.....	49
1.5.6.1 Staining of mitochondria on the basis of mitochondrial membrane potential.....	49
1.6 Current status of cryopreservation in aquatic species.....	50
1.6.1 Difficulties associated with the cryopreservation of fish oocytes.....	51
1.6.2 Principle of cryobiology.....	52
1.6.2.1 Chilling injury.....	52
1.6.2.2 Freezing injury.....	53
1.6.2.3 Controlled slow cooling and vitrification.....	54
1.6.3 Cryoprotectants.....	56
1.6.3.1 CPAs toxicity.....	58
1.7 The present study.....	61
1.7.1 Relevance of the research to society.....	61
1.7.2 The selection of subject material for this study.....	62
1.7.3 The aim and the approach of this study.....	63
<u>Chapter 2: Material and methods</u>	65
2.1 Introduction.....	65
2.2 General methods.....	65
2.2.1 Maintenance of zebrafish (<i>Danio rerio</i>).....	65
2.2.1.1 Zebrafish (<i>Danio rerio</i>) care.....	65
2.2.1.2 Separation of stage III ovarian follicle from ovarian masses.....	66

2.2.1.2.1 Mechanical method.....	66
2.2.1.2.2 Enzymatic method.....	67
2.2.2. Chemicals.....	67
2.2.3. Data analysis.....	69
2.2.3.1. Experimental design and statistical analysis.....	69
2.3 Development of new assay for zebrafish oocytes viability using vital stains.....	70
2.3.1 FDA-PI staining and fluorescence microscopy.....	70
2.3.2 Application of FDA-PI.....	71
2.3.2.1 Controls.....	71
2.3.2.2 Comparisons of FDA-PI with other viability assessment methods after follicle isolation.....	71
2.3.2.3 Comparisons of FDA-PI, TB and GVBD in cryoprotective agents (CPAs) toxicity tests.....	72
2.3.2.4 Comparisons of FDA-PI and TB following cryopreservation procedure.....	72
2.3.3 Other viability assays.....	73
2.3.3.1 Ovarian follicle staining by Trypan Blue.....	73
2.3.3.2 Observation of Germinal Vesicle Breakdown (GVBD).....	73
2.4 Observation of mitochondria distribution and activity in stage III ovarian follicles.....	73
2.4.1. Staining of Mitochondria.....	74
2.4.1.1 Confocal microscopy.....	74
2.4.1.2 Mitochondria inhibitors.....	75
2.4.2 Assessment of ATP level.....	75
2.4.2.1 Preparation of extract from ovarian follicle.....	75
2.4.2.2 Preparation of FL-AA reagent.....	76
2.4.2.3 Determination of ATP level.....	77
2.5 Examination by Scanning Electron Microscopy (SEM) and Transmission Electron of stage III zebrafish (<i>Danio rerio</i>) ovarian follicle structure to support observation of mitochondrial distribution obtained by confocal microscopy.....	78

2.5.1 Cryo - Scanning Electron Microscopy (Cryo - SEM).....	78
2.5.2 Transmission Electron Microscopy (TEM).....	79
2.6 Evaluation of mitochondrial activity and distribution as biological marker in stage III ovarian follicle of zebrafish (<i>Danio rerio</i>) following CPAs exposure....	81
2.6.1 CPA treatment.....	81
2.6.2 Observation of mitochondrial activity and distribution by confocal microscopy.....	82
2.6.2.1 Staining of Mitochondria with JC-1.....	82
2.6.2.2 Confocal microscopy.....	82
2.6.3. Viability assay.....	82
2.6.3.1 Viability assessed by FDA-PI staining.....	82
2.6.3.2 Viability assessed by TB staining.....	82
2.6.4 mtDNA copy number determination.....	82
2.6.4.1 DNA extraction from ovarian follicle.....	83
2.6.4.2.1 PCR.....	83
2.6.4.2.2 Agarose gel electrophoresis.....	83
2.6.4.2.3 DNA extraction from gels.....	84
2.6.4.3 Real time PCR.....	84
2.6.5 ATP levels and ADP/ ATP ratio determination.....	85

Chapter 3: Development of new assay for zebrafish oocytes viability using vital stains..... 87

3.1 Introduction.....	87
3.2 Results.....	89
3.2.1 Reliability of FDA-PI.....	89
3.2.2 Comparisons of FDA-PI, TB and GVBD tests after follicles isolation.....	91
3.2.3 Comparisons of FDA-PI, TB and GVBD in cryoprotective agents (CPAs) toxicity tests.....	92
3.2.4 Comparisons of FDA-P and TB following cryopreservation procedure...	96
3.3 Discussion.....	97

3.4 Summary.....	100
------------------	-----

Chapter 4: Observation of mitochondria distribution and activity in stage III

ovarian follicles.....	101
4.1 Introduction.....	101
4.2 Results.....	103
4.2.1 Mitochondrial distribution and activity investigation by confocal microscopy.....	103
4.2.2 Effect of mitochondrial inhibitors on mitochondria distribution and activity and on ATP concentration.....	106
4.3 Discussion.....	112
4.4 Summary.....	114

**Chapter 5: Examination by Scanning Electron Microscopy (SEM) and
Transmission Electron Microscopy (TEM) of stage III zebrafish (*Danio Rerio*)
ovarian follicle structure to support observation of mitochondria distribution
obtained by confocal microscopy.....**

5.1 Introduction.....	116
5.2 Results.....	117
5.2.1 Cryo-SEM.....	117
5.2.2 TEM.....	119
5.3 Discussion.....	124
5.4 Summary.....	126

**Chapter 6: Evaluation of mitochondrial activity and distribution as biological
marker in stage III ovarian follicles of zebrafish (*Danio Rerio*) following CPAs
exposure**

6.1 Introduction.....	128
-----------------------	-----

6.2 Results.....	130
6.2.1 Effect of methanol assessed by confocal microscopy.....	130
6.2.2 Viability assessed by TB and FDA-PI staining.....	131
6.2.3 Effect of cryoprotectants on mtDNA copy number.....	134
6.2.4 Effect of cryoprotectants on ATP content and ADP/ATP ratio.....	136
6.3 Discussion.....	138
6.4 Summary.....	141

Chapter 7:

Conclusions	142
7.1 Summary of the aims and objectives.....	142
7.2 Review of main findings.....	143
7.2.1 Development of new assay for zebrafish ovarian follicle viability using vital stain.....	143
7.2.1.1 Conclusions and suggestions for future work.....	144
7.2.2 Observation of mitochondria distribution and activity in stage III ovarian Follicles.....	145
7.2.2.1 Conclusions and suggestions for future work.....	146
7.2.3 Examination by Scanning Electron Microscopy (SEM) and Transmission Electron of stage III zebrafish (<i>Danio rerio</i>) ovarian follicle structure to support observation of mitochondrial distribution obtained by confocal microscopy.....	148
7.2.3.1 Conclusions and suggestions for future work.....	149
7.2.4 Evaluation of mitochondrial activity and distribution as biological marker in stage III ovarian follicle of zebrafish (<i>Danio rerio</i>) following CPAs exposure.....	150
7.2.4.1 Conclusions and suggestions for future work.....	151
7.3 In Summary.....	153
7.4 Future studies	154

References	156
Appendix A: Mitochondrial distribution and nuclei localization in the granulosa cells of stage III ovarian follicles.....	188
Appendix B: Publications.....	191

LIST OF TABLES

Chapter 1: Introduction

Table 1.1 Factors which affect ovarian egg quality in fish.....	24
Table 1.2 Viability methods commonly used to assess zebrafish ovarian follicles viability.....	27
Table 1.3 Stage III zebrafish follicle	37

Chapter 2: Material and methods

Table 2.1 Chemicals	67
---------------------------	----

Chapter 4: Observation of mitochondria distribution and activity in stage III ovarian follicles

Table 4.1 Effect of oligomycin on ATP level in zebrafish stage III ovarian follicles.....	111
Table 4.2 Effect of FCCP on ATP level in zebrafish stage III ovarian follicles.....	111

LIST OF FIGURES

Chapter 1: Introduction

Figure 1.1	29
Cystovarian type ovaries	
Figure 1.2	36
Diagrammatic representation of the follicle and oocyte during early vitellogenesis in teleosts	

Chapter 3: Development of new assay for zebrafish oocytes viability using vital stains

Figure 3.1	90
Dead stage III ovarian follicles exposed to 99% methanol for 10 min and visualized by PI (a) and by FDA (b). Viable stage III ovarian follicles, unstained by PI (c) and showing bright green after staining by FDA (d).	
Figure 3.2	90
Numbers of stage III zebrafish follicles stained by PI and FDA. Control represents follicles in KCL buffer. Negative control represents follicles exposed to 99% Methanol for 10 min.	
Figure 3.3	91
Comparisons of viability of stage III ovarian follicles using three viability assessment methods. Control: TB, FDA-PI and GVBD tests were performed immediately after follicle separation from the ovaries. Control 30: follicles incubated at 22 °C for 30 min in 50% Leibovitz L-15. Columns and error bars represent means \pm SEM of three experiments each with three replicates. *Significantly different from corresponding control value, $P < 0.05$.	
Figure 3.4	93

Comparisons of follicle viability assessed by TB, FDA-PI and GVBD tests following exposure to different concentrations of methanol (A), DMSO (B) and EG (C), in Leibovitz L-15 medium. Control: TB, FDA-PI and GVBD tests were performed after incubation of ovarian follicles at 22 °C for 30 min in 50% Leibovitz L-15; treated: TB, FDA-PI and GVBD were conducted after ovarian follicles were exposed to 1-4M methanol, DMSO or EG for 30 min at 22 °C. Columns and error bars represent means ± SEM of three experiments each with three replicates. *Significantly different from corresponding control value, P < 0.05.

Figure 3.594

Comparisons of follicle viability assessed by TB and FDA-PI tests following exposure to different concentrations of methanol (A), DMSO (B) and EG (C), in Hanks' solution. Control: TB and FDA-PI tests were performed after incubation of ovarian follicles at 22 °C for 30 min in Hanks' solution; treated: TB and FDA-PI were conducted after ovarian follicles were exposed to 1-4M methanol, DMSO or EG for 30 min at 22 °C. Columns and error bars represent means ± SEM of three experiments each with three replicates. *Significantly different from corresponding control value, P < 0.05.

Figure 3.695

Comparisons of follicle viability assessed by TB and FDA-PI tests following exposure to different concentrations of methanol (A), DMSO (B) and EG (C), in KCl buffer. Control: TB and FDA-PI tests were performed after incubation of ovarian follicles at 22 °C for 30 min in KCl buffer; treated: TB and FDA-PI were conducted after ovarian follicles were exposed to 1-4M methanol, DMSO or EG for 30 min at 22 °C. Columns and error bars represent means ± SEM of three experiments each with three replicates. *Significantly different from corresponding control value, P < 0.05.

Figure 3.796

Comparisons of TB and FDA-PI tests on stage III follicles exposed to two cryoprotectant solutions - 4M methanol or 4M methanol + 0.2M glucose - made up in Hanks' solution (A) and KCl buffer (B). Control t0: viability was assessed after

ovarian follicles separation. Control 30 min: ovarian follicles were incubated at 22°C for 30 min in KCl buffer. Treated: TB and FDA-PI were conducted after incubation of follicles in 4M methanol or 4M methanol + 0.2M glucose. Columns and error bars represent means \pm SEM of three experiments each with three replicates. *Significantly different from corresponding control value, $P < 0.05$.

Figure 3.8.....97
 Comparisons of TB and FDA-PI viability tests of stage III follicles following cryopreservation, using 4M methanol with 0.2M glucose as cryoprotectants in either Hanks' solution or KCl buffer. Control: TB, FDA+PI were performed on ovarian follicles held at 22 °C; treated: TB and FDA-PI were conducted after cryopreservation of follicles in 4M methanol and 0.2 M glucose. Columns and error bars represent means \pm SEM of three experiments each with three replicates; bars with different superscripts differ significantly ($P < 0.05$).

Chapter 4: Observation of mitochondria distribution and activity in stage III ovarian follicles

Figure 4.1105
 Mitochondria distribution in stage III zebrafish follicle exposed to 5 μ M JC1. JC-1 is a sensitive marker for $\Delta\Psi_m$. JC-1 accumulates in monomeric form within the mitochondria matrix and its fluorescence emission characteristics are a function of the magnitude of $\Delta\Psi_m$. Low polarized organelles fluoresce green (A,D), while higher polarized organelles fluoresce orange-red owing to multimerization of JC-1 and formation of J-aggregates (B,E.). Merged images showing mitochondria with both red and green fluorescence, suggesting a metabolic turnover of activity (C,F).

Figure 4.2106
 Mitochondria distribution in stage III zebrafish follicle exposed to 5 μ M Mitotracker Green FM. The green represents mitochondria stained on the basis of the membrane potential. Mitochondria stained by Mitotracker green FM shows the same pattern

obtained with JC-1 (A). (B) Optical section showing the incapacity of stain to penetrate in the oocyte.

Figure 4.3107

Ovarian follicle viability assessed by TB and GVBD tests following exposure to different concentration of Triton X-100 in Leibovitz L-15 medium. Control: TB and GVBD tests were undertaken after follicles separation from ovaries; 0.01% Triton: TB and GVBD tests were conducted after the exposure of follicles to 0.01% (v/v) Triton X-100 for 15 min; 0.1% (v/v) Triton: TB and GVBD tests were conducted after the exposure of follicles to 0.1% Triton X-100 for 15 min. Error bars represent S.E.M. Bars with different superscripts differ significantly ($P < 0.05$).

Figure 4.4109

Mitochondria distribution in stage III zebrafish follicle exposed to 5 μ M JC1 following a permeabilization treatment with 0.01% (v/v) Triton X-100 for 15 min (A,B,C) followed by 5 μ M (D-F) or 50 μ M (G-I) of FCCP in Hanks' solution for 15 min. FCCP causes a structural breakdown of the mitochondria patterns (D,G) and no red fluorescence was found (E,H). C, F and I represent merged images.

Figure 4.5110

Mitochondria distribution in stage III zebrafish follicle exposed to 5 μ M MitoTracker green FM following a permeabilization treatment with 0.01% (v/v) Triton X-100 for 15 min (A-B); followed by 5 μ M (C) or 50 μ M (D) of FCCP in Hanks' solution for 15 min. 5 μ M FCCP causes a decrease of green fluorescence (C) whilst 50 μ M FCCP causes a structural breakdown of the mitochondria patterns (D).

Chapter 5: Examination by Scanning Electron Microscopy (SEM) and Transmission Electron Microscopy (TEM) of stage III zebrafish (*Danio rerio*) ovarian follicle structure to support observations of mitochondria distribution obtained by confocal microscopy

Figure5.1118

Micrographs of stage III follicle obtained by Cryo-SEM (A-B) showing the oocyte (O) and the outer layer (OL). (C) Fracture surface inside stage III ovarian follicle obtained by Cryo-SEM. Particular hexagonal - polygonal structure belonging to the vitelline envelope (VE), which surrounded the oocyte (O), is shown. Each hexagonal – polygonal structure showed a diameter of 10 – 15 μm (square). Bar, 10 μm .

Figure 5.2120

(A-B) High-power TEM showing a portion of a granulosa cell, which presents steroids producing cells features: round and oval mitochondria (m), abundant globular smooth endoplasmic reticulum (arrows), basement membrane (Bm). (C) Electron micrograph of granulosa cell of vitellogenic follicle, which contains abundant free ribosomes (square), elongated mitochondria and rough endoplasmic reticulum (RER).

Figure 5.3121

(A) Electron micrograph of stage III follicle separated using enzymatic method, showing the layers (VE-vitelline envelope, F-granulosa cells layers, T-thecal layer) of a vitellogenic oocyte (O). The oocyte displays endocytic activity (arrows). The vitelline envelope shows pore canals (pc). (B) Electron micrograph of stage III follicle separated using mechanical method, indicating cortical alveoli (CA) and mitochondria (arrow) in the ooplasm (O). The vitelline envelope (VE) shows masses of electron dense material (*) next to its external surface. (C) High-power TEM in the ooplasm of a portion of developing cortical alveoli (CA) with a distinct central core surrounded by light flocculent material. Mitochondria appear randomly dispersed (arrow) in the ooplasm.

Figure 5.4122

(A) High-power TEM indicating the cortical cytoplasm of the oocyte (O). Yolk body (Y) has a smooth contour, homogeneous interiors. Microvilli (arrow) from the oocytes extend to the follicle cells through the vitelline envelope. (B) High-power TEM showing microvilli from the oocyte (O) passing through are the pore canals (pc) of the vitelline envelope (VE). (C) High-power TEM showing the pore canals (pc),

whit a diameter of 0.39 micron, of the vitelline envelope (VE). The vitelline envelope shows a thickness of 2.9 micron and an outer layer of 0.19 micron.

Figure 5.5123

Electron micrographs of stage III follicle separated using enzymatic (A-B) and mechanical (C-D) method. The ooplasm (O) was surrounded by the vitelline envelope (VE), which showed pore canals (pc). External to the granulosa layer (F) was the thecal layer (T). In micrograph D, part of the thecal layer (arrow) has been removed by the mechanical separation. The granulosa cell layer remains (F) beneath the basal lamina. Electron dense material (E) between the follicle cell and the vitelline envelope (VE).

Chapter 6: Evaluation of mitochondrial activity and distribution as biological marker in stage III ovarian follicles of zebrafish (*Danio rerio*) following CPAs exposure

Figure 6.1131

Mitochondrial distribution in stage III zebrafish follicle exposed to 5 μ M JC1. JC-1 is a sensitive marker for mitochondrial membrane potential ($\Delta\Psi_m$). JC-1 accumulates in monomeric form within the mitochondrial matrix and its fluorescence emission characteristics are a function of the magnitude of $\Delta\Psi_m$. Low polarised organelles fluoresce green, while higher polarised organelles fluoresce red, owing to multimerisation of JC-1 and formation of J-aggregates. The green represents mitochondria with low membrane potential while the red represents those with high membrane potential. Effect of different concentrations of methanol on mitochondrial membrane potential are shown (C, D, E, F, G, H, I, J) in zebrafish stage III ovarian follicles. 1 M methanol causes a decrease in both green (C) and red (D) fluorescence. 2 M methanol also causes a decrease in green fluorescence (E) and loss of red fluorescence (F). 3 M (G, H) and 4 M methanol (I, J) cause a structural breakdown of the mitochondrial patterns.

Figure 6.2133

Viability assessed by TB and FDA – PI staining after exposure to methanol (A) or DMSO (B) followed by incubation in Hanks’ solution for 5h at 28°C. Bars and error bars represent means \pm SEM of three experiments each with three replicates. Bars with different superscripts differ significantly ($P < 0.05$).

Figure 6.3135

Effect of methanol (A) and DMSO (B) exposure on mtDNA on zebrafish stage III ovarian follicles. mtDNA copy number was measured 1 h and 5h after 30 min exposure to cryoprotectant. Error bars represent Standard Error of the Mean. Different letters represent significant differences between control and treated groups ($P < 0.05$). # represents significant differences between the 1h and 5h pair values.

Figure 6.4137

Effect of methanol (A-B) and DMSO (C-D) exposure on ATP level and ADP/ATP ratio on zebrafish stage III ovarian follicles. ATP level and ADP/ATP ratio were measured 1 h and 5 h after the exposure to cryoprotectant for 30 min. Error bars represent Standard Error of the Mean. Significant difference in ATP level between control and treated groups are indicated (*) ($P < 0.05$).

Chapter 1: Introduction

1.1 Quality of fish oocytes

High quality fish oocytes are essential for *in vitro* maturation (IVM), *in vitro* fertilization (IVF) protocols, and for use in cryopreservation. However, although progress has been made in understanding the developmental mechanism of mammalian and certain invertebrate oocytes, very limited progress has been reported for fish. It is important to develop new methods for assessing the quality of fish oocytes for their role in the aquaculture system, in the preservation of endangered species and managing fish models used in biomedical research. The lack of reliable methods of evaluating oocyte quality limits progress in these areas.

The quality concept is not easy to define in fish, it depends on several factors determined by the intrinsic properties of the egg itself and the environment in which the egg is fertilised and incubated (Brooks et al.1997). Good quality eggs in the fish farming industry have been defined by Bromage et al. (1992) as those eggs which exhibit low mortalities at fertilisation, eyeing, hatching and first feeding. Kjorsvik et al. (1990) and Bromage et al., (1994) suggested the shape of the egg, its transparency, the distribution of oil globules and also the appearance of the zone pellucida can be indicators of quality.

The quality of an egg is determined by its genes, by maternal mRNA and the nutrients contained within the yolk. After fertilisation, the quality of the embryo will depend also on the contribution of the paternal genes. In multiple spawning fish, there are also variations in the quality of eggs produced in different batches over a single spawning season. It is known that nutrients sequestered by the oocyte during the growing phase influence embryonic growth and survival. The embryo development in fish depends also on the types and the amount of lipids, fatty acids, water, proteins, minerals and vitamins present in the egg (Speake et al., 1994; Bell and Sargent, 2003;

Royle et al.,2003; Tveiten et al., 2004). Large lipoglycophosphoproteins and vitellogenins are essential nutrients for the developing oocytes. Besides their role as a source of nutrients for the developing embryo, vitellogenins serve as co-transporter of immunoglobulins and hormones to the oocytes (Babin, 1992; Specker and Sullivan, 1994; Montorzi et al., 1995; Picchietti et al., 2001). A decline in these proteins could induce alteration of the egg composition and lead to a compromised embryo survival. The physiological conditions of the fish, including hormonal status, which affects the incorporation of the compounds into the egg, also have an influence on the quality.

A better understanding of the mechanisms of oocyte growth and development is essential as during those processes the oocyte acquires components such as yolk, vitelline envelope materials and most of the components for DNA, protein synthesis and mRNA. The developmental competence of the oocyte is acquired during its growth and maturation. Although meiosis may be completed successfully, there are a variety of other processes occurring within the cytoplasm of the oocyte that are required for complete developmental competence following fertilization, these events are called cytoplasmic maturation. An oocyte that has not completed cytoplasmic maturation is of poor quality (Krisher, 2004).

In fish and oviparous vertebrates, the major constituents of the egg are the yolk and the vitelline envelope. These proteins are synthesized in the liver and transported to the oocyte. Their synthesis is under endocrine control and a major role is played by estradiol-17B. Vitellogenesis and zonagenesis (formation of vitelline envelope) are crucial for reproduction and also for successful embryo development.

The quality of the follicular environment from which the oocyte originates also has an impact on the quality of the oocyte. The oocyte, together with somatic cells by which it is surrounded, forms a functional unit. They are in contact with each other by a dense network of gap junctions, and a paracrine signaling system. This communication is bidirectional. Communication between the oocyte and the

surrounding cells takes place through specialised membrane channels, called gap-junctions, that allow the transfer of low molecular weight molecules (Eppig, 1991). The molecules involved in cellular communication include glucose metabolites, amino acids, and nucleotides, but a special role is played by cyclic adenosine monophosphate (cAMP) and purines, which are small regulatory molecules that regulate the oocyte meiotic process at the time of ovulation or *in vitro* maturation (Conti et al., 2002; Eppig and Downs, 1988; Ge, 2005). Cyclic AMP acts as the intracellular messenger for gonadotropin stimulation (Conti et al., 2002). However, the precise mechanism by which changes in the intracellular concentration of cAMP affect oocyte maturation is not fully understood. High levels of cAMP have been proposed as the regulatory mechanism responsible for maintaining the oocyte in meiotic arrest. Cyclic AMP is only one of a complex network of paracrine regulators that orchestrate the follicular changes leading to ovulation and full oocyte competence (Fair, 2003).

The ability of an oocyte to develop into a viable embryo also depends on the accumulation of specific maternal information and molecules. Information stored in the oocyte is particularly critical during the interval between fertilization and the zygotic genome activation which occurs at the midblastula transition. During this period, all processes are under control of the maternal products. Maternal ribonucleic acids (RNAs) and proteins synthesized during oogenesis support the embryonic development. This transcriptional activity occurring in the oocyte allows the build up of cytoplasmic stores of messenger molecules, which will be translated up to, and possibly beyond, the midblastula transition. Therefore, the formation and stability of the oocyte mRNA is crucial for normal embryo development, and any perturbation of this process is likely to reduce oocyte developmental competence and cause an arrest of embryonic development that could occur at any given stage. Mitochondrial DNA (mtDNA) which is maternally inherited also represents a vital contribution to embryo development.

Cytoplasmic compartmentalisation has also been suggested to be an important factor in the coordination of nuclear and cytoplasmic oocyte maturation (Combelles and Albertini, 2001). The activity and cytoplasmic distribution of mitochondria can be used as a marker of cytoplasm compartmentalisation and is one of the many diverse features of cytoplasmic maturation (Van Blerkom and Runner, 1984).

Table 1.1 Factors which affect ovarian egg quality in fish

<p><i>Environment in which the egg is fertilised and incubated</i></p> <ul style="list-style-type: none"> - physiochemical conditions of the water
<p><i>Endocrine status of the female during the growth of the oocyte affected by</i></p> <ul style="list-style-type: none"> - photoperiod
<p><i>Morphology of the egg</i></p> <ul style="list-style-type: none"> - the shape - its transparency - the distribution of oil globules - the appearance of the zone pellucida
<p><i>Successful completion of physiological events during oogenesis and folliculogenesis</i></p> <ul style="list-style-type: none"> - vitellogenesis - zonagenesis - nuclear maturation - cytoplasmic maturation
<p><i>Amount of substances present in the egg</i></p> <ul style="list-style-type: none"> - lipids, - fatty acids, water, - proteins, - minerals and vitamins
<p><i>Successful synthesis and transcriptional activity of</i></p> <ul style="list-style-type: none"> - maternal RNAs - proteins - Mitochondrial DNA (mtDNA)
<p><i>Cytoplasmic compartmentalisation</i></p> <ul style="list-style-type: none"> - the coordination of nuclear and cytoplasmic oocyte maturation - organelles distribution (mitochondria)
<p><i>Follicular environment from which the oocyte originates</i></p> <ul style="list-style-type: none"> - communication between the oocyte and the surrounding cells - efficient paracrine regulators system

1.2 Viability assays

The assessment of ovarian follicle viability is an important step before undertaking further and more complicated study to identify ovarian follicles of good quality. Viability assays attempt to measure the percentage of cells that are viable. They can be classified on the basis of the characteristics being assessed - physical integrity, metabolic activity, mechanical activity, mitotic activity and *in vivo* function (fertilization and development).

The evaluation of viability by dye exclusion, or by dye uptake, is one of the most common methods used. Dye exclusion is based on membrane integrity; cells with an intact membrane are able to exclude the dye, whilst cells with a damaged membrane take up the colouring agent (e.g. Trypan Blue). In the case of a dye uptake assay, the dye is normally taken up by viable cells but not by non-viable cells. Moreover, the use of a combination of tests for the viability assessment has been preferred because it gives the opportunity of evaluating more than one parameter, such as physical integrity and metabolic activity. A range of vital stains and other methods have been used with the goal of assessing the zebrafish oocytes viability; these include, trypan blue (TB) staining, thiazolyl blue (MTT) and *in vitro* maturation followed by observation of germinal vesicle breakdown (GVBD) (Plachinta et al. 2004a, Selman et al. 1994; Isayeva et al. 2004). The observation of germinal vesicle breakdown (GVBD) is the most sensitive method, but this test can only be applied to stage III as the later stages have already gone through maturation and germinal vesicle breakdown. While the vital stains are applicable to all stages, they have several limitations. Plachinta et al. (2004a) pointed out that TB test may not be ideal as it only assesses the membrane damage as oppose to whole cell physiological status. In their study, MTT was also shown to be the least sensitive method, giving poor correlation to subsequent GVBD results.

The resumption of meiosis, indicated by germinal vesicle breakdown (GVBD), has certainly been the best test as it is based on a physiological state, but even this test has some limitations due to its stage specific applicability and to the lack of reliable protocols for *in vitro* maturation of oocytes in zebrafish. Indeed, unlike the maturation in mammals where, in domestic livestock species, offspring have been produced using *in vitro* oocyte maturation, in zebrafish there are very limited reports of offspring production deriving by *in vitro* oocyte maturation (Seki et al., 2008).

Proteomics analysis has been also used to find correlations between oocyte viability and their associated protein repertoires (Rime et al., 2004). Proteomics analysis allows the investigation of protein constituents of oocyte; also changes in the amounts of the proteins and in the patterns of postranslational modifications can be followed. Proteomic technologies have been used to analyse the protein repertoires of zebrafish oocytes at different stages of development. The effect of two most commonly used cryoprotectants (methanol and DMSO) has been investigated on the repertoire of the oocyte proteins. Very small changes appear following the exposure to cryoprotectant (CPA), indicating that the loss of viability may be due to physical changes and not changes in the protein repertoire (Chapovetsky et al., 2007).

Table 1.2 Viability methods commonly used to assess zebrafish ovarian follicles viability

<i>Viability method</i>	<i>Mode of action</i>	<i>Advantages</i>	<i>Disadvantages</i>
Trypan Blue (TB)	Membrane integrity test; cells with an intact membrane are able to exclude the dye, whilst cells with a damaged membrane take up the colouring agent	Fast	It only assess the membrane integrity. No indication of metabolic status.
Methyl thiazolyl blue (MTT)	Conversion of methyl thiazole by mitochondrial enzyme succinate dehydrogenase.	Fast	Low sensitivity as shown by Plachinta et al., (2004a)
Observation of germinal vesicle breakdown (GVBD)	Prematurational follicles are opaque becoming translucent following GVBD. Follicles failing to undergo maturation and GVBD remained opaque	Physiological marker.	limitations due to its stage specific applicability and to the lack of reliable protocols for <i>in vitro</i> maturation of oocytes in zebrafish

1.3 Using zebrafish as a model system

Zebrafish (*Danio rerio*) is a tropical freshwater fish belonging to the minnow family (Cyprinidae) and it is native to India and Pakistan. Among teleosts, the zebrafish is an important experimental animal in developmental biology, physiology, genetics and biomedical research (Buono and Linser, 1992; Leff, 1992; Squire et al., 2008; Westerfield, 2000). Zebrafish as a model has become popular in the past two decades (Udvardia and Linney, 2003). Zebrafish exhibit many features of an ideal model organism as they are easy to maintain and manipulate in the laboratory. The eggs are

externally fertilised and, under simple laboratory conditions, zebrafish can produce a large number of fertilised eggs on a daily basis. Their embryos are large, easy to obtain and embryo development is rapid (Fishman et al., 1997; Stainier and Fishman, 1992; Strehlow et al., 1994; Westerfield, 2000). Furthermore, the zebrafish is being established as a genetic and physiological model for vertebrate-specific processes such as organogenesis (Zhong et al., 1984). It has also been considered an emerging model system for human disease (Zon, 1999).

Their short generation time of three months makes zebrafish an ideal model for genetic studies and also their susceptibility to the mutagens, teratogens, carcinogens and toxins makes this breed an ideal environmental model. Furthermore, the genome of this fish has already been sequenced. Zebrafish is also very useful for the investigation of ovarian follicle development, as its ovary contains follicles at different stages of development. The results obtained in zebrafish also contribute towards a better understanding of oogenesis and folliculogenesis processes in fish in general and therefore would be supportive to the undergoing research in fish reproduction and related fields.

1.4 Structure of zebrafish ovary

Zebrafish present cystovarian type ovaries with a true ovarian capsule. The oocytes are ovulated into the intraovarian space and move down to the cloaca, without entering the peritoneal cavity, by ciliated epithelium and smooth muscles (Fig1.1). Zebrafish possess group-synchronous ovaries, meaning that all stages of oocyte development are present in the ovaries during the breeding period. Adult zebrafish spawn several times in a month. Each follicle consists of an oocyte surrounded by more than one layer. The structure of the follicle changes during growth, maturation and ovulation of the oocyte. Oocyte development has been divided into five stages, stage I, II, III, IV and V (Selman et al. 1993).

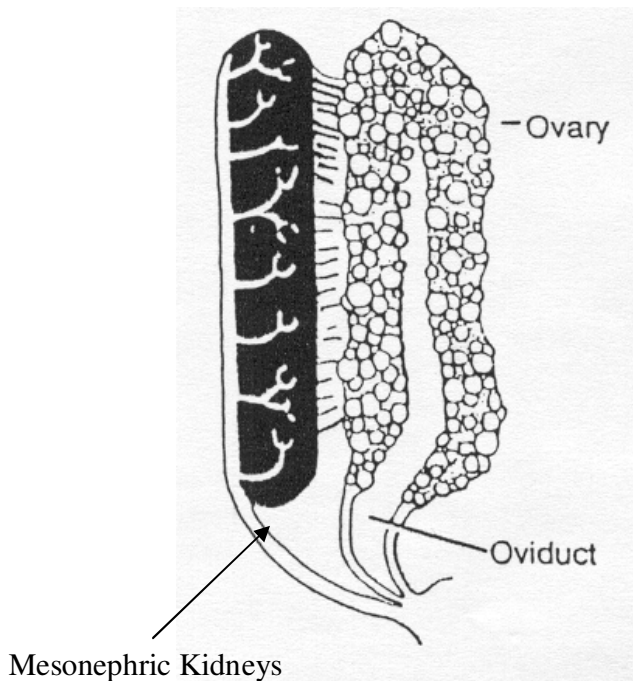


Fig.1.1 Cystovarian type ovaries. (downloaded from <http://www.iim.csic.es/pesqueras/Pesca/Biologia/reproduccion/Repro452%20Fish.ppt#302,17,Slide 17>)

1.4.1 Stage I (the primary growth stage)

The oocyte is surrounded by a single layer of squamous follicle cells and as the oocyte grows, the ooplasm becomes more basophilic and intracellular organelles proliferate. Shortly after the beginning of stage IB, the chromosomes begin to decondense and enter diplotene, where they arrest for the remainder of oocyte development. One to a few large nucleoli are evident within the germinal vesicles but as the oocyte grows, the nucleoli proliferate and decrease in size, and move peripherally within the enlarging germinal vesicle. The ovarian follicle is formed when the oocyte leaves the nest enveloped by layers of somatic tissues. The ovarian follicle is formed of an oocyte surrounded by a single layer of squamous follicle cells that lie on a distinct basement membrane. By the end of this stage, annulated lamellas are noticeable, and mitochondria, Golgi complex and cisterns of rough endoplasmic

reticulum are abundant in the cortical ooplasm. Extracellular material (amorphous electron-dense material) between the microvilli extend from the oocyte, and the microvilli of the overlying follicle cells start to appear.

Stage IB

In the follicle phase, the oocyte leaves the nest and resides within a definitive follicle. It is surrounded by a single layer of follicle cells that lie on a distinct basement membrane. This complex is surrounded by a vascularised connective tissue compartment, the theca, which is covered by a surface epithelium.

1.4.2 Stage II (follicle diameter = 0.14-0.34 mm)

Follicles increase in size and cortical alveoli proliferate, oocytes become opaque and the centrally germinal vesicles are difficult to discern. This stage is also known as the cortical alveolus stage and is characterized by the appearance of cortical alveoli within the oocyte. During this stage the formation of tripartite vitelline envelope begins, the newly formed vitelline envelope is perforated by patent channels (pore canals) which contain long microvilli (macrovilli) from both the oocyte and the follicle cells. During stage II, the follicle cells external to the oocyte and to the vitelline envelope, become cuboidal and are attached to each other by numerous desmosomes as well other intracellular junctions.

Special cells appear within the theca, the “special thecal cells or ovarian interstitial cells”, they are thought to be steroid-secreting cells. They are not numerous or well developed in stage I, but from the stage II and throughout the rest of development they increase in number and size, appearing more differentiated. Ultrastructurally, they have numerous mitochondria packed with tubular cristae in a dense matrix and display many profiles of smooth endoplasmic reticulum. Also fibroblasts in the theca layer have been observed.

1.4.3 Stage III Vitellogenesis stage (follicle diameter 0.34-0.69 mm)

During stage III (Fig. 1.2), the vitellogenic oocyte is surrounded by two major cell layers, the thecal and follicular layers, which are separated from each other by a distinct basement membrane (Nagahama, 1994). The theca contains collagen fibres, fibroblasts and capillaries, and in zebrafish follicles special thecal cells have been found. Fibroblasts, which are most numerous within the theca, have fewer mitochondria (with flattened cristae), and contain free ribosomes and moderate amounts of both rough and smooth endoplasmic reticulum. The special thecal cells continue to enlarge and increase in number, while the follicle cells remain cuboidal with both lysosomes and endoplasmic reticulum proliferating.

During stage III the oocyte accumulates the yolk containing nutritional reserves for embryo development, and completes differentiation of its cellular and a-cellular envelope. Stage III has been divided into two sub-stages, stage III a and stage III b (Selman et al., 1993).

Stage IIIa, the first entry of vitellogenin (Vtg) into the oocyte and in many species by the accumulation of lipid globules. Cortical alveoli are observed in the vicinity of numerous Golgi apparatus resulting from the biosynthesis activity of the oocyte. The alveoli are distributed in a single layer underlying the oolemma. During fertilisation they fuse with the oolemma and discharge their glycoprotein content at the oocyte surface during the cortical reaction by exocytosis (Selman and Wallace, 1989). Shibata et al. (2000) reported that the release of the cortical alveoli leads to a restructuring and hardening of the vitelline envelope to become a chorion. In zebrafish, the presence of lipid globules has not been observed, while they have been reported in other teleosts. During this stage mitochondria are scattered throughout the ooplasm.

During stage III b, Vtg endocytosis is considerable, indicating a rapid growth of the follicle and formation of zona radiate. The micropyle is fully formed during this stage. The micropylar cells originate from the granulosa cells and invade the zona radiate (ZR) to the oolemma. The micropyle represents the only entrance for the spermatozoa (Dumont and Brummett, 1980), and the animal pole formation is determined by the location of the micropyle.

1.4.3.1 The Vitelline Envelope

The vitelline envelope is an acellular structure which surrounds the oocyte. In most animals, including fish, one of the envelope's roles is to protect the egg (and embryo) from the mechanical and physiological damages during and after the ovulation until hatching. Other roles of the vitelline envelope include the uptake of nutrients, functional buoyancy (Podolsky, 2002), protection of the oocyte, species-specific sperm binding, guidance of the sperm to the micropyle (Dumont and Brummet, 1980) and it also has bactericides proprieties (Kudo and Inoue, 1989).

In teleosts fish, vitelline envelope glycoproteins are provided by the liver (Murata et al. 1997). The vitelline envelope structure is completely assembled while the oocyte is still in the ovary, and remains closely opposed to its surface during ovulation and is separated from the oocyte by the perivitelline space. Depending on the animal species, the envelope is not modified until the oocyte is activated (sea urchin, fish, etc.) or interacts with oviduct secretions (amphibians) (Barisone, et al. 2003). In zebrafish, the vitelline envelope begins to form during Stage IB (follicle phase of primary growth) and by the end of this stage it is <0.15 μm thick. It appears as an amorphous electron-dense material, initially as isolated patches, between numerous microvilli that extend from oocyte surface to the overlying follicle cells, which have also microvilli projecting toward the oocytes. During stage II growth, a tripartite vitelline envelope is formed, the envelope develops a second layer, between the initial layer developed in stage I and the oolemma. At the beginning of the vitellogenesis,

the vitelline envelope reaches its maximum thickness of approximately 6.0 μm (Selman et al. 1993).

The vitelline envelope is characterized by pores (pore canals) which contain microvilli from both the follicle cells and the oocytes. Processes from both cells type lie in the same pores, but while the microvilli from the oocytes are long (Kessel et al. 1988 reported a length of 8.0 μm) and extend deep into the space between follicle cells, the processes from the follicular layer do not always reach the oocytes surface. Dumont and Brummet (1980) reported that the function of the pore canals is to support the transfer of yolk proteins and other metabolites from the inside to the outside of the developing oocyte and vice versa.

Whilst the follicle matures, the vitelline envelope becomes compact and more homogeneous in appearance. The pore canals become narrower as the microvilli from both oocytes and follicle cells begin to retract and the vitelline envelope is penetrated by only a single canal, the micropyle, which permits fertilization by providing a portal through which the sperm can reach the egg. The outer coat of the vitelline envelope (chorion) of a mature egg displays a filamentous nature (Selman et al., 1993). The vitelline envelope is separated from the oocyte by the perivitelline space; this space is necessary for allowing division of the oocyte and for harbouring the first polar body formed in the division.

The general understanding of the vitelline envelope formation in fish is that the envelope is formed by the oocyte itself or the follicle cells (Anderson, 1967; Dumont and Brummett, 1985; Wourms, 1976; Wourms and Sheldon, 1976). Studies on the *de novo* synthesis of components of the egg envelope in pipefish, *Syngnathus scovelli*, also supported the above concept, reporting that all 3 major components of the envelope were produced by the oocyte and/or the follicle cells (Begovac and Wallace, 1989). However, the components of zebrafish vitelline envelope are synthesized in the ovary, as reported by Chang et al. (1996).

1.4.3.2 Vitellogenesis and vitellogenin uptake

Vitellogenesis represents one of the most important reproductive phenomena in egg-laying animals and it is well known that many proteins and lipids are actively synthesised and transported to the oocyte during the vitellogenic process. Vitellogenesis also represents the major growth stage, in which the oocyte increases in size due to accumulation of yolk. The yolk is sequestered as vitellogenin, a yolk precursor protein. The oocyte's yolk proteins in oviparous animals are synthesised by the liver as lipophosphoglycoprotein precursor vitellogenin (Vtg), which represents a source of nutrients for developing larvae.

The vitellogenin is produced in the liver and is sequestered by the oocyte via endocytosis and then processed into yolk proteins (lipovitellin and phosvitin, a protein heavily phosphorylated on its serines stretch), which accumulate within membrane-limited yolk bodies. The Vtg gene is sensitive to estrogens and other steroid hormones and it is the principal precursor of egg-yolk proteins. The Vtg is the major circulating protein in the blood stream during estrogen induced vitellogenesis. Vtg are large phospholipoglycoproteins, varying in size from 200 to 700 KDa. Membrane-bound vitellogening receptors (VtgR) are found on the oocyte surface; these receptors belong to the low density lipoprotein receptor family and allow the uptake of vitellogenin by the oocyte through the interaction with N-terminal region of Vtg via electrostatic attraction. Vtg dimmers are sequestered via membrane-bound Vtg receptors-mediated endocytosis, Vtg is then cleaved in the oocyte into yolk protein, lipovitellin and phosvitin, which represent stored nutrients for the developing embryo. The role of estradiol (E2) in inducing vitellogenin mRNA synthesis in oviparous vertebrates such as amphibians, avians, reptiles and fish, has been well documented.

Three different forms of vitellus of the teleosts oocyte are oil droplets, yolk vesicles and yolk globules. However, the first one is absent in zebrafish (Leug et al., 2000). Despite the general agreements on the function of the droplets for buoyancy and

energy supply, little is known about their structural functions. Based on the conclusion of Kayaba et al. (2001), it is plausible that the phospholipidic content of the droplets are consumed in the organelles such as mitochondria and Golgi apparatus.

1.4.3.3 Cortical alveoli

Cortical alveoli are membrane limited vesicles of variable size. The mature cortical alveolus consists of a distinct central core surrounded by light flocculent material and a membrane. Their appearance within the oocytes characterize the stage II, also known as the cortical alveolus stage. The proliferation of the cortical alveoli during this stage causes the oocyte to become opaque. In zebrafish, during stage II, the cortical alveoli appear in proximity to the Golgi complex, which have been shown to participate in the synthesis of their content (Selman and Wallace, 1989), but during vitellogenesis, due to the accumulation of protein yolk in the centre, the cortical alveoli are pushed to the cortex of the ooplasm. During fertilization, the content of the cortical alveoli is released to the outside of the plasma membrane by exocytosis as part of cortical reaction (Selman et al. 1993). The cortical reaction provides a block to polyspermy and is brought into play as soon as the first sperm fuses with the plasma membrane of the oocyte. Two different types of cortical alveoli have been found in *Blennius pholis* (Shackley and King, 1977) and *Anguilla japonica* (Kayaba et al., 2001), cortical alveoli containing filamentous and those containing latticed material. While in *Fundulus heteroclitus*, only the presence of cortical alveoli containing flocculent material was reported by Anderson (1968).

1.4.3.4 Maturation competence

Oocytes undergo maturation prior to becoming eggs, and this occurs subsequent to the major growth phase, or vitellogenesis (Selman and Wallace, 1989). During this final maturation, the germinal vesicle (GV) migrates towards the periphery of the

oocyte, its envelope breaks down, the first meiotic division occurs, and the chromosomes progress to and arrest at the second meiotic metaphase. In zebrafish, prematurational follicles are opaque, and as maturation progresses, they become more translucent and increase slightly in size. Selman et al. (1993) reported an increase in volume of 10-15% during oocyte maturation *in vivo* and a slightly less increase for *in vitro* matured follicle, in this case probably due to the osmolarity of the culture medium employed. During maturation, the yolk bodies change their structure, losing their crystalline main bodies and developing a homogeneous interior (Selman et al., 1993). Prior to ovulation, the microvilli of the follicle cells are retracted from the pore canals of the vitelline envelope. After hormonal stimulation, translucent eggs (0.73-0.75mm in diameter) are ovulated out of their follicle into the ovarian lumen and subsequently spawned.

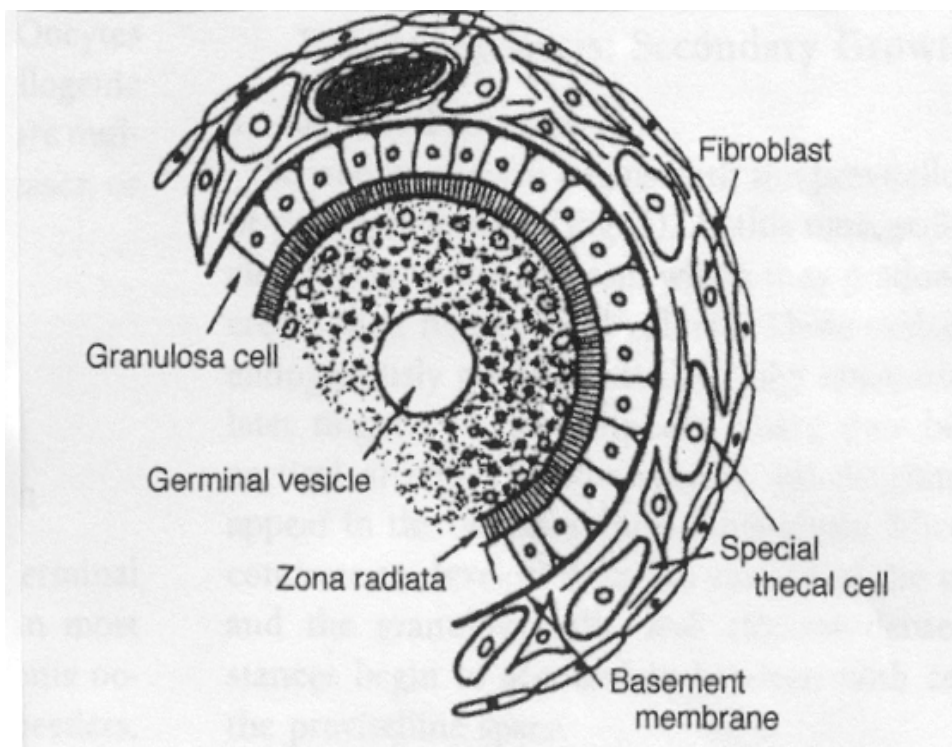


Fig. 1.2 Diagrammatic representation of the follicle and oocyte during early vitellogenesis in teleosts (Nagahama, 1983).

Table 1.3 Stage III zebrafish follicle

<i>Diameter:</i> 0.34-0.69 mm
General appearance: follicle becomes increasingly opaque, the germinal vesicle is completely obscured (GV is not visible).
<i>Follicle cells:</i> cuboidal; increased amount of rough endoplasmic reticulum; lysosome apparent.
<i>Vitelline envelope:</i> Tripartite; begins to get thinner; retains pore canals with microvilli.
<i>Cortical alveoli:</i> Numerous throughout ooplasm; move toward periphery.
<i>Yolk bodies:</i> yolk bodies accrue throughout ooplasm; contain crystalline inclusions.
<i>Endocytosis:</i> Maximal
<i>Nucleus:</i> Begin to move towards periphery develops smoother contour.
<i>Nucleoli:</i> Fewer than stage II; spherical to oval; smallest remain central in GV
Stage of meiosis: Arrested in prophase I.
Maturation competence: in follicle > 0.52mm in diameter.

From Selman et al. (1993)

1.4.4 Stage IV Final stage of oocyte maturation (follicle diameter 0.69-0.730 mm)

During this stage, the oocyte leaves the diplotene stage and restarts the first meiotic division. The nucleus migrates towards the animal pole, in response to hormonal stimulation, where germinal vesicle breakdown (GVBD) takes place. The nuclear membrane is constructed from a class of intermediate filament proteins called lamins, the phosphorylation of lamin proteins induces the disassembly of GV lamina. Metaphase of the first meiotic division occurs, producing a large secondary oocyte and a small first polar body, which degenerates. The secondary oocyte undergoes the second meiotic division, which is arrested in metaphase. This stage is characterised by changes in the organization of cytoskeletal components to promote these events during maturation (Kotani and Yamashita, 2005). In zebrafish, a light flocculent

material has been reported (Selman et al., 1993), which covers the outer surface of the zona radiata externa, periodically interrupted by masses of electron-dense material. All these processes are under hormonal stimulation.

1.4.5 Stage V (Egg)

This stage is characterized by ovulation, which results in the release of mature oocytes from their follicular cells. It involves opening of the follicular wall surrounding the oocyte (follicular rupture) and active expulsion of the oocyte through the opening site (Cerda' et al. 1999, Bolamba et al. 2003). The follicular rupture is caused by the dissolution of the extracellular matrix of the follicular wall. The oocyte is then released into the lumen of the ovary.

1.5 Mitochondria

1.5.1 Structure of mitochondria

Mitochondria are especially abundant in cells and regions of cells that are associated with active processes. Mitochondria contain two membranes, separate by an intermembrane space. The two membranes are very different in structure and in function. The composition of the outer membrane has a 50:50 lipid protein ratio and contains protein structures, porins, which render it permeable to molecules with molecular weights of up to 10000 dalton (Lodish et al, 1995). Ions, nutrient molecules, ATP, ADP, can pass through the outer membrane.

The inner membrane is relatively impermeable, it is permeable only to oxygen, carbon dioxide, and water and it is made by 80% protein and contains all of the complexes of the electron transport system, the ATP synthetase complex, and transport proteins. This complex of proteins is encoded by two genomes, the nuclear and the mitochondrial genomes. The inner membrane forms internal compartments called cristae, which increase the reaction surface area available.

The membranes create two compartments. The region between the inner and outer membranes is the intermembrane space. The main function of this space is nucleotide phosphorylation. Its content is similar to that of the cytoplasm, due to the presence of porins in the outer membrane allowing free movement of ions and small molecules into the intermembrane space. It has an important role in the primary function of mitochondria, which is oxidative phosphorylation. The space enclosed by the inner membrane is the matrix, which contains enzymes responsible for the citric acid cycle. It also contains the recyclable intermediates that serve as energy shuttles.

Mitochondria can be free in the cytoplasm or packed in among more rigid structures. They form tubular and reticular networks and their interaction with the cytoskeleton provides a clue to their distribution, movement and inheritance (Rube and van der Bliet, 2004). The shape of mitochondria varies with cell type. In some tissues, the mitochondria are almost filamentous, in others cells they can assume spherical or ellipsoid shape. The size of a mitochondrion is about 0.5 by 1 μm , however, they vary widely in shape and size. They reproduce by fission in a manner similar to that of bacterial cells.

1.5.2 Mitochondrial distribution in oocyte and their role in reproduction

Mitochondria have a wide range of functions that affect reproduction. Structural and quantitative variation in mtDNA has been associated with gamete quality and reproductive success. Adequate ATP reserves in oocytes and embryos are critical for normal nucleic acid and protein synthesis, and they have been suggested to be an indicator of the developmental potential of mouse (Calarco 1995) and bovine embryos (Stojkovic 2001). Van Blerkom (2004) has reported that factors such as mitochondrial complement size, mitochondrial DNA copy numbers and defects, levels of respiration, and stage-specific spatial distribution, influence the developmental normality and viability of human oocytes and preimplantation- stage embryos.

The distribution of mitochondria in oocytes of fish and amphibian has been studied mainly in perivitellogenic stages of oogenesis. In *Xenopus laevis*, in diplotene oocytes (stage I and II), the presence of a mitochondrial cluster called “yolk nucleus” (Billet and Adam, 1976) or “mitochondrial mass” (Callen et al. 1980) has been identified. It originates from small mitochondrial aggregates already present in primordial germ cells which become spherical in growing oocytes. It consists of numerous long intermingled mitochondria in 200 µm oocytes of young females, whilst in adult females numerous small vesicles are found among mitochondria.

Little attention has been paid to the way that mitochondrial mass is fragmented after the beginning of vitellogenesis. Data concerning the size of the oocytes in which the disaggregation begins are contradictory. Tourte and co-authors (1984) investigated mitochondria distribution during vitellogenesis in *Xenopus laevis* oocyte and they reported two populations of mitochondria, the first involved in the elaboration of a cortical layer at the vegetative hemisphere of the cells and the second around the nucleus. They also reported that the density of organelles inside each population stays constant during vitellogenesis up to the middle of stage V and the crown is always less compact than the mitochondrial mass. Studies have been carried out on mitochondrial DNA in zebrafish (Broughton et al., 2001) and on mitochondrial behavior in early stage (stage I) of zebrafish oocyte (Zhang et al. 2008), but little is known about mitochondrial distribution and activity in later stage zebrafish follicles/oocytes. Only the study conducted by Selman et al. (1993) identified aggregations of mitochondria and endoplasmic reticulum in the cortical ooplasm of early stage III zebrafish oocytes.

1.5.3 Mitochondrial DNA (mtDNA)

Mitochondria possess their own genome. It was firstly observed in 1924 by Bresslau and Scremin using light microscopy and a Feulgen stain (Sawyer and Van Houten,

1999). It is circular, comprising two strands. The individual strands of the mtDNA molecules are denoted heavy (H) and light (L) strand because of their different buoyant densities in a cesium chloride gradient. The observed difference is due to the nucleotide content of the two strands, the H strand is guanine rich, whilst the L strand is guanine poor. The control region (mtDNA-CR), also known as D-loop, is the most rapidly evolving region of the mtDNA, with a mutation rate up to 20 times that of the nuclear genome. It results in approximately one mutation every 33 generations. It is an unstable and hypervariable region, with a triplex DNA structure at the site of origin of the H-strand. This region is important for the initiation of the transcription and translation.

The mitochondrial genome lacks introns and the only significant noncoding sequence is the control region, which is involved in regulating transcription and replication (Shadel and Clayton 1997) and is usually <5% of the total genome size (Broughton et al. 2001). In human cells each strand contains a single promoter region for transcriptional initiation, the light-strand promoter (LSP) and the heavy-strand promoter (HSP). The two strands of mtDNA have two different origins of replication, for the H-strand it is within the D-loop, whereas that for the L-strand is about one third of the way around the genome. Replication is dependent on the binding of the nuclear encoded transcription factor A to its binding site or sites. Mitochondria contain enzyme systems responsible for mtDNA replication and expression, which are distinct from those found in the nucleus.

The respiratory complexes are encoded by both the nuclear and mitochondrial genomes. The mitochondrial genes encode for a small number of these subunits while the nuclear genes encode for the majority of them. The nuclear genes encode the remaining components of the respiratory chain which are imported to the mitochondrion via specialized import systems (Mokranjac and Neupert, 2005). The genes encoded in mtDNA are all essential for cellular ATP production by oxidative phosphorylation. The mitochondrial genome encodes 13 polypeptides, 22 tRNAs and

2 rRNAs, necessary for mRNA expression. The 13 proteins encoded by the mtDNA are essential subunits of the electron transport chain and ATP synthase.

Mitochondrial genetics differ from nuclear genetics in three respects. Firstly, mitochondrial genes do not follow a Mendelian pattern of inheritance as they are maternally inherited. Secondly, the mitochondrial genome is polyploid. Normally, only one form of mtDNA is present (state of homoplasmy). Mutation can lead to a state of heteroplasmy (two or more forms of mtDNA coexist within a cell). Thirdly, unlike a diploid nuclear gene that can normally only assume certain states (homozygous wild type, heterozygous, or homozygous mutant), mtDNA heteroplasmy does not vary by discrete steps (Lemire, 2005). Mitochondria replicate their DNA and synthesise proteins even if the major part of these proteins are encoded by the nuclear DNA.

1.5.3.1 MtDNA copy number

The number of mitochondria and mitochondrial genome copy number vary between tissues. The number of mitochondrial genomes seems to be correlated with the organelle number and it indicates that the nucleus has the potential to increase the amounts of mitochondrial components as this correlation is tissue-specific. Different factors are involved in the maintenance of mtDNA copy number in animal cells, although the mechanism by which mtDNA levels are controlled is unknown. Moraes (2001), in a detailed review, reported that the major factors involved in mtDNA replication, such as a DNA polymerase, RNA polymerase, single-stranded-DNA-binding proteins (mtSSBB) and RNA processing enzymes, were all encoded by the nuclear genome. Many nuclear genes are needed to replicate, transcribe and maintain the mtDNA.

The mitochondrial transcription factor (mtTFA) and mitochondrial RNA polymerase are required for mtDNA maintenance, as transcription is essential for mtDNA

replication because an RNA primer is necessary to start DNA polymerization. The increase in energy production might be achieved mainly by an overall increase in mitochondria biogenesis (Moares, 2001).

In mammals, most cells contain between 10^3 and 10^4 copies of mtDNA. The mature oocyte contains higher copy number (10^5), this could be explained by the fact that replication does not occur during early embryogenesis and the high copy number is required for building up a reservoir or maybe in preparation for energetic demands of embryogenesis (Piko and Matsumoto, 1976).

1.5.3.2 Mechanism of mtDNA damage

The mitochondrial genome lies at the site of the electron transfer chain and it is vulnerable to oxidative attack, being exposed to free radicals generated by electron transport chain. It lacks protective histones and it mutates 10 or more times faster than nuclear DNA. Various mutations and deletions have been identified in mtDNA under some extreme conditions and they have been divided into: base modifications leading to double-strand separation (Hayakawa et al. 1992), strand breaks and deletions (Hayakawa et al. 1995). A higher concentration of active intermediates is produced in mitochondrial matrices than in nuclei because of the presence of protein containing Fe-S clusters in the mitochondrion. Accumulation of mtDNA damage and mutations can contribute to ageing process and degenerative disease (Wei 1998). DNA damage blocks the activity of the transcription machinery, leading to a decline in mitochondrial mRNA and protein synthesis. Because mtDNA codes for protein of the electron chain, the reduced expression leads to a decline in oxidative phosphorylation, increased reactive oxygen species (ROS) production and further damage (Sawyer and Van Hovten, 1999).

1.5.3.3 MtDNA repair

The high rate of mtDNA mutation can be attributed to two general factors: an increased susceptibility of mtDNA to mutation and to an insufficient presence of enzymatic DNA repair activities devoted to the removal of damaged nucleotides. The susceptibility to mutation is due to the constant exposure of mitochondria to an oxidative environment. Mitochondria are the major potential source for ROS production, being the compartment where about 95% of O₂ is consumed (Turrens 2003). Furthermore, other factors could affect mtDNA, such as errors incurred during replication, incorporation of uracil, modifications resulting from UV exposure and ionizing radiation and also following the exposure to certain chemicals. The absence of histones and efficient DNA repair mechanism make the mtDNA more vulnerable to mutation showing a 10-20 higher mutational frequency than the nuclear DNA (Richter et al. 1988; Yakes and Van Houten 1997). Mitochondria lack the necessary enzymes for nucleotides excision repair (Clayton et al., 1974), the principal pathway for the removal of oxidative DNA damage (Alexeyev et al., 2004; Sawyer and Van Houten, 1999). All the mtDNA repair genes are encoded in the nucleus and the corresponding gene products are then transported into the mitochondria through the membrane potential and a mitochondrial targeting sequence, which comprises 20-25 N-terminal aminoacids that are cleaved off during the transport process (Pettepher et al., 1991; Driggers et al., 1993).

1.5.4 Role of mitochondria

In addition to this role in production of most cellular energy, in the form of ATP, through the oxidative phosphorylation system, mitochondria are involved in other metabolic functions such as heme and non-heme iron biogenesis, urea production and steroid biogenesis. These organelles also control the homeostasis of intracellular Ca²⁺. Calcium ion concentration is an important second messenger in cells. They also play an important role in the apoptotic-signaling pathway. A variety of key events in

apoptosis focus on mitochondria, such as the release of caspase activators (e.g. cytochrome c), changes in electron transport, loss of mitochondria transmembrane potential, altered cellular oxidation-reduction, and the participation of pro- and anti-apoptotic Bcl-2 family protein (Green, 1998; Green and Reed, 1998).

1.5.4.1. The respiratory chain

The respiratory chain is composed by four complexes. The electrons enter the chain either through complex I or II and they are passed on from these complexes to complex III by the coenzyme Q carrier (ubiquinone). Cytochrome c carries electrons from complex III to cytochrome oxidase (complex IV), where they react with oxygen and protons to form water. The respiratory chain forms a succession of linked redox reactions, each carrier being reduced (gaining electrons) and successively oxidized (losing electrons) by the next carrier. These redox reductions release energy.

1.5.4.2 ATP

Energy is stored in living systems as adenosine triphosphate (ATP), which consists of a nitrogenous base, adenine, linked to ribose. A string of three phosphate residues is attached to the sugar molecule. ATP can be hydrolysed to adenosine diphosphate (ADP) and inorganic phosphate (Pi) according to the following reaction:



Two processes convert ADP into ATP: 1) substrate-level phosphorylation; and 2) chemiosmosis. Substrate-level phosphorylation occurs in the cytoplasm when an enzyme attaches a third phosphate to the ADP.

Enzymes in chemiosmotic synthesis are arranged in an electron transport chain that is membrane embedded. In eukaryotes, this membrane is in either the chloroplast or

mitochondrion. According to the chemiosmosis hypothesis proposed by Peter Mitchell in 1961, a special ATP-synthesizing enzyme (ATP synthase) is also located in the membranes. During chemiosmosis in eukaryotes, H^+ ions are pumped across an organelle membrane by membrane "pump proteins" into a confined space (bounded by membranes) that contains numerous hydrogen ions. The energy for the pumping comes from the coupled oxidation-reduction reactions in the electron transport chain. Electrons are passed from one membrane-bound enzyme to another, losing some energy with each transfer (as per the second law of thermodynamics). This "lost" energy allows for the pumping of hydrogen ions against the concentration gradient (there are fewer hydrogen ions outside the confined space than there are inside the confined space). The confined hydrogens cannot pass back through the membrane. Their only exit is through the ATP synthesizing enzyme that is located in the confining membrane. As the hydrogen passes through the ATP synthesizing enzyme, energy from the enzyme is used to attach a third phosphate to ADP, converting it to ATP.

1.5.4.3 ADP:ATP ratio

A fast conversion of ADP to ATP in the mitochondria keeps a high ATP/ADP ratio in the cells. There is much more ATP than ADP in the cell, the ADP is continually converted in ATP to generate a reservoir of potential energy in the form of ATP. The energy required for this conversion is supplied by respiration, which maintains high level of ATP, against the normal chemical equilibrium.

When ATP is hydrolysed to ADP and P_i in physiological condition, ΔG (free energy variation) is between -11 and -13 Kcal/mol. The ΔG depends on the high concentration of ATP if compared to ADP and P_i and it describes how far the reaction is from the equilibrium. When the concentrations of ATP, ADP and P_i are the same (1 mol/l as standard condition), ΔG_0 (standard Gibbs free energy variation) can be just -7.3

Kcal/mole. ΔG_0 depends on the characteristics of the molecules involved. When the concentration of ATP is much lower than ADP and P_i , ΔG is equal to zero, the velocity of hydrolysis of ATP is equal to the velocity of synthesis of ATP from ADP and P_i , the reaction reaches the equilibrium.

In the cell there is an efficient conversion of ADP to ATP, which keeps a very high concentration of ATP, high ATP/ADP ratio and ΔG is very negative.

$$\Delta G = \Delta G_0 + RT \ln \frac{[B]}{[A]}$$

$$\Delta G = \Delta G_0 \text{ when } [B] = [A] \text{ (ln 1 = 0)}$$

In the cell, the very high negative value of ΔG for the hydrolysis of ATP depends on the fact that the cell keeps this reaction ten orders of magnitude above the equilibrium. The equilibrium is reached when the major part of the ATP has been hydrolysed, as occurs in dead cells (Alberts et al., 1995).

1.5.5 Uncoupling and inhibition of oxidative phosphorylation

Oxidative phosphorylation is influenced by different chemical agents, which have been classified into three major classes (Lehninger, 1977):

The uncoupling agents, allow electron transport to continue but prevent the phosphorylation of ADP to ATP. Characteristically they stimulate the rate of oxygen uptake by mitochondria even in the absence of ADP. Moreover, they cause a large amount of ATP-hydrolyzing activity in mitochondria. In the absence of uncoupling agents, mitochondria have very little ATPase activity (Lehninger, 1977). Many different uncoupling agents are known, among these is 2,4-dinitrophenol (DNP). This compound reduces the mitochondrial membrane potential and uncouples oxidative phosphorylation from ATP production by facilitation of proton flux back into the mitochondrial matrix (Loomis and Lipmann, 1948). Carbonyl cyanide p-

[trifluoromethoxy]-phenyl-hydrozone (FCCP) is another uncoupling agent. It acts as an ionophore and uncouples oxidation from phosphorylation by dissipating the chemiosmotic gradient (Mitchell and Moyle, 1967). This action depolarizes the mitochondria (Aronis et al., 2002), thereby inhibiting ATP production (Luo et al., 1997).

Inhibitors of oxidative phosphorylation, they prevent both the stimulation of oxygen consumption by ADP and the phosphorylation of ADP to ATP. They do not directly inhibit any of the electron carriers of the respiratory chain. Instead, they prevent the ATP-forming mechanism from utilizing the high-energy intermediate generated by electron transport. As a consequence, electron transport cannot continue unless the high energy intermediate is used up. Oligomycin is one example of this class. This antibiotic acts by binding ATP synthase hence blocking the proton channel (Grover et al. 2004).

Ionophores are able to dissipate the electric gradient, allowing the entrance of cations such as potassium and sodium, inducing the breakdown of the high energy intermediate state. These agents are called ionophores since they form lipid-soluble complexes with specific cations, which are thus carried through the mitochondria membrane. Antibiotics as valinomycin and gramicidin are known to selectively mediate K^+ and K^+ or Na^+ transport, respectively, in mitochondria. For example, the valinomycin- K^+ complex readily passes through the membrane: in the absence of antibiotic, K^+ passes only very slowly. Valinomycin prevents oxidative phosphorylation because it forces the mitochondria to use the energy of respiration to pump K^+ into the matrix, instead of using the energy to make ATP. The K^+ leaks out as fast as it pumped in, thus dissipating the respiratory energy (Moore and Pressman, 1964).

1.5.6 Evaluation of mitochondria distribution and activity

The mitochondrial membrane potential ($\Delta\Psi_m$) is a key marker of mitochondrial function, generated by the pumping of protons across the inner mitochondrial membrane in association with electron transport. The proton pumping generates an electrochemical gradient, composed of $\Delta\Psi_m$ and ΔpH . The electrochemical gradient is used for ATP synthesis, ADP-ATP exchange, uptake of respiratory substrates and inorganic phosphate, transport of K^+ , Na^+ , and anions to regulate volume, and regulation of protons to control heat production (Bernardi, 1999). Depolarization of $\Delta\Psi_m$ can lead to alterations of intracellular calcium dynamic and to the opening of the mitochondrial permeability transition pore (PTP) (Vergun et al., 1999; Nieminen et al., 1996).

1.5.6.1 Staining of mitochondria on the basis of mitochondrial membrane potential

Conventional mitochondria stains, such as rhodamine 123 and tetramethylrhodamine, are sequestered by functional mitochondria, but are washed out once the mitochondrial membrane potential is lost. A novel cationic carbocyanine dye JC-1, accumulates in mitochondria on the basis of membrane potential. The dye exists as a monomer at low concentrations or low membrane potential and yields green fluorescence, similar to fluorescein. At higher concentrations or higher membrane potential, the dye forms J-aggregates that exhibit a broad excitation spectrum and an emission maximum at ~ 590 nm (Smiley et al., 1991; Reers et al., 1995). These characteristics make JC-1 a sensitive marker for mitochondrial membrane potential (Feldkamp et al., 2005). The ratio of red to green fluorescence of JC-1 is dependent only on membrane potential, and not influenced by mitochondrial size, shape, or density.

Other mitochondrial probes which also stain mitochondria on the basis of membrane potential are the Mitotracker probes. These probes are cell-permeant mitochondrion-selective dyes that contain a mildly thiol-reactive chloromethyl moiety, the

chloromethyl group is responsible for keeping the dye associated with the mitochondria after fixation. Mitotracker passively diffuses across the plasma membrane and accumulates in active mitochondria (Hallap et al. 2005; Agnello et al., 2008).

1.6 Current status of cryopreservation in aquatic species

Cryopreservation of fish gametes is of great importance in aquaculture, conservation of endangered species and in human genomic research. The creation of gamete cryobanks allows the storage of genetic material of targeted species for almost unlimited time periods. Furthermore, cryopreservation has a significant role in aquatic biodiversity, eco-toxicology, and environmental conservation.

Advances in research on cryopreservation of gametes and embryos of aquatic organisms are modest compared with work done in mammals. Some success has been achieved in the cryopreservation of shellfish embryos and early larvae. Bivalves are currently the most studied group. Pacific oyster (*Crassostrea gigas*) embryos have been successfully cryopreserved by slow cooling (Rana et al., 1992; Lin et al., 1993; Chao et al., 1997; and by vitrification (Lin et al., 1993). Pacific oyster eggs have been cryopreserved with up to 50% post-thaw survival using slow cooling and 10% ethylene glycol as cryoprotectant (Tervit et al., 2005). In sea urchin (*Evechinus chloroticus*), although sperm and larvae have been cryopreserved efficiently, the successful cryopreservation of oocytes and fertilized eggs still remain elusive (Adams, 2003). Starfish (*Nardoa variolata*) immature oocytes have not survived cryopreservation by controlled slow cooling to-date, but vitrification has brought some limited success, with 51% of frozen-thawed oocytes which have been able to complete maturation, and a low percentage of these eggs were able to be fertilized (Kaseoglu et al., 2001; Hamaratoglu et al., 2005).

Cryopreservation has been successfully achieved for fish sperm of many species (Rana, 1995; Ranson and Zon, 1999; Lahnsteiner et al., 2000a, 2000b; Rurangwa et

al., 2001), but there has been no success with fish embryos and oocytes. Although few studies reported successful recovery of few embryo following cryopreservation (Zhang et al., 1989), there are no any reproducible cryopreservation protocols. Attempts to cryopreserve zebrafish ovarian follicles have been conducted although low viability has been shown (Plachinta et al., 2007 and also it was accompanied by depletion of ATP levels indicating compromised of the energy machinery suppliers (Guan et al., 2008b).

1.6.1 Difficulties associated with the cryopreservation of fish oocytes

Although oocyte cryopreservation represents an important tool for preserving the female genome, there are many obstacles to fish oocyte cryopreservation, they include: their high chilling sensitivity, especially at subzero temperatures (Isayeva et al., 2004); a much lower surface area to volume ratio of the egg in many species (many fish eggs are greater than 1 mm in diameter), restrictively diffusion of the cryoprotectants and water throughout the cytoplasm; and low membrane permeability, especially for later stages of development (Guan et al. 2008a; Loeffler and Lovestrup, 1970; Isayeva et al., 2004), to water and solutes, including cryoprotectants, when compared to other cell types .

Studies on zebrafish oocyte chilling sensitivity have been done on oocytes at later developmental stages, and have shown them to be very sensitive to chilling. Their survival at low temperatures is influenced by membrane permeability; the developmental stage; exposure temperature; exposure periods and individual females (Isayeva et al. 2004; Pearl and Arav, 2000). Tsai et al (2009) reported that stage I and II ovarian follicles are less sensitive to chilling than stage III follicles. A number of studies have shown that immature oocytes (ovarian follicles) of aquatic species, such as amphibian and teleosts fish, are much more permeable to water and solute than mature eggs (Ecker and Smith, 1971) including data on zebrafish stage III and V ovarian follicles (Seki et al, 2007; Zhang et al., 2005). They are also less hydrated

than mature ovarian follicles (Wallace and Selamn, 1981) which brings benefits for their cryopreservation. However, cryopreservation of immature ovarian follicles has disadvantages when compared to mature eggs as, after thawing, immature ovarian follicles need to be incubated and undergo *in vitro* maturation before to be fertilised. This represents a further limitation as there are no successful protocols for *in vitro* culture of early stages ovarian follicles.

1.6.2 Principle of cryobiology

Cryopreservation is a process by which cells or whole tissue are preserved at low sub-zero temperatures (below -130C), in a state of suspended animation. At this low temperature, no biological activity occurs, as the kinetic energy levels are too low to allow the necessary molecular motion (Grout et al. 1990). The cryopreservation procedure can be divided in two major steps, chilling, which includes a reduction of temperature from physiological temperature to the freezing point, and freezing, which implied a further reduction of temperature to storage temperature. During cooling to freezing temperature and warming to physiological temperature, cells are exposed to many types of injury. Chilling injury and freezing injury are the two major damages that can occur when cells or tissue have been exposed to low temperature. Chilling injury refers to the damage following exposure to low temperature without freezing. Whilst freezing injury is due to solidification of water.

1.6.2.1 Chilling injury

Chilling injury is permanent damage that occurs upon cooling to low but not freezing temperatures. Chilling injury can modify the structure of membranes and, therefore, their integrity (Arav et al., 1996; Zeron et al., 1999). The cell membrane consists of three classes of lipids: phospholipids, glycolipids and steroids (Alberts et al., 2002). It also contains a wide variety of integral membrane proteins. Phospholipids are major components of cellular membranes; the membrane proprieties are influenced by the

length of the fatty acid acyl chain, and the number and positions of the double bonds within the phospholipids (Stubbs and Smith, 1984). The sensitivity and fluidity of the plasma membrane to chilling injury is influenced by high concentrations of cholesterol and polyunsaturated fatty acids (PUFA) (Quinn, 1985; White, 1993). Membrane fluidity depends on the cholesterol level, the phospholipid composition, the degree of unsaturation and the protein content, the membrane composition is used as an indicator of changes in membrane fluidity (Giraud et al., 2000). Temperature has an effect on membrane fluidity due to membrane lipid phase transitions. Lipid in cell membranes would undergo a liquid-to-gel phase transition in the temperature range of 0°C and 20°C, the temperature range of maximum chilling injury. During chilling, lipid phase transitions result in membrane disorganization and membrane leakiness, which can affect cell viability. Another cause of chilling injury is due to denaturation of proteins, due to heat or low temperature (Lattman et al., 1994). As the structure of water molecules and hydrogen bonding becomes more ordered by low temperature treatment, it is thought that the hydrophobic bonds among the side chains of protein molecule are loosened, and consequently, the conformation of the protein molecule changes resulting in denaturation (Tajima and Shimizu, 1973). Chilling can also induce oxidative stress leading to the production of reactive oxygen species (ROS) (McKersie et al., 1990; Scandalios, 1993; Tsang et al., 1991), which can cause protein denaturation, lipid peroxidation and cell apoptosis (Prasad, 1996; Wood and Youle, 1995).

1.6.2.2 Freezing injury

During freezing, the cells are exposed to the mechanical effect of ice crystals forming in the extracellular environment, alterations in the physical properties of the extracellular solution such as concentration of the solution following nucleation phenomena of water, and also to the intracellular freezing (Grout and Morris, 1987). Between -5°C and -15°C, ice forms in the extracellular solution either spontaneously or as a result of “seeding” of ice, but cell content remains unfrozen and supercooled.

The presence of extracellular ice affects the composition of unfrozen fraction of the extracellular solution, leading to an increase of solute concentration and to a growth of the ice phase. This results in an imbalance between the cell and the unfrozen extracellular solution. The increased osmotic pressure in the extracellular space creates an osmotic gradient across the cell's plasma membrane, which results in water flowing out of the cells and freezing externally (Mazur, 1963; Mazur et al., 1984). If the cooling is slow enough, the cells lose water rapidly enough through the semipermeable plasma membrane to concentrate the intracellular solute, eliminating supercooling and maintaining the equilibrium of the chemical potential between the intracellular and the extracellular water. As a result, the cell dehydrates and does not freeze. If cooling is too rapid, the rate at which the chemical potential in the extracellular solution decreases is faster than the rate at which water can diffuse out of the cell and results in intracellular ice formation, which is lethal to cells (Mazur, 2004). If the cooling rate is too slow, the cells will be exposed to a hypertonic condition in the residual liquid fraction for a sufficient long period to experience damage before reaching the ultra-low temperature used for storage. This has been called solution effects injury (Mazur, 1970). The solution effects injury have not been satisfactorily demonstrated (Watson and Fuller, 2001), different aspects of this event could be considered: high salt concentration, the physical relationship between the cells and the surrounding ice matrix, pH, fluctuations with temperature and concentration of buffers, the physical reduction in liquid space compacting the cells.

1.6.2.3 Controlled slow cooling and vitrification

A major factor determining whether or not cells survive freezing to low subzero temperatures is the rate at which they are cooled. The controlled slow-cooling procedure is characterised by the addition of molar concentration of cryoprotectants (CPA) to the cell suspension and by the use of a controlled freezing to the storage temperature. There are several crucial parameters that needed to be considered, such as the cooling rate, ice seeding temperature, liquid nitrogen plunging temperature,

thawing protocol, removal of cryoprotectants and post-thawing handling. Cooling rate is one of the major factors which affects cell survival. Different types of cells have different optimal cooling rates (Konc et al., 2005; Eriksson et al., 2001). The size of the cells and their membrane permeability to water and cryoprotective agents influence the optimal cooling rate. Ice seeding is often used in controlled slow cooling procedures for artificially initiating the controlled formation of extracellular ice to decrease the incidence of intracellular ice formation and increase the cells survival rate. During cryopreservation, the process of thawing is as important as that of cooling. The effects of thawing rates are influenced by the prior rate of cooling, whether the prior rate of cooling has been high enough to induce intracellular freezing or low enough to produce cell dehydration. Although high cooling rates lead to intracellular ice formation, the ice crystals tend to be small. Small crystals have higher surface free energies than larger crystals due to their small radii of curvature, and because of this higher free energy they tend to recrystallize or fuse together to form larger crystals. The extent of such phenomenon depends on temperature and time. Consequently, recrystallization is enhanced when warming is slow and it is suppressed when warming is rapid. The enlargement of the ice crystals formed by recrystallization is damaging, probably because it disrupts intracellular membranes (Farrant et al. 1977). Whilst if the cells are cooled slowly enough avoiding intracellular freezing, the response to warming rate is highly variable depending also on the cell type (Mazur, 2004). After thawing, cells are exposed to hypotonic solutions, which may be damaging to the post-thawed cells, especially to osmotically sensitive cells. Therefore dilution of cryoprotective agents needs to be carried out in a controlled manner (Wessel and Ball, 2004).

Vitrification is the solidification of a liquid in a glass-like state by an extreme elevation of viscosity during cooling. During vitrification the molecular motions are arrested and there is no ice crystal formation or solution effect injury. However, vitrification requires the optimisation of several steps, such as the concentration and composition of vitrification solution, procedures to equilibrate the cells in the

solution, cooling and warming rates and procedures to dilute the vitrification solution from the cells (Rall, 1987). Vitrification requires rapid cooling rates. Vitrification of water inside cells can be achieved only when an extremely rapid rate of cooling is reached and high concentrations of cryoprotectants diffuse into cells, which increase viscosity and depress the freezing temperature inside cells. When the solution is rapidly cooled and formed into a glass during vitrification, the entire solution contains no ice crystals (Fahy, 1986b). Vitrification has been used for cryopreservation of different cells type, among these human oocytes, embryos and blastocyst (Liebermann et al., 2003), goat and bovine oocytes (Begin et al., 2003; Dinnyes et al., 2000).

1.6.3 Cryoprotectants

Cryoprotectants (CPAs) are substances characterised by their ability to reduce cryoinjury of biological materials during the course of freezing. Cryoprotectants have been divided in two categories: permeating and non-permeating CPA. Permeating CPAs such as methanol, dimethyl sulfoxide (DMSO), ethylene glycol (EG) and propylene glycol (PG) are low-molecular weight substances that penetrate cell membranes. Non-permeating CPAs such as various sugars, hydroxyethyl starch and polyvinyl pyrrolidone, are high-molecular weigh agents which cannot penetrate the cells. These two groups of CPAs behave in different ways during cooling and thawing.

Penetrating CPAs have an effect on the freezing point, their presence lowers salt concentration normally found in physiological solution, which reduces the solute-effect injury, they lower the amount of ice (Mazur et. 1984; Woods et al., 1999). Their presence results in cells osmotic dehydration leading to a decreasing of the amount of intracellular ice formation. When cryoprotective agents diffuse into cells, they displace a certain amount of water and form hydrogen bonds with biological molecules, such as protein, RNA and DNA. Hydrogen bonding in aqueous solutions

is very important for the function of the biological molecules, as the biological molecules can keep their functional structure, and the cryoprotective agents can form strong hydrogen bonds with numerous substances in the cytoplasm. Therefore, this can increase cytoplasm stability and influence the emergence and growth of ice. Cryoprotective agents can provide osmotic buffering for the cells during freezing and thawing by acting as a secondary solvent for salts (Pegg, 1984).

Non-penetrating CPAs dehydrate the cell before cooling, reducing the amount of water that cells need to lose to remain close to osmotic equilibrium during freezing. They stabilize both proteins and membranes during freezing (Nounou et al., 2005) by formation of interactions with the phospholipids, through hydrogen bonding between hydroxyl groups of the sugars molecules with the phosphate moiety of the phospholipids in the membrane. They can also have an effect as inhibitors on ice growth during freezing and thawing, as they can influence the size and form of ice crystal to decrease the damage to membranes. Trehalose and sucrose can inhibit ice crystal growth (Nicolajsen and Hvidt, 1994).

Unfortunately, CPAs can be toxic for cells, and it is important to determine the effect of cryoprotectants on oocytes as the first step in freezing protocol design. Cryoprotectants should have low toxicity. DMSO is the most widely used CPA and has been used in the cryopreservation of a wide range of cell types, tissue and organs. Methanol has been shown to be the most effective CPA for zebrafish embryo (Zhang et al., 1993) and sperm of several fish species (Lahnsteiner et al., 2000a, 2000b). EG promotes small-granular crystallisation and amorphous solidification due to its high viscosity at low temperatures. It also reduces the quantity of unbound water within the cell, therefore suppressing intracellular ice formation. Glucose together with sucrose are widely used as extracellular cryoprotectants, often in combination with permeating cryoprotectants. They induce dehydration and osmotic shrinkage of the cells, therefore lowering the risk of intracellular ice crystallisation. Glucose was also

found to be a membrane-stabilising agent, binding to lipids and proteins of the bilayer, stabilising it against compression (King et al., 1993, Suzuki et al., 1996).

1.6.3.1 CPAs toxicity

All known CPAs, despite their protective proprieties, can have a toxic effect on biological materials (Fahy, 1986a). Methanol and DMSO are both penetrating cryoprotectants which exert their effect by replacing the free intracellular water, although other actions such as positive effect on protein stabilization have been proposed (Tajima and Shimizu, 1973; Penninckx et al., 1983; Van der Elst et al., 1988). It is also know that cryoprotectants may cause of damage to the meiotic spindle, cytoskeleton, membranes and zona pellucida.

The toxicity of methanol (Fahy, 1986a) is linked to the action of the cellular enzyme alcohol dehydrogenase (ADH), which converts methanol to toxic formaldehyde. Formaldehyde is an extremely strong denaturant agent due to its high chemical activity. It forms abnormal cross linkages between molecules of proteins and lipids, irreversibly inhibiting their normal functioning. Methanol is first oxidized to formaldehyde, which is further oxidized to formic acid very rapidly. Since most investigations have not been able to demonstrate even traces of formaldehyde in the organs during oxidation of methanol (Roe,1955), the toxicity of methanol is attributable to its metabolite, formic acid, which is responsible for the metabolic acidosis and visual toxicity observed in human methanol poisoning (Seme et al., 2001). Formic acid has been hypothesized to produce retinal and optical nerve toxicity by disrupting mitochondrial energy production. It has been reported that formate inhibits the activity of cytochrome oxidase, the terminal electron acceptor of mitochondrial electron transport chain involved in ATP synthesis. Inhibition occurs subsequent to the binding of formic acid to the ferric heme iron in cytochrome oxidase, with inhibition constants between 5 and 300 Mm. Additional *in vitro* studies in isolated mitochondria and cultured neuronal cells have shown that formate inhibits mitochondrial ATP synthesis and decreases cellular ATP content. These studies

document formate-induced depletion of retinal ATP and ADP and a corresponding increase in retinal AMP after methanol intoxication. These findings strongly support the hypothesis the formate inhibits mitochondrial energy metabolism and oxidative phosphorylation in methanol intoxication and are consistent with the documented actions of formate in isolated mitochondria (Seme et al., 2001).

Unconverted methanol can also have a damaging effect on cell structures. Methanol and other alcohols have been demonstrated to interact with phospholipids to destabilise the lipid bilayers of artificial membranes. Short chain alcohols, such as methanol and ethanol, interact more directly with the polar head group of lipids in bilayers due to their low hydrophobicity. However, the short non polar region of the alcohol can create voids between the lipid chains in the membrane interior and introduce instability within the bilayer. At high concentrations, methanol renders the cell membrane unstable resulting in lipid phase transition: lipids acyl-chains from opposing monolayers are shifted from their normal opposite-facing orientation to an interspersed arrangement that exposes the ends of the hydrophobic tails.

The toxic effect of DMSO on cells has been linked to labilisation of membranes and denaturation of proteins (Henderson et al., 1975). DMSO can also increase the concentration of calcium ions in cytoplasm, causing a variety of chronic negative metabolic responses such as cytoskeleton depolymerisation and reassembly (Yamamoto, 1989). DMSO may also affect RNA splicing (Bolduc et al., 2001), lipid, protein and DNA synthesis (Nilsson, 1980). DMSO penetrates membranes much more slowly than water, resulting in rapid plasmolysis as water exits cells during its addition to the cells, and swelling when DMSO is removed from extracellular medium after thawing. Therefore, osmotic stresses may aggravate the toxicity of dimethyl sulfoxide. Karran and Legge (1996) proposed an alternative explanation for some of the damages; they identified the presence of formaldehyde in the cryoprotectant solution containing DMSO, providing an alternative mechanism for cellular damage. The formaldehyde could be formed via a non-enzymatic reaction

taking place in the solvent and the cryoprotectant solution. This hypothesis was also supported by Klein et al. (1981), they demonstrated that formaldehyde can form in DMSO via hydroxyl-mediated non-enzymatic reaction creating a methoxyl radical species which subsequently forms formaldehyde.

EG has been suggested to have a destabilising effect on protein secondary structure, causing unfolding of alpha-helices (Arakawa et al., 1990). Moreover, due to the action of enzyme alcohol dehydrogenase, EG inside the cells may be converted to a number of highly toxic derivatives, such as glycolic acids and salts of oxalic acid. Metabolites of EG suppress oxidative phosphorylation, inhibit sulfhydryl-group-containing enzymes, inhibit protein synthesis and cause severe acidification of cytoplasm.

The cell damaging effects of non- penetrating compounds, such as sucrose, are mainly osmotic. Cell shrinkage due to water loss induced by presence of non penetrating CPAs results in undesired changes of the plasma membrane, which may include lateral separation of membrane lipids, lipid phase transitions, formation of protein clusters, speculation and vesiculation of plasmatic membrane (Meryman, 1971).

1.7 The present study

1.7.1 Relevance of the research to society

Development of methods to assess ovarian follicle viability/quality has a significant role in assisting progress of cryopreservation. The assessment of ovarian follicles is an important step before and following the cryopreservation procedure, allowing the preservation of good quality material and also the investigation of possible effects of cryopreservation.

Cryopreservation of gametes offers a promising method to preserve fish genetic material, which is of great importance in preserving species diversity, aquaculture, and managing fish models used in biomedical research.

Fish population are globally threatened due to overfishing and pollution. More than 65% of the European fish species are threatened (Kirchofer, 1996) and worldwide the number of species listed as endangered is growing rapidly. Cryopreservation of germoplasm is a good *ex situ* strategy to conserve rare or important genetic material for future use, but it also has other important applications.

The use of cryopreserved gametes in aquaculture is growing. With cryopreservation, the genes from selectively brood stock individuals can be stored, well beyond the lifetime of the donor. Once frozen, the gametes can be transported great distances in the frozen state without loss of fertilization success. Gametes preservation would help in genetic selection programmes, by providing easy access to a reserve of genetic material of known and desired qualities.

Fish gametes play also an important role in human genome studies. The small size of fish genomes make them easier for sequencing, and an ideal model for studies on vertebrate development and human diseases (Barbazuk et al., 2000; Brownlie et al.,

1998). Cryopreservation of fish gametes will be of benefit of embryological and molecular biological studies.

1.7.2 The selection of subject material for this study

The majority of the studies on oocyte cryopreservation have been conducted in mammals with oocytes at the metaphase II (MII) stage. Stage III zebrafish ovarian follicle are used in this study. Stage III zebrafish oocyte is at the germinal vesicle (GV) stage and is considered to be more resistant to freezing and thawing than later stages (stage V). During GV stage, the GV chromatin is protected by a nuclear envelope, microtubules are depolymerised and thecal and follicle cells protect the oocyte from rapid influx or efflux of cryoprotectants. However, several authors have reported that cryopreservation can be detrimental to the functionality of cumulus-oocyte communication in mouse (Ruppert-Lingham et al, 2003, 2006), cow (Modina et al 2004) and porcine oocytes (Wu et al., 2006). Communication between follicle cells and oocyte permits the transfer of small molecules, such as nutrients and signaling molecules for oocyte growth as well as nuclear and cytoplasmic maturation *in vitro* after hormonal stimulation (Comizzoli et al. 2003; Luvoni et al. 2006; Luciano et al. 2004).

Seki et al. (2007) suggested that immature zebrafish oocytes would be more suitable for cryopreservation, as their permeability to water and to CPAs such as EG, propylene glycol and *dymetil* sulfoxide (DMSO) at 25°C was substantially higher than that of mature oocytes (stage V). In terms of permeability, EG and DMSO would be more suitable for cryopreservation than glycerol and PG as the authors showed that EG and DMSO permeate more efficiently than other cryoprotectants. Furthermore, Zhang et al. (2005) showed that the membrane permeability of stage III oocytes decreased significantly with temperature. No significant changes in cell volume during methanol treatment were observed. Membrane permeability parameters values obtained for stage III zebrafish oocytes were generally lower than those obtained

from other aquatic invertebrates and higher than those obtained with fish embryos (Zhang and Rawson, 1998). Plachinta et al. (2004a) also reported that the sensitivity of oocyte to cryoprotectants appeared to increase with the developmental stage with stage V oocytes being the most sensitive.

1.7.3 The aims and the approaches of this study

The present study aimed to develop new methods for assessing the viability and the quality of zebrafish ovarian follicles and in particular to investigate the possible potential use of mitochondria as markers for ovarian follicle quality. The methods developed were then applied to study the impact of cryoprotectant and/or cryopreservation procedures. The study can be divided into three main parts.

Part I. To develop a new vital staining assay for assessing zebrafish ovarian follicle viability. Fluorochromic markers, previously used in mammalian cells, have been investigated in zebrafish ovarian follicles. The results are presented in Chapter 3.

Part II. To investigate mitochondrial activity and distribution in zebrafish ovarian follicles with a view to their use as markers for ovarian follicle quality. Mitochondrial activity and distribution were investigated using confocal microscopy and mitochondrial probes. Scanning and Transmission Electron Microscopy studies of ovarian follicle structure were also undertaken to verify the results obtained by confocal microscopy. In addition, the electron microscopy studies were also used to evaluate differences between mechanical and enzymatic methods for separation of ovarian follicles from ovaries. The results are presented in Chapters 4 and 5.

Part III. To determine whether mitochondrial activity and distribution can be markers for ovarian follicle quality. The impact of CPAs exposure on structural and functional integrity of mitochondrial in stage III ovarian follicle, as a prerequisite to formulating a successful cryopreservation protocol, was investigated. Specifically, the effect of

CPAs exposure on mitochondria distribution, membrane potential, ATP levels and mtDNA copy number was examined. Results of this study are presented in Chapter 6.

Chapter 2: Material and methods

2.1 Introduction

Three main areas of study were carried out in the project: (i) development of a new method for assessing zebrafish ovarian follicles viability; (ii) investigation of mitochondrial activity and distribution in stage III zebrafish ovarian follicles with the view to their use as markers for ovarian follicle quality. Mitochondrial activity and distribution were investigated using confocal microscopy and mitochondrial probes, also including determination of cell ATP levels. The structure of stage III ovarian follicle and mitochondrial distribution were also evaluated using scanning electron microscopy (SEM) and transmission electron microscopy (TEM); (iii) studies on the effect of cryoprotectants on mitochondrial activity and distribution in zebrafish ovarian follicles, including determination of mtDNA copy number and ADP/ATP ratio. All experiments were carried out in the laboratories at the Institute of Research in the Applied Natural Sciences (LIRANS), University of Bedfordshire, except for the SEM, TEM and confocal microscopy studies, which were carried out at the Centre for Bioimaging, Plant Pathogen and Microbiology Department, Rothamsted Research, Harpenden, UK.

2.2 General methods

2.2.1 Maintenance of zebrafish (*Danio rerio*)

2.2.1.1 Zebrafish (*Danio rerio*) care

Adult zebrafish (*Danio rerio*) 12-14 weeks old were obtained from Aquascape Ltd (Birmingham, UK). They were maintained in 45 l (28x28x58 cm) glass fish tanks at 28 °C with approximately 40 fish per tank. Tanks were cleaned by siphoning debris from the bottom and one third of the tank water was replaced once per week. Tap

water aged at least for 2 days was used as tank water; alternatively tank water was made up from deionised water by adding 2.5 g of sea salt per 10 l of water. The tanks were constantly aerated. Filtration of the water in the tanks was carried out using an electric pump connected to an upturned funnel which was surrounded by filter floss in a beaker (1 l) immersed in the fish tank. The funnel and floss were held in position by a layer of smooth gravel. Water was pulled through the gravel and floss by the suction effect generated by the rising air. Fish were fed three times per day, twice with dry flake food Tetra Brand (ingredients: fish and fish derivatives, cereals, yeast, vegetable protein extracts, molluscs and crustaceans, oils and fats, derivatives of vegetable origin, algae, various sugars contains EEC permitted colorants) and once with live food: Premium Grade brine shrimp (*Artemia salina*) (ZM Fish Food and Fishroom Equipment, Winchester, UK). Brine shrimp cysts were approximately 200 µm in diameter and newly hatched brine shrimp measured approximately 500 µm.

2.2.1.2 Separation of stage III ovarian follicle from ovarian masses

Stage III ovarian follicles used in this study were obtained from zebrafish on a regular basis, without any hormonal treatment to induce oocyte maturation.

2.2.1.2.1 Mechanical method

To obtain oocytes, gravid female zebrafish were anaesthetised with a lethal dose of tricaine (0.6 mg/ml) for 5min and decapitated before the ovaries were removed. The ovaries were gently placed immediately into a Petri dish containing Hanks' solution (246mOsm, pH 8.2) (0.137M NaCl, 5.4mM KCl, 0.25mM Na₂HPO₄, 0.44mM KH₂PO₄, 1.3mM CaCl₂, 1mM MgSO₄, 4.2mM NaHCO₃) at 22°C. Ovarian follicles were separated manually using forceps (Plachinta, 2007), and stage III ovarian follicles selected.

2.2.1.2.2 Enzymatic method

To collect follicles, adult female zebrafish (*Danio rerio*) were anaesthetized with a lethal dose of tricaine (0.6mg/ml) for 5 min and decapitated before the ovaries were removed. The ovaries were immersed in 1.6mg/ml hyaluronidase (Guan et al. 2008a) made up in either Hanks' solution, KCl buffer (55mM KCl, 55mM C₂H₃O₂K, 1mM MgCl₂, 2 mM CaCl₂, 10mM HEPES; pH 7.4) or 50% Leibovitz L-15 medium for 10 min at room temperature. Follicles were separated by gentle pipetting, and then washed three times in Hanks' solution, KCl buffer or 50% Leibovitz L-15 and stage III follicles selected.

2.2.2. Chemicals

Information on the chemicals used in this study is listed in Table 2.1. Fresh aqueous solutions were prepared with deionised water shortly before use.

Table 2.1 Chemicals

Chemical	Source	Product No.
Acetone	Aldrich	179973
Adenosine	Sigma	A9251
ADP	Sigma	A2754
ApoSENSOR™ ADP/ATP Ratio Assay Kit	BioVision	K254-200
ATP analysis kit	Sigma	FL-AA
CaCl ₂	Aldrich	22,231-3
Choline chloride	Sigma	C1879
C ₂ H ₃ O ₂ K	Sigma	P1190
DHP (17(, 20(-dihydroxy-4-pregnen-3-one)	Sigma	P6285

Dimethyl sulfoxide (DMSO)	Sigma-Aldrich	154938
EDTA	BDH	16079
Ethanol	Sigma	R8382
Ethidium bromide	Sigma	E1510
Ethylene glycol	BDH	10324
FCCP	Sigma	C2920
Fluorescein diacetate	Sigma	F7378
Formaldehyde	Sigma	F1635
Formvar	Agar Scientific	R1201
Gentamicin	Sigma	G1272
Glucose	Sigma	G5767
Glutaraldehyde	TAAB	G002/1
HCl	Aldrich	31,894-9
HClO ₄	Aldrich	24,425-2
HEPES	Sigma	H3375
Hyaluronidase	Sigma	H2126
JC-1	Fluka	40882
KCl	Sigma	P3911
KH ₂ PO ₄	BDH	10203
KOH	Aldrich	22,147-3
Lead Citrate	Agar Scientific	R1210
Leibovitz (L15) cell medium pre-mixed powder	Sigma	L4386
Methanol	Sigma	M3641
MgSO ₄	BDH	10151
MitoTracker Green FM	Molecular Probe	M-7514
Na ₂ HPO ₄	Sigma	S9390
NaOH	Sigma	S2770

NaCl	Aldrich	43,320-9
NaHCO ₃	BDH	10247
Oligomycin	Fluka	75352
Osmium Tetroxide	TAAB	O001
Paraformaldehyde	Sigma-Aldrich	158127
Propidium Iodide	Sigma	P4170
Sea salt	ZM Ltd	
Spurr's Epoxy resin	TAAB	ERL 4206
Tricaine	Sigma	A5040
Tris acetate-EDTA (TAE)	Sigma	T4038
Triton X-100	Aldrich	234729
Trypan blue	Sigma	T8154
Uranyl Acetate	BDH Chemicals	100504-336

2.2.3. Data analysis

2.2.3.1. Experimental design and statistical analysis

One-way ANOVA test was used to examine the differences between different treatments ($p < 0.05$). If significant differences were shown, least significant difference (LSD) or Tukey's tests were used post hoc to determine pairwise differences between treatments ($p < 0.05$). The fit of the model with the data was checked with a normality test. Homogeneity of variance was confirmed to determine whether ANOVA assumptions were valid. When two groups were compared, results were analyzed using Student's t-tests ($p < 0.05$). All statistical analysis was carried out using SPSS (SPSS for Windows Version 12.01) and Microsoft Excel.

2.3 Development of new assay for zebrafish oocytes viability using vital stains

Following the studies on the efficacy of the FDA, PI and FDA-PI methods, FDA-PI (fluorescein diacetate-propidium iodide) staining was compared with TB (Trypan blue) staining and GVBD (Germinal vesicle breakdown) test in a series of cryoprotectant (CPA) toxicity tests in different media commonly used with zebrafish follicles – Hanks' solution, KCl buffer and Leibovitz L-15. The GVBD test was only carried out when the Leibovitz L-15 was used as the medium is commonly used for zebrafish *in vitro* maturation. The FDA-PI test was also used, in comparison with TB, to assess ovarian follicle viability following cryopreservation. The optimum cryoprotective media and cooling rates for stage III zebrafish follicles that were previously identified in this laboratory were used (Guan et al., 2008b; Plachinta et al., 2004b).

2.3.1. FDA-PI staining and fluorescence microscopy

For FDA-PI staining, a stock solution of FDA was prepared by dissolving 5 mg FDA in 1 ml of acetone. The FDA working solution was freshly prepared before use by adding 40 μ l of stock to 10 ml of PBS. The propidium iodide stock solution was made by dissolving 1 mg PI in 50 ml PBS. For FDA-PI staining, 100 μ l (2 μ g) of FDA working solution and 30 μ l (0.6 μ g) of PI stock solution were added directly to the follicles. The follicles were stained in the dark for 3 min (Jones and Senft, 1985). The non-polar fluorescein-diacetate molecules enter the cell, and are hydrolyzed by cellular esterases to produce the polar compound fluorescein. In viable cells, the fluorescein is unable to pass through the intact membrane, accumulating in the cytoplasm of the cell, whilst damaged cells show a distinct loss of fluorescein through the cell membrane. Live cells with intact membranes are distinguished by their ability to exclude the PI that easily penetrates dead or damaged cells, intercalating with DNA and RNA to form bright red fluorescence. Follicles fluorescing bright green were considered to be viable, while nonviable cells stained bright red. FDA-PI

stained follicles were examined with a fluorescence microscope (LEICA DM IL) with two filter cubes: I3 (excitation filter: bandpass (BP) 450-490 nm; dichromatic mirror: 510; suppression filter: longpass (LP) 515) and N.2.1 filter excitation filters: BP: 515-560 nm; dichromatic mirror: 580; suppression filter: LP: 590). This filter arrangement did not permit both green and red fluorescing follicles to be seen simultaneously. At least 90 ovarian follicles in each group were assessed in three repeated experiments.

2.3.2 Application of FDA-PI

2.3.2.1 Controls

Two controls were required in order to assess the reliability of FDA and PI stains and the combination of these two fluorochromes, a negative control was established by exposing ovarian follicles to 99% methanol for 10 min at 22°C, while follicles for the untreated control were held in Hanks' solution or KCl buffer. Follicle viability of control and treated groups were assessed by FDA and PI alone, and in combination (FDA-PI).

2.3.2.2 Comparisons of FDA-PI with other viability assessment methods after follicle isolation

The FDA-PI test was subsequently compared with two other viability assessment methods routinely used in this laboratory, the Trypan blue (TB) and germinal vesicle breakdown (GVBD) tests. The viability of ovarian follicles was assessed both immediately after follicle separation from the ovaries and after 30 min in L-15 medium at room temperature.

2.3.2.3 Comparisons of FDA-PI, TB and GVBD in cryoprotective agents (CPAs) toxicity tests

Follicles were exposed to 3 different cryoprotectants (CPAs), ethylene glycol (EG), methanol or DMSO in the concentration range of 1 to 4M (made up in Hanks', KCl buffer or 50% Leibovitz L-15 medium) for 30 min at 22°C. Control follicles were incubated in the corresponding CPA-free medium under the same conditions. For the assessment of CPA on ovarian follicle viability, 15-40 follicles were exposed to CPA supplemented medium. After incubation in CPAs for 30 min at 22°C, follicles were washed twice with bathing media and viability tests were conducted. Hanks' solution and KCl buffer were used for TB and FDA+PI tests, whilst 50% L-15 medium was used for TB, FDA+PI and GVBD tests. L-15 was used to carry out GVBD test as it is the medium commonly used for *in vitro* maturation.

2.3.2.4 Comparisons of FDA-PI and TB following cryopreservation procedure

The optimal CPA media and cooling protocol for stage III zebrafish follicles previously identified in this laboratory (Guan et al. 2008b; Plachinta et al., 2007) were used in this study. Solutions of the CPAs (4M Methanol in combination with 0.2 M glucose) were made up in KCl buffer or Hanks' solution. After 30 min incubation in CPAs solution, follicles were loaded into 0.5 ml plastic straws and put into a programmable cooler (Planer KRYO 550). The following cooling protocol was used: cooling at 2°C/min from 20°C to -12.5°C (seeding temperature), manual seeding and hold for 5 min, freezing from -12.5°C to -40°C at 0.3°C/min, from -40°C to -80°C at 10°C/min and from -80 to -160°C at 50°C/min, samples were then plunged in liquid nitrogen (LN₂) at -196°C and held in LN₂ for at least 10 min. Samples were thawed using a water bath at 27°C. Cryoprotectants were removed in 4 steps (2M, 1M and 0.5M methanol in Hanks' solution or KCl buffer, 2.5 min for each step); the samples were then transferred to Hanks' solution or KCl buffer. Viability was assessed by FDA-PI and TB tests.

2.3.3 Other viability assays

2.3.3.1 Ovarian follicle staining by Trypan Blue

TB was used to assess membrane integrity. Follicles were incubated in 0.2% of Trypan Blue for 3-5 min at room temperature and then washed in Hanks' solution, KCl buffer or L15 medium. Unstained follicles were considered viable, the follicles stained blue were considered non-viable. At least 90 ovarian follicles in each group were assessed in three repeated experiments.

2.3.3.2 Observation of Germinal Vesicle Breakdown (GVBD)

Examination of the physiological event of GVBD involved the incubation of stage III follicles in 50% L15 medium supplemented with 100 ng/ml DHP (17 α -Hydroxy-20 β dihydroprogesterone) for 24h at 25°C. Prematurational follicles are opaque but become translucent following GVBD. Follicles that did not undergo maturation and germinal vesicle breakdown remained opaque.

2.4 Observation of mitochondrial distribution and activity in stage III ovarian follicles

In this study, investigations of mitochondrial activity and distribution in stage III zebrafish ovarian follicle under normal physiological conditions were carried out. Confocal microscopy and two mitochondrial fluorescent probes were used. In order to verify that the staining obtained by confocal microscopy was specific for mitochondria, the effects of mitochondrial inhibitors on staining patterns were investigated. Furthermore, the ATP levels of the ovarian follicles were measured following the exposure to the inhibitors to see whether the maintenance of mitochondrial organisation within the ovarian follicle was an ATP-dependent process.

2.4.1. Staining of Mitochondria

Stage III ovarian follicles were stained with JC-1. A 1.5 mM stock solution of the dye was prepared in DMSO according to the manufacturer's instructions. JC-1 stains mitochondria with low membrane potential green and mitochondria with high membrane potential red. The dye was used at a concentration of 5 μ M in Hanks' solution for 30 min at room temperature. Subsequently the follicles were washed three times with Hanks' solution, transferred into a 35 mm glass bottom dish and were observed by confocal microscopy. For MitoTracker[®] Green FM staining, a 1 mM stock solution of the dye was prepared in DMSO. The dye was used at a concentration of 5 μ M in Hanks' solution for 30 min at room temperature. Subsequently the follicles were washed three times with Hanks' solution, transferred into a 35 mm glass bottom dish (WillCo Wells) and analysed by confocal microscopy.

2.4.1.1 Confocal microscopy

Stained samples were examined using a Leica TCS-SP/DM IRBE (Leica, Microsystems (UK) Ltd, Milton Keynes, Bucks, UK) confocal microscope equipped with Ar/Kr laser. Active mitochondria distribution was assessed through a series of optical sections. Objectives (20X, 40X and 63X water immersion), pinhole, filters, gain and offset were kept constant throughout the experiments. Laser excitation and emission filters for the different labelled dyes were as follows: JC-1 FM: λ_{ex} =488 nm (excitation), (green) λ_{em} =510/550 nm (emission), red) λ_{em} =580/610 nm (emission), MitoTracker[®] Green FM λ_{ex} =488 nm (excitation), λ_{em} =500/600 nm (emission). Digital images were obtained with Leica TCS software and stored in TIFF format. The TIFF images were processed with Adobe PhotoShop (V7). At least 30 samples in each group were analysed in three repeated experiments.

2.4.1.2. Mitochondria inhibitors

The follicles were exposed to 5 and 50 μ M of p-trifluoromethoxy carbonyl cyanide phenyl hydrazone (FCCP) for 15 min at room temperature following a treatment of permeabilisation with 0.01% (v/v) Triton X-100 for 15 min. Triton X-100 was used as a permeabiliser to allow the entrance of FCCP in the ovarian follicle. For the oligomycin exposure, ovarian follicles were exposed to 100 μ M oligomycin for 15 or 30 min at room temperature following a treatment with 0.01% (v/v) Triton X-100 for 15 min.

2.4.2 Assessment of ATP level

ATP is a vital substance, the main transporting agent of energy inside the living cells. The presence of ATP in the oocyte is essential for their survival, normal development and reproduction potential. ATP content in the cell is a reliable parameter for evaluation of viability of different types of cells, including fish sperm cells (Perchec et al. 1995) and fish oocytes (Boulekbache et al., 1989; Wendling et al., 2004). ATP content of zebrafish ovarian follicles was evaluated using the commercially available ATP Bioluminescent Assay Kit (FL-AA, Sigma). The protocol is based on reaction of the luciferin protein with ATP, catalysed by the enzyme luciferase. The product of this reaction, adenylyl-luciferin, is oxidized with emission of light within the optical range (λ_{\max} = 560).

2.4.2.1 Preparation of extracts from ovarian follicles

Follicles from control groups and follicles exposed to different conditions such as mitochondrial inhibitors (FCCP and Oligomycin), with or without pre-exposure to Triton X-100, were used for the preparation of extracts for ATP determination. In all experiments, three replicates were used for each treatment and experiments were repeated three times. The following procedure was used for extract preparation: 30

stage III zebrafish ovarian follicles were added to 1 ml of ice cold 0.5 M perchloric acid + 4 mM EDTA and homogenized with a conical glass pestle. The homogenate was centrifuged at 20,000 g for 5 min at 0-2 °C in a refrigerated centrifuge. Supernatant was separated and neutralised with 2.5 M KOH to adjust the pH to 7-6, centrifuged for 5 min at 8000 g and the supernatant collected. This extract was loaded into an Eppendorf tube and stored at -20 °C until ATP determination.

2.4.2.2 Preparation of FL-AA reagent

FL-AAM (ATP Assay Mix): The contents of one vial of Assay Mix ATP ASSAY MIX (a lyophilized powder containing luciferase, luciferin, MgSO₄, DTT, EDTA, bovine serum albumin and tricine buffer salts) was dissolved in 5 ml of sterile deionised water to generate a stock solution with pH 7.8. This stock solution could be stored at 0-5 °C up to 2 weeks. Immediately before experiments, FL-AMM solution was diluted with FL-AAB (ATP Assay Mix Dilution Buffer) a 25-fold dilution can be used for ATP concentrations of 2×10^{-10} to 2×10^{-7} mol/l.

FL-AAB (ATP Assay Mix Dilution Buffer): Contents of one vial of FL-AAB (lyophilizes powder containing MgSO₄, DTT, EDTA, bovine serum albumin and tricine buffer salts) was dissolved in 50 ml of sterile deionised water. This solution could be stored for 2 weeks at 0-5 °C.

FL-AAS (ATP Standard): One vial of FL-AAS contains approx. 1 mg (2.0×10^{-6} mole) of ATP. Solutions of ATP were made in sterile deionised water. Solutions are stable for 2 weeks when stored at -20°C, or up to 24 hours at 0-5 °C. A number of solutions of decreasing ATP concentration were prepared in sterile deionised water: 2×10^{-5} , 2×10^{-6} , 2×10^{-7} , 2×10^{-8} , 2×10^{-9} , 2×10^{-10} , 2×10^{-11} and 2×10^{-12} M. A calibration curve was established from the fluorescence measurements emitted during reaction with FL-AAM.

2.4.2.3 Determination of ATP level

0.1 ml of ATP Assay Mix solution was added to a reaction vial, gently swirled and left to stand at room temperature for approximately 3 min before 0.1 ml of sample was added. The mixture was then swirled quickly and light emitted was immediately measured with a luminometer. To determine the amount of background light produced, 0.1 ml of deionised water was added to 0.01 ml of ATP Assay Mix solution, the mixture was swirled and the luminescence measured. The value obtained was subtracted from that of the samples. The final value was proportional to the amount of ATP in the sample. A calibration curve was established from different dilutions of FL-AAS (ATP Standard), and this curve was used for determining concentrations of ATP in the samples. ATP content of ovarian follicles was measured using the luciferin – luciferase bioluminescence assay provided by a FL-AA kit. A luminometer (TD-20/20 Luminometer – Turner Designs) was used for all measurements. Background light was measured and subtracted by running an appropriate blank. As directed by the manufacturer’s assay instructions (Sigma-AI), a fresh calibration curve was constructed for each assay. The curve was constructed by plotting the log of relative luminescence intensity (RLI) against the log of ATP concentration (moles/l) using a serial dilution of an ATP standard. The “least square” method was used to convert ATP-induced light to moles of ATP according to the calibration plot prepared each day. The LINEST function in Microsoft Office Excel 2003 was used to fit a linear regression line to the log-log data. The regression parameters (slope and intercepts) were used to convert test measurements to [ATP]:

$$\log_{10} (RLI_{\text{measure}} - RLI_{\text{background}}) = \text{slope} \times \log_{10} \left[\frac{ATP}{M} \right] + \text{intercept} \quad (1)$$

$$\log_{10} \left[\frac{ATP}{M} \right] = \frac{\log_{10} (RLI_{\text{measure}} - RLI_{\text{background}}) - \text{intercept}}{\text{slope}} \quad (2)$$

$$\frac{[\text{ATP}]}{\text{M}} = 10^{\left\{ \frac{\log_{10} (\text{RLI}_{\text{measure}} - \text{RLI}_{\text{background}}) - \text{intercept}}{\text{slope}} \right\}} \quad (3)$$

ATP released from follicles was monitored using the luciferin-luciferase bioluminescence assay in a luminometer (TD-20/20 Luminometer). 10 sec integration period was used, with 2 sec delay period before each integration period. The total amount of light produced by the sample during 10 sec interval was determined. Luminescence of each sample was measured 5 times over a period of 11 minutes, in order to eliminate the quenching of luminescence with time. The mean luminescence level of each sample was then calculated. For each treatment, three replicates (three samples) were measured.

2.5 Examination by Scanning Electron Microscopy (SEM) and Transmission Electron of stage III zebrafish (*Danio rerio*) ovarian follicle structure to support observation of mitochondrial distribution obtained by confocal microscopy

In this study, Cryo-SEM and TEM studies were undertaken in order to identify the mitochondrial probe stained layer obtained in the confocal microscopy studies within the ovarian follicles from the enzymatic isolation method. Cryo-SEM and TEM studies were also carried out to compare stage III zebrafish follicles obtained by both mechanical and enzymatic isolation methods.

2.5.1 Cryo - Scanning Electron Microscopy (Cryo - SEM)

Follicles, obtained by separation from the ovaries, were held in Hanks' solution before specimen preparation. Ovarian follicles were mounted onto a cryo stub smeared with Tissue-Tek OCT Compound (Sakura Finetechnical Co. Ltd, Tokyo, Japan) and plunged into pre-slushed LN₂. The sample was then transferred under

vacuum to the Gatan (Gatan UK, Abingdon, UK) Alto 2500 cryo chamber and fitted onto the cold stage where the temperature was maintained at -180°C . Here it was fractured using the cold knife blade to allow visualisation of the inner structures. The specimen was then etched by warming the stage to -95°C for 1min to remove any contaminating ice. The stage temperature was then returned to -150°C or colder and the specimen was coated with AuPd (gold-palladium) for 90secs. The sample was then transferred to the Jeol FEG 6700 (Jeol (UK) Ltd, Welwyn Garden City, UK.) Scanning Electron Microscope chamber for imaging. Images were recorded using the on-board software system.

2.5.2 Transmission Electron Microscopy (TEM)

Follicles, obtained both from mechanical and enzymatic method of separation, were prepared for electron microscopy. Follicles were held in Hanks' solution before specimen preparation for electron microscopy. Follicles were fixed for 2 hours in a combination of 2% glutaraldehyde and 1% formaldehyde, 10X Hanks' solution was used as the vehicle. The glutaraldehyde reacts very rapidly with proteins and, being a dialdehyde, it stabilizes structures by cross-linking before there is any opportunity for extraction by the buffer to occur. Glutaraldehyde alone is not an adequate fixative, since certain cell components, especially lipids, are not fixed and may be extracted during dehydration. The formaldehyde was made fresh from paraformaldehyde and NaOH was added. Formaldehyde reacts with proteins but there is less cross-linking than with glutaraldehyde, since formaldehyde is mono-functional, being a monoaldehyde. It reacts with lipids, and it has the advantages of a considerably higher rate of penetration than either glutaraldehyde or osmium tetroxide, this allows large blocks of tissue to be fixed. Formaldehyde and glutaraldehyde are not osmotically active. It is thought that formaldehyde temporarily stabilizes structures which are subsequently fixed more permanently by the glutaraldehyde (Karnovsky 1965). The primary fixation was followed by three washings each of 10 min (the first washing with Hanks' solution, the second with Hanks' solution and distilled water with a ratio of 1:1, and the third one only

with distilled water) to remove all unreacted fixative. Follicles were then postfixed for 1 hour in 1% osmium tetroxide in distilled water, washed three times in distilled water.

Most embedding media are not soluble in water and consequently fixed specimens are dehydrated by passing them through a sequence of solutions, the last of which is miscible with the embedding medium. Dehydration was achieved by passing the fixed specimen through a graded series of solutions of increasing concentration of acetone in distilled water, ending with absolute dehydrating agent (acetone series of 10% increments in distilled water for 30 minutes at each concentration). Once the concentration of acetone reached 100%, the follicles were left for one hour and the 100% acetone was exchanged three times. The final step was to infiltrate the specimens with a liquid embedding medium which was then polymerized to produce a solid block suitable for thin-sectioning. Spurr's resin (TAAB Laboratories Equipment Ltd, Aldermaston, Berks, UK) was used as the embedding medium. The specimens were infiltrated with the embedding medium by passing through a sequence of solution until the dehydrating agent has been completely replaced by the final embedding mixture (25%, 50%, 75% and 100% for 1 hour at each concentration). The 100% resin was exchanged three times. Once the specimens were completely infiltrated by pure resin, they were placed in moulds and polymerized in an oven at 65°C overnight. BEEM polyethylene capsules (TAAB Laboratories) were used as embedding moulds to provide a block of a convenient size for the thin sectioning. These capsules had a pyramid-shaped ends that produced blocks that required the minimum of trimming before sectioning. One to five ovarian follicles were placed at the bottom of the capsule and the capsule was filled with the final embedding medium.

Ultrathin resin sections (90-100 nm thickness) were cut with a Reichert-Jung Ultracut microtome (Leica, Microsystems (UK) Ltd, Milton Keynes, Bucks, UK), mounted on mesh copper grids coated with Formvar. The sections were stained with 2% uranyl

acetate in 50% EtOH:ddH₂O and Reynold's lead citrate (Reynolds, 1963) and examined in a JEOL 2011 (Jeol (UK) Ltd, Welwyn Garden City, UK.) transmission electron microscope and imaged using an Ultrascan CCD camera (Gatan UK, Abingdon, UK). Measurements were made on digital electron micrographs of fixed specimens using Digital Micrograph (Gatan UK).

2.6 Evaluation of mitochondrial activity and distribution as biological marker in stage III ovarian follicles of zebrafish (*Danio rerio*) following CPAs exposure

In this study, the impact of CPA exposure on structural and functional integrity of mitochondria in stage III ovarian follicle was investigated in order to determine whether mitochondrial activity and distribution can be markers for ovarian follicle quality. The effect of CPA on mitochondrial distribution, membrane potential, ATP levels and mtDNA copy number was examined.

2.6.1 CPA treatment

Follicles were exposed for 30 min at 22°C to methanol or DMSO in Hanks' solution in the concentration range of 1 to 4 M. Control follicles were incubated in Hanks' solution under the same conditions. For the cryoprotective toxicity test, 15-40 follicles were held in Hanks' solution (10 min) followed by replacement of the medium with CPA supplemented medium. After incubation in CPA for 30 min at 22°C, follicles were washed twice with Hanks' solution and held in Hanks' solution at 27°C. Mitochondrial activity and distribution were assessed for ovarian follicles exposed to methanol. Assessment of ATP, ADP/ATP ratio, mtDNA copy number were carried out after 1h and 5h incubation following the CPA (methanol or DMSO) removal. FDA-PI test was carried out after 5h incubation following the methanol or DMSO removal.

2.6.2 Observation of mitochondrial activity and distribution by confocal microscopy

2.6.2.1 Staining of Mitochondria with JC-1

Stage III ovarian follicles were stained with JC-1 (Sigma) after the exposure to different methanol concentrations (for staining procedure see paragraph 2.4.1).

2.6.2.2 Confocal microscopy

Stained samples were examined using a Leica TCS-SP/DM IRBE confocal microscope equipped with Ar/Kr laser (see paragraph 2.4.1.1)

2.6.3 Viability assay

2.6.3.1 Viability assessed by FDA-PI staining

See paragraph 2.3.1

2.6.3.2 Viability assessed by TB staining

See paragraph 2.3.3.1

2.6.4 mtDNA copy number determination

mtDNA copy number was measured for follicles after 1 and 5 h incubation following 30 min CPA exposure, holding the follicles in Hanks' solution at 27°C. Treated and control follicles were stored at -80°C prior to DNA extraction.

2.6.4.1 DNA extraction from ovarian follicle

DNA was extracted from individual ovarian follicles using the EZNA Gel extraction kit (Omega Bio-tek, via VWR, Lutterworth, UK) with a slightly modified protocol. Samples were dissolved in 150µl binding buffer and vortexed vigorously before being added to the spin columns provided. The remainder of the procedure was carried out according to the manufacturer's instructions.

2.6.4.2.1 PCR

The external standards for mtDNA copy number calculation were generated using conventional PCR with primers designed to amplify a region of the mitochondrial genome (F: TAC AAT CCG CCG CCT AAA CAC T, R: AAG TGC TCC TGG TTG GCT AAG T). Reactions were performed in 20µl using 1x PCR buffer (Bioline, London, UK), 1.5mM MgCl₂ (Bioline), 0.5µM each primer, 200µM dNTP mix (Bioline), and 2U BioTaq polymerase (Bioline). Reaction conditions were 1 cycle of 95°C for 5 min followed by 35 cycles of 95°C for 30 sec, 59°C for 30 sec and 72°C for 30 sec, with a final extension at 72°C for 5 min. PCR products were run on 2% agarose gels (see section 2.6.4.2.2).

2.6.4.2.2 Agarose gel electrophoresis

2% (w/v) agarose gels were made by mixing 2g agarose (Bioline) with 100 ml Tris acetate- EDTA (TAE) buffer in an appropriately sized Duran bottle. The mixture was heated in a microwave for about 1 min, to dissolve the agarose. The gel was allowed to cool before it was poured into an electrophoresis tank (MAXI –VG (700-7213), VWR International) and covered with TAE buffer. Firstly, 5 µl Ethidium Bromide (EthBr), a DNA intercalating dye visible in ultraviolet (UV) light, was added to the cooled gel. Combs were used to create a horizontal line to load the samples. Combs were removed and 20 µl sample and 4 µl of marker were loaded. Gels were run at 100V for 60 minutes to separate, on the basis of the size, the DNA fragments of interest in each lane. Gels were viewed using a UV transilluminator and images of the

gel were captured and processed using the onboard software of the gel documentation system (VWR).

2.6.4.2.3 DNA extraction from gels

DNA was extracted from the excised bands using the EZNA Gel extraction kit (Omega Bio-tek) according to the manufacturer's instructions. Samples were quantified using spectrophotometry at 260 nm, they were initially diluted to 2ng/μl and then serially diluted 10 fold for use as standards for real-time PCR.

2.6.4.3 Real time PCR

Real time PCR allows quantification of double-stranded DNA using the intercalating dye Sybr Green. When Sybr Green binds to double-stranded DNA, it emits green fluorescence (λ_{max} = 522 nm), such as during the extension phase of a PCR cycle, but the dye does not fluoresce when no double-stranded DNA is present, such as during the denaturation phase of the PCR cycle. An increase in DNA products during PCR therefore leads to an increase in fluorescence intensity, which is measured at each cycle.

The conventional PCR method uses agarose gels for detection of PCR amplification at the final phase or plateau of the PCR reaction. At the plateau the reaction has stopped, no more products are being made. Whilst during the exponential phase (phase of detection for real time PCR) doubling of product is accumulating at every cycle and the reaction is very specific and precise.

In this study, Real-time PCR was performed on a Rotorgene 6000 cycler (Corbett Research, UK) using a 72 well rotor. Reaction tubes contained 7.5μl SensiMix dT 2x mix and 0.3μl SYBR Green (both from Quantace), 333 nM each primer and 2μl each sample or standard, made up to 15μl with molecular biology grade water. The reaction conditions were 1 cycle at 95°C for 10 min followed by 50 cycles of 95°C for 10 sec, 59°C for 15 sec and 72°C for 15 sec, with data being acquired on the

FAM/SYBR channel at the end of each extension step. Melt curves were analysed to check for the absence of mispriming. Each experiment was carried out three times and all samples were run in triplicate. The concentration of each standard was converted into mtDNA copy number and the number of mtDNA molecules per follicle for each treatment was subsequently calculated using the RotorGene software (Version 1.7, Corbett Research) and Microsoft Excel.

2.6.5 ATP levels and ADP/ ATP ratio determination

Additional information on mitochondrial energetic status can be obtained by measurement not only the ATP content but also of ADP and ATP and calculation of ATP/ADP ratio. ADP/ATP ratio and ATP levels were evaluated in follicles 1 and 5 h incubation following CPA removal, during which the ovarian follicles were held in Hanks' solution at 27°C. Follicles from control groups and follicles exposed to 1-4 M methanol or to 1-4 M DMSO for 30 min, were used for the preparation of extracts for determination of ATP+ADP levels. For all experiments, three replicates were used for each treatment and experiments were repeated three times. For the extract preparation, the procedure has been already described in section 2.4.2.1.

ATP content of ovarian follicle extracts was measured using the luciferin – luciferase bioluminescence assay provided by a commercial kit (ApoSENSOR™ ADP/ATP Ratio Assay Kit, BioVision). A luminometer (TD-20/20 – Turner Designs) was used for all measurements. Background light was measured and subtracted by running a blank containing water. The measurements were expressed as the number of relative light units (RLU). The nucleotides were released from the extract by addition of 100 µl nucleotide releasing reagent. 1 µl of ATP monitoring enzyme was added to the lysate and a reading was taken at one minute to determine the ATP level (A). To measure the ADP levels in the cells, the samples were read at 10 minutes (B). The ADP in the wells was converted to ATP by the addition of 1µl of ADP converting enzyme and a reading was taken after one minute (C).

The ratio of ADP: ATP for each well was calculated from these three readings as follows:

$$\frac{C - B}{A} = \frac{ADP}{ATP}$$

The mean and standard error of the triplicates were calculated.

Chapter 3: Development of new assay for zebrafish oocytes viability using vital stains

3.1 Introduction

A range of vital stains and other methods have been studied for assessing the viability of follicles at different stages, and among these TB staining and *in vitro* maturation followed by observation of germinal vesicle breakdown (GVBD) have been routinely used. The GVBD test is the most sensitive method, but this test can only be applied to stage III follicles as later stages have already undergone maturation and germinal vesicle breakdown. Indeed, unlike maturation in mammals, where offspring have been produced using *in vitro* matured oocytes, in zebrafish there are few reports (Li et al., 1993; Seki et al., 2008) of offspring production derived by *in vitro* ovarian follicle maturation, and the stage used in these studies was late vitellogenic follicles (Stage III) with a diameter between 0.65-0.69 mm. Whilst vital stains such as the TB are suitable for their applicability to all stages, they do have several limitations. TB only assesses membrane integrity and it does not provide any information on the metabolic activity of the cells (Plachinta et al., 2004a).

The fluorescein diacetate (FDA) test has been found to be suitable for assessing animal cells viability (Widholm, 1972). Rotman and Papermaster (1966), in a detailed investigation, demonstrated the mode of action of this compound, providing evidence indicated that the intracellular retention of fluorescein is dependent on the integrity of the cell membrane. The non-polar fluorescein-diacetate molecules enter the cell, are hydrolyzed by cellular esterases to produce the polar compound fluorescein. The resulting reaction, characterised by the appearance of bright-green fluorescence inside the cell, is termed *fluorochromasia*. In viable cells, the fluorescein is unable to pass through the intact membrane, accumulating in the cytoplasm of the cell, whilst damaged cells show a distinct loss of fluorescein through the cell membrane. The FDA test has been successfully employed to assess viability of pig oocytes (Albertini,

1984, Didion et al., 1990), mouse embryo (Mohr and Trounson, 1980), and human cells (Frim and Mazur, 1983) and ram spermatozoa (Holt and North 1994).

Staining of nonviable cells with propidium iodide (DNA-binding probe) has been performed on most cell types (Sauch et al., 1991) as single or in combination with other fluorochromes (Cai et al., 2005; Garner and Johnson, 1995). Live cells with intact membranes are distinguished by their ability to exclude the dye that easily penetrates dead or damaged cells, intercalating with DNA and RNA to form bright red fluorescence. Since the dye is excluded by intact cell membranes, propidium iodide (PI) is an effective stain to identify non viable cells. The combination of FDA and PI has been used to determine viability of protozoa cyst (Schupp and Erlandsen, 1987), parasites spores (Yokoyama et al., 1997) and mammalian cells (Harrison and Vickers, 1990; Jones and Senft, 1985); it is used here for the first time to investigate zebrafish ovarian follicles.

In this study stage III zebrafish ovarian follicles were used. During this stage the oocyte is surrounded by several cell layers and acellular structures (thecal layer, basement membrane, granulosa cells layer and vitelline envelope). Following initial checks to test the efficacy of the FDA and PI methods, FDA-PI staining was compared with TB staining and GVBD test in a series of cryoprotectant (CPA) toxicity tests in different media commonly used with zebrafish follicles – Hanks' solution, KCl buffer and Leibovitz L-15. The GVBD test was only carried out when the Leibovitz L-15 was used as it is the medium normally employed for zebrafish *in vitro* maturation. The FDA-PI test was also used, in comparison with TB, to assess ovarian follicle viability following cryopreservation. The GVBD test was not applicable after cryopreservation procedure as the follicles became transparent. This study used the optimum cryoprotective media and cooling rates for stage III zebrafish follicles that were previously identified in this laboratory (Guan et al., 2008b; Plachinta et al., 2004b; Plachinta 2007).

3.2 Results

3.2.1 Reliability of FDA-PI

Simultaneous staining with FDA-PI showed distinctive differences between control and negative control. After exposure to 99% methanol for 10 min, dead follicles showed bright red staining due to propidium iodide penetration, while the same follicles were only faintly stained green by FDA. Viable follicles produced fluorochromasia, represented by bright green staining and remain unstained by PI. Fig. 3.1a shows oocytes in KCl buffer after exposure for 10 min to 99% methanol, dead cells showed bright red staining due to propidium iodide penetration, while in Fig. 3.1b the same oocytes were only faintly stained green by FDA. Living oocytes produced fluorochromasia (Rotman and Papermaster 1966), and are bright green (Fig. 3.1d) and remain unstained by PI (Fig.3.1c). Fig 3.2. shows the number of follicles of the control group and treated group indicating the proportion of follicles stained red by PI and stained green by FDA.

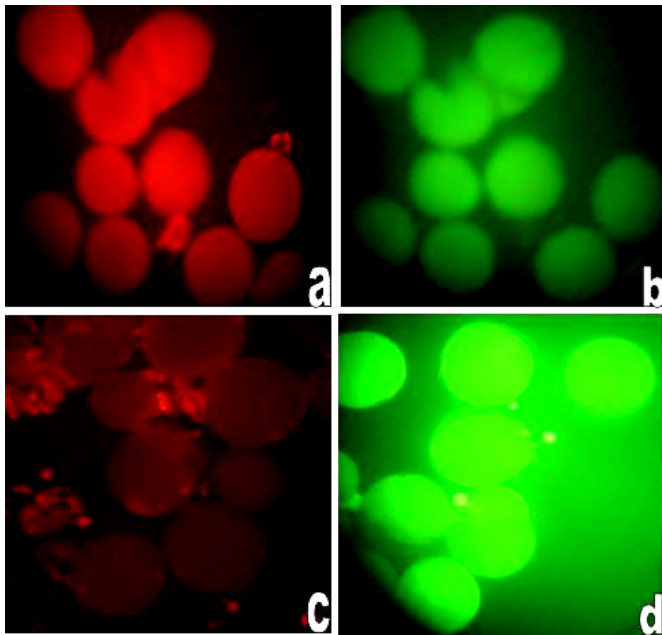


Fig. 3.1 Dead stage III ovarian follicles exposed to 99% methanol for 10 min and visualized by PI (a) and by FDA (b). Viable stage III ovarian follicles, unstained by PI (c) and showing bright green after staining by FDA (d)

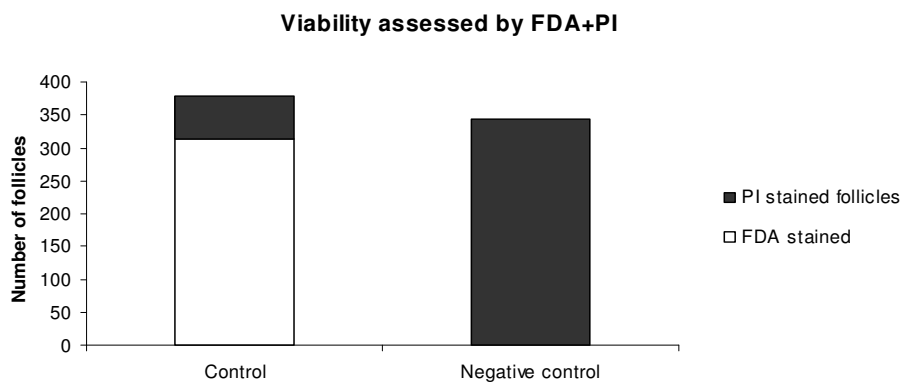


Fig 3.2 Numbers of stage III zebrafish follicles stained by PI and FDA. Control represents follicles in KCL buffer. Negative control represents follicles exposed to 99% Methanol for 10 min.

3.2.2 Comparisons of FDA-PI, TB and GVBD tests after follicles isolation

Viability assessment with FDA-PI, TB and GVBD was performed immediately after the separation of the follicles from the ovaries and after 30 min incubation in L-15 medium. The results showed that the percentage viability assessed by TB was always higher than the viability assessed by FDA-PI (Fig. 3.3). There were significant differences between the group obtained immediately after follicle separation and the group held at room temperature for 30 min in L-15 medium when the viability was assessed by TB, whilst there were no significant differences when the viability was assessed by FDA-PI and GVBD test (Fig 3.3).

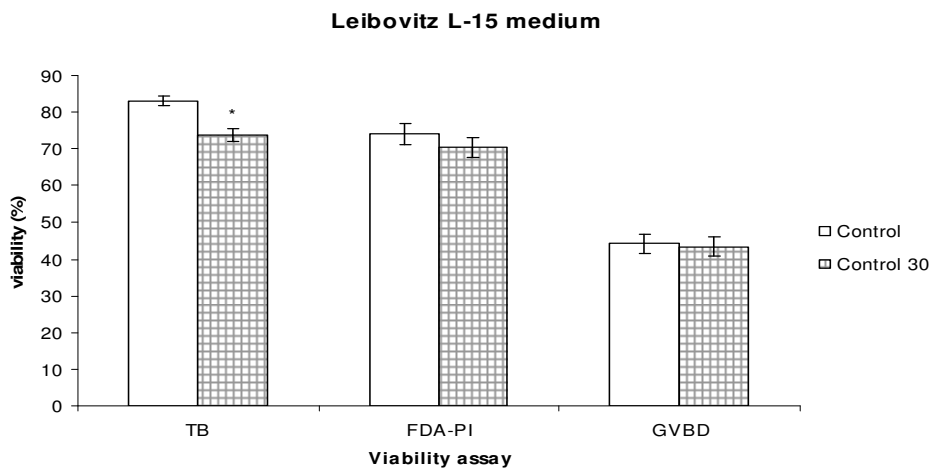


Fig. 3.3 Comparisons of viability of stage III ovarian follicles using three different viability assessment methods. Control: TB, FDA-PI and GVBD tests were performed immediately after follicle separation from the ovaries. Control 30: follicles incubated at 22 °C for 30 min in 50% Leibovitz L-15. Columns and error bars represent means \pm SEM of three experiments each with three replicates. *Significantly different from corresponding control value, $P < 0.05$.

3.2.3 Comparisons of FDA-PI, TB and GVBD in cryoprotective agents (CPAs) toxicity tests

Results showed that the FDA-PI staining is more sensitive than TB staining and the sensitivity appeared to increase with concentration of cryoprotectants. The study also showed that the toxicity of cryoprotectants generally increased with concentration using all three viability assessment methods (Fig. 3.4-3.5-3.6). Methanol was the least toxic cryoprotectant to zebrafish ovarian follicles in all three different media. DMSO and EG were more toxic to stage III follicles and significantly reduced the viability of follicles when assessed by GVBD, FDA-PI or TB in all media (Fig. 3.4-3.5-3.6). The medium employed to make up the cryoprotectant solutions had no effects on follicle viability assessed after 30 min exposure to cryoprotectants at room temperature, as similar results were obtained with all three different media (Fig. 3.4-3.5-3.6). Viabilities assessed by TB and FDA-PI were also compared when follicles were exposed to 4M methanol with and without 0.2M glucose in Hanks' solution and KCl buffer, as this cryoprotectant solution was identified as the optimum for zebrafish oocytes cryopreservation (Guan et al., 2008b). Results showed that there were no significant differences between the control and treated groups when 4M methanol + 0.2 M glucose was used and viability was assessed by FDA-PI and TB tests (Fig. 3.7).

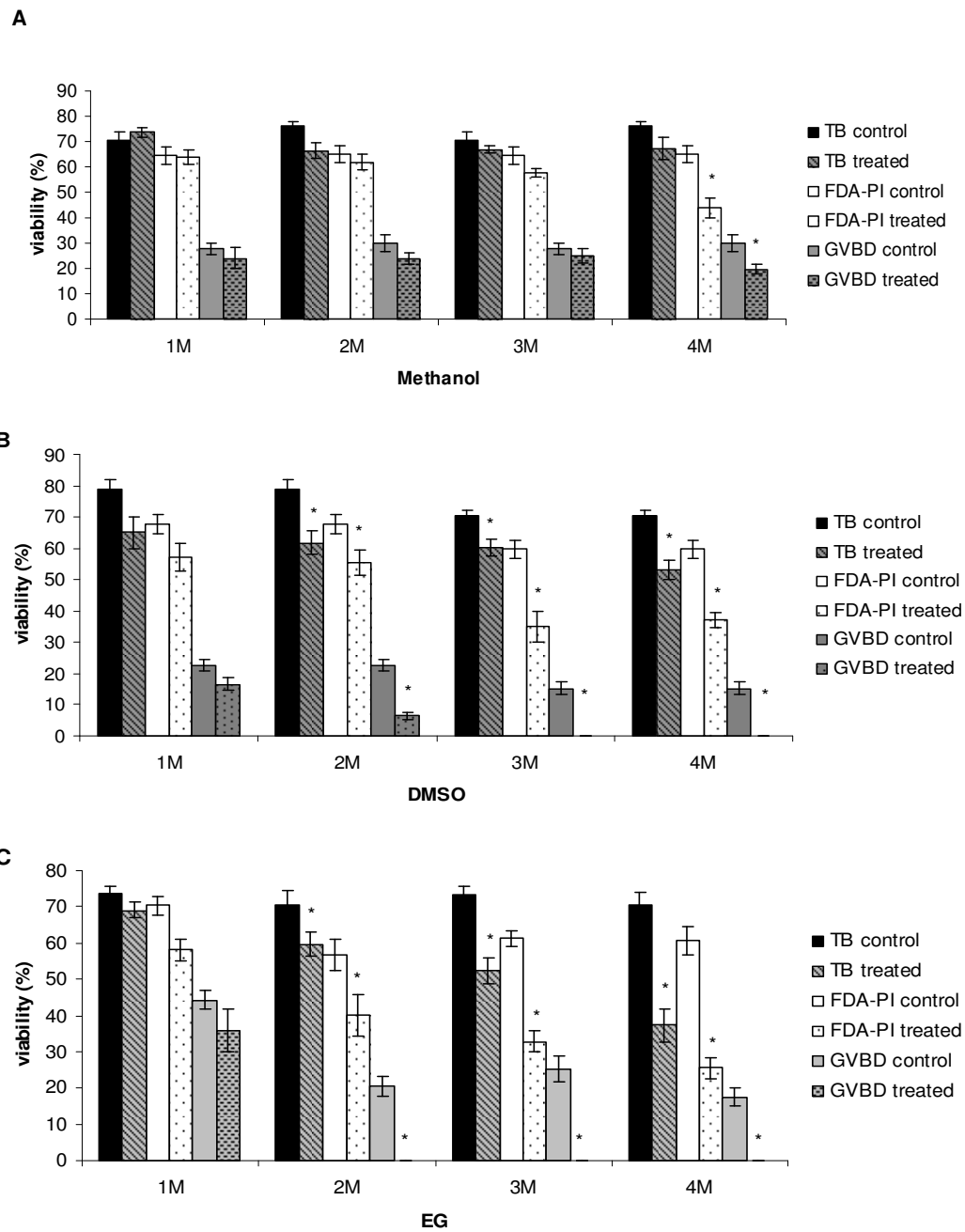


Fig. 3.4 Comparisons of follicle viability assessed by TB, FDA-PI and GVBD tests following exposure to different concentrations of methanol (A), DMSO (B) and EG (C), in Leibovitz L-15 medium. Control: TB, FDA-PI and GVBD tests were performed after incubation of ovarian follicles at 22 °C for 30 min in 50% Leibovitz L-15; treated: TB, FDA-PI and GVBD were conducted after ovarian follicles were exposed to 1-4M methanol, DMSO or EG for 30 min at 22 °C. Columns and error bars represent means \pm SEM of three experiments each with three replicates. *Significantly different from corresponding control value, $P < 0.05$.

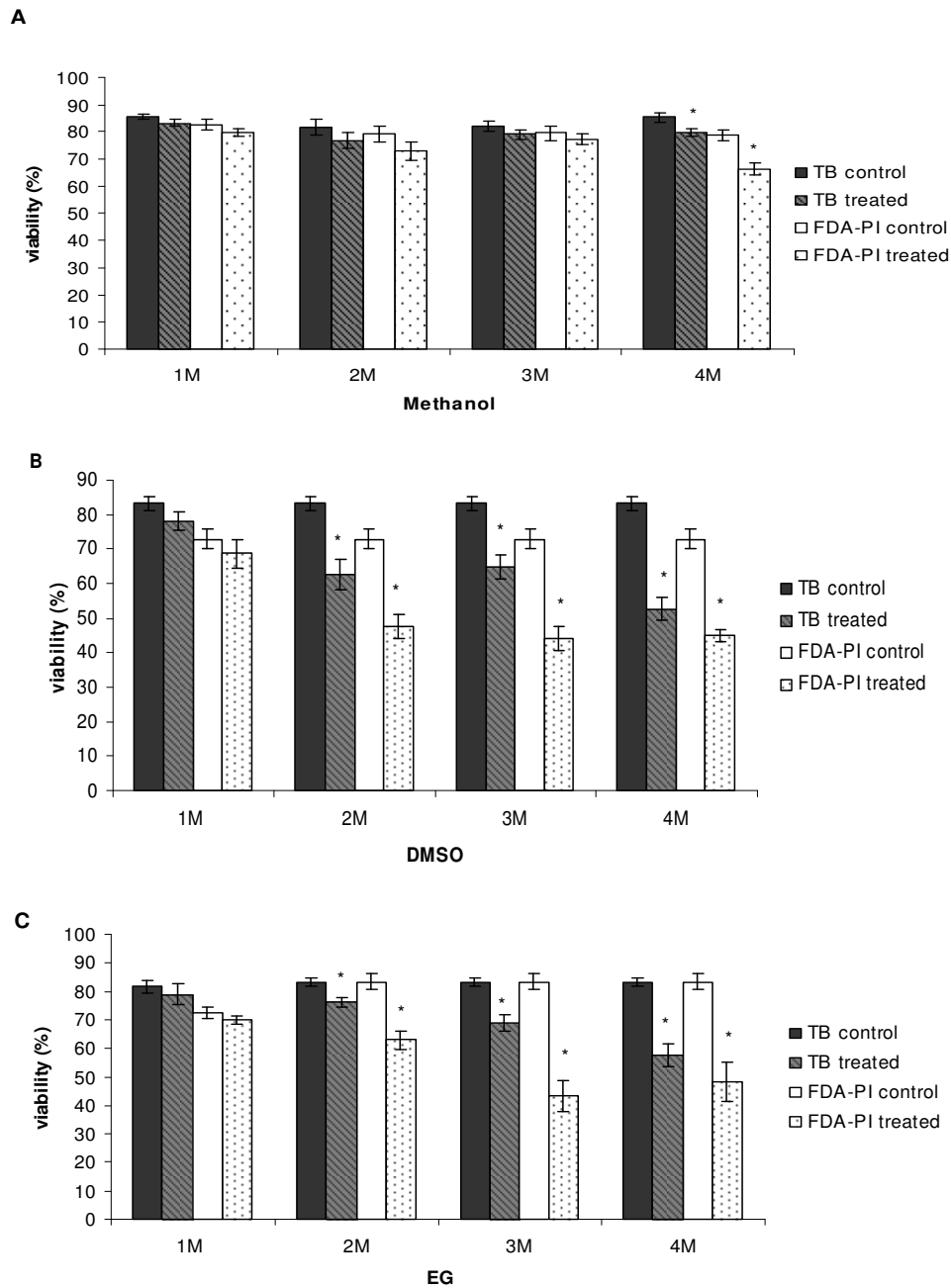


Fig. 3.5 Comparisons of follicle viability assessed by TB and FDA-PI tests following exposure to different concentrations of methanol (A), DMSO (B) and EG (C), in Hanks' solution. Control: TB and FDA-PI tests were performed after incubation of ovarian follicles at 22 °C for 30 min in Hanks' solution; treated: TB and FDA-PI were conducted after ovarian follicles were exposed to 1-4M methanol, DMSO or EG for 30 min at 22 °C. Columns and error bars represent means \pm SEM of three experiments each with three replicates. *Significantly different from corresponding control value, $P < 0.05$.

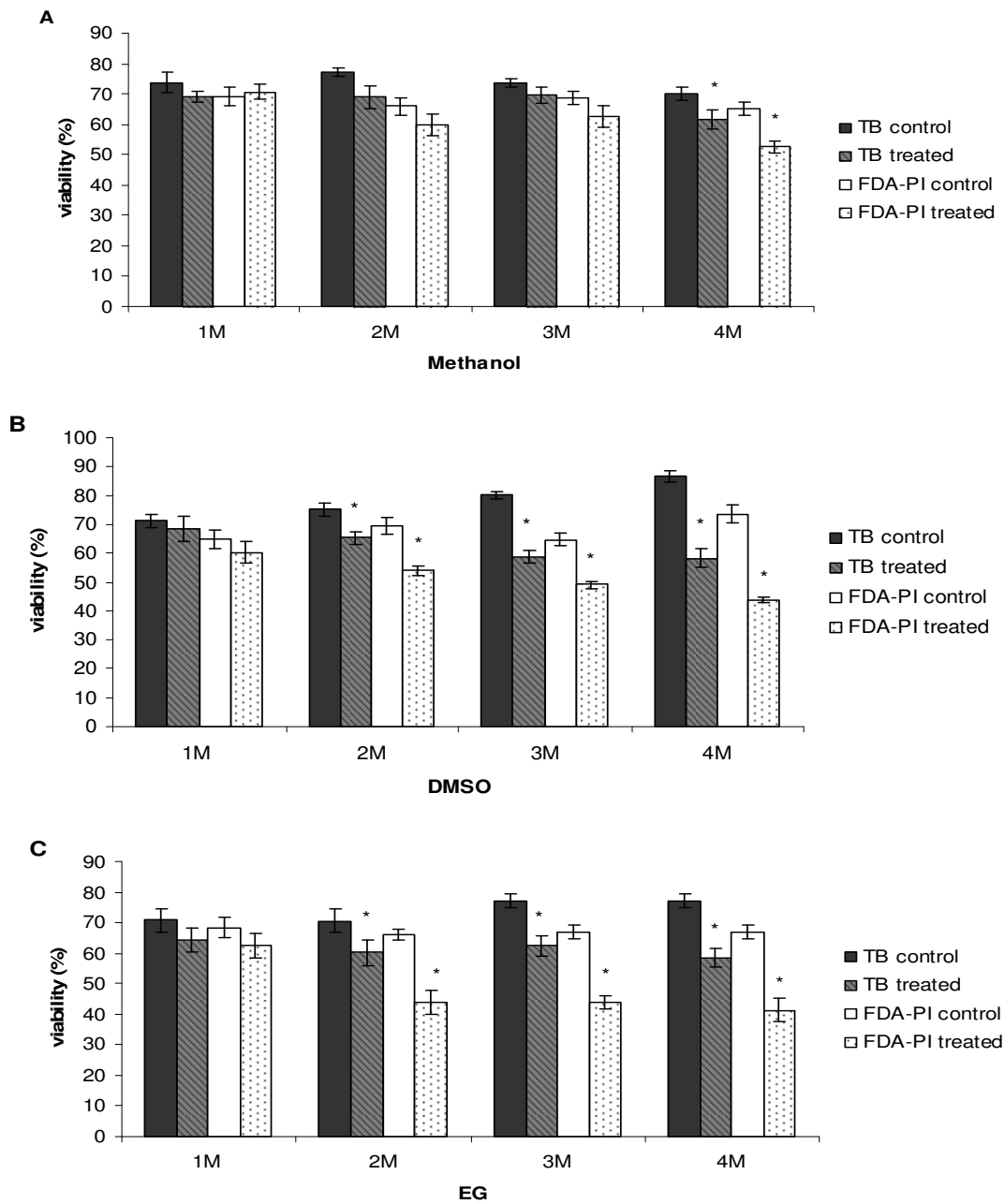


Fig. 3.6 Comparisons of follicle viability assessed by TB and FDA-PI tests following exposure to different concentrations of methanol (A), DMSO (B) and EG (C), in KCl buffer. Control: TB and FDA-PI tests were performed after incubation of ovarian follicles at 22 °C for 30 min in KCl buffer; treated: TB and FDA-PI were conducted after ovarian follicles were exposed to 1-4M methanol, DMSO or EG for 30 min at 22 °C. Columns and error bars represent means \pm SEM of three experiments each with three replicates. *Significantly different from corresponding control value, $P < 0.05$.

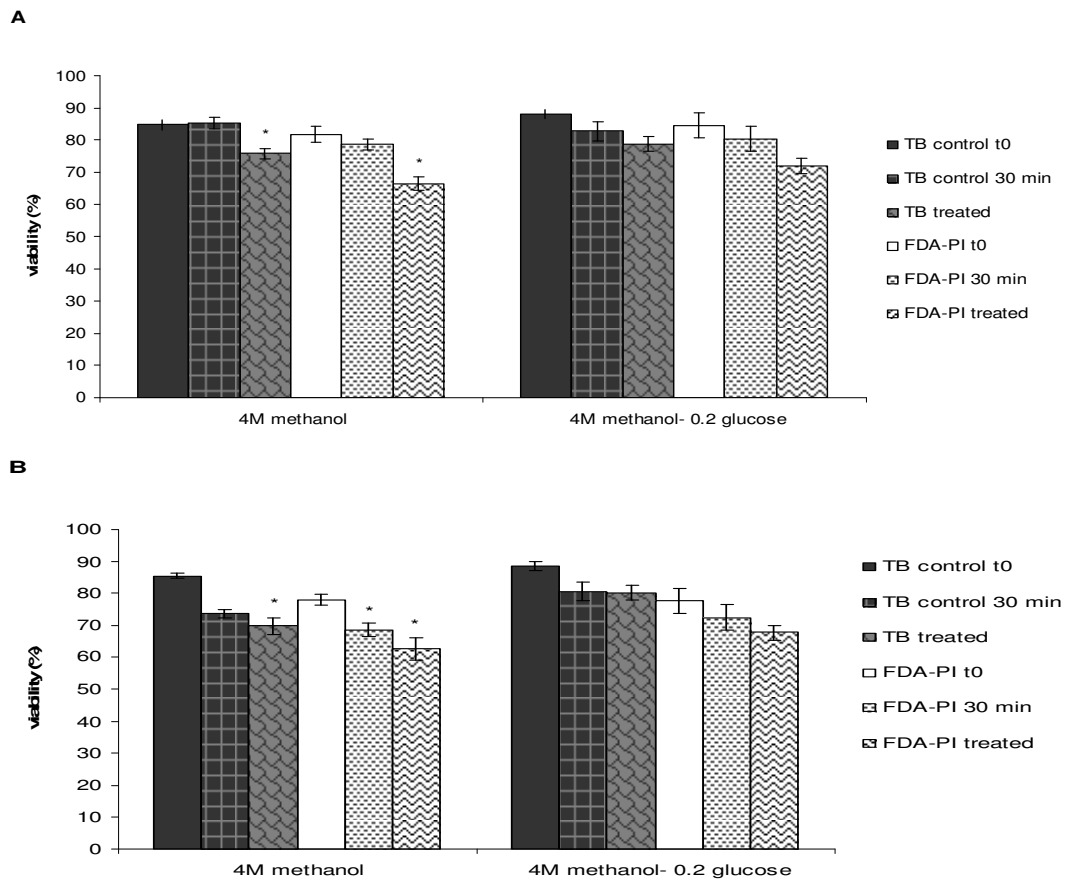


Fig. 3.7 Comparisons of TB and FDA-PI tests on stage III follicles exposed to two cryoprotectant solutions - 4M methanol or 4M methanol + 0.2M glucose - made up in Hanks' solution (A) and KCl buffer (B). Control t0: viability was assessed after ovarian follicles separation. Control 30 min: ovarian follicles were incubated at 22°C for 30 min in KCl buffer. Treated: TB and FDA-PI were conducted after incubation of follicles in 4M methanol or 4M methanol + 0.2M glucose. Columns and error bars represent means \pm SEM of three experiments each with three replicates. *Significantly different from corresponding control value, $P < 0.05$.

3.2.4 Comparisons of FDA-P and TB following cryopreservation procedure

The percentage of viable follicles after cryopreservation assessed by FDA-PI was always lower than the viability evaluated by TB both with Hanks' solution ($28.9 \pm 2.5\%$ and $38.9 \pm 4.0\%$) and KCl buffer ($35.2 \pm 3.5\%$ and $45.2 \pm 4.3\%$) (Fig. 3.8). Moreover, there were no significant differences between KCl buffer and Hanks' solution after cryopreservation procedure when the viability was assessed by FDA-PI and TB (Fig. 3.8). The FDA-PI

proved to be more sensitive than TB test as microscopic observation showed a decrease of green fluorescence in the follicles with intact membranes after cryopreservation compared to the control follicles.

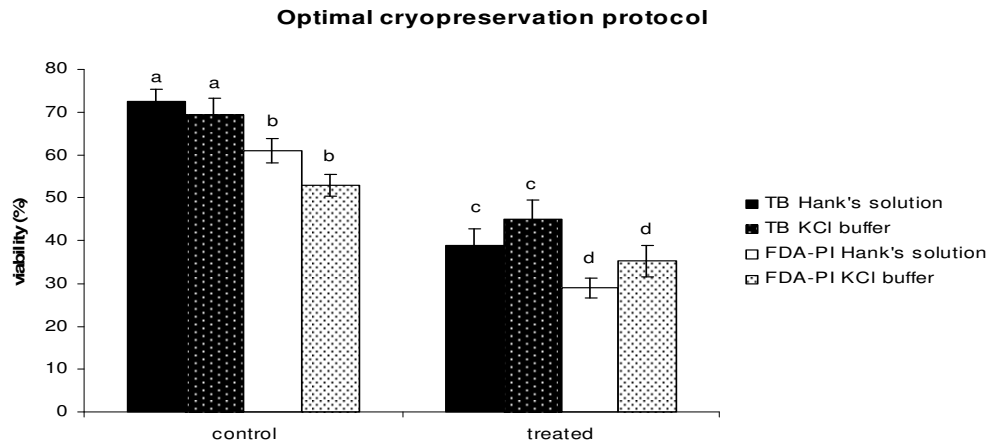


Fig. 3.8 Comparisons of TB and FDA-PI viability tests of stage III follicles following cryopreservation, using 4M methanol with 0.2M glucose as cryoprotectants in either Hanks' solution or KCl buffer. Control: TB, FDA+PI were performed on ovarian follicles held at 22 °C; treated: TB and FDA-PI were conducted after cryopreservation of follicles in 4M methanol and 0.2 M glucose. Columns and error bars represent means \pm SEM of three experiments each with three replicates; bars with different superscripts differ significantly ($P < 0.05$).

3.3 Discussion

There are a limited number of studies in the literature on zebrafish ovarian follicle viability assessment. In these studies, carboxyfluorescein diacetate (Pearl and Arav, 2000), TB, MTT and GVBD (Plachinta et al., 2004a) were used. The GVBD test is the most sensitive method for assessing follicles viability as it assesses oocytes developmental capability; however, it can only be applied to stage III follicles as later stages have already undergone maturation and germinal vesicle breakdown *in vivo*. Moreover, the GVBD test is not applicable in all experimental conditions. The TB test is one of the most common method to assess cell viability and it has been performed on many cell types (Allison and Ridolpho, 1980; Narayanan et al., 2005), but it only assess membrane integrity. TB is a vital dye, its reactivity is based on the fact that the chromophore is negatively charged and does not penetrate the cell unless the membrane

is damaged. The results in this study showed that the FDA-PI test can be successfully employed to assay fish follicle viability following exposure to different experimental conditions. This test proved to be more sensitive than TB but less sensitive than GVBD test.

The results from the present study also showed that L-15 medium is the most suitable medium for zebrafish follicles, when compared with two other solutions (Hanks' solution and KCl buffer). This is thought to be because Leibovitz L-15 is a bicarbonate-free medium, which uses a high level of amino acids in the free base form with buffering capacity, and has galactose as a carbohydrate source which produces lactic acid at a slower rate than glucose. It also contains pyruvate and alanine to generate bicarbonate for synthesis reaction. This medium has been designed for use in cell culture in free exchange with room air (Barngrover et al., 1985; Leibovitz, 1963).

The results from the present study showed that the toxicity of cryoprotectants generally increased with concentration, using all three viability assessment methods. As previously reported (Plachinta et al., 2004a), methanol is the least toxic cryoprotectant to stage III zebrafish follicles, followed by DMSO and EG. However, the results of this study showed that 4M methanol had a toxic effect on zebrafish follicles since significant differences were observed between the control and the treated follicles where the viability was assessed by FDA-PI and TB; these results are not in agreement with previous studies (Plachinta et al., 2004a; 2004b). The use of high concentrations of CPA may induce osmotic damage and damage induced by the toxicity of the CPA itself. The use of 4 M methanol with 0.2 M glucose gave better results probably due to the combination of permeating and non-permeating cryoprotectants with their different mechanisms of action. The beneficial effect of the addition of low concentration of sugars to a freezing medium on zebrafish oocytes has already been reported (Plachinta, 2007). Plachinta et al. (2004a) also reported that exposure of stage III zebrafish follicles to glucose concentrations <0.25 M has no toxic effect.

With both FDA-PI and TB assessment methods, there were no significant differences between KCl buffer and Hanks' solution when these two solutions were used for the cryopreservation procedure, this result is not in agreement with those previously reported (Plachinta et al., 2004b; Plachinta, 2007).

The FDA-PI test proved to be more sensitive than Trypan Blue, because after cryopreservation the follicles stained by FDA-PI showed a lower level of green fluorescence when compared to control follicles. Moreover, in the follicles following cryopreservation, the green fluorescence seeped out of the follicles. The fluorescence decreasing could be due to the partial loss of esterase activity, whilst the damage of the membrane could be the cause of the fluorescence seeping out of the cells. These results are in agreement with those from mammalian oocytes (Boender, 1984) where in heavily damaged oocytes with the esterase activity still intact, the fluorescein leaks through the cell membrane into the extracellular space. Follicles stained by PI showed the red fluorescence more delimited at the periphery of the follicles, probably involving the granulosa cells layer.

The combined FDA-PI test showed that cryopreservation induced damage to the follicles, and the FDA-PI microscopic observations are supported by the fact that the follicle became translucent after thawing, making it difficult to use the GVBD test. This phenomenon has already been reported in previous studies (Guan et al., 2008b; Isayeva et al., 2004). Furthermore, the FDA-PI microscopic observation showed follicles leaking their content. Further studies to identify an optimal protocol for cryopreservation are needed considering the low percentage of survivals based on vital staining after cryopreservation. The results obtained from FDA-PI test showed a decrease of fluorescein production, providing evidence of compromised metabolic activity even if the membrane could remain intact.

The FDA-PI method informs on both the physiological state and membrane integrity, as the FDA requires cellular esterase activity in addition to an intact membrane, and PI, an intercalating dye, is known to pass only through the membranes of dead or dying cells.

This approach can also be applied to follicles at all stages. FDA-PI assay was chosen because it has been widely and successfully used in others cell studies. The main advantages of FDA-PI test are its speed, high sensitivity and simplicity.

In this study, FDA-PI staining was tested on fish follicles for the first time. The results show the method to be promising and offers a new test of the viability for fish follicles. Ultimately, for a full assessment of ovarian follicle viability, further studies are needed. Additional biological markers need to be considered to allow a more detailed assessment of the effects of treatments such as cryopreservation on fish ovarian follicles.

3.4 Summary

Reliable fish oocyte quality assessment methods are essential in developing protocols for cryopreservation as well as their *in vitro* maturation and fertilisation. Current ovarian follicle viability assessment methods either lack sensitivity (e.g. Trypan Blue staining-TB) or are stage dependent (e.g. *in vitro* maturation and observation of germinal vesicle breakdown-GVBD). The aim of the present study was to develop a new viability assessment method for zebrafish ovarian follicles that is reliable, sensitive and not-stage specific. Fluorescein Diacetate (FDA) and Propidium Iodide (PI) were used for the first time to assess viability of zebrafish ovarian follicles. After preliminary studies to evaluate the efficacy of FDA and PI, a combination of these two fluorochromes was subsequently chosen and compared with TB staining and GVBD test in a series of cryoprotectant toxicity studies and following cryopreservation using stage III ovarian follicles. In all cases the FDA-PI test proved to be more sensitive than TB staining but less sensitive than the GVBD test. Ovarian follicle survivals after 4M Methanol treatment for 30 min at 22 °C were $67.4 \pm 4.4 \%$, $43.9 \pm 3.8 \%$ and $19.6 \pm 1.9 \%$ using TB, FDA-PI and GVBD test respectively. Survivals after cryopreservation procedure were $38.9 \pm 4.0 \%$ and $28.9 \pm 2.5 \%$ using TB and FDA-PI respectively when Hanks' solution was used as medium and $45.2 \pm 4.3 \%$ and $35.2 \pm 3.5 \%$ when KCl buffer was used. The results showed the method to be promising, and it may offer a new approach for viability assessment of fish ovarian follicles.

Chapter 4: Observation of mitochondria distribution and activity in stage III ovarian follicles

4.1 Introduction

The aim of this part of the study was to investigate the potential role of mitochondria as a biological marker for ovarian follicle quality. Mitochondrial activity and distribution were investigated using confocal microscopy and two mitochondrial fluorescent probes.

Stage III oocytes are surrounded by cellular and acellular layers. These layers have an important role in supporting oogenesis, steroidogenesis and vitellogenesis. Communication between the oocyte and its surrounding follicle cells is critical for the development of a competent oocyte at ovulation. Within the ovarian follicle, oocyte growth and maturation are dependent on the association between granulosa/thecal cells and oocyte. Homologous gap junctions between follicular cells and heterologous gap junctions between follicular cells and oocytes allow an efficient communication network to support oocyte development. Several processes in the oocyte, such as metabolism, growth, meiotic arrest and maturation are dependent upon factors from follicular cells (Cerdeira et al., 1993). Observation of the granulosa cell layer during oocyte development, suggests that within this layer there is an efficient system for energy production.

Several processes occurring in the stage III ovarian follicle strongly suggest the potential involvement of mitochondria in supporting the growth phase of the oocyte, not only as sources of energy in the form of ATP, but also in signal transduction pathways. If the ATP, as a source of energy, is not taken up efficiently through the oocyte plasma membrane, then it is probably delivered to the oocyte using the gap junctional pathway (Eppig, 1991). ATP is also used as a substrate by kinases that phosphorylate proteins and lipids, and by adenylate cyclase which uses ATP to produce the second messenger molecule cyclic adenosine monophosphate (cAMP). In zebrafish, it has already been reported that cAMP is the major second messenger that mediates gonadotrophin actions in the ovary, also involving growth factors that serve as intraovarian modulators (Wang and Ge, 2003). Wang and Ge (2005) reported the role of cAMP in the differential

regulation of the intraovarian mediators, activin β A and β B, expression in zebrafish ovarian follicle cells, through cAMP-dependent signal transduction pathways.

Mitochondria are also involved in the process of steroid biosynthesis, taking part in the metabolism of cholesterol to pregnenolone. This is the first intermediate, and also the rate-determining step, in the steroid biosynthesis pathway in mitochondria (Hall, 1984; Jefcoate, 2002, Simpson and Waterman, 1983; Crivello and Jefcoate, 1980; Privalle et al., 1983). The main event occurring during this stage is vitellogenesis, which represents the major growth stage in which the oocyte increases in size due to accumulation of yolk. The yolk is sequestered as vitellogenin, which is produced by the liver of female fish under hormonal control, in particular estradiol (E2) synthesised from the follicular/thecal layer following gonadrophin stimulation (Polzonetti et al., 2004). The estradiol also has critical roles in oocyte development, induction of female secondary sex characteristics and negative feedback linkage to the hypothalamus and hypophysis (Ankley and Johnson, 2004).

In this study, mitochondrial distribution and activity were investigated in stage III zebrafish ovarian follicles by confocal microscopy, using the fluorescent probe JC-1 (5,5',6,6'-Tetrachloro-1,1',3,3'-tetraethyl-imidacarbocyanine iodide) to discriminate high and low mitochondrial membrane potential. JC-1 fluorescence has two emission peaks, with red fluorescence of j-aggregates indicating hyperpolarised mitochondria (high membrane potential) and green fluorescence (JC-1 monomers) due to low membrane potential (Reers et al., 1991, 1995). JC-1 allows both the mitochondria metabolic status and distribution to be determined.

Another mitochondrial stain, Mito Tracker green FM, was used with confocal microscopy to support the results obtained with JC-1. MitoTracker Green FM (Ex 488 nm, Em 516 nm) is a green-fluorescent mitochondrial stain which appears to accumulate in mitochondria regardless of mitochondrial membrane potential. This mitochondrial probe is essentially nonfluorescent in aqueous solutions, only becoming fluorescent once it accumulates in the lipid environment of mitochondria.

To provide further evidence of the mitochondrial origin of fluorescence obtained with JC-1 and MitoTracker Green FM, the follicles were exposed to a range of conditions that are known to affect the mitochondrial membrane potential ($\Delta\Psi_m$). This involved the use of the mitochondrial inhibitor p-trifluoromethoxy carbonyl cyanide phenyl hydrazone (FCCP). The follicles were exposed to an increasing concentration of FCCP following a permeabilisation pre-treatment with 0.01% (v/v) Triton X-100, to enable the FCCP to penetrate into the ovarian follicle. Exposure of follicles to 0.01% (v/v) and 0.1% (v/v) of Triton X-100 were tested by TB and GVBD tests to evaluate the effect of the detergent on ovarian follicles viability. Following the detergent and inhibitor exposure, the follicles were stained with JC-1 or MitoTracker Green FM and observed by confocal microscopy. Levels of ATP in the ovarian follicles were also measured after the exposure to the mitochondrial inhibitor to determine the relationship between mitochondria distribution and ATP levels. For the ATP measurement the follicles were also exposed to oligomycin, an inhibitor of the ATP-synthase. The oligomycin treatment was used to test the efficacy of the ATP assay for zebrafish ovarian follicles.

4.2 Results

4.2.1 Mitochondrial distribution and activity investigation by confocal microscopy

More than 150 good quality, live ovarian follicles were screened by confocal microscopy after exposure to JC-1 or MitoTracker Green FM; all the ovarian follicles examined presented a contiguous peripheral aggregation of mitochondria in the granulosa cells which surround the oocytes. A series of optical sections were undertaken of 40-50 intact ovarian follicles. The photomicrographs shown in this thesis are representative examples of ovarian follicles obtained by confocal microscopy.

Both the JC-1 and the MitoTracker Green FM were consistently unable to penetrate the oocytes, and no mitochondrial staining in the ooplasm was found (4.2B).

The fluorescence pattern shown by the mitochondria distribution was consistent in every normal follicle and represented a well organised distributional arrangement, with each

fluorescence pattern having a diameter of 10-15 μm . The fluorescence was concentrated at the margins of the each granulosa cell (Fig. 4.1, 4.2A).

Individual mitochondria consistently exhibited either green or red fluorescence, suggesting the possibility that these could be functionally distinct subsets or that metabolic turnover of activity (Fig. 4.1) is a normal feature of the oocyte-follicle complex.

The exposure of ovarian follicles to a second mitochondrial probe, MitoTracker Green FM, supported the results from the JC-1 staining, showing the same fluorescent patterns of mitochondria in the granulosa cells layer (Fig. 4.2A).

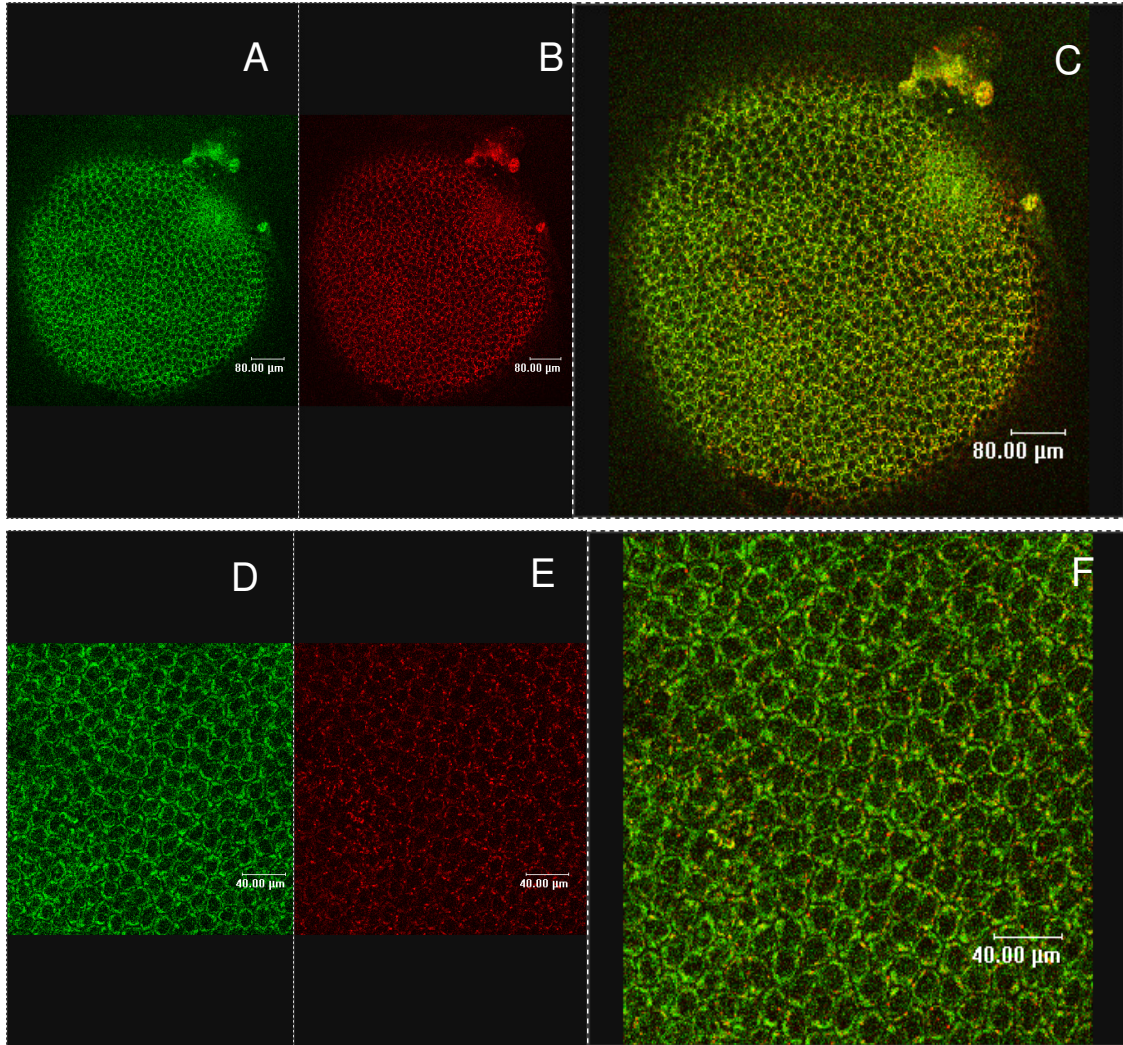


Fig. 4.1 Mitochondria distribution in stage III zebrafish follicle exposed to 5 μM JC1. JC-1 is a sensitive marker for $\Delta\Psi\text{m}$. JC-1 accumulates in monomeric form within the mitochondria matrix and its fluorescence emission characteristics are a function of the magnitude of $\Delta\Psi\text{m}$. Low polarized organelles fluoresce green (A,D), while higher polarized organelles fluoresce orange-red owing to multimerization of JC-1 and formation of J-aggregates (B,E). Merged images showing mitochondria with both red and green fluorescence, suggesting a metabolic turnover of activity (C,F).

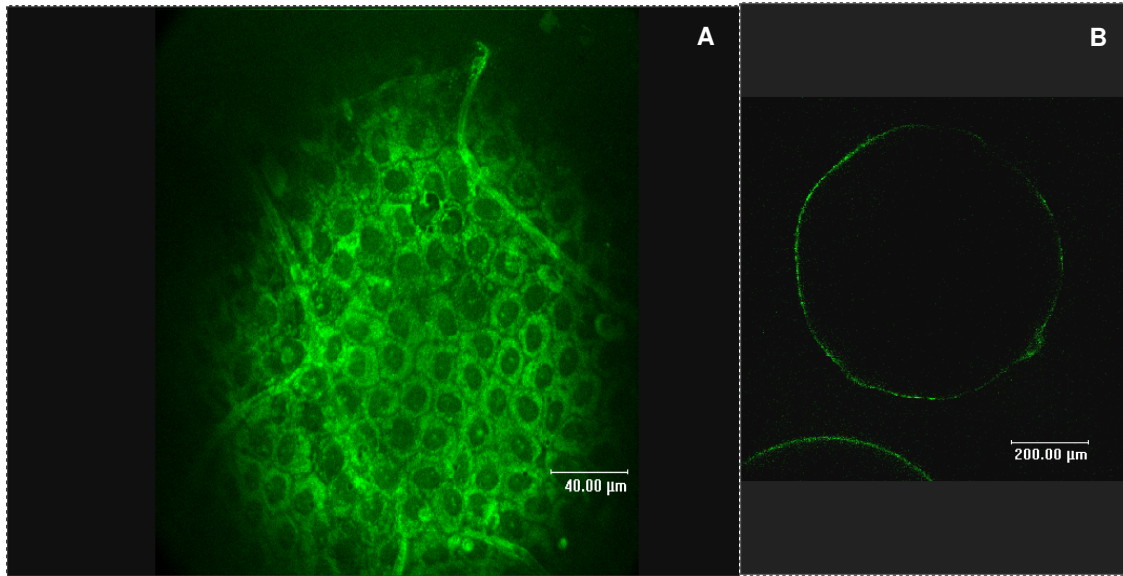


Fig. 4.2 Mitochondria distribution in stage III zebrafish follicle exposed to 5 μ M Mitotracker Green FM. The green represents mitochondria stained on the basis of the membrane potential. Mitochondria stained by Mitotracker green FM shows the same pattern obtained with JC-1 (A). (B) Optical section showing the incapacity of stain to penetrate in the oocyte.

4.2.2 Effect of mitochondrial inhibitors on mitochondria distribution and activity and on ATP concentration

Results from TB and GVBD tests showed that 0.01% Triton did not affect the ovarian follicle survival and did not compromise the GVBD (Fig 4.3). Whilst exposure to 0.1% Triton induced a decrease of ovarian follicle survival assessed by TB and also compromised the capability of ovarian follicles to go through GVBD.

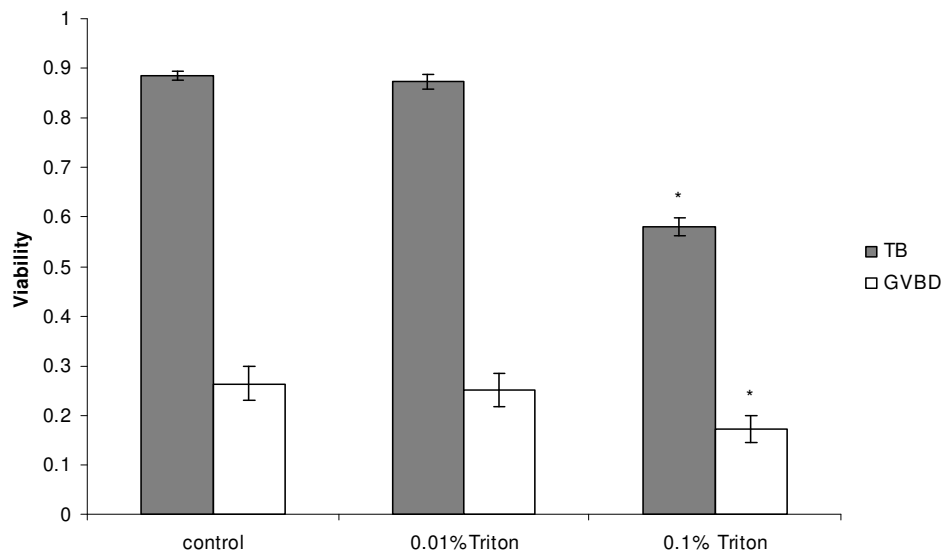


Fig 4.3 Ovarian follicle viability assessed by TB and GVBD tests following exposure to different concentration of Triton X-100 in Leibovitz L-15 medium. Control: TB and GVBD tests were undertaken after follicles separation from ovaries; 0.01% Triton: TB and GVBD tests were conducted after the exposure of follicles to 0.01% (v/v) Triton X-100 for 15 min; 0.1% (v/v) Triton: TB and GVBD tests were conducted after the exposure of follicles to 0.1% Triton X-100 for 15 min. Error bars represent S.E.M. Bars with different superscripts differ significantly ($P < 0.05$).

Images obtained after the exposure to Triton X-100 (between 40-50 ovarian follicles were examined) showed no effect of this substance on the follicle cells, as the same pattern of mitochondrial distribution was found (Fig. 4.4A-B-C); these results were also supported by the results of the ATP assay, which indicated no decrease of ATP in follicles exposed to 0.01% (v/v) Triton X-100 (Table 4.1). Results also showed that exposure of ovarian follicles to Triton X-100 alone, employed as a membrane permeabiliser, did not allow the penetration of mitochondrial probes into the oocytes (Fig. 4.5B).

Images obtained with the JC-1 after exposure of ovarian follicles to FCCP showed the loss of structural integrity when 5 or 50 μM FCCP (between 40-50 ovarian follicles were examined for each group) (Fig. 4.4D-E-F; 4G-H-I) was used. It was still possible to identify some green fluorescence, indicating that a certain level of membrane potential

(above background) still remained, although the mitochondria were no longer held in a well organised pattern. Images obtained with MitoTracker Green FM after the exposure of ovarian follicles to FCCP showed reduced fluorescence when 5 μ M FCCP (Fig. 4.5C) was used and the loss of structural integrity and fluorescence when 50 μ M FCCP was used (Fig. 4.5D).

Results obtained after the exposure to 0.01% (v/v) Triton X-100 showed that this substance had no effect on the intracellular ATP concentration, as there were no significant ($P > 0.05$) differences between the control follicles and those exposed to Triton X-100, whilst there were significant ($P < 0.05$) differences between the control follicles, the follicles exposed to Triton X-100 and those exposed to oligomycin for 15 and 30 min (Table 4.1). The concentrations of ATP within the follicle also showed a progressive decline after exposure to FCCP following a pre-treatment with 0.01% (v/v) Triton X-100 (15 min); there were also significant differences ($P < 0.05$) between the control follicles and the follicles treated with 5 μ M and 50 μ M FCCP for 15 min respectively (Table 4.2).

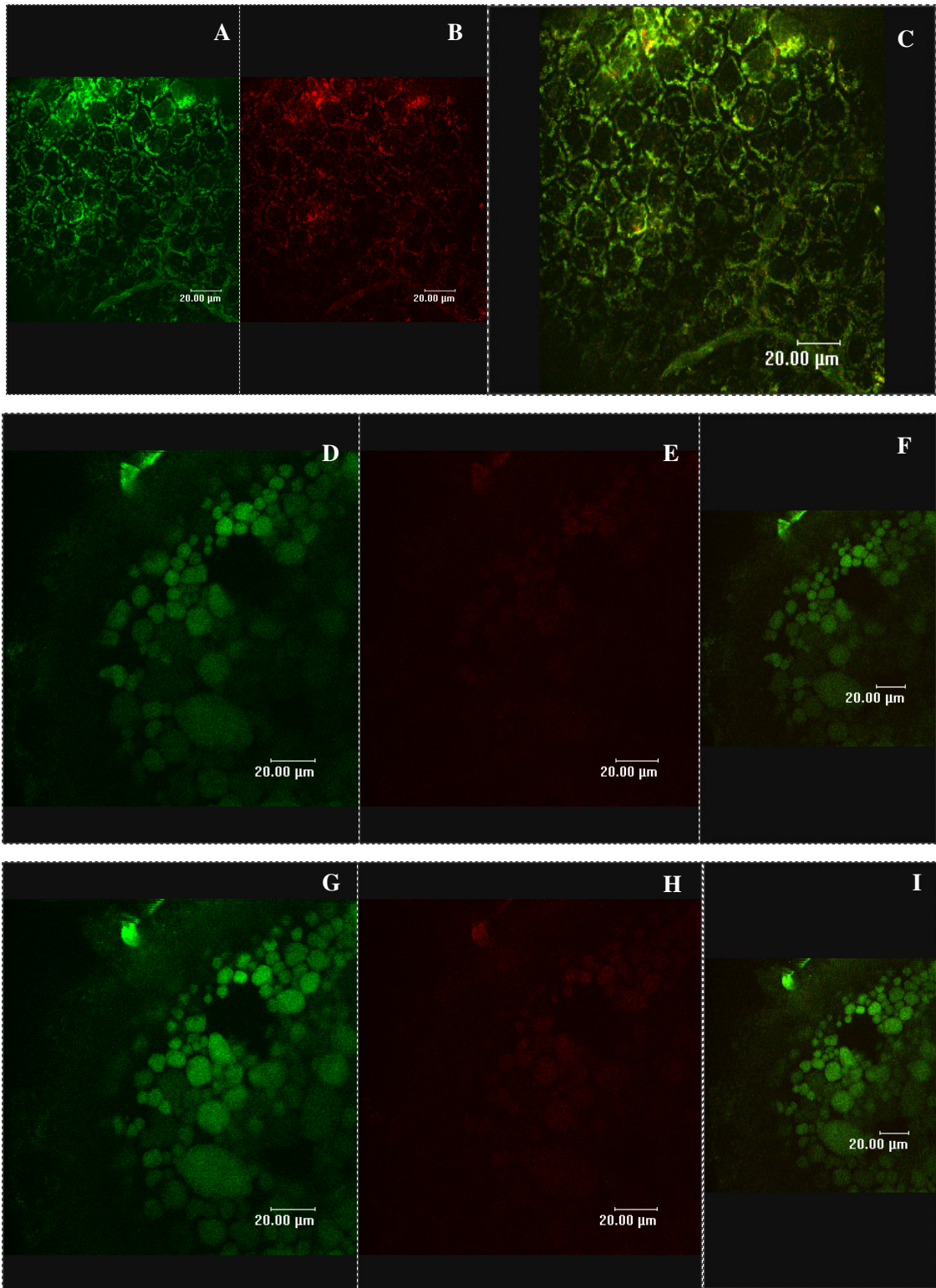


Fig 4.4 Mitochondria distribution in stage III zebrafish follicle exposed to 5 μM JC1 following a permeabilization treatment with 0.01% (v/v) Triton X-100 for 15 min (A,B,C) followed by 5 μM (D-F) or 50 μM (G-I) of FCCP in Hanks' solution for 15 min. FCCP causes a structural breakdown of the mitochondria patterns (D,G) and no red fluorescence was found (E,H). C, F and I represent merged images.

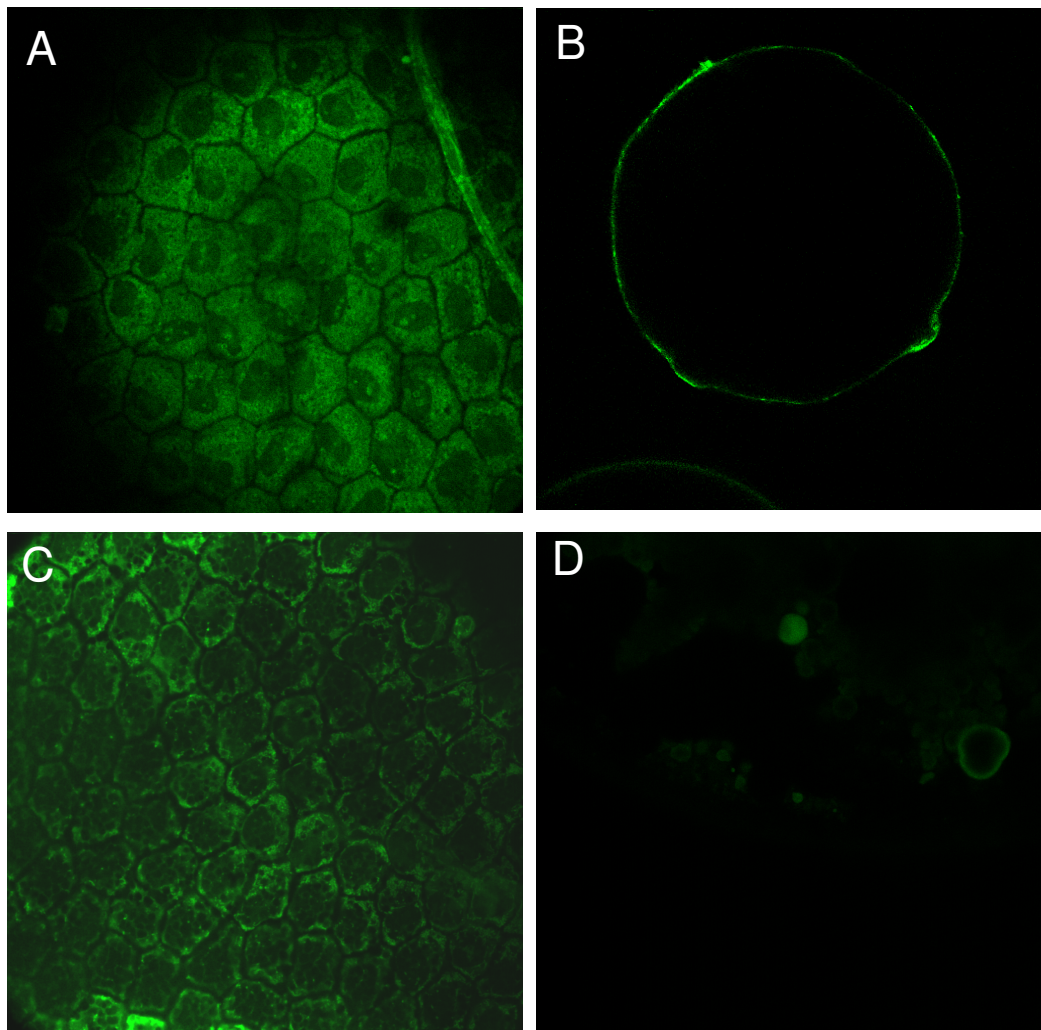


Fig. 4.5 Mitochondria distribution in stage III zebrafish follicle exposed to 5 μ M MitoTracker green FM following a permeabilization treatment with 0.01% (v/v) Triton X-100 for 15 min (A-B); followed by 5 μ M (C) or 50 μ M (D) of FCCP in Hanks' solution for 15 min. 5 μ M FCCP causes a decrease of green fluorescence (C) whilst 50 μ M FCCP causes a structural breakdown of the mitochondria patterns (D).

Table 4.1 Effect of oligomycin on ATP level in zebrafish stage III ovarian follicles

<i>Treatment</i>	<i>ATP concentration / ovarian follicle (Mol)</i>
Control	$1.51 * 10^{-11} \pm 2.19 * 10^{-12}$ a
0.01% (v/v) Triton X-100	$1.32 * 10^{-11} \pm 9.67 * 10^{-13}$ ab
0.01% (v/v) Triton X-100 + 100 μ M oligomycin (15 min)	$9.48 * 10^{-12} \pm 2.03 * 10^{-12}$ bc
0.01% (v/v) Triton X-100 + 100 μ M oligomycin (30 min)	$7.09 * 10^{-12} \pm 8.83 * 10^{-13}$ c

Data shown as mean \pm S.E.M. Data with different letter differ significantly (P < 0.05).

Table 4.2 Effect of FCCP on ATP level in zebrafish stage III ovarian follicles

<i>Treatment</i>	<i>ATP concentration / ovarian follicle (Mol)</i>
Control	$2.83 * 10^{-11} \pm 4.43 * 10^{-12}$ a
0.01% (v/v) Triton X-100 + 5 μ M FCCP	$1.93 * 10^{-11} \pm 4.37 * 10^{-12}$ b
0.01% (v/v) Triton X-100 + 50 μ M FCCP	$5.13 * 10^{-12} \pm 5.57 * 10^{-13}$ c

Data shown as mean \pm S.E.M. Data with different letter differ significantly (P < 0.05).

4.3 Discussion

This study has shown that mitochondria are spatially and systematically distributed within the granulosa cell layer (chapter 5) surrounding the oocytes in stage III zebrafish ovarian follicles and suggests a location-dependent function at this stage to support oocyte maturation.

To validate the mitochondrial staining, the mitochondrial inhibitor FCCP was used to uncouple mitochondrial oxidative phosphorylation. This compound is known as a proton ionophore that uncouples oxidation from phosphorylation by dissipating the chemiosmotic gradient while leaving the electron transport system functional (Mitchell and Moyle, 1967). As previously reported by Van Blerkom et al. (2003), the exposure of follicles to FCCP is characterized by the development of the characteristic pattern of fluorescence. In the zebrafish follicles the development of a characteristic pattern of fluorescence following FCCP exposure was also visible and it was accompanied by a loss of the organised spatial distribution of the mitochondria. Furthermore, after uncoupler treatment, mostly green JC-1 staining was observed, which was more diffused throughout the cells, indicating the loss of membrane potential. These findings are also in agreement with results obtained in *Xenopus laevis* oocytes (Wilding et al. 2001a), where FCCP caused the immediate destruction of the membrane potential and loss of fluorescence. Staining with MitoTracker green FM showed a loss of structure and decrease of green fluorescence. These results are in agreement with results previously reported by Keij et al. (2000) in HL60 cells, where exposure to common mitochondrial potential altering drugs caused fluorescence changes. These findings showed that FCCP caused a loss of membrane potential, a decrease of ATP, and a loss of mitochondrial spatial pattern. This suggests that ATP is essential for maintaining the correct spatial arrangement of mitochondria, and that mitochondria are held in a specific pattern by an energy-dependent process.

The well organised distribution of mitochondria shown by confocal microscopy analysis leads me to consider that the cytoskeleton could be involved in holding the mitochondria

in such a pattern and the results also suggest that this interaction between cytoskeleton and mitochondria is energy-dependent. The association of mitochondria with cytoskeleton fibrillar elements has been described previously. Mitochondrial distribution is established by movement along the cytoskeletal elements and by anchoring at the site where their function is required. They are concentrated in areas of increased energy consumption, where they provide ATP. Furthermore, Hall and Almahbobi (1997) reported the involvement of the cytoskeleton in the steroidogenic process and the interactions among mitochondria and microtubules, microfilaments and intermediate filaments in steroidogenic cells for the intracellular transport of cholesterol.

The presence of abundant and active mitochondria in the granulosa cells layer, shown by confocal microscopy, was also supported by electron micrographs (chapter 5), confirming that the layer stained by the mitochondria-specific probes was the granulosa cell layer.

The selective probes, JC-1 and MitoTracker Green FM, allowed mitochondrial distribution and activity to be determined. JC-1 staining showed a more definite structure, probably due to the characteristics of the dye. JC-1 responds differentially to high or low membrane potential. In cells with intact mitochondria, JC-1 accumulates in the mitochondria as aggregates and exhibits a fluorescence emission shift from red (600 nm) to green (525 nm) (Reers et al., 1991, 1995; Smiley et al., 1991; Chen et al., 1993; Plasek and Sigler, 1996). JC-1 has been used in somatic cells, amphibian oocytes (Wilding et al. 2001a), and mammalian oocytes and embryos (Wilding et al., 2001b, Van Blerkom et al., 2002; Van Blerkom, 2004). Images from confocal microscopy showed the presence of mitochondria both with high and low membrane potential, this is in accordance with what has been reported by Zhang et al. (2008) in early stage zebrafish oocyte, where the green and red fluorescence intensity were almost the same in the oocyte. This phenomenon could be due to a metabolic turnover, as mitochondria have different roles at this stage of folliculogenesis, not only as source of ATP but also of cAMP and in steroidogenesis. MitoTracker Green FM stains only metabolically active mitochondria, as it accumulates in mitochondria regardless of mitochondrial membrane potential.

The results obtained by confocal microscopy showed the inability of the mitochondrial stains to penetrate the oocyte. Even after exposure to Triton, no mitochondrial staining in the ooplasm was found. This is probably due to the low permeability of the thick vitelline envelope which surrounded the zebrafish oocytes (Selman et al., 1993), as TEM results showed randomly dispersed mitochondria in the oocytes (discussed in chapter 5). Exposure to Triton X-100 had no effect on the follicle cells as the same pattern of mitochondria distribution was found with JC-1 and MitoTracker green FM staining, results also supported by the ATP production assay which indicated no decrease of ATP in follicles exposed to 0.01% (v/v) of Triton X-100. Exposure to Triton X-100 did not affect the viability and the capacity of ovarian follicle to undergo through GVBD.

The spatial organisation of mitochondria in the granulosa cell layer observed by confocal microscopy in stage III zebrafish ovarian follicles is reported here for the first time. The decline of ATP following FCCP exposure and the results obtained by confocal microscopy showing decrease of fluorescence and loss of peripherally contiguous aggregation of mitochondria after the exposure to FCCP support the hypothesis that the mitochondria distribution in the granulosa cells of zebrafish stage III ovarian follicle is energy dependent.

4.4 Summary

Fluorescent probes, JC- 1 (5,5',6,6'-Tetrachloro-1,1',3,3'-tetraethyl-imidacarbocyanine iodide) and Mitotracker green FM, have been used to investigate mitochondrial distribution and activity in stage III zebrafish ovarian follicles by confocal microscopy. The distributional arrangement of mitochondria in the granulosa cell layer is reported here for the first time. Mitochondria exhibited a contiguous distribution at the margin of the granulosa cell layer surrounding stage III zebrafish oocytes (chapter 5); the pattern became disrupted when the follicle-oocyte complexes were exposed to the mitochondrial inhibitor carbonyl cyanide 4-(trifluoromethoxy) phenylhydrazone (FCCP). This suggested that the distribution of mitochondria is itself energy dependent. This hypothesis was verified by the fact that both FCCP and oligomycin treatments reduced the concentrations of ATP in the oocytes. These results lead the conclusions that

maintenance of the spatial mitochondrial distribution in the zebrafish stage III ovarian follicle is an energy dependent process.

To confirm the location of mitochondria within the ovarian follicle shown by confocal microscopy and also to confirm that the mitochondrial probes were unable to penetrate the oocytes, it was decided to undertake cryo- and transmission-electron microscopy studies (reported in Chapter 5).

Chapter 5: Examination by Scanning Electron Microscopy (SEM) and Transmission Electron Microscopy (TEM) of stage III zebrafish (*Danio rerio*) ovarian follicle structure to support observations of mitochondria distribution obtained by confocal microscopy

5.1. Introduction

In this study, Cryo-SEM and TEM analyses were undertaken to identify the mitochondrial probe-stained layer obtained in the confocal microscopy studies with stage III ovarian follicles isolated by enzymatic method. The confocal studies were based on optical sections and surface views of external ovarian follicle stained for mitochondria. This microscopy technique did not allow the precise location of the mitochondria-stained layer to be identified. Cryo-SEM and TEM studies could provide these details.

These studies also allowed a comparison to be made of ovarian follicles isolated by mechanical and enzymatic separation following the Guan et al. (2008a) protocol. This part of my study was carried out to determine whether there were any differences between the two treatments with regard to possible removal of any of the cellular layers which surround the oocyte during its development. Zebrafish ovarian follicles have been previously separated from ovaries mechanically and the method is laborious and time consuming (Plachinta, 2007). A new method of separating ovarian follicles was recently developed by Guan et al. (2008a) to obtain large numbers of morphologically intact zebrafish ovarian follicles at different stages of development. 1.6 mg/ml hyaluronidase treatment for 10 min at 22 °C has been reported as the optimal enzymatic separation, following this treatment survival rates of $96.6 \pm 0.7\%$, $92.9 \pm 1.3\%$ and $94.6 \pm 0.9\%$ for stages I, II and III oocytes, respectively using trypan blue staining have been reported (Guan et al. 2008a).

5.2 Results

5.2.1 Cryo-SEM

Cryo-SEM and TEM analyses of stage III ovarian follicles were undertaken to identify the mitochondrial probe-stained layer obtained in the confocal microscopy studies and also to assess the effect of mechanical and enzymatic separation on ovarian follicle structure. Preliminary results obtained by Cryo-SEM did not allow the layer to be identified (Fig. 5.1A-B), but the fracture surface inside the ovarian follicle, obtained by Cryo-SEM, showed a hexagonal-polygonal structure surrounding the oocyte (Fig 5.1C). Each hexagonal-polygonal structure had a diameter of 10-15 μm (Fig. 5.1C).

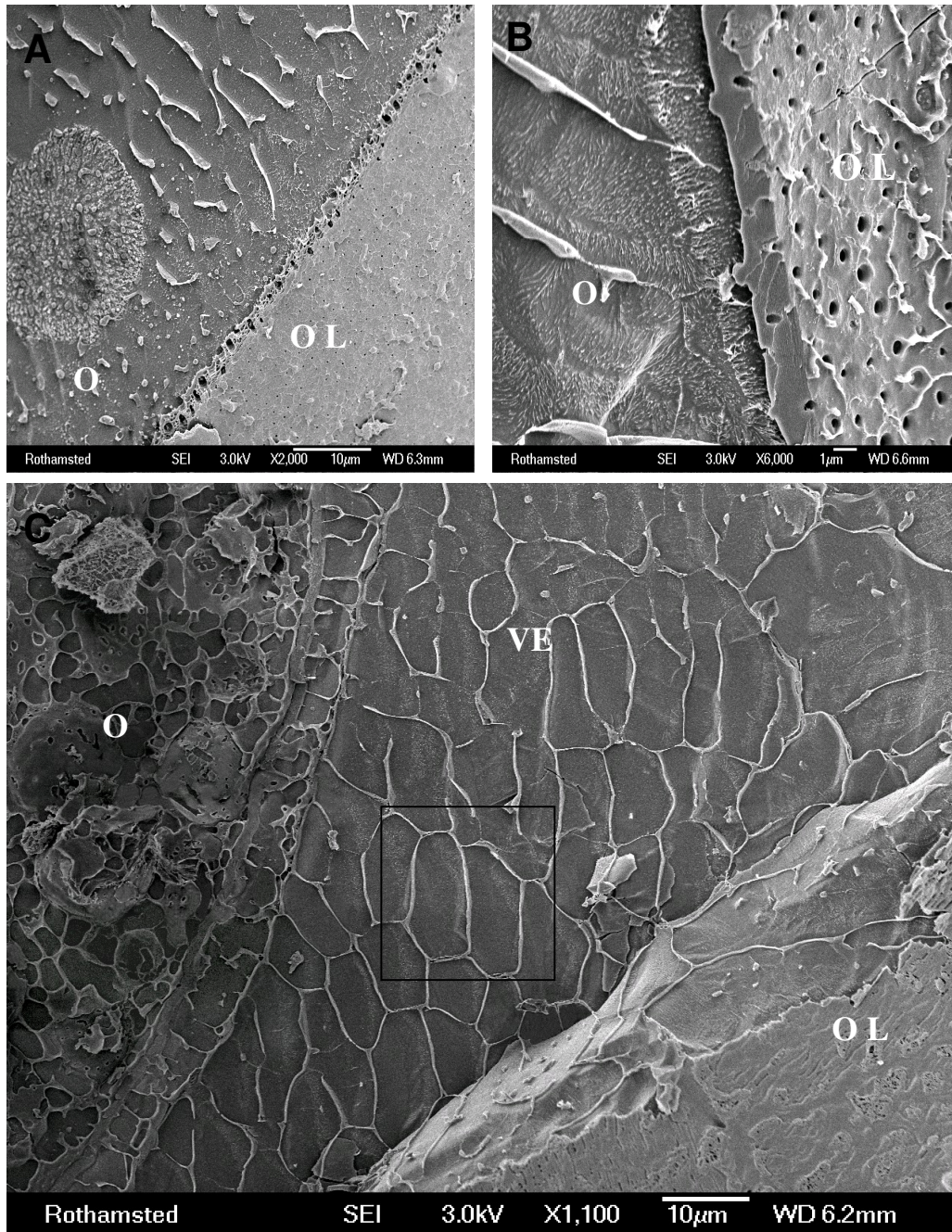


Fig. 5.1 Micrographs of stage III follicle obtained by Cryo-SEM (A-B) showing the oocyte (O) and the outer layer (OL). (C) Fracture surface inside stage III ovarian follicle obtained by Cryo-SEM. Particular hexagonal - polygonal structure belonging to the vitelline envelope (VE), which surrounded the oocyte (O), is shown. Each hexagonal – polygonal structure has a diameter of 10 – 15 μm (square). Bar, 10 μm.

5.2.2 TEM

TEM results for the granulosa cell layer showed characteristics of steroid secreting cells, with abundant round, oval and elongated mitochondria with tubular cristae. (Fig. 5.2A-B). Furthermore, it was possible to observe granulosa cells containing features suggestive of protein synthesis i.e. elongate mitochondria, electron dense material, tubular rough endoplasmic reticulum (RER) and abundant free ribosome (Fig. 5.2C).

The oocyte surface displayed endocytic activity during vitellogenesis (Fig. 5.3A); the cortical cytoplasm contained yolk bodies, cortical alveoli and mitochondria that seemed randomly dispersed (Fig. 5.3B-C). The external layer of the vitelline envelope is characterized by masses of dense material (Fig. 5.5D-3D). The surface of the oocyte presented numerous microvilli, which are long and penetrate the pore canals of the vitelline envelope (Fig 5.4).

From the TEM results, it was ascertained that the both mechanical and enzymatic method of follicles separation from the ovaries induced the removal of the surface epithelium and may induce the removal of the thecal layer or damage the thecal layer. As shown in Fig. 5.5 the follicles derived from both methods of separation showed an oocyte surrounded by the vitelline envelope, the granulosa cells layer and the thecal layer which is separated from the follicle layer by a basal membrane. From the Fig 5.5D was actually possible see that part of the thecal layer has been completely removed.

Although, the TEM preparation could induce artefacts, in this case the samples from both treatments were processed simultaneously for TEM specimens preparation, for this reason no difference due to artefacts should be present.

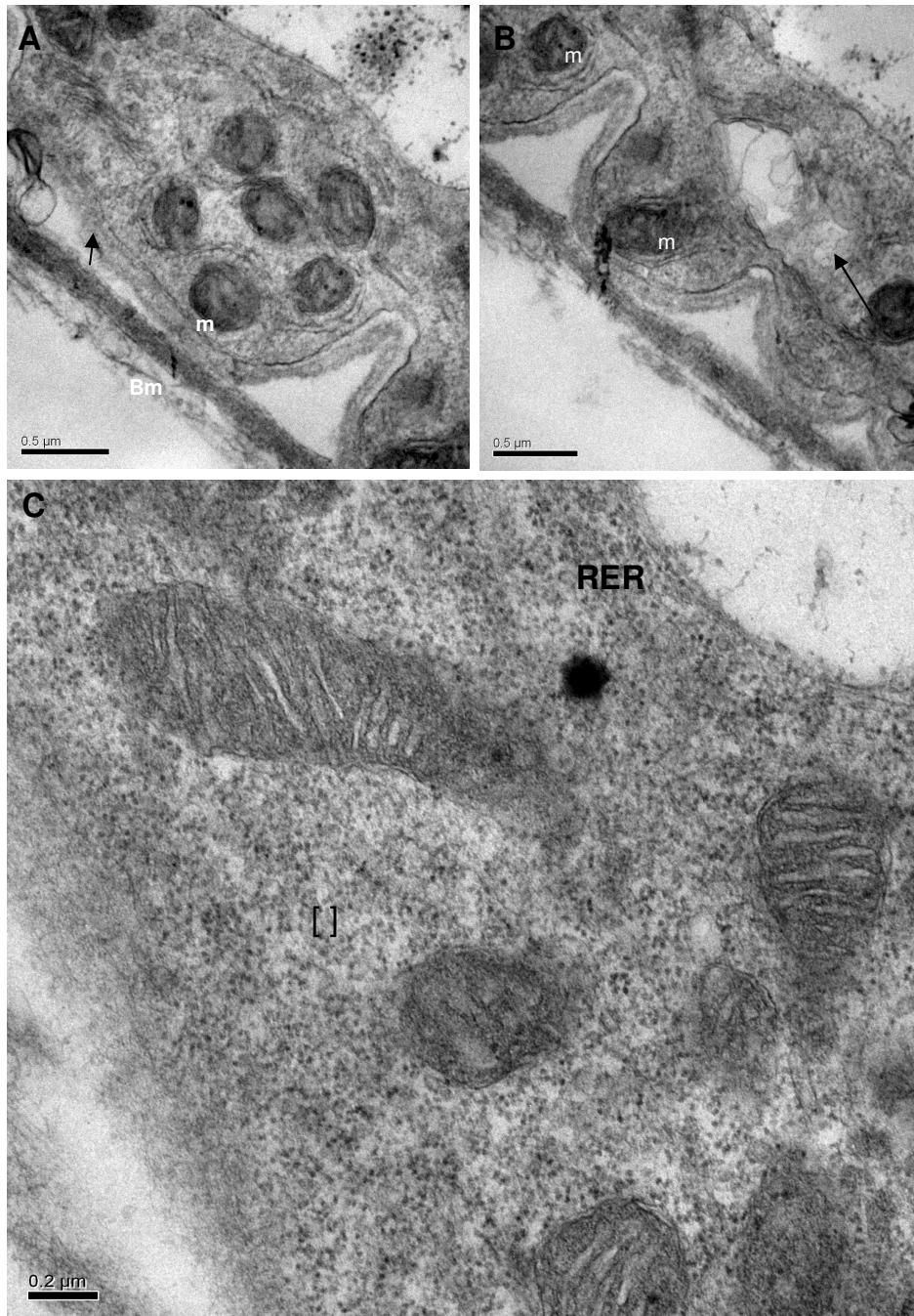


Fig. 5.2 (A-B) High-power TEM showing a portion of a granulosa cell, which presents steroids producing cells features: round and oval mitochondria (m), abundant globular smooth endoplasmic reticulum (arrows), basement membrane (Bm). (C) Electron micrograph of granulosa cell of vitellogenic follicle, which contains abundant free ribosomes (square), elongated mitochondria and rough endoplasmic reticulum (RER).

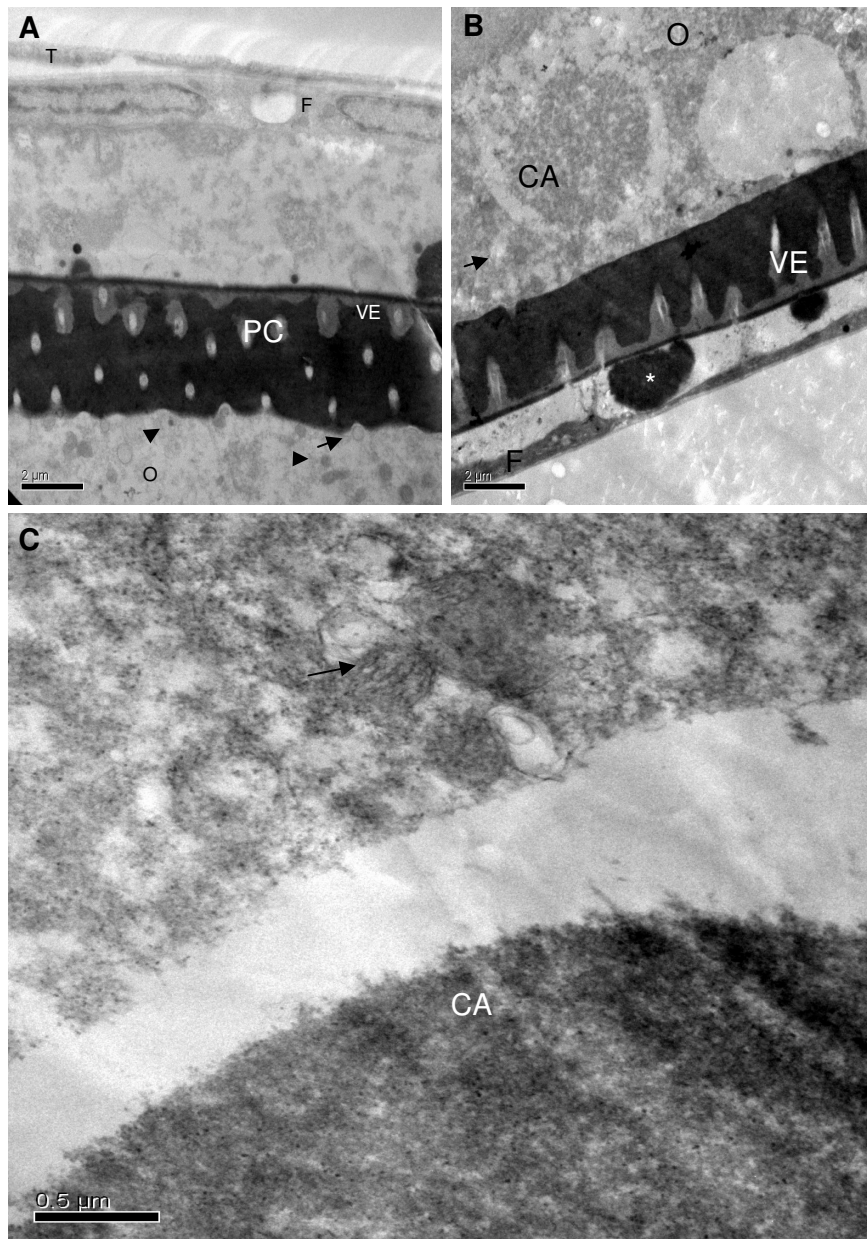


Fig. 5.3 (A) Electron micrograph of stage III follicle separated using enzymatic method, showing the layers (VE-vitelline envelope, F-granulosa cells layers, T-thecal layer) of a vitellogenic oocyte (O). The oocyte displays endocytic activity (arrows). The vitelline envelope shows pore canals (pc). (B) Electron micrograph of stage III follicle separated using mechanical method, indicating cortical alveoli (CA) and mitochondria (arrow) in the ooplasm (O). The vitelline envelope (VE) shows masses of electron dense material (*) next to its external surface. (C) High-power TEM in the ooplasm of a portion of developing cortical alveoli (CA) with a distinct central core surrounded by light flocculent material. Mitochondria appear randomly dispersed (arrow) in the ooplasm.

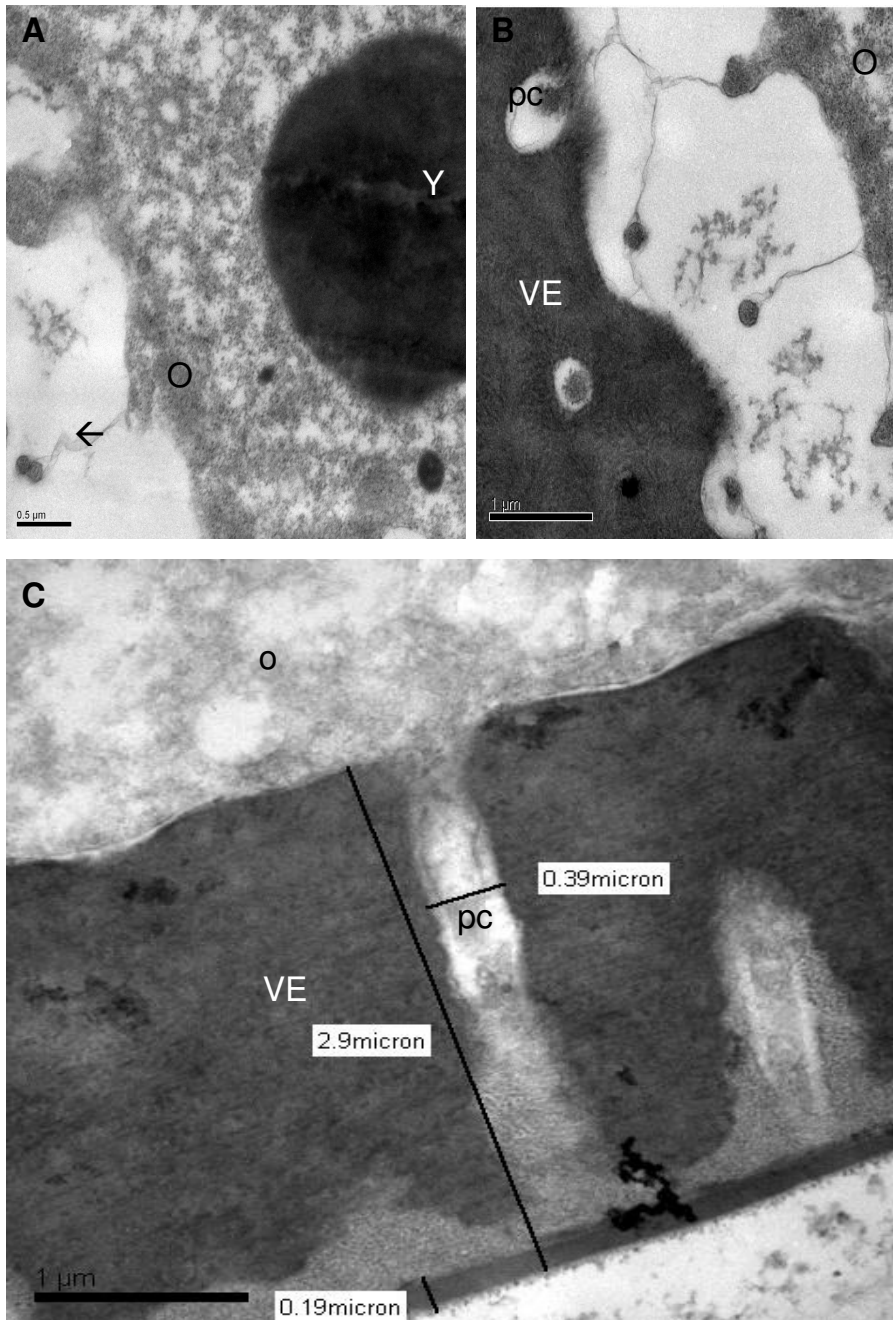


Fig. 5.4 (A) High-power TEM indicating the cortical cytoplasm of the oocyte (O). Yolk body (Y) has a smooth contour, homogeneous interiors. Microvilli (arrow) from the oocytes extend to the follicle cells through the vitelline envelope. (B) High-power TEM showing microvilli from the oocyte (O) passing through are the pore canals (pc) of the vitelline envelope (VE). (C) High-power TEM showing the pore canals (pc), diameter of 0.39 micron, of the vitelline envelope (VE). The vitelline envelope has a thickness of 2.9 micron and an outer layer of 0.19 micron.

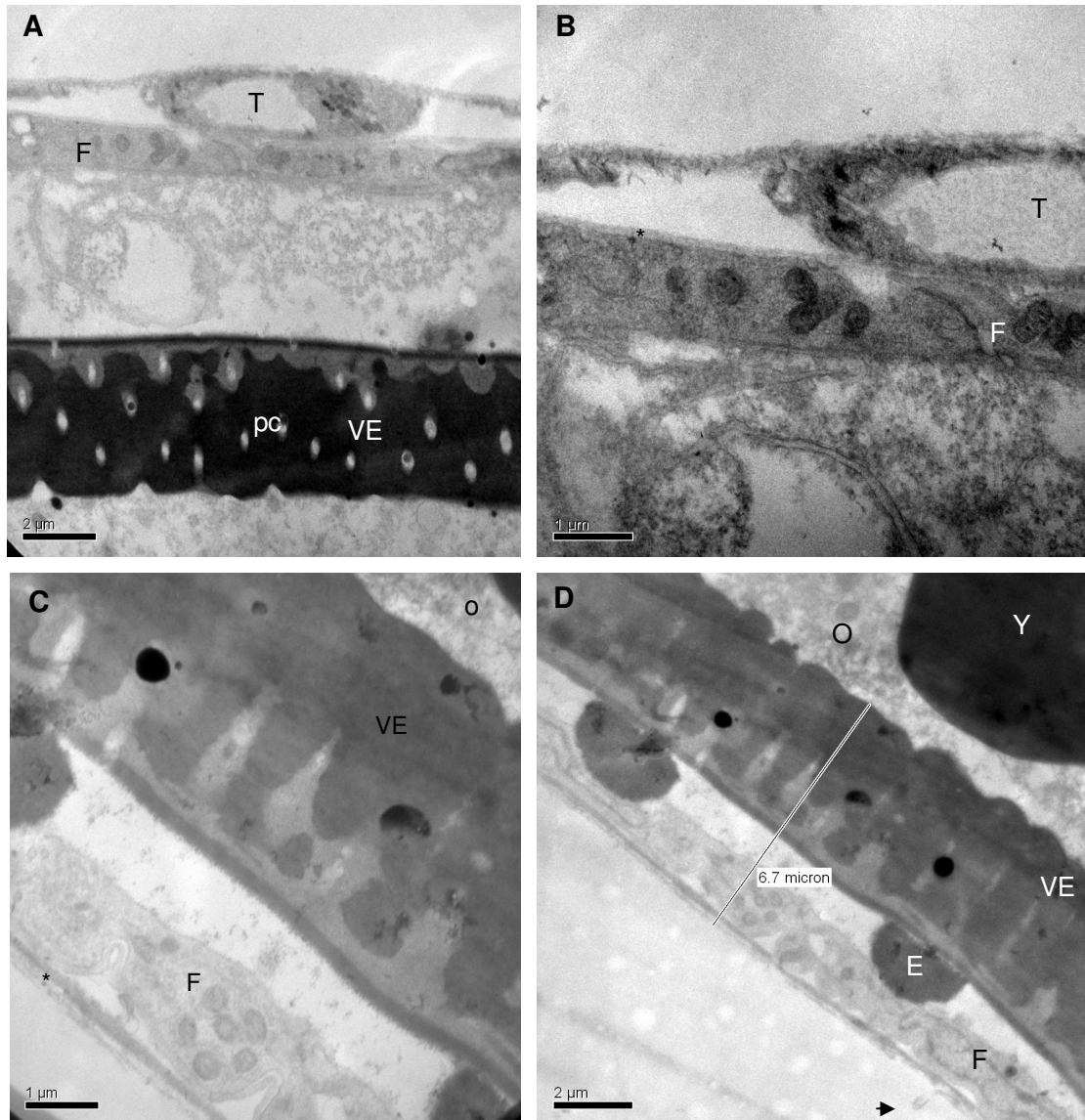


Fig. 5.5 Electron micrographs of stage III follicle separated using enzymatic (A-B) and mechanical (C-D) method. The ooplasm (O) was surrounded by the vitelline envelope (VE), which showed pore canals (pc). External to the granulosa layer (F) was the thecal layer (T). In micrograph D, part of the thecal layer (arrow) has been removed by the mechanical separation. The granulosa cell layer remains (F) beneath the basal lamina. Electron dense material (E) between the follicle cell and the vitelline envelope (VE).

5.3 Discussion

Cryo-SEM did not allow the identification of the layer stained by mitochondrial probes in the confocal microscopy study (chapter 4) and also it did not identify any differences between enzymatic and mechanical methods of separation of ovarian follicles. However, the fracture surface obtained by Cryo-SEM showed a polygonal patterns. The polygonal patterns could be due to the presence of a hexagonally structured egg envelope, as reported for Sole (*Pleuronichthys coenosus*), where ultrastructural evidence has shown (Stehr and Hawkes, 1983; Wallace and Selman, 1990) that a single granulosa cell is associated with each hexagonal chamber. In support of this hypothesis, comparison of the follicle cells from the confocal images (discussed in chapter 4) with the polygonal structure obtained by cryo-SEM, showed they had similar dimensions of 10-15 μm . From cryo-SEM micrographs this polygonal structure seems to belong to the vitelline envelope. These results suggested that the granulosa cells are polygonally shaped and the fact that the mitochondria are arranged in such a pattern at the periphery of the granulosa cells surrounding the nucleus, suggesting the presence of nuclear-mitochondria interactions and also the association of mitochondria with the plasma membrane. These possible interactions need further investigation.

The TEM results showed that both the enzymatic and the mechanical methods of follicles separation from the zebrafish ovaries induced the removal of the surface epithelium and may also induce the removal of the thecal layer.

The presence of abundant and active mitochondria in the granulosa cells layer, shown by confocal microscopy (discussed in the chapter 4), was also supported by electron micrographs confirming that the layer stained by the mitochondria-specific probes was the follicular layer. This layer was rich in mitochondria, and showed features consistent with steroid secreting cells; i.e. abundant round and oval mitochondria with tubular cristae, elongated mitochondria and smooth endoplasmic reticulum (Prince, 2002; Srijunngam et al., 2005). The granulosa cells and thecal cells have previously been shown to be sites of steroid synthesis in the teleost ovary (Nagahama et al., 1994; Nakamura and Nagahama, 1985; Nakamura et al., 1993; Petrino et al., 1989). The abundant

mitochondria in the follicular cells could have a role in the synthesis of steroids (Crivello and Jefcoate, 1980; Privalle et al., 1983).

The first, and also the rate-determining, step (Jefcoate, 2002) in steroid biosynthesis is the transport of cholesterol to the inner mitochondria membrane by the steroid acute regulatory protein (StAR) (Stocco and Clark, 1996; Stocco et al. 2005; Miller 2007), where it is converted by enzymes of the cytochrome P450 superfamily and auxiliary electron transferring proteins into pregnenolone (Catt et al., 1980; Jefcoate, 2002). Also Papadopoulos et al. (2007) reported, in a detailed review, the possible involvement of a larger multimeric mitochondrial complex of proteins assembled to facilitate the import of the cholesterol into mitochondria.

From the results of TEM study, it was not possible to identify the presence of the special thecal cells in ZF, as previously reported by Selman et al. (1993), and in some other teleosts by Srijunngam et al. (2005). One possibility is that they were removed during both the mechanical and enzymatic separation. The special thecal cells were reported (Selman et al., 1993) to have the characteristics of active steroid producing cells with abundant round and oval mitochondria with tubular cristae and elongated mitochondria.

It has been reported (Nagahama, 1987; Matsuyama et al., 1991) that granulosa cells of vitellogenic oocytes of several teleosts contain organelles typical of protein secreting cells. The protein secreting character of these cells correlates with the fact that there is a high level of production of enzymes involved in the conversion of steroid precursor (Guraya, 1986), and furthermore, it could be involved in the synthesis of the vitelline envelope. Similarly, the granulosa cells of vitellogenic oocytes in zebrafish contained features suggestive of protein synthesis i.e. elongate mitochondria, electron dense material, tubular rough endoplasmic reticulum (RER), and abundant free ribosomes. Free ribosomes usually make proteins that will function in the cytosol, while bound ribosomes produce proteins that are exported or included in the cell's membrane (Alberts et al., 1995).

The external layer of the vitelline envelope was characterized by the presence of dense materials. As reported by Selman et al. (1989, 1993), the formation of this dense material starts during stage II and gets larger and remains associated with the vitelline envelope throughout development and ovulation. The origin, composition and function of these aggregates have not been determinate, but they may be homologous to the chorionic fibrils associated with the vitelline envelope of other teleosts (Selman et al., 1993).

Selman et al. (1993) have already reported the presence of endocytic vesicles at the periphery of the oocyte. Le Mann et al (2007) described the role of these vesicles as being involved in the transfer of vitellogenin towards the multivesicular bodies (MVB) centripetally. The MVB are coated vesicles containing vitellogenin, fuse with lysosomes and they originate from the Golgi apparatus (Busson-Mabillot, 1984; Wallace and Selman, 1990). Whereas dense-cored vesicles originating from the Golgi apparatus reach the oolemma centrifugally to deposit the zona radiata interna at the oocytes surface by exocytosis. Furthermore, the same authors reported that large numbers of endocytic vesicles bud off from the oocyte cytoplasm near the bases of the oocyte microvilli, in correlation with the enormous amount of yolk stored in the oocyte.

From TEM micrographs it was also possible to observe numerous microvilli. The presence of the microvilli, which extended from both the oocyte and the follicle cells, has been already reported by Selman et al. (1993). These microvilli from both cells lie within the same pore canals, which perforate the vitelline envelope.

5.4 Summary

In this part of the study, SEM and TEM were carried out to confirm the results obtained by confocal microscopy (described in chapter 4), investigating mitochondrial distribution within the ovarian follicle. These studies were undertaken to identify the mitochondrial probe stained layer obtained in the confocal microscopy study. The effects of the two ovarian follicles isolation procedures were also investigated. Ovarian follicles obtained both from mechanical separation and enzymatic separation were used for preparation of specimens for Cryo-SEM and TEM. Micrographs obtained by TEM showed that the

granulosa cell layer was rich in mitochondria. Furthermore, TEM images showed randomly dispersed mitochondria in the oocyte, which were not stained by the mitochondrial probes used in confocal microscopy study described in chapter 4, leading to the conclusion that the mitochondrial stains were unable to penetrate into the oocytes. Associated cryo-electron microscopy studies also showed that the follicle surface is covered by an hexagonal-polygonal pattern of ridges with the same geometric dimensions as indicate by the fluorescent staining of mitochondria. Micrographs obtained also showed that there were no differences between enzymatic and mechanical separation. However, both enzymatic and mechanical separation may induce the removal of the epithelial cells and part of the thecal cell layer of the follicle.

Chapter 6: Evaluation of mitochondrial activity and distribution as biological marker in stage III ovarian follicles of zebrafish (*Danio rerio*) following CPAs exposure

6.1 Introduction

Each late stage ovarian follicle of the zebrafish is a complex system of acellular and cellular structures surrounding the developing egg, the oocyte. The large size of fish ovarian follicles, their high yolk content and their chilling sensitivity (Isayeva et al. 2004) have been a barrier to their successful cryopreservation. Previous cryopreservation studies have focused on the use of cryoprotectants (CPAs) to reduce the risk of chilling injury and intra-cellular ice formation. CPAs can suppress most cryoinjuries but when used at high concentrations, they become toxic to biological material (Leung, 1991).

Detailed information on the toxicities of cryoprotectants is essential for the development of cryopreservation protocols for ovarian follicles. To date, the effect of cryoprotectants on zebrafish ovarian follicles has been evaluated only by viability tests such as Trypan Blue (TB) staining, thiazolyl blue MTT test, Fluorescein diacetate (FDA) and Propidium iodide (PI) and by the observation of germinal vesicle breakdown (GVBD) (Plachinta et al., 2004a; discussed in chapter 3). These tests have known limitations, they are stage-specific as in the case of GVBD or evaluate only one (TB, MTT) or two (FDA-PI) parameters. However, there are other possible subtle impacts of CPAs use which may not result in cell death, but can compromise future development.

The detrimental effect of cryoprotectants may be osmotic or due to direct biochemical injury. Osmotic injury results from changes in cell volume which may be induced by cryoprotectant addition or removal (Renard and Cochard 1989). The biochemical injury could be due to direct interaction of cryoprotectant and cell enzymes or by indirect action of cryoprotectant by altering the environment of cellular biomolecules that can modify redox potential, dielectric constant, ionic strength, pH, and surface tension (Adam et al., 1995; Arakawa et al., 1990; Fahy, 1986a). Mitochondria are susceptible to

cryopreservation damage (O'Connell et al., 2002), and can mediate both apoptosis and necrosis (Green, 1998).

Mitochondria have a wide range of cellular functions that affect metabolism and reproduction. They are responsible for the production of most cellular energy, in the form of ATP, through oxidative phosphorylation, and are also implicated in triggering cell aging and death (apoptosis) following cellular insult. Quantitative variation in mitochondrial DNA (mtDNA) has been associated with gamete quality and reproductive success in other animals (Hiendleder and Wolf, 2003; Tamassia et al., 2004), including humans (May-Panloup et al., 2005, Díez-Sánchez et al., 2003). The number of mitochondria and mitochondrial genomes or DNA molecules vary between tissues (Moraes 2001). Different factors are involved in the maintenance of mtDNA copy number in animal cells, although the mechanism by which mtDNA levels are controlled is uncertain.

The quantity of mitochondria in the oocyte affects its ability to produce ATP (Van Blerkom et al., 1998). Measurement of ATP content is a common method to quantify cellular energetics because the maintenance of high intracellular ATP means that mitochondria and the ATP- generating mechanism are functionally intact.

The aim of this study was to investigate the use of mitochondrial distribution and function as biological marker to assess ovarian follicle quality following CPAs exposure. The effects of methanol and DMSO, known to be the least toxic to zebrafish ovarian follicles (Isayeva et al., 2004, Plachinta et al., 2004a), on mitochondria of stage III ovarian follicles were evaluated. Mitochondrial activity and distribution were investigated using confocal microscopy with the mitochondrial probe JC-1. To further investigate the effect of methanol, quantitative methods were considered. The determination of ovarian follicle mtDNA copy number, measurements of ATP and ADP/ATP ratio were undertaken following cryoprotectant exposure. The effect of DMSO, a more toxic cryoprotectant to zebrafish ovarian follicles was also investigated,

to determine whether mitochondrial function was decreased further with a potentially more toxic CPA.

As set out in the Materials and Methods section (Chapter 2), in these studies assessments of viability evaluation were undertaken 1 and 5 h following 30 min CPA exposure and removal of CPA.

6.2 Results

6.2.1 Effect of methanol assessed by confocal microscopy

It has been previously demonstrated that methanol was a relatively non-toxic CPA, the No Observed Effect Concentrations (NOECs) for stage III ovarian follicle was > 3 M assessed by GVBD, TB and FDA-PI tests (see chapter 3). In order to determine whether this CPA had any effect on mitochondria, JC-1 staining was carried out. This allowed observation of changes in distribution, network formation, and membrane potential ($\Psi\Delta m$). The results obtained using confocal microscopy after exposure of zebrafish stage III ovarian follicles to methanol showed that even low concentrations of methanol induced changes in mitochondrial membrane potentials in the granulosa cells which surrounded the oocyte, resulting in a loss of red fluorescence and decrease of green fluorescence (Fig 6.1 C, D, E, F, G, H, I, J) compared with control group (Fig. 6.1A, B). Red fluorescence, an indicator of mitochondria with high membrane potential, decreased with 2M methanol, whilst higher concentrations, 3 or 4 M, also caused a loss of the mitochondrial distribution pattern (6.1 G, H, I, J)

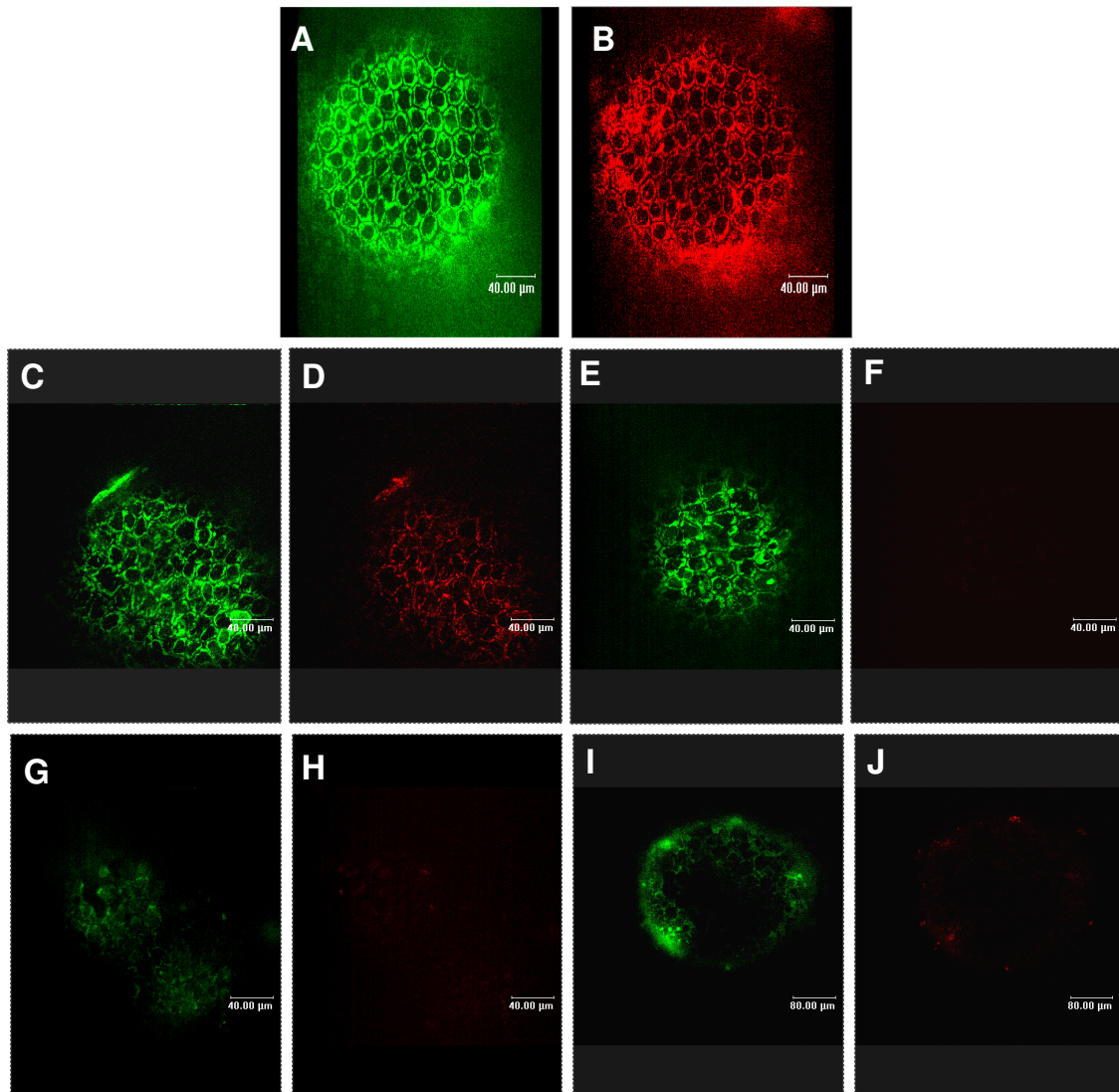


Fig. 6.1 Mitochondrial distribution in stage III zebrafish follicle exposed to 5 μ M JC1. JC-1 is a sensitive marker for mitochondrial membrane potential ($\Delta\Psi_m$). JC-1 accumulates in monomeric form within the mitochondrial matrix and its fluorescence emission characteristics are a function of the magnitude of $\Delta\Psi_m$. Low polarised organelles fluoresce green, while higher polarised organelles fluoresce red, owing to multimerisation of JC-1 and formation of J-aggregates. The green represents mitochondria with low membrane potential while the red represents those with high membrane potential. Effect of different concentrations of methanol on mitochondrial membrane potential are shown (C, D, E, F, G, H, I, J) in zebrafish stage III ovarian follicles. 1 M methanol causes a decrease in both green (C) and red (D) fluorescence. 2 M methanol also causes a decrease in green fluorescence (E) and loss of red fluorescence (F). 3 M (G, H) and 4 M methanol (I, J) cause a structural breakdown of the mitochondrial patterns.

6.2.2 Viability assessed by TB and FDA-PI staining

In order to determine the toxicity of two commonly used CPAs, methanol and DMSO, two viability assessments were carried out after 1 and 5 h incubation post-treatment. The viability of ovarian follicles assessed by TB and FDA-PI staining at 1 h after the CPA removal is not presented here as these data have been previously discussed in chapter 3. No Observed Effect Concentrations (NOECs) for stage III ovarian follicle were > 3 M and 1M for methanol and DMSO, respectively (see chapter 3).

There was a decrease of viability of the control groups following 5 h incubation at 27°C in Hanks' solution when the viability was assessed by both TB and FDA-PI. However, there were no significant differences ($P > 0.05$) between the control group at 5 h post-treatment and the equivalent groups treated with methanol when the viability was assessed by TB. When FDA-PI was used, there were significant decreases in viability after 5 h incubation following 30 min exposure to 3 or 4 M methanol (Fig. 6.2A).

There were no significant differences between the control group after 5 h incubation and the groups treated with 1 M DMSO when the viability was assessed by TB. When assessed using FDA-PI staining, there were significant decreases in viability after 5 h incubation following DMSO removal (Fig. 6.2B). Methanol was the least toxic cryoprotectant to zebrafish ovarian follicles, as there were significant decreases in viability after 5 h incubation following 30 min exposure to 3 or 4 M methanol assessed by FDA-PI; DMSO was more toxic to stage III follicles as it significantly reduced the viability of follicles when assessed both by FDA-PI or TB (Fig. 6.2B).

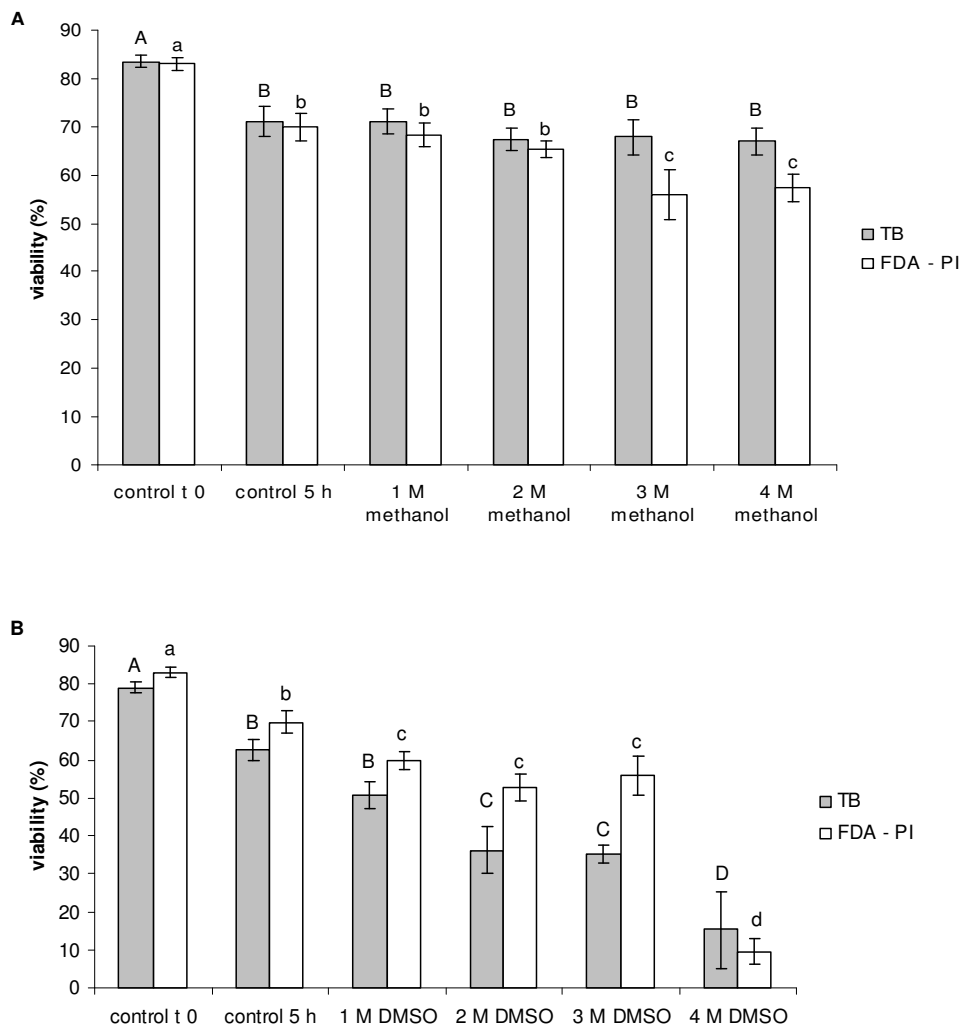


Fig. 6.2 Viability assessed by TB and FDA – PI staining after exposure to methanol (A) or DMSO (B) followed by incubation in Hanks' solution for 5h at 27°C. Bars and error bars represent means \pm SEM of three experiments each with three replicates. Bars with different superscripts differ significantly ($P < 0.05$).

6.2.3 Effect of cryoprotectants on mtDNA copy number

As mtDNA copy number is reported to correlate with mitochondrial number and potential activity, mtDNA copy number was measured to enable quantification of the effect of cryoprotectant incubation. Results showed that there were no significant differences ($P>0.05$) between the control and treated follicles when the mtDNA copy number was evaluated 1 h after the 30 min exposure to methanol (Fig. 6.3A). Since no effect was observed at 1 h post-treatment, the mtDNA copy number was measured at 5h after 30 min CPA exposure. There were significant ($P<0.05$) decreases in mtDNA copy number between untreated follicles and those exposed to concentrations of 3 or 4 M methanol when the mtDNA copy number was evaluated 5 h following the removal of the cryoprotectant (Fig. 6.3A). Furthermore, there were significant differences between the groups assessed for mtDNA copy number after 1 h incubation and those measured after 5 h incubation following methanol treatment when 2, 3 or 4 M was used, which was not the case for control samples. As effects were observed with a relatively non-toxic CPA, it was investigated whether a larger effect would be observed with DMSO, which is known to be more toxic than methanol.

An increase in mtDNA copy number was obtained between 1 and 5 h in control samples and for 1M DMSO. Such increase was not present in samples treated with 2, 3 and 4 M DMSO. There was a significant early increase ($P>0.05$) between the untreated ovarian follicles and those exposed to 2 M DMSO when the mtDNA copy number was measured 1 h after the CPA removal (Fig. 6.3B). Significant decreases ($P<0.05$) were found between the untreated ovarian follicles and those exposed to 3 and 4 M DMSO when the mtDNA copy number was measured after 5 h incubation following the CPA removal (Fig. 6.3B).

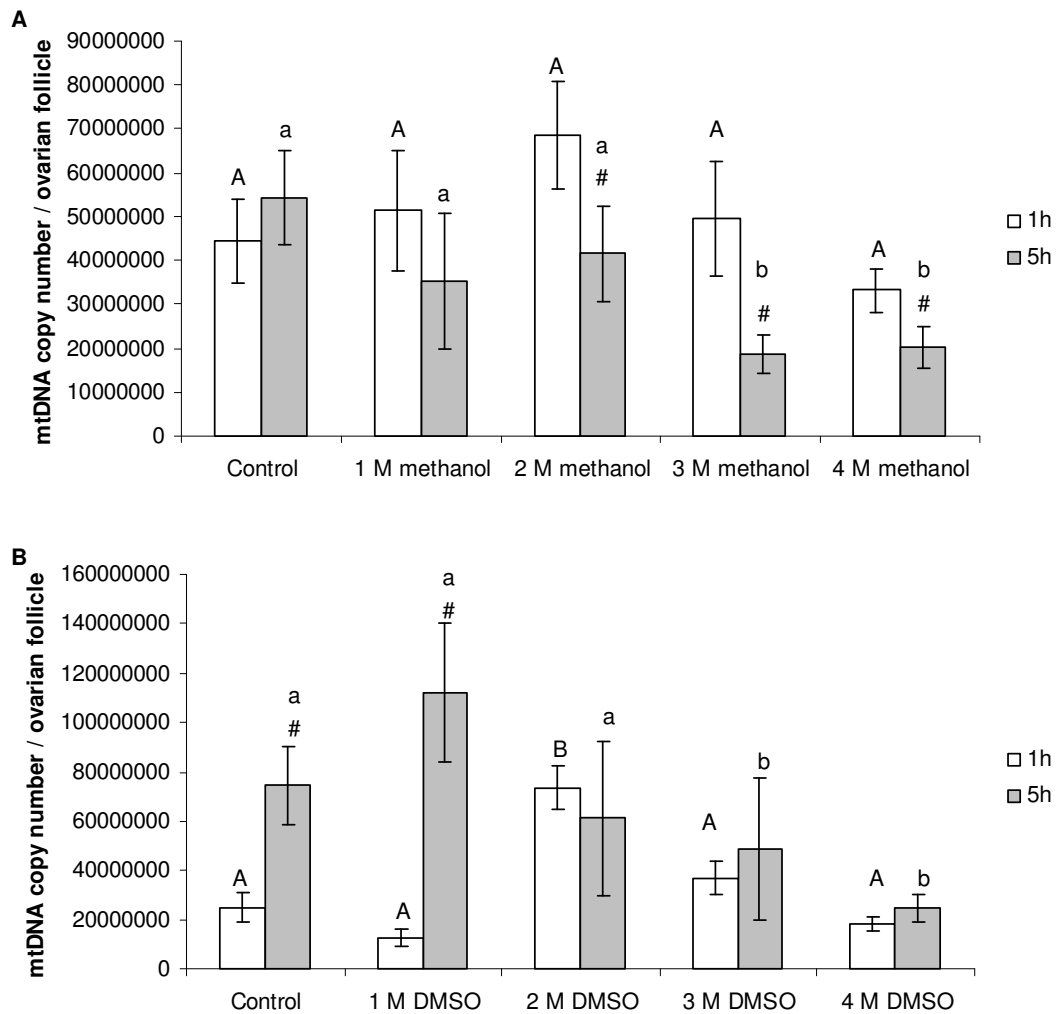


Fig 6.3. Effect of methanol (A) and DMSO (B) exposure on mtDNA on zebrafish stage III ovarian follicles. mtDNA copy number was measured 1 h and 5h after 30 min exposure to cryoprotectant. Error bars represent Standard Error of the Mean. Different letters represent significant differences between control and treated groups ($P < 0.05$). # represents significant differences between the 1h and 5h pair values.

6.2.4 Effect of cryoprotectants on ATP content and ADP/ATP ratio

In order to determine whether the changes observed in mitochondrial distribution, membrane potential and mtDNA copy number actually affected mitochondrial function, ATP levels and ADP/ATP ratios were determined.

Results from these studies showed that the ATP content was not significantly affected after 1 h or 5 h incubation following 30 min exposure to 1 to 4 M methanol (Fig. 6.4 A), there were no significant differences between the control group and the treated groups ($P > 0.05$). Similarly, at 1 h following 30 min exposure to methanol, there were no significant differences between control groups and treated groups when the ADP/ATP ratio was calculated. However, all the treated groups had lower ADP/ATP ratios than the control groups at 5 h following CPAs removal, although the differences were not statistically significant (Fig. 6.4B).

The results also showed that ATP content significantly decreased ($P < 0.05$) following exposure to 2, 3 and 4 M DMSO when measured both at 1 h and 5 h following CPA exposure for 30 min (Fig. 6.4 C). At 1 h following DMSO removal the ADP/ATP ratio decreased compared to the control group when 2 and 3 M were used, whilst at 5 h post-treatment there was a decrease of ADP/ATP ratio for all the treated groups (Fig. 6.4D), however the differences were not statistically significant.

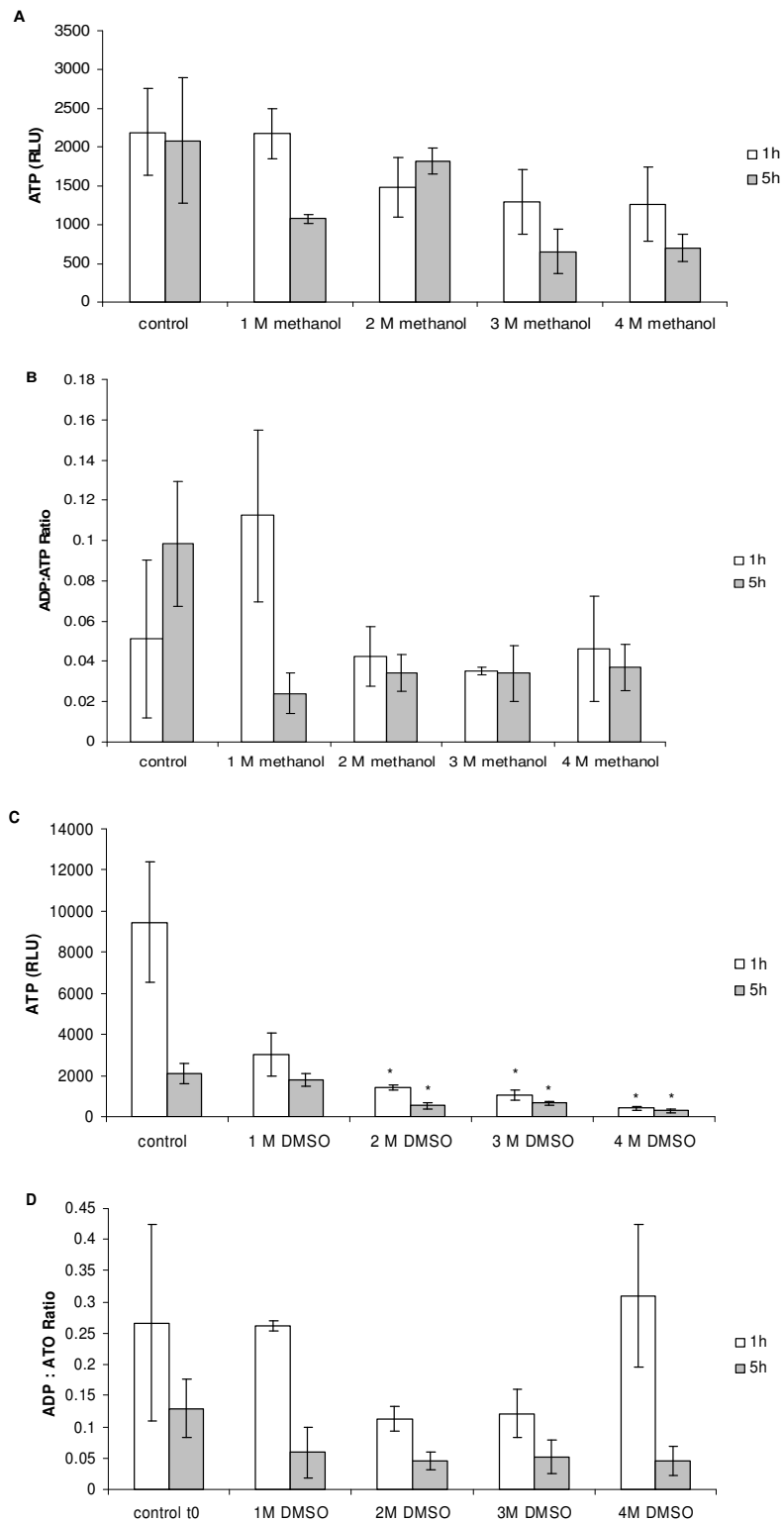


Fig 6.4. Effect of methanol (A-B) and DMSO (C-D) exposure on ATP level and ADP/ATP ratio on zebrafish stage III ovarian follicles. ATP level and ADP/ATP ratio were measured 1 h and 5 h after the exposure to cryoprotectant for 30 min. Error bars represent Standard Error of the Mean. Significant difference in ATP level between control and treated groups are indicated (*) ($P < 0.05$).

6.3 Discussion

Cryoprotectants are essential for the successful freezing and thawing of viable cells but are known to be toxic at high concentrations. The results obtained from viability tests previously performed in zebrafish ovarian follicles (Plachinta et al., 2004a) and from the present study showed the relatively low toxicity of methanol at concentrations of 3M or 4M, when the viability was assessed based on membrane integrity (see chapter 3). These results could be due to the fact that cell membranes are generally highly permeable to methanol and that the methanol does not induce any damage in terms of membrane integrity. Zhang et al., (2005) reported that methanol penetrates ovarian follicles at a rate comparable with the rate of water transport and, therefore, incubation of cells with this cryoprotectant does not lead to osmotic stress.

In this study, it has been hypothesised that even cells that appear unaffected by freezing or CPA exposure may suffer more subtle effects. In support of this, the data obtained by JC-1 staining with confocal microscopy indicate a reduced fluorescence and an increasing loss of mitochondrial distributional arrangement with increasing concentration of methanol. Images obtained by confocal microscopy showed the disruptive effect of methanol on mitochondrial distribution and mitochondrial membrane potential in the granulosa cells, which surround the stage III zebrafish oocyte. These findings showed that methanol exposure, even at concentrations that did not affect survival, resulted in a loss of the mitochondrial membrane potential. JC-1 has been used to estimate variation in membrane potential. It is known that mitochondrial membrane potential is a key indicator of cellular viability, as it reflects the pumping of hydrogen ions across the inner membrane during the process of electron transport and oxidative phosphorylation, responsible for ATP production. Many mitochondrial functions, including protein import, ATP generation and lipid biogenesis, depend on the maintenance of $\Psi\Delta m$ (Voisine et al. 1999). JC-1 proved to be a useful marker of mitochondrial activity and mitochondrial distributional arrangement.

The role of granulosa/thecal cells has already been established in supporting oogenesis, vitellogenesis and maturation (Eppig and Downs, 1988; Cerda' et al., 1999). Also, the mitochondria in the granulosa layer have different functions, not only as a source of ATP, but also as source of cAMP and in the synthesis of steroids (discussed in chapter 4 and 5). Therefore, a compromised mitochondrial activity might result in failure of oocyte maturation. In these experiments it was not possible to observe mitochondria in the oocyte itself due to the thickness of the vitelline envelope and the consequent failure of the mitochondrial probe to penetrate the oocyte. Should the methanol reach the oocyte and compromise the mitochondria, its impact may severely affect the success of *in vitro* maturation and later on embryo development, taking into consideration the critical role that mitochondria, which are maternally inherited organelles, have during early embryonic development.

It has previously been reported that cryopreservation of zebrafish (*Danio rerio*) blastomeres (Kopeika et al., 2005) increases the frequency of mtDNA mutations. In order to see if CPA treatment could also affect mtDNA and to quantify the effects seen with methanol exposure, mtDNA copy number was measured.

Data obtained with FDA-PI test (discussed in chapter 3) suggest that methanol is less toxic to ovarian follicles than DMSO, in agreement with other studies (Plachinta et al 2004a, Isayeva et al 2004). Exposure to DMSO reduced the viability and also the lower concentrations used had a larger effect than methanol. In this study, it has been further shown that this is also the case when viability is assessed 5 h after the removal of CPAs. At 1 h after exposure to methanol for 30 min, no changes in mtDNA copy number were obtained, despite structural damage observed by confocal microscopy. A decrease of copy number was obtained at 5 h after the exposure to 3 and 4 M methanol for 30 min. 3 and 4 M methanol also resulted in a decrease in viability when FDA-PI was used. The decrease in copy number could be due to a compromised synthesis mechanism of mtDNA following methanol exposure.

The effect of DMSO, another commonly used CPA for zebrafish ovarian follicles, was also investigated. A marked increase in mtDNA copy number was observed at 1 h after the exposure to 2 M DMSO for 30 min. This increase could be an attempt by the cells to correct for the insult. At 3M and 4M DMSO, there was no increase in mtDNA copy number, possibly due to the synthesis mechanism or repair mechanisms being damaged.

MtDNA encodes vital components of the electron transport chain, essential for efficient production of cellular ATP. It is also known that the impact of depletion of cellular ATP in oocytes induces dramatic disruption of microfilaments, as well as cessation of the many other vitally important processes (Lahnsteiner, 2000b).

The ADP/ATP ratio showed a similar trend as the ATP content but in this case, a larger decrease was noted after 5 h from the treatment. While necrotic cell death may be associated with an early decrease in the ability of the cells to synthesize ATP, cells undergoing apoptosis may retain a high concentration of ATP until relatively late in the progression of events leading to cell death (Leist et al., 1997; Eguchi et al., 1997). With the exception of 1M DMSO, the exposure to DMSO induced a decrease of ATP content. The ADP/ATP ratio showed a trend of decrease after 5 h from the CPA removal; whilst at 1 h only for 2 and 3 M DMSO a decrease was observed. These results could indicate that most of the intracellular ATP and probably ADP stocks have been consumed in coping with stress associated with cryoprotectant exposure, or an irreversible damage of the cells vital energy system. The results from methanol exposure, together with the results obtained measuring the ADP/ATP ratio after DMSO exposure, suggested a very large variation in ATP content among ovarian follicles. Perhaps this variation could be minimised by increasing the size of the sample. In the present work, 30 ovarian follicles were used per group. Although effects were not large enough to show statistical difference, the observation of similar trends between treatments and between copy number, ATP content and ADP/ATP ratio suggests that there are biological effects present. However, Suszynski et al. (2008) indicated the ATP/DNA ratio is a better indicator of islet cell viability than the ADP/ATP ratio, as dead cells are rapidly depleted of their ADP and ATP. If dead cells are rapidly depleted of their ATP and ADP content,

then ADP/ATP ratio would be incapable of accounting for any dead cells found and would be effectively overestimating the viability of the cells. This needs further investigation.

6.4 Summary

The aim of this study was to investigate the use of mitochondrial distributional arrangement and activity as biological marker to assess ovarian follicle quality. In order to achieve this goal, the effect of cryoprotectants known to be the least toxic to zebrafish ovarian follicles (methanol and DMSO) on mitochondria of stage III ovarian follicles was evaluated. The mitochondrial distributional arrangement was determined using confocal microscopy, and the mitochondrial membrane potential, the mtDNA copy number, ATP levels and ADP/ATP ratios were assessed following exposure to cryoprotectants.

Results obtained by confocal microscopy showed that 2M methanol induced a loss of membrane potential, although viability tests showed no decrease in survival even after 5 h incubation post-exposure. Higher concentrations of methanol (3M and 4M) induced not only a decrease of mitochondrial membrane potential but also the loss of mitochondrial distributional arrangement, which suggested a compromised mitochondrial function. Furthermore, 3M and 4M treatments resulted in a decrease in viability assessed by FDA-PI after 5 h incubation post-exposure. A decrease in mtDNA copy number and ADP/ATP ratio was reported after 5 h incubation following methanol exposure, indicating a delayed effect. The use of DMSO, which is considered to be a more toxic CPA to zebrafish ovarian follicles than methanol, induced a decrease of viability and it caused an immediate and sustained decrease of ATP levels, accompanied by failure to maintain mtDNA copy number. These results indicated that even CPAs that are considered to have no toxicity as determined by TB and FDA-PI tests can have a deleterious effect on mitochondrial activity, potentially compromising oocyte growth and embryo development. Therefore, the assessment of mitochondria activity and distributional arrangement can be used as a more sensitive measure of viability.

Chapter 7: Conclusions

7.1 Summary of the aims and objectives

The aim of the present work was to develop new methods to assess ovarian follicle viability and quality for use in cryopreservation studies. In order to achieve this aim the following investigations were undertaken:

1. The first part of this study, reported in chapter 3, focused on the development of a new vital stain assay for zebrafish ovarian follicles. The combination of two fluorochromic markers, FDA and PI, previously used in mammalian cells, were investigated for use with zebrafish ovarian follicles. The applicability of the FDA-PI assay to ovarian follicles was evaluated in comparison with currently used viability assays in a series of cryoprotectant toxicity studies. Although FDA-PI was shown to be a suitable method for assessment of ovarian follicle viability, it only provided an assessment of two gross parameters, the membrane integrity and cytoplasmic esterase activity.
2. The second part of the study, reported in chapter 4, focused on more detailed analysis of the potential role of mitochondria in the determination of ovarian follicle/oocyte quality. As there were no report on mitochondria distribution and activity in stage III zebrafish ovarian follicles, the first approach was to investigate mitochondrial activity and distribution in stage III zebrafish ovarian follicle in normal physiologically condition. Confocal microscopy and two mitochondrial fluorescent probes were used. To show that the staining obtained by confocal microscopy was specific for mitochondria, the effects of mitochondrial inhibitors on staining patterns were also investigated. Furthermore, ATP levels were measured following the exposure to the inhibitors, to see whether the maintenance of mitochondrial organisation within the ovarian follicle was an ATP-dependent process.

3. The third part of the study, reported in chapter 5, focused on transmission electron microscopy and scanning electron microscopy analysis of the mitochondrial location in the ovarian follicle, to further validate the results obtained with mitochondrial fluorescent staining and confocal microscopy reported in chapter 4. Electron microscopy was also undertaken to identify whether any damage occurred during the separation of ovarian follicle from ovaries following both enzymatic and mechanical isolation methods.
4. The fourth part of the study, reported in chapter 6, was carried out to evaluate the mitochondrial activity and distributional arrangement (investigated in chapter 4) as a marker for ovarian follicle viability/quality. In order to test this hypothesis, a series of CPA toxicity studies were conducted. The mitochondrial probe JC-1 was used to determine changes in mitochondrial activity in ovarian follicles following exposure to commonly used CPAs. Quantitative approaches for mitochondrial activity were also used, ATP level, ADP/ATP ratio and mtDNA copy number were investigated following CPAs exposure. FDA-PI assay was also undertaken and the results were compared with those obtained by mitochondrial analysis to see whether there was any correlation between the viability tests and mitochondrial distribution and activity analyses.

In the following sections, a summary of the main findings, general conclusion and directions for future work are discussed.

7.2 Review of main findings

7.2.1 Development of new assay for zebrafish ovarian follicle viability using vital stains

Reliable fish oocyte quality assessment methods are essential in developing protocols for cryopreservation, as well as for their *in vitro* maturation and fertilisation. Current ovarian follicle viability assessment methods either lack sensitivity (e.g. Trypan Blue staining-TB) or are stage dependent (e.g. *in vitro* maturation and observation of germinal vesicle

breakdown-GVBD). The aim of this study was to develop a new viability assessment method for zebrafish ovarian follicles that is reliable, sensitive and not stage-specific. Fluorescein Diacetate (FDA) and Propidium Iodide (PI) were used for the first time to assess viability of zebrafish ovarian follicles. After preliminary studies to evaluate the efficacy of FDA and PI, a combination of these two fluorochromes was subsequently chosen and compared with TB staining and the GVBD test in a series of cryoprotectant toxicity studies and following cryopreservation of stage III ovarian follicles. In all cases the FDA-PI test proved to be more sensitive than TB staining, but less sensitive than the GVBD test. The results showed the FDA-PI method to be promising, and it offers an additional approach for viability assessment of fish ovarian follicles that is able to inform on both membrane integrity and metabolic activity. This work has been published in *CryoLetters* (Vol. 29(6) 2008 pp. 463-475).

7.2.1.1 Conclusions and suggestions for future work

From the present study, it is evident that FDA-PI staining is a useful method for the differentiation of viable and nonviable ovarian follicles. The applicability of FDA-PI to assess zebrafish ovarian follicle viability has been shown under a series of different experimental conditions, and the method also does not present any limitations linked to developmental stage. It is a more sensitive vital stain than TB, although less sensitive than assessment based on the observation of GVBD. FDA-PI staining allows the assessment of both membrane integrity and the cytoplasmic esterase activity. Although methanol was shown to be the least toxic CPA (Plachinta et al., 2004a), the present study showed that 4 M methanol had a toxic effect on zebrafish ovarian follicle viability assessed by both TB and FDA-PI staining. Exposure to 4M methanol also had a negative effect on the capability of developing from stage III to stage IV through *in vitro* maturation assessed by GVBD. As 4M methanol + 0.2 M glucose has been used in this and previous studies (Plachinta et al., 2004b; Guan et al., 2008b) as the optimal cryoprotectant treatment, further investigations in the identification of the optimal protocol for cryopreservation are needed, and especially as studies have shown a

depletion of ATP levels in stage III ovarian follicles following cryopreservation using 4M methanol based cryoprotectant medium (Guan et al., 2008b).

The FDA-PI test represents a reliable method to assess ovarian follicle viability. It is simple, does not require a long incubation time and can be applied to different stages of development. Its applicability to different conditions such as following CPA exposure or cryopreservation makes it a useful screening test in assessing viability, before further and more laborious methods are carried out.

Although, following cryopreservation a similar percentage viability was achieved by TB and FDA-PI, the ovarian follicles stained by FDA-PI showed a decrease in green fluorescence when compared to viable ovarian follicles from the control group. It was possible to observe high intensity fluorescence in control ovarian follicle and low intensity fluorescence among ovarian follicles following cryopreservation. This decrease in green fluorescence indicates a compromised esterase activity. Shi et al. (2006) used FDA for viability assessment of porcine oocytes and reported that the degree of fluorescein accumulation was a reflection of oocyte cytoplasm status. Boender (1984) reported the use and quantification of FDA to assess viability of bovine oocyte. The fluorescence of cells stained by FDA could be also measured by fluorimetry, allowing the quantification of the variation in fluorescence intensity following cryopreservation. The quantification of FDA would render this method even more sensitive. The decrease in fluorescein also suggests that “viable” cells may still be damaged, hence further studies on more subtle defects are needed.

7.2.2 Observation of mitochondria distribution and activity in stage III ovarian follicles

Fluorescent probes, JC- 1 (5,5',6,6'-Tetrachloro-1,1',3,3'-tetraethyl-imidacarbocyanine iodide) and Mitotracker Green FM, were used to investigate mitochondrial distribution and activity in stage III zebrafish ovarian follicles by confocal microscopy. Mitochondria exhibited a contiguous distribution in the granulosa cell layer surrounding stage III

zebrafish oocytes. The mitochondrial pattern in the granulosa cells became disrupted when the follicle-oocyte complexes were exposed to the mitochondrial inhibitor carbonyl cyanide 4-(trifluoromethoxy) phenylhydrazone (FCCP). This suggested that the distribution of mitochondria is itself energy dependent. This hypothesis was supported by the findings that both FCCP and oligomycin treatments reduced the concentrations of ATP in the ovarian follicles. These results suggested that maintenance of the mitochondrial spatial distribution in the granulosa cells of zebrafish stage III ovarian follicle is an energy dependent process.

7.2.2.1 Conclusions and suggestions for future work

In this part of the study mitochondrial distribution and activity was investigated in stage III ovarian follicles with the goal of using mitochondrial membrane potential and mitochondria distribution as a marker for the evaluation of mitochondrial function in ovarian follicle. This study showed that mitochondrial probes were not able to penetrate the oocyte, indicating a low permeability of the vitelline envelope. The mitochondrial probes showed the granulosa cells to be rich in mitochondria, which assumed a contiguous peripheral pattern aligned with the margins of each cell.

The evidence of a mitochondrial origin of fluorescence derived by JC-1 exposure was confirmed using a second mitochondrial stain, MitoTracker Green FM, which showed similar mitochondrial patterns and also using mitochondrial inhibitors such as FCCP. JC-1 staining showed a mixed population of mitochondria with high and low membrane potential in the granulosa cell layer leading to the conclusion that this could be due to a metabolic turnover of activity or could be due to a functionally distinct subset. The phenomenon of mitochondrial heterogeneity has been studied in several cell types (Kirischuk et al., 1995; Salvioli et al., 2000; Wikstrom et al., 2007). Mitochondria display a wide range of morphologies and are functionally heterogeneous. The morphological and functional heterogeneity of mitochondria raises the possibility that subpopulations of

these organelles can carry out diverse processes within different areas of a cell (Cossarizza et al., 1996; Collins et al. 2002; Andrey et al., 2004).

The exposure to the mitochondrial inhibitor, FCCP, induced a loss of fluorescence and the destruction of the hexagonal-polygonal pattern. The loss of the hexagonal-polygonal pattern was also accompanied by a decrease in ATP levels, suggesting that ATP is essential for maintaining the spatial arrangement of mitochondria and that the maintenance of mitochondria in a specific pattern is an energy-dependent process. The ATP assay was able to measure the changes in mitochondrial ATP concentrations following the exposure to oligomycin, an inhibitor of ATP synthesis. In order to obtain more detailed information with regards to energy dependent distribution of mitochondria, future work should investigate the dose-response inhibition of ATP levels following FCCP and oligomycin treatment. Also, time-lapse confocal studies following mitochondrial inhibitors exposure could be undertaken to gain more detailed information on the effect of those inhibitors on mitochondrial activity. The assessment of recovery of staining after inhibitors removal should also be considered.

To further confirm the arrangement of mitochondria in the granulosa cell layer, a counter stain with a fluorescent DNA probe (e.g. DAPI or Hoechst) to show nuclear location and size should be considered. This could clarify whether the distribution of mitochondria along the cell margin was due to mitochondria specialisation or spatial specification related to levels of metabolism or the state of polarisation, or simply by default due to the nucleus occupying a high percentage of the cytoplasm, inducing the distribution of mitochondria to the margins (See appendix A). The interaction between mitochondria and cytoskeleton elements could also be investigated using cytoskeleton inhibitors.

As Triton treatment did not allow the mitochondrial probes to penetrate into the oocyte, the use of a different detergent (such as BRij-35) as membrane permeabiliser could be investigated. A defolliculation procedure should be also considered, as it could allow the analysis of mitochondria in the oocyte, allowing more detailed information on both

mitochondria in the surrounding layers and in the oocyte to be gained. Viewing the mitochondrial distribution within the oocyte might generate more detailed information on oocyte development and also it could facilitate additional methods to assess oocyte quality in fish such as Brilliant Cresyl Blue (BCB) dye which has been reported in mammalian studies (Roca et al. 1998; Alm et al. 2005; Rodriguez-Gonzalez et al. 2002).

Studies on the reversibility of mitochondrial spatial organisation and reactive oxygen species (ROS) production could be considered in order to determine whether inhibitor treatment is accompanied by an elevation of ROS to levels that can compromise cell function and integrity. Furthermore, as only the present study and Zhang et al. (2008) report the mitochondrial distribution in zebrafish stage III and stage I ovarian follicles, respectively, there is a need for further investigation of mitochondrial distribution in the other stages, including the determination of mitochondria in the layers surrounding the oocyte and the oocyte itself, perhaps following a defolliculation procedure.

The identification of mitochondrial activity and distribution in stage III ovarian follicles obtained in this study not only contributes to the field of developmental biology, being the first report on mitochondrial observation in a later stage of zebrafish ovarian follicle development, but also provides details of the physiological distribution and activity of mitochondria that can be used as a marker of ovarian follicle viability/quality (as shown in chapter 6 of this thesis).

7.2.3 Examination by Scanning Electron Microscopy (SEM) and Transmission Electron Microscopy (TEM) of stage III zebrafish (*Danio rerio*) ovarian follicle structure to support observation of mitochondria distribution obtained by confocal microscopy

In this part of the study, SEM and TEM were carried out to verify the results obtained by confocal microscopy (described in chapter 4), investigating mitochondrial distribution within the ovarian follicle. The effects of the two separation procedures of ovarian

follicles from the ovarian mass were also investigated. Ovarian follicles obtained both from mechanical separation and enzymatic separation were used for preparation of specimens for Cryo-SEM and TEM. Micrographs obtained by TEM showed that the granulosa cell layer was rich in mitochondria. Associated cryo-electron microscopy studies also showed that the follicle surface is covered by an hexagonal-polygonal pattern of ridges with the same geometric dimensions as indicate by the fluorescent staining of mitochondria. Furthermore, TEM images showed randomly dispersed mitochondria in the oocyte, which were not stained by the mitochondrial probes used in confocal microscopy study described in chapter 4 leading to the conclusion that the mitochondrial stains were unable to penetrate into the oocytes. Micrographs obtained showed that there were no differences between enzymatic and mechanical separation. However, both enzymatic and mechanical separation may induce the removal of the epithelial cells and part of the thecal cell layer of the follicle.

The electron microscopy studies provided new information on follicle structure and effect of different isolation methods. The study of organelle distribution and organization could support the *in vitro* maturation and oocyte development fields, as well as their use as biological markers for quality determination. These findings will contribute in a better understanding of oocyte/folliculogenesis processes in fish. Work carried out in sections 7.2.2 and 7.2.3 has been accepted for publication in *Theryogenology* (Zampolla et al., Distributional arrangement of mitochondria in the granulosa cells surrounding stage III zebrafish (*Danio rerio*) oocytes. 2009, in press).

7.2.3.1 Conclusions and suggestions for future work

Although there were no differences between the two procedures used to separate ovarian follicles from the ovarian mass, further studies on ovarian follicle structure using TEM and SEM are needed to see if the separation method itself may induce potentially damaging changes to the follicle. As shown from both mechanical and enzymatic separation, some of the epithelial and thecal layers may be removed which could

compromise the success of *in vitro* growth/maturation of ovarian follicles. The majority of studies conducted on zebrafish ovarian follicles use mechanical separation of ovarian follicles (Selman et al., 1993; Plachinta et al., 2004a; Isayeva et al., 2004; Seki et al., 2008), although Guan et al. (2008b) reported the successful use of hyaluronidase treatment to separate ovarian follicles which allow the collection of large numbers of apparently morphologically intact zebrafish ovarian follicles at different stages of development.

7.2.4 Evaluation of mitochondrial activity and distributional arrangement as biological marker in stage III ovarian follicle of zebrafish (*Danio rerio*) following CPAs exposure

The aim of this study was to investigate the use of mitochondrial distributional arrangement and activity as biological marker to assess ovarian follicle quality. In order to achieve this goal, the effect of cryoprotectants known to be the least toxic to zebrafish ovarian follicles (methanol and DMSO) on mitochondria of stage III ovarian follicles were evaluated. The mitochondrial distributional arrangement was determined using confocal microscopy and the mitochondrial probe JC-1, and the mtDNA copy number, ATP levels and ADP/ATP ratios were measured following exposure to cryoprotectants. Results obtained by confocal microscopy showed that methanol exposure led to loss of mitochondrial membrane potential and disruption of mitochondrial distributional arrangement at high concentrations (3M and 4M). Both methanol and DMSO exposures induced changes in mtDNA copy number. Methanol exposure did not change ATP levels, but, exposure to DMSO did cause a decrease in ATP levels. The ADP/ATP ratio generally decreased following the exposure to CPAs. These results showed that even CPAs that are considered to be relatively non toxic as determined by TB and FDA-PI tests can have a deleterious effect on mitochondrial activity, potentially compromising oocyte growth and embryo development. Therefore, the assessment of mitochondria activity and distributional arrangement can be used as a more sensitive measure of viability.

7.2.4.1 Conclusions and suggestions for future work

As already pointed out, the large size of later stage ovarian follicles (0.39-0.69 mm), the complex system of acellular and cellular structures surrounding the oocyte, the low membrane permeability, and the high yolk content are obstacles to their successful cryopreservation.

In this study JC-1 was used as a marker of mitochondrial function that can be used to estimate changes in membrane potential following CPA exposure. The mitochondrial membrane potential influences ADP/ATP ratio, redox state (Nicholls, 2004), and reactive oxygen species (ROS), as well as calcium sequestration (Lowell and Shulman, 2005). The ADP/ATP ratios, ATP levels and mtDNA copy number were measured following CPA exposure. The mitochondrial probe JC-1 and confocal microscopy provided qualitative results of mitochondrial membrane potential and mitochondrial distributional arrangement whilst the ADP/ATP ratios, ATP levels and mtDNA copy number allowed the quantification of functional changes in mitochondria following CPA exposure. Quantitative methods have additional advantage of being able to assess the whole follicle, whilst the evaluation of mitochondrial membrane potential by confocal microscopy and JC-1 allowed the evaluation only of the follicle cells on the margin of the ovarian follicle.

Detailed information on the toxicities of cryoprotectants is essential for development of cryopreservation protocols for ovarian follicles. So far, the effect of cryoprotectants in zebrafish ovarian follicles has been evaluated only by viability test such as trypan blue (TB) staining, MTT test, fluorescein diacetate and propidium iodide and by the observation of GVBD (Plachinta et al., 2004a; Isayeva et al., 2004; Guan et al., 2008b; Tsai et al., 2008). Also the limitations of the viability tests are well known, they relate to stage-specific assays e.g. GVBD, or the evaluation of only one (TB, MTT) or two parameters (FDA-PI). TB and FDA-PI viability assays assess only large and significant effects, not the more subtle effects that the mitochondrial evaluation could offer.

The results obtained showed the applicability of confocal microscopy and mitochondrial staining with JC-1 probe for assessment of ovarian follicle viability/quality following CPA exposure. An immediate result can be obtained with minimal processing of sample, whilst ATP levels, ADP/ATP ratio or mtDNA copy number required extraction and further processing of samples, but do provide quantitative data.

Although methanol has been considered a relatively non-toxic CPA (Plachinta et al., 2004a; Guan et al., 2008a), exposure to methanol resulted in the loss of mitochondrial pattern and changes in fluorescence shifting from red to green, indicating loss of membrane potential and therefore mitochondrial function. The results reported in chapter 6 compared to TB and FDA-PI results showed that the assay of mitochondrial activity and distribution gave more detail of the effect of substances such as CPAs on ovarian follicles. The results obtained in this study suggest that only low concentrations of methanol should be used for cryopreservation, therefore a further optimisation of the currently used protocols may need to be considered.

Exposure to methanol and DMSO, two commonly used CPAs for zebrafish ovarian follicles, induced a decrease of mtDNA copy number 5 hours following CPA exposure as discussed in chapter 6. The decrease could be due either to a compromised synthesis mechanism, a damaged repair mechanisms or to a reduction in cell viability. Ovarian follicle survival may be disturbed by mitochondrial dysfunction caused by depletion of mitochondrial DNA in response to CPA exposure. MtDNA encodes vital components of the electron transport chain, essential for ATP production. ATP molecules are involved in several vitally important processes. Decreases in mtDNA are significant as it has been reported that there is a threshold number of mtDNA molecules essential for successful embryogenesis in variety of mammalian species (Reynier et al., 2001; Tamassia et al., 2004). Alteration of mtDNA copy number following CPA exposure is reported here for the first time. Further studies on the changes in mtDNA could be considered as in this study, only the levels of mtDNA have been considered here.

The evaluation of the ADP/ATP ratios have been used in a range of cell types to distinguish between necrosis and apoptosis induced cell death (Bradbury et al., 2000). The effect of CPAs in inducing necrosis or apoptosis should be further investigated. Studies of ADP/ATP ratios following exposure to necrosis and apoptosis inducers should be carried out in order to have a better understanding of the CPA effects. ATP/DNA ratio could be also evaluated following CPA exposure. Suszynski et al. (2008) reported that the ATP/DNA ratio was a better indicator of islet cell viability than the ADP/ATP ratio as dead cells may be rapidly depleted of both ATP and ADP, which would render the ratio incapable of accounting for dead cells. Whilst the DNA of dead cells is expected to remain stable over prolonged periods of time.

7.3 In Summary

The aim of this research was to develop new methods to assess viability/quality of zebrafish ovarian follicles. Progress has been made in the following areas:

1. The new vital staining procedure, FDA-PI, was found to be more sensitive than TB although less sensitive than GVBD but it can be applied to all stages and different conditions. Overall, it provided an improvement on the screening viability methods. However, the FDA-PI allows only discrimination between live and dead cells.
2. The analysis of mitochondrial distributional arrangement and activity, and their use as biological markers, proved to be useful for ovarian follicle viability assessment following CPA exposure. The qualitative assay by confocal microscopy with JC-1 and the Cryo-SEM provided new information on zebrafish ovarian follicle structure, identifying a polygonal structure of the vitelline envelope, which is reported here for the first time. The electron microscopy studies also provided new information on follicle structure and effect of different isolation methods.

The study of organelle distribution and organization will inform future work on *in vitro* maturation and oocyte development, as well as their use as biological markers for quality determination.

3. Quantitative studies on mtDNA copy number, ATP and ADP/ATP ratios provided information on mitochondria activity in physiological conditions as well as following CPAs exposure. Additional information on the effect of methanol, considered before as the least toxic CPA for zebrafish ovarian follicles, showed the CPA to be more toxic than previously reported. These changes in mitochondrial activity could inform the development of optimal cryo-protocols for ovarian follicles.

7.4 Future studies

The results obtained in this work point to two areas that merit further investigation:

- The development of specific markers for the oocyte. The defolliculation procedure would allowed the isolation of the oocyte and the application of tests which are currently used in mammals (BCB staining), as the intricate structures of fish oocyte does not allow the application of such stains.
- The development of non-invasive markers. This could include the use of markers to monitor the metabolic activity of the ovarian follicle. The study of denudated fish oocyte and ovarian follicle metabolic profiles of carbohydrates, amino acids or oxygen consumption may also serve as a potential marker of oocyte viability, and inform on the folliculogenesis/oogenesis process.

To date, all attempts of cryopreservation of fish eggs and embryos have failed and advances in their cryopreservation remain difficult to predict. Results obtained in this work on mitochondrial activity of ovarian follicles following cryoprotectants exposure highlights the need for more studies to be undertaken on the subcellular impact of cryoprotectants to inform future protocol design.

The failure in cryopreservation of fish eggs has implications in two main areas: aquaculture and conservation, although alternative approaches to overcome this issue could be considered.

In aquaculture failure in cryopreservation of fish eggs limits progress in selective breeding, and extension of the breeding period throughout the year. Although further studies still need to be carried out, ovarian tissue cryopreservation could offer a valid alternative to cryopreservation of oocytes or ovarian follicles.

Cryopreservation can assist in maintain species diversity and long-term storage of genetic information. Fish populations are globally threatened due to overfishing and pollution. Although biological diversity is being lost through extinction, efforts to conserve genetic material through the institution of gene banking can mitigate some of the losses. Collection and cryo-banking of genetic material from threatened species as DNA samples, frozen cells or tissues, is already underway and also an alternative approach to germoplasm collection. New technologies providing pluripotent stem (iPS) cells from somatic cell lines could also offer an additional way to maintain cell lines for future use.

References:

Adam M, Rana KJ and McAndrew BJ (1995) Effect of cryoprotectants on activity of selected enzymes of fish embryos *Cryobiology* **32**, 92-104

Adams S (2003) Cryopreservation of gametes and larvae of the sea urchin, *Evechinus chloroticus* and of other marine invertebrate species. PhD Thesis, University of Otago, New Zealand

Agnello M, Morici G and Rinaldi AM (2008) A method for measuring mitochondrial mass and activity *Cytotechnology* **56(3)**, 145-9

Albertini DF (1984) Novel morphological approaches for the study of oocyte maturation *Biol Reprod* **30**, 13-28

Alberts B, *Biologia molecolare della cellula*, Terza edizione, Zanichelli Editore, Bologna, 1995

Alberts B, Johnson A, Lewis J, Roberts K and Walter P (2002) *Molecular biology of the cell*: Garland Science, pp.1463

Alexeyev MF, Ledoux SP and Wilson GL (2004) Mitochondrial DNA and aging *Clinical Science* **107**, 355-364

Allison DC and Ridolpho P (1980) Use of a trypan blue assay to measure the deoxyribonucleic acid content and radioactive labeling of viable cells *J Histochem Cytochem* **28**, 700-3

Alm H, Torner H, Lohrke B, Viergutz T, Ghoneim IM and Kanitz W (2005) Bovine blastocyst development rate in vitro is influenced by selection of oocytes by brilliant cresyl blue staining before IVM as indicator for glucose-6-phosphate dehydrogenase activity *Theriogenology* **63(8)**, 2194-205

Anderson E (1967) The formation of the primary envelope during oocyte differentiation in teleosts. *J Cell Biol* **35(1)**, 193-212

Anderson E (1968) Cortical alveoli formation and vitellogenesis during oocyte differentiation in the pipefish, *Syngnathus fuscus*, and the killifish, *Fundulus heteroclitus* *J Morphol* **125(1)**, 23-59

Andrey K, Yves U, Xavier L and Raimund M (2004) Subcellular heterogeneity of mitochondrial function and dysfunction: Evidence obtained by confocal imaging *Molecular and Cellular Biochemistry* **256(1-2)**, 359-365

Ankley GT and Johnson RD (2004) Small Fish Models for Identifying and Assessing the Effects of Endocrine disrupting Chemicals *ILAR J.* **45**, 469-83

Arakawa T, Carpenter JF, Kita YA and Crowe JH (1990) The basis for toxicity of certain cryoprotectants: a hypothesis. *Cryobiology* **27**, 401-415

Arav A, Zeron Y, Leslie SB, Behboodi E, Anderson GB, and Crowe JH (1996) Phase transition temperature and chilling sensitivity of bovine oocytes *Cryobiology* **33(6)**, 589-599

Aronis A, Komarnitsky R, Shilo S and Tirosh O (2002) Membrane Depolarization of Isolated Rat Liver Mitochondria Attenuates Permeability Transition Pore Opening and Oxidant Production *Antioxidants & Redox Signaling* **4(4)**, 647-654

Babin PJ (1992) Binding of thyroxine and 3,5,3'-triiodothyronine to trout plasma lipoproteins *Am J Physiol* **262**, E712-E720

Barbazuk WB, Korf I, Kadavi C, Heyen J, Tate S, Wun E, Bedell JA, McPherson JD, Johnson SL (2000) The syntenic relationship of the zebrafish and human genomes, *GenomeRes.* **10**, 1351-1358

Barisone GA, Albertali IE, Sánchez M and Cabada MO (2003) The envelopes of amphibian oocytes: physiological modifications in *Bufo arenarum* *Reprod Biol Endocrinol* **1**, 18

Barngrover D, Thomas J and Thilly WG (1985) High density mammalian cell growth in Leibovitz bicarbonate-free medium: effects of fructose and galactose on culture biochemistry *J Cell Sci* **78**, 173-189

Begin I, Bhatia B, Baldassarre H, Dinnyes A and Keefer CL (2003) Cryopreservation of goat oocytes and in vivo derived 2- to 4- cell embryos using the cryoloop (CLV) and solid-surface vitrification (SSV) methods *Theriogenology* **59**, 1839-1850

Begovac PC and Wallace RA (1989) Major vitellins envelope proteins in piperfish oocytes originate within the follicle and are associated with the Z₃ layer. *J. Exp. Zool.*, **251**, 56-73

Bell JG and Sargent JR (2003) Arachidonic acid in aquaculture feeds: current status and future opportunities *Aquaculture* **218**, 491 -499

Bernardi P (1999) Mitochondrial Transport of Cations: Channels, Exchangers, and Permeability Transition *Physiol. Rev.* **79**, 1127-1155

Billet FS and Adam E (1976) The structure of the mitochondrial cloud of *Xenopus laevis* oocytes *J Embryol Exp Morphol* **33**, 697-710

Boender J (1984) Fluorescein-diacetate, a fluorescent dye compound stain for rapid evaluation of the viability of mammalian oocytes prior to in vitro studies *Vet Q* **6(4)**, 236-240

Bolamba D, Patiño R, Yoshizaki G and Thomas P (2003) Changes in homologous and heterologous gap junction contacts during maturation-inducing hormone-dependent meiotic resumption in ovarian follicles of Atlantic croaker *Gen Comp Endocrinol* **131(3)**, 291-5

Bolduc L, Labrecque B, Cordeau M, Blanchette M, and Chabot B (2001) Dimethyl Sulfoxide Affects the Selection of Splice Sites *J. Biol. Chem* **276** (20), 17597-17602

Boulekbache H, Bastin J, Andriamihaja M, Lefebvre B and Joly C (1989) Ageing of fish oocytes: effects on adenylic nucleotides content, energy charge and viability of carp embryo *Comp. Biochem. Physiol.* **93**, 471-476

Bradbury DA, Simmons TD, Slater KJ and Crouch SP (2000) Measurement of the ADP:ATP ratio in human leukaemic cell lines can be used as an indicator of cell viability, necrosis and apoptosis *J Immunol Methods* **240**, 79-92

Brooks S, Tyler CR, Sumpter JP (1997) Egg quality in fish: what makes a good egg? *Reviews in Fish Biology and Fisheries* **7**(4) 387-416

Bromage N, Jones J, Randall C, Thrush M, Springate J, Duston J and Barker G (1992) Broodstock management, fecundity, egg quality and the timing of egg production in the rainbow trout (*Oncorhynchus mykiss*). *Aquaculture* **100**, 141-166

Bromage N, Bruce M, Basavaraja N, Rana K, Shields R, Young C, Dye J, Smith P, Gillespie M and Gamble J (1994) Egg Quality Determinants in Finfish The Role of Overripening with Special Reference to the Timing of Stripping in the Atlantic Halibut *Hippoglossus hippoglossus* *Journal of the World Aquaculture Society* 25(1), **13 - 21**

Broughton RE, Milam JE and Roe BA (2001) The complete sequence of the zebrafish (*Danio rerio*) mitochondrial genome and evolutionary patterns in vertebrate mitochondrial DNA *Genome Res* **11**(11), 1958-67

Brownlie A, Donovan A, Pratt SJ, Paw BH, Oates AC, Brugnara C, Witkowska HE, Sassa S, Zon LI (1998) Positional cloning of zebrafish sauternes gene: A model for congenital sideroblastic anemia *Nat Genet* **20**, 244-250

Buono RJ and Linser PJ (1992) Transient expression of RSV-CAT in transgenic zebrafish made by electroporation *Mol Mar Biol Biotechnol* **1(4-5)**, 271-275

Busson-Mabillot S (1984) Endosomes transfer yolk proteins to lysosomes in the vitellogenic oocyte of the trout *Biology of the Cell* **51**, 53-66

Cai K, Yang J, Guan M, Ji W, Li Y and Rens W (2005) Single UV excitation of Hoechst 33342 and propidium iodide for viability assessment of rhesus monkey spermatozoa using flow cytometry *Arch Androl* **51(5)**, 371-383

Calarco PG (1995) Polarization of mitochondria in the unfertilized mouse oocytes *Developmental genetics* **16**, 36-43

Callen JC, Dennebouy N, Mounolou JC (1980) Development of the mitochondrial mass and accumulation of mtDNA in previtellogenic stages of *Xenopus laevis* oocytes *J Cell Sci* **41**, 307-20

Catt KJ, Hardwood JP, Clayton RN, Davies TF, Chan V, Katikineni M, Nozu K and Dufau MI (1980) Regulation of peptide hormone receptors and gonadal steroidogenesis *Rec Prog Horm Res* **36**, 557-662

Cerdà J, Petrino TR, Wallace RA (1993) Functional heterologous gap junctions in *Fundulus* ovarian follicles maintain meiotic arrest and permit hydration during oocyte maturation *Developmental biology* **160(1)**, 228-235

Cerdà J, Reidenbach S, Prätzel S and Franke WW (1999) Cadherin-Catenin Complexes During Zebrafish Oogenesis: Heterotypic Junctions Between Oocytes and Follicle Cells *Biology of Reproduction* **61**, 692-704

Chang YS, Wang SC, Tsao CC and Huang FL (1996) Molecular cloning, structural analysis, and expression of carp ZP3 gene *Mol Reprod Dev* **44(3)**, 295-304

Chao NH, Lin TT, Chen YL, Hsu HW and Liao IC (1997) Cryopreservation of early larvae and embryos in oyster and hard clam *Aquaculture* **155**, 31–44

Chapovetsky V, Gattegno T and Admon A (2007) Proteomics analysis of the developing fish oocyte *The Fish Oocyte From Basic Studies to Biotechnological Applications* Patrick J. Babin, Joan Cerdà and Esther Lubzens, pp 105

Chen LB, Smiley ST and Mason WT (1993) ed. *Fluorescent and Luminescent Probes for Biological Activity*, 124

Clayton DA, Doda JN, Friedberg EC (1974) The absence of a pyrimidine dimer repair mechanism in mammalian mitochondria. *Proc. Natl. Acad. Sci. USA* **71**, 2777-2781

Collins TJ, Berridge MJ, Lipp P and Bootman MD (2002) Mitochondria are morphologically and functionally heterogeneous within cells *EMBO J.* **21(7)**,1616-27

Combelles CM and Albertini DF (2001) Microtubule patterning during meiotic maturation in mouse oocytes is determined by cell cycle-specific sorting and redistribution of gamma-tubulin *Dev Biol* **239(2)**, 281-94

Comizzoli P, Wildt DE and Pukazhenthil BS (2003) Impact of Anisotonic Conditions on Structural and Functional Integrity of Cumulus–Oocyte Complexes at the Germinal Vesicle Stage in the Domestic Cat *Mol Reprod Dev* **75(2)**, 345–354

Conti M, Andersen CB, Richard F, Mehats C, Chun SY, Horner K, Jin C and Tsafiri A (2002) Role of cyclic nucleotide signaling in oocyte maturation *Mol Cell Endocrinol* **187(1-2)**, 153-9

Cossarizza A, Ceccarelli D and Masini A (1996) Functional heterogeneity of an isolated mitochondrial population revealed by cytofluorometric analysis at the single organelle level *Exp Cell Res* **222(1)**, 84-94

Crivello JF, Jefcoate CR (1980) Intracellular movement of cholesterol in rat adrenal cells. Kinetics and effects of inhibitors *J Biol Chem* **255**, 8144–8151

Didion BA, Pomp D, Martin MJ, Homanics GE and Markert CL (1990) Observations on the cooling and cryopreservation of pig oocytes at the germinal vesicle stage *J Anim Sci* **68**, 2803-10

Díez-Sánchez C, Ruiz-Pesini E, Lapeña AC, Montoya J, Pérez-Martos A, Enríquez JA and López-Pérez MJ (2003) Mitochondrial DNA content of human *spermatozoa* *Biol Reprod* **68(1)**, 180-5

Dinnyes A, Daí Y, Jiang S and Yang X (2000) High developmental rates of vitrified bovine oocytes following parthenogenetic activation, in vitro fertilization, and somatic cell nuclear transfer *Biol Reprod* **63**, 513-518

Driggers WJ, LeDoux SP and Wilson GL (1993) Repair of Oxidative Damage within the Mitochondrial DNA of RINr 38 Cells *J Biol Chem* **268**, 22042-22045

Dumont J and Brummett A (1980) The vitelline envelope, chorion. and micropyle of *Fundulus heteroclitus* eggs *Gamete Res* **3**, 25-44

Dumont JN and Brummett AR (1985) Egg Envelope in vertebrates. In "Developmental Biology: A Comprehensive Synthesis." (R.W. Browder, Ed.) Vol. 1, pp.235-288. Plenum, New York, N.Y.

Eguchi Y, Shimizu S and Tsujimoto T (1997) Intracellular ATP levels determine cell death fate by apoptosis or necrosis *Cancer Res* **57**, 1835-1840

Ecker RE, Smith LD (1971) Influence of exogenous ions on the events of maturation in *Rana pipiens* oocytes *Journal of Cell Physiology* **77**, 61-70

Eppig JJ (1991) Intercommunication between mammalian oocytes and companion somatic cells. *Bioessays* **13**, 569-74

Eppig JJ and Downs SM (1988) Gonadotropin-induced murine oocyte maturation in vivo is not associated with decreased cyclic adenosine monophosphate in the oocyte-cumulus cell complex *Gamete Res* **20(2)**, 125-31

Eriksson BM, Vazquez JM, Martinez E, Roca J, Lucas X and Rodriguez-Martinez H (2001) Effect of holding time during cooling and of type of package on plasma membrane integrity, motility and in vitro oocyte penetration ability of frozen-thawed boar spermatozoa. *Theriogenology* **55**, 1593 -1605

Fahy GM (1986a) The relevance of cryoprotectant "toxicity" to cryobiology *Cryobiology* **23(1)**, 1-13

Fahy GM (1986b) Vitrification: a new approach to organ cryopreservation *Prog Clin Biol Res* **224**, 305-335

Fair T (2003) Follicular oocyte growth and acquisition of developmental competence *Anim Reprod Sci* **78(3-4)**, 203-16

Farrant J, Walter CA, Lee H and McGann LE (1977) Use of two-step cooling procedures to examine factors influencing cell survival following freezing and thawing *Cryobiology* **14(3)**, 273-286

Feldkamp T, Kribben A and Weinberg JM (2005) Assessment of mitochondrial membrane potential in proximal tubules after hypoxia-reoxygenation *Am J Physiol Renal Physiol* **288(6)**, 1092-102

Fishman MC, Stainier DY, Breitbart RE and Westerfield M (1997) Zebrafish: genetic and embryological methods in a transparent vertebrate embryo. *Methods Cell Biol* **52**, 67-82

Frim J and Mazur P (1983) Interactions of cooling rate, warming rate, glycerol concentration, and dilution procedure on the viability of frozen-thawed human granulocytes *Cryobiology* **20(6)**, 657-76

Garner DL and Johnson LA (1995) Viability assessment of mammalian sperm using SYBR-14 and propidium iodide *Biol Reprod* **53(2)**, 276-284

Ge, W (2005) Intrafollicular paracrine communication in the zebrafish ovary: The state of the art of an emerging model for the study of vertebrate folliculogenesis. *Molecular and Cellular Endocrinology* **237**,1-10

Giraud MN, Motta C, Boucher D and Grizard G (2000) Membrane fluidity predicts the outcome of cryopreservation of human spermatozoa *Hum Reprod* **15**, 2160–2164

Green DR and Reed JC (1998) Mitochondria and apoptosis *Science* **1(5381)**, 1309-12

Green DR (1998) Apoptosis. Death deceiver *Nature* **396(6712)**, 629-30

Grover GJ, Atwal KS, Sleph PG, Wang FL, Monshizadegan H, Monticello T, Green DW (2004) Excessive ATP hydrolysis in ischemic myocardium by mitochondrial F₁F₀-ATPase: effect of selective pharmacological inhibition of mitochondrial ATPase hydrolase activity *Am J Physiol Heart Circ Physiol* **287**, 1747–1755

Grout BWW and Morris GJ (1987) Freezing and cellular organization. In: Grout BW and Morris GJ (eds.) *Effect of low temperatures on biological systems*. Arnold, London, pp. 147-173

Grout B, Morris J and McLellan M (1990) Cryopreservation and the maintenance of cell lines *Trends Biotechnol* **8(10)**, 293-7

Guan M, Rawson DM and Zhang T (2008a) Development of a new method for isolating zebrafish oocytes (*Danio rerio*) from ovary tissue masses *Theriogenology* **69(3)**, 269-75

Guan M, Rawson DM and Zhang T (2008b) Cryopreservation of zebrafish (*Danio rerio*) oocytes using improved controlled slow cooling protocols *Cryobiology* **56(3)**, 204-8

Guraya SS. (1986) The cell and molecular biology of fish oogenesis Monogr Dev Biol **18**, 1-223

Hall PF (1984) Cellular organization for steroidogenesis *Int Rev Cytol* **86**, 53-95

Hall PF and Almahbobi G (1997) Roles of microfilaments and intermediate filaments in adrenal steroidogenesis *Histology of the mammalian adrenal cortex*. Microscopy research and technique Nussdorfer, G.G. (ed). 1997, vol. **36**, Los Alamos, New Mexico. pp 463-479

Hallap T, Nagy S, Jaakma U, Johannisson A, Rodriguez-Martinez H (2005) Mitochondrial activity of frozen-thawed spermatozoa assessed by MitoTracker Deep Red 633. *Theriogenology* **63(8)**, 2311-22

Hamaratoglu F, Eroglu A, Toner M, Sadler KC (2005) Cryopreservation of starfish oocytes *Cryobiology* **50(1)**, 38-47

Harrison RA and Vickers SE (1990) Use of fluorescent probes to assess membrane integrity in mammalian spermatozoa *J Reprod Fertil* **88(1)**, 343-52

Hayakawa M, Hattori K, Sugiyama S, Ozawa T (1992) Age-associated oxygen damage and mutations in mitochondrial DNA in human hearts *Biochem Biophys Res Commun* **189**, 979-985

Hayakawa M, Katsumata K, Yoneda M, Tanaka M, Sugiyama S, Ozawa T (1995) Mitochondrial DNA minicircles, lacking replication origins, exist in the cardiac muscle of a young normal subject *Biochem Biophys Res Commun* **215(3)**, 952-60

Henderson TR, Henderson RF, York JL (1975) Effects of dimethyl sulfoxide on subunit proteins *Ann N Y Acad Sci.* **243**, 38-53

Hiendleder S and Wolf E (2003) The Mitochondrial Genome in Embryo Technologies *Reproduction in Domestic Animals* **38(4)**, 290 - 304

Holt WV and North RD (1994) Effects of temperature and restoration of osmotic equilibrium during thawing on the induction of plasma membrane damage in cryopreserved ram spermatozoa *Biol Reprod* **51(3)**, 414-24

Isayeva A, Zhang T and Rawson DM (2004) Studies on chilling sensitivity of zebrafish (*Danio rerio*) oocytes *Cryobiology* **49(2)**, 114-22

Jefcoate CR (2002) High-flux mitochondrial cholesterol trafficking, a specialized function of the adrenal cortex *J Clin Invest* **110**, 881-890

Jones KH and Senft JA (1985) An improved method to determine cell viability by simultaneous staining with fluorescein diacetate-propidium iodide *J Histochem Cytochem* **33(1)**, 77-9

Karnovsky, M.J. 1965. A formaldehyde-glutaraldehyde fixative of high osmolarity for use in electron microscopy. *J. Cell Biol.* **27**,137

Karran G and Legge M (1996) Non-enzymatic formation of formaldehyde in mouse oocyte freezing mixtures *Hum Reprod* **11(12)**, 2681-6

Kaseoglu M, Eroglu A, Toner M, Sadler KC (2001) Starfish oocytes form intracellular ice at unusually high temperatures *Cryobiology* **43(3)**, 248-59

Kayaba T, Takeda N, Adachi S and Yamauchi K (2001) Ultra-. structure of the oocytes of the Japanese eel *Anguilla japonica* during artificially induced sexual maturation *Fish Sci* **67(5)**, 870-879

Keij JF, Bell-Prince C, Steinkamp JA (2000) Staining of mitochondrial membranes with 10-nonyl acridine orange, MitoFluor Green, and MitoTracker Green is affected by mitochondrial membrane potential altering drugs *Cytometry* **39(3)**, 203-10

Kessel RG, Roberts RL and Tung HN (1988) Intercellular junctions in the follicular envelope of the teleost, *Brachydanio rerio* *J Submicrosc Cytol* **20**, 415–424

King PA, Roshol MNt and Storey KB (1993) Adaptations of plasma membrane glucose transport facilitate cryoprotectant distribution in freeze-tolerant frogs *Am J Physiol Regul Integr Comp Physiol* **265**, 1036-1042

Kirchofer A, (1996) Conservation of Endangered Freshwater Fish in Europe, Birkhauser, Basel, 341.

Kirischuk S, Neuhaus J, Verkhatsky A, Kettenmann H (1995) Preferential localization of active mitochondria in process tips of immature retinal oligodendrocytes *Neuroreport* **6**, 737–741

Kjørsvik E, Mangor-Jensen A and Holmefjord I (1990) Egg quality in fishes *Advances in marine Biology* **26**, 71-113

Klein H, Puschmann S, Schaper J and Schaper W (1981) The mechanism of the tetrazolium reaction in identifying myocardial infarction. *Virchows Arch* **393**, 287-297

Konc J, Kanyó K and Cseh S (2005) Clinical experiences of ICSI-ET thawing cycles with embryos cryopreserved at different developmental stages *J Assist Reprod Genet* **22(5)**, 185-90

Kopeika J, Zhang T, Rawson DM, Elgar G (2005)_Effect of cryopreservation on mitochondrial DNA of zebrafish (*Danio rerio*) blastomere cells *Mutat Res* **570(1)**, 49-61

Kotani T and Yamashita M (2005) Behavior of delta-tubulin during spindle formation in *Xenopus* oocytes: requirement of cytoplasmic dynein-dependent translocation *Zygote* **13(3)**, 219-26

Krisher RL (2004) The effect of oocyte quality on development *J Anim Sci* **82**, E14-E23

Kudo S and Inoue M (1989) Bacterial action of fertilization envelope extract from eggs of the fish *Cyprinus carpio* and *Plecoglossus altivelis* *J Exp Zool* **250(2)**, 219-28

Lahnsteiner, F. (2000a) Cryopreservation protocols for sperm of salmonid fishes. In *Cryopreservation in Aquatic Species* (T.R. Tiersch, and P.M. Mazik, eds), Baton Rouge, Louisiana, USA: The World Aquaculture Society, 91-100

Lahnsteiner F, Berger B, Horvath A, Urbanyi B and Weismann T (2000b) Cryopreservation of spermatozoa in cyprinid fishes *Theriogenology* **54(9)**, 1477-98

Lattman EE, Fiebig KM and Dill KA (1994) Modeling compact denatured states of proteins *Biochemistry* **33(20)**, 6158-6166

Leff D (1992) Zebrafish: a virus with a backbone *Mosaic* **23**, 25-35

Leibovitz A (1963) The growth and maintenance of tissue-cell cultures in free gas exchange with the atmosphere *Am F Hyg* **78**, 173-180

Leist M, Single B, Castoldi A, Kühnle S and Nicotera P (1997) Intracellular adenosine triphosphate (ATP) concentration: a switch in the decision between apoptosis and necrosis *J Exp Med* **185**, 1481–1486

Le Mann F, Cerda J, Babin PJ (2007) Ultrastructural aspects of the ontogeny and differentiation of ray-finned fish ovarian follicle. In *The fish oocytes: from basic studies to biotechnological applications*. (Babin PJ, Cerda J, and Lubzens E, eds): Springer

Lemire, B (2005) Mitochondrial genetics. In: The *C elegans* Research Community, editor. *WormBook*

Lehninger AL (1977) *Biochemistry* Second Edition Worth Publishers, Inc, New York

Leung LKP (1991) Principles of biological cryopreservation. In: Jamienson, B.G.M. (Ed.). *Fish evolution and systematics: evidence from spermatozoa*. New York

Leung CF, Webb SE, Miller AL (2000) On the mechanism of ooplasmic segregation in single-cell zebrafish embryos *Dev Growth Differ* **42(1)**, 29-40

Li S, Mao Z, Han W, Yan W, Chen H and Yan S (1993) In vitro oocyte maturation in the zebra fish, *Brachydanio rerio*, and the fertilization and development of the mature egg *Chin J Biotechnol* **9(4)**, 247-255

Liebermann J, Dietl J, Vanderzwalmen P and Tucker MJ (2003) Recent developments in human oocyte, embryo and blastocyst vitrification: where are we now? *Reprod Biomed Online* **7**, 623-33

Lin TT, Tung HT, Chao HH (1993) Cryopreservation of oyster embryos with conventional procedure and vitrification *Cryobiology* **30**, 614 (Abstract)

Lodish H, Baltimore D, Berk A, Zipursky SL, Matsudaira P and Darnell J (1995) *Molecular Cell Biology* (3rd Edn) W.H. Freeman and Company, New York

Loeffler CA and Lovtrup S (1970) Water balance in the salmon egg *J exp Biol* **52**, 291-8

Loomis WF and Lipmann F (1948) Reversible inhibition of the coupling between phosphorylation and oxidation *J Biol Chem* **173(2)**, 807

Lowell BB and Shulman GI (2005) Mitochondrial dysfunction and type 2 diabetes. *Science* **307**, 384–387

Luciano AM, Modena S, Vassena R, Milanesi E, Lauria A and Gandolfi F (2004) Role of intracellular cyclic adenosine 3',5'-monophosphate concentration and oocyte-cumulus cells communications on the acquisition of the developmental competence during in vitro maturation of bovine oocyte *Biol Reprod* **70(2)**, 465-72

Luo Y, Bond JD, and Ingram VM (1997) Compromised mitochondrial function leads to increased cytosolic calcium and to activation of MAP kinases. *Proc Natl Acad Sci USA* **94**, 9705-9710

Luvoni GC, Chigioni S, Perego L, Lodde V, Modena S and Luciano AM (2006) Effect of gonadotropins during in vitro maturation of feline oocytes on oocyte-cumulus cells functional coupling and intracellular concentration of glutathione *Anim Reprod Sci* **96(1-2)**, 66-78

Matsuyama M, Nagahama Y and Matsuura S (1991) Observations on ovarian follicle ultrastructure in the marine teleost, *Pagrus major*, during vitellogenesis and oocyte maturation *Aquaculture* **92**, 67-82

May-Panloup P, Chrétien MF, Jacques C, Vasseur C, Malthièry Y and Reynier P (2005) Low oocyte mitochondrial DNA content in ovarian insufficiency *Hum Reprod* **20(3)**, 593-597

Mazur P (1963) Kinetics of Water Loss from Cells at Subzero Temperatures and the Likelihood of Intracellular Freezing *J Gen Physiol* **47**, 347-369

Mazur P (1970) Cryobiology: the freezing of biological systems *Science* **168(934)**, 939-949

Mazur P, Rall WF and Leibo SP (1984) Kinetics of water loss and the likelihood of intracellular freezing in mouse ova. Influence of the method of calculating the temperature dependence of water permeability *Cell Biophys* **6(3)**, 197-213

Mazur P (2004) Principles of cryopreservation. In *Life in the Frozen State* (B. Fuller, N. Lane, and E. Benson, eds): CRC press, pp 3-66

Meryman HT (1971) Cryoprotective agents *Cryobiology* **8**, 173-183

McKersie, BD, Hoekstra, FA and Krieg, LC (1990) Differences in the susceptibility of plant membrane lipids to peroxidation *Biochim Biophys Acta* **1030(1)**, 119-126

Miller WL (2007) Steroidogenic acute regulatory protein (StAR), a novel mitochondrial cholesterol transporter *Biochimica et Biophysica Acta* **1771**, 663-676

Mitchell P and Moyle J (1967) Chemiosmotic hypothesis of oxidative phosphorylation. *Nature* **213**, 137–139

Modina S, Beretta M, Lodde V, Lauria A and Luciano AM (2004) Cytoplasmic changes and developmental competence of bovine oocytes cryopreserved without cumulus cells *Eur J Histochem* **48(4)**, 337-46

Mohr LR and Trounson AO (1980) The use of fluorescein diacetate to assess embryo viability in the mouse *J Reprod Fertil* **58(1)**, 189-96

Mokranjac D and Neupert W (2005) Protein import into mitochondria *Biochemical Society Transactions* **33**, 1019–1023

Montorzi M, Falchuk KH, Vallee BL (1995) Vitellogenin and lipovitellin: zinc proteins of *Xenopus laevis* oocytes *Biochemistry* **34(34)**, 10851-8

Moraes CT (2001) What regulates mitochondrial DNA copy number in animal cells? *Trends Genet* **17(4)**, 199-205

Moore, C, Pressman B. C, (1964). Mechanism of action of valinomycin on mitochondria. *Biochem. Biophys. Res. Commun* **15**, 562-567

Murata K, Sugiyama H, Yasumasu S, Iuchi I, Yasumasu I and Yamagami K (1997) Cloning of cDNA and estrogen-induced hepatic gene expression for choriogenin H, a precursor protein of the fish egg envelope (chorion) *Proc Natl Acad Sci USA* **94**, 2050–2055

Nagahama Y, Hirose K, Young G, Adachi S, Suzuki K and Tamaoki B (1983) Relative in vitro effectiveness of 17 alpha, 20 beta-dihydroxy-4-pregnen-3-one and other pregnene derivatives on germinal vesicle breakdown in oocytes of ayu (*Plecoglossus altivelis*), amago salmon (*Oncorhynchus rhodurus*), rainbow trout (*Salmo gairdneri*), and goldfish (*Carassius auratus*) *Gen Comp Endocrinol* **51(1)**, 15-23

Nagahama Y (1987) 17 α , 20 β -Dihydroxy-4-pregnen-3-one: A teleost Maturation-Inducing Hormone *Develop Growth and Differ* **29(1)**, 1-12

Nagahama Y (1994) Endocrine regulation of gametogenesis in fish. *Int. J. Dev. Biol.* **38**, 217-229

Nakamura M and Nagahama Y (1985) Steroid Producing Cells during Ovarian Differentiation of the Tilapia, *Sarotherodon niloticus*. *Dev Growth Differ* **27 (6)**, 701–708

Nakamura Y, Specker JL and Nagahama Y (1993) Ultrastructural analysis of the developing follicle during early vitellogenesis in tilapia, *Oreochromis niloticus*, with special reference to the steroid-producing cells *Cell Tissue Res* **272**, 33-39

Narayanan R, Kenney MC, Kamjoo S, Trinh TH, Seigel GM, Resende GP and Kuppermann BD (2005) Trypan blue: effect on retinal pigment epithelial and neurosensory retinal cells *Invest Ophthalmol Vis Sci* **46(1)**,304-9

Nicholls DG (2004) Mitochondrial membrane potential and aging *Aging Cell* **3**, 35–40

Nicolajsen H and Hvidt A (1994) Phase behaviour of the system trehalose-NaCl-water *Cryobiology* **31**, 199-205

Nieminen AL, Petrie TG, Lemasters JJ and Selman WR (1996) Cyclosporin A delays mitochondrial depolarization induced by *N*-methyl-D-aspartate in cortical neurons: evidence of the mitochondrial permeability transition. *Neuroscience* **75**, 993–997

Nilsson JR (1980) Effects of dimethyl sulphoxide on ATP content and protein synthesis in *Tetrahymena Protoptasma* **103(2)**, 189-200

Nounou M, El-khordagui L, Khallafallah N and Khalil S (2005) influence of different sugar cryoprotectants on the stability and physico-chemical characteristics of freeze-dried 5-fluorouracil plurilamellar vesicles. *DARU*, **13(4)**, 133-142

O'Connell M, McClure N and Lewis SE (2002) The effects of cryopreservation on sperm morphology, motility and mitochondrial function *Hum Reprod* **17(3)**, 704-9

Papadopoulos V, Liu J and Culty M (2007) Is there a mitochondrial signaling complex facilitating cholesterol import? *Molecular and Cellular Endocrinology* **256-266**, 59-64

Pearl M and Arav A (2000) Chilling sensitivity in zebrafish (*Brachydanio rerio*) oocytes is related to lipid phase transition *Cryo Letters* **21(3)**, 171-178

Pegg DE. (1984) Red cell volume in glycerol/sodium chloride/water mixtures *Cryobiology* **2**, 234-9

Penninckx F, Cheng N, Kerremans R, Van Damme B and De Loecker W (1983) The effects of different concentrations of glycerol and dimethylsulfoxide on the metabolic activities of kidney slices *Cryobiology* **20(1)**, 51-60

Perchee G, Jeulin C, Cosson J, Andre F and Billard R (1995) Relationship between sperm ATP content and motility of carp spermatozoa *Journal of Cell Science* **108**, (2) 747-753

Petrino TR, Greeley M.S., Jr., Selman K, Lin YW and Wallace RA (1989) Steroidogenesis in *Fundulus heteroclitus*. II. Production of 17 alpha-hydroxy-20 beta-dihydroprogesterone, testosterone, and 17 beta-estradiol by various components of the ovarian follicle *Gen Comp Endocrinol* **76**, 230–240

Pettepher CC, LeDoux SP, Bohr VA and Wilson GL (1991) Repair of Alkali-labile Sites within the Mitochondrial DNA of RINr 38 Cells after Exposure to the Nitrosourea Streptozotocin *J Biol Chem* **266**, 3113-3117

Picchietti S, Scapigliati G, Fanelli M, Barbato F, Canese S, Mastrolia L, Mazzini M and Abelli L (2001) Sex-related variations of serum immunoglobulins during reproduction in gilthead sea bream and evidence for a transfer from the female to the eggs *J Fish Biol* **59(6)**, 1503-1511

Piko L and Matsumoto L (1976) Number of mitochondria and some properties of mitochondrial DNA in the mouse egg *Dev Biol* **49(1)**, 1-10

Plachinta M, Zhang T, Rawson DM (2004a) Studies on cryoprotectant toxicity to zebrafish (*Danio rerio*) oocytes *Cryo Letters* **25(6)**, 415-24

Plachinta M, Zhang T and Rawson DM (2004b) Preliminary studies on cryopreservation of zebrafish (*Danio rerio*) vitellogenic oocytes using controlled slow cooling *Cryobiology* **49**, 347

Plachinta M (2007) Studies on Cryopreservation of Zebrafish (*Danio rerio*) Oocytes Using Controlled Slow Cooling. Luton Institute of Research in the Applied Natural Sciences, University of Bedfordshire, Luton (2007)

Plasek J and Sigler K (1996) Slow fluorescent indicators of membrane potential: a survey of different approaches to probe response analysis *J Photochem Photobiol B* **33(2)** 101-24

Podolsky RD (2002) Fertilization ecology of egg coats: physical versus chemical contributions to fertilization success of free-spawned eggs *J Exp Biol* **205**, 1657-68

Polzonetti A, Mosconi G, Soverchia L, Carnevali O and Kikuyama S (2004) Multihormonal control of vitellogenesis in lower vertebrates *Int Rev Cytol* **239**, 1 – 46

Prasad TK (1996) Mechanisms of chilling-induced oxidative stress injury and tolerance in developing maize seedlings: changes in antioxidant system, oxidation of proteins and lipids, and protease activities *The Plant Journal* **10**, 1017-1026

Prince FP (2002) Lamellar and tubular association of the mitochondrial cristae: unique forms of the cristae present in steroid-producing cells *Mitochondrion* **1**, 381-389

Privalle CT, Crivello JF and Jefcoate CR (1983) Regulation of intramitochondrial cholesterol transfer to side-chain cleavage cytochrome P-450 in rat adrenal gland *Proc Natl Acad Sci U S A* **80**, 702–706

Quinn PJ (1985) A lipid-phase separation model of low-temperature damage to biological membranes *Cryobiology* **22**,128–146

Rall WF (1987) Factors affecting the survival of mouse embryos cryopreserved by vitrification *Cryobiology* **24(5)**, 387-402

Rana KJ, McAndrew BJ, Musa MA (1992) Cryopreservation of oyster (*Crassostrea gigas*) eggs and embryos. Workshop on gamete and embryo storage and cryopreservation in aquatic organisms, Paris, p 25 (Abstract)

Rana KJ (1995) Cryopreservation of Fish Spermatozoa *Methods Mol Biol* **38**, 151-165

Ransom DG and Zon LI (1999) Collection, storage, and use of zebrafish sperm *Methods Cell Biol* **60**, 365-72

Reers M, Smith TW and Chen LB (1991) J-aggregate formation of a carbocyanine as a quantitative fluorescent indicator of membrane potential *Biochemistry* **30(18)**, 4480–4486

Reers M, Smiley ST, Mottola-Hartshorn C, Chen A, Lin M and Chen LB (1995) Mitochondrial membrane potential monitored by JC-1 dye *Methods Enzymol* **260**, 406–417

Renard P and Cochard JC (1989) Effects of various cryoprotectants on Pacific oyster *Crassostrea gigas*, Thunberg, Manila clam, *Ruditapes philippinarum* Reeve and king scallop *Pecten maximus* (L) embryos: influence of the biochemical and osmotic effects *Cryo-Letters* **10(3)**, 169-180

Reynier P, May-Panloup P, Chrétien M, Morgan CJ, Jean M, Savagner F, Barrière P and Malthièry Y (2001) Mitochondrial DNA content affects the fertilizability of human oocytes *Molecular Human Reproduction* **7 (5)**, 425-429

Reynolds ES (1963) Use of lead citrate at high pH as an electron-opaque stain in electron microscopy *Journal of Cell Biology* **17**, 208-212

Rime H, Guitton N, Pineau C, Bonnet E, Bobe J, and Jalabert B (2004) Post-ovulatory ageing and egg quality: a proteomic analysis of rainbow trout coelomic fluid *Reproductive biology and endocrinology* **2**, 26

Richter C, Park JW and Ames B (1988) Normal Oxidative Damage to Mitochondrial and Nuclear DNA is Extensive *Proc. Natl. Acad. Sci. USA* **85**, 6465-6467

Roca J, Martinez E, Vazquez JM and Lucas X (1998) Selection of immature pig oocytes for homologous in vitro penetration assays with the brilliant cresyl blue test *Reprod Fertil Dev* **10(6)**, 479-85

Rodriguez-Gonzalez E, Lopez-Bejar M, Velilla E and Paramio MT (2002) Selection of prepubertal goat oocytes using the brilliant cresyl blue test *Theriogenology* **57(5)**, 1397-409

- Roe O (1955) The metabolism and toxicity of methanol *Pharmacol Rev* **7(3)**, 399–412
- Rotman B and Papermaster BW (1966) Membrane properties of living mammalian cells as studied by enzymatic hydrolysis of fluorogenic esters *Proc Natl Acad Sci U S A* **55 (1)**, 134-41
- Royle NJ, Surai PF and Hartley IR (2003) The Effect of Variation in Dietary Intake on Maternal Deposition of Antioxidants in Zebra Finch Eggs *Funct Ecol* **17**, 472-481
- Rube DA and van der Blik AM (2004) Mitochondrial morphology is dynamic and varied *Mol Cell Biochem* **256-257(1-2)**, 331-9
- Rurangwa E, Volckaert FA, Huyskens G, Kime DE and Ollevier F (2001) Quality control of refrigerated and cryopreserved semen using computer-assisted sperm analysis (CASA), viable staining and standardized fertilization in African catfish (*Clarias gariepinus*) *Theriogenology* **55(3)**,751-69
- Ruppert-Lingham CJ, Paynter SJ, Godfrey J, Fuller BJ and Shaw RW (2003) Developmental potential of murine germinal vesicle stage cumulus-oocyte complexes following exposure to dimethylsulphoxide or cryopreservation: loss of membrane integrity of cumulus cells after thawing *Human reproduction* (Oxford, England) **18(2)**, 392-8
- Ruppert-Lingham CJ, Paynter SJ, Godfrey J, Fuller BJ and Shaw RW (2006) Membrane integrity and development of immature murine cumulus-oocyte complexes following slow cooling to -60 degrees C: the effect of immediate rewarming, plunging into LN2 and two-controlled-rate-stage cooling *Cryobiology* **52(2)**, 219-27
- Salvioli S, Dobrucki J, Moretti L, Troiano L, Fernandez MG, Pinti M, Pedrazzi J, Franceschi C and Cossarizza A (2000) Mitochondrial heterogeneity during staurosporine-

induced apoptosis in HL60 cells: analysis at the single cell and single organelle level. *Cytometry* **40**, 189–197

Sauch JF, Flanigan D, Galvin ML, Berman D and Jakubowski W (1991) Propidium iodide as an indicator of Giardia cyst viability *Appl Environ Microbiol* **57(11)**, 3243-7

Sawyer DE and Van Houten B (1999) Repair of DNA damage in mitochondria *Mutation Research/DNA Repair* **434(3)**,161-176

Scandalios JG (1993) Oxygen Stress and Superoxide Dismutases *Plant Physiol* **101(1)**, 7-12

Schupp DG and Erlandsen SL (1987) A new method to determine Giardia cyst viability: correlation of fluorescein diacetate and propidium iodide staining with animal infectivity *Appl Environ Microbiol* **53(4)**, 704-7

Seki S, Kouya T, Valdez DM, Jr Jin B, Hara T, Saida N, Kasai M and Edashige K (2007) The permeability to water and cryoprotectants of immature and mature oocytes in the zebrafish (*Danio rerio*) *Cryobiology* **54(1)**, 121-124

Seki S, Kouya T, Tsuchiya R, Vldez Jr DM, Jin B, Hara T, Saida N, Kasai M and Edashige K (2008) Development of a reliable in vitro maturation system for zebrafish oocytes *Reproduction* **135(3)**, 285-9

Seme MT, Summerfelt P, Neitz J, Eells JT and Henry MM (2001) Differential recovery of retinal function after mitochondrial inhibition by methanol intoxication *Inves. Ophthalmol. Vis Sci* **42**, 834–841

Selman K and Wallace RA (1989) Cellular aspects of oocyte growth in teleosts *Zool Sci* **6**, 211-231

Selman K, Wallace AR, Sarka A, Qi X (1993) Stage of oocyte development in the Zebrafish, *Brachydanio rerio* *Journal of Morphology* **218**, 203-224

Selman K, Petrino TR and Wallace R (1994) Experimental conditions for oocyte maturation in the zebrafish *Brachydanio rerio*. *Journal of Experimental Zoology* **269** 538-550

Shackley SE and King PE (1977) Oögenesis in a marine teleost, *Blennius pholis* L. *Cell Tissue Res* **181(1)**, 105-28

Shadel GS and Clayton DA (1997) Mitochondrial DNA maintenance in vertebrates *Annu Rev Biochem* **66**, 409-35

Shi W, Zhu S, Zhang D, Wang W, Tang G, Hou Y and Tian S (2006) Improved development by Taxol pretreatment after vitrification of *in vitro* matured porcine oocytes *Reproduction* **131** 795-804

Shibata Y, Iwamatsu T, Oba Y, Kobayashi D, Tanaka M, Nagahama Y, Suzuki N and Yoshikuni M. (2000) Identification and cDNA cloning of alveolin, an extracellular metalloproteinase, which induces chorion hardening of medaka (*Oryzias latipes*) eggs upon fertilization *J Biol Chem* **275(12)**, 8349-54

Simpson ER and Waterman MR (1983) Regulation by ACTH of steroid hormone biosynthesis in the adrenal cortex *Can J Biochem Cell Biol* **61(7)**, 692-707

Smiley ST, Reers M, Mottola-Hartshorn C, Lin M, Chen A, Smith TW, Steele GD and Jr Chen LB (1991) Intracellular heterogeneity in mitochondrial membrane potentials revealed by a J-aggregate-forming lipophilic cation JC-1 *Proc Natl Acad Sci U S A*. **88(9)**, 3671-3675

Speake BK, Noble RC, McCartney RJ and Ferguson MWJ (1994) Differences in Tissue-Specific Lipid Composition Between Embryos of Wild and Captive-Breeding Alligators (*Alligator mississippiensis*) *J Zool* **234**, 565–576

Specker JL and Sullivan CV (1994) Vitellogenesis in fishes: status and perspectives. In: Davey, K.G., Peter, R.E., Tobe, S.S. (Eds.), *Perspectives in Comparative Endocrinology*. National Research Council Canada, Ottawa, pp. 304-315

Squire JM, Knupp C and Luther PK (2008) Zebrafish--topical, transparent, and tractable for ultrastructural studies *J Gen Physiol* **131(5)**, 439-443

Srijunngam J, Kitana N, Callard IP and Wattanasirmit K, (2005) Ultrastructural changes in the ovarian follicular wall during oocytes growth in the Nile Tilapia, *Oreochromis niloticus* Linn *The Natural History Journal of Chulalongkorn University* **5(1)** 21-30

Stainier DY and Fishman MC (1992) Patterning the zebrafish heart tube: acquisition of anteroposterior polarity *Dev Biol* **153(1)** 91-101

Stehr CM and Hawkes JW (1983) The development of the hexagonally structured egg envelope in the C-O Sole (*Pleuronichthys coenosus*) *J Morphol* **178**, 267-284

Stocco DM and Clark BJ (1996) Role of the steroidogenic acute regulatory protein (StAR) in steroidogenesis *Biochem Pharmacol* **51(3)**, 197–205

Stocco DM, Wang X, Jo Y and Manna PR (2005) Multiple signaling pathways regulating steroidogenesis and steroidogenic acute regulatory protein expression: more complicated than we thought *Mol Endocrinol* **19(11)**, 2647–2659

Stojkovic SA, Zakhartchenko PV, Hutzler P, Goncalves PB and Wolf E (2001) Mitochondrial distribution and adenosine triphosphate content of bovine oocytes before and after in vitro maturation: correlation with morphological criteria and developmental capacity after in vitro fertilization and culture *Biol Reprod* **64(3)**, 904-9

Strehlow D, Heinrich G and Gilbert W (1994) The fates of the blastomeres of the 16 cell zebrafish embryo *Development* **120(7)**, 1791-1798

Stubbs CD and Smith AD (1984) The modification of mammalian membrane polyunsaturated fatty acid composition in relation to membrane fluidity and function *Biochim Biophys Acta* **779(1)**, 89-137

Suszynski TM, Wildey GM, Falde EJ, Cline GW, Stewart Maynard K, Ko N, Sotiris J, Naji-A, Hering BJ and Papas KK (2008) The ATP/DNA Ratio Is a Better Indicator of Islet Cell Viability Than the ADP/ATP Ratio *Transplantation Proceedings* **40(2)**, 346-350

Suzuki T, Komatsu H and Miyajima K (1996) Effects of glucose and its oligomers on the stability of freeze-dried liposomes. *Biochim Biophys Acta* **1278(2)**, 176–182

Tamassia M, Nuttinck F, May-Panloup P, Reynier P, Heyman Y, Charpigny G, Stojkovic M, Hiendleder S, Renard JP and Chastant-Maillard S (2004) In vitro embryo production efficiency in cattle and its association with oocyte adenosine triphosphate content, quantity of mitochondrial DNA, and mitochondrial DNA haplogroup *Biol Reprod* **71(2)**, 697-704

Tajima K and Shimizu N (1973) Effect of Sterol, Alcohol and Dimethylsulfoxide on Sorghum Seedling Damaged by Above-Freezing Low Temperature *Proc. Crop Sci. Soc. Japan* **42(2)**, 220-226

Tervit HR, Adams SL, Roberts RD, McGowan LT, Pugh PA, Smith JF and Janke AR (2005) Successful cryopreservation of Pacific oyster (*Crassostrea gigas*) oocytes. *Cryobiology* **51**,142–151.

Tourte M, Mignotte F and Mounolou JC (1984) Heterogeneous distribution and replication activity of mitochondria in *Xenopus laevis* oocytes *Eur J Cell Biol* **34(1)**, 171-8

Tsai S, Rawson DM and Zhang T (2008) Studies on cryoprotectant toxicity to early stage zebrafish (*Danio rerio*) ovarian follicles *CryoLetters* **29(6)**, 477-483

Tsai S, Rawson DM and Zhang T (2009) Studies on chilling sensitivity of early stage zebrafish (*Danio rerio*) ovarian follicles *Cryobiology* **58(3)**, 279-286

Tsang EW, Bowler C, Herouart D, Van Camp W, Villarroel R, Genetello C, Van Montagu M and Inze D (1991) Differential regulation of superoxide dismutases in plants exposed to environmental stress *Plant Cell* **3(8)**, 783-792

Turrens JF (2003) Mitochondrial formation of reactive oxygen species *J Physiol* **552**, 335-344

Tveiten H, Jobling M and Andreassen I (2004) Influence of egg lipids and fatty acids on egg viability, and their utilization during embryonic development of spotted wolf-fish, *Anarhichas minor* Olafsen *Aquacult Res* **35**, 152-161

Udvardia AJ and Linney E (2003) Windows into Development: Historic, Current and Future Perspectives on Transgenic Zebrafish *Developmental Biology* **256**, 1-17

Van Blerkom J and Runner MN (1984) Mitochondrial reorganization during resumption of arrested meiosis in the mouse oocyte *Am J Anat* **171(3)**, 335-55

Van Blerkom J, Sinclair J and Davis P (1998) Mitochondrial transfer between oocytes: potential applications of mitochondrial donation and the issue of heteroplasmy *Hum Reprod* **13(10)**, 2857-68

Van Blerkom J, Davis P, Mathwing V and Alexander S (2002) Domains of high-polarized and low-polarized mitochondria may occur in mouse and human oocytes and early embryos *Hum Reprod* **2**, 393-406

Van Blerkom J, Davis P and Alexander S (2003) Inner mitochondrial membrane potential ($\Delta\psi$), cytoplasmic ATP content and free Ca^{2+} levels in metaphase II mouse oocytes *Hum Reprod* **18**(11), 2429-40

Van Blerkom J (2004) Mitochondria in human oogenesis and preimplantation embryogenesis: engines of metabolism, ionic regulation and developmental competence *Reproduction* **128**, 269-280

Van der Elst J, Van den Abbeel E, Jacobs R, Wisse E and Van Steirteghem A (1988) Effect of 1,2-propanediol and dimethylsulphoxide on the meiotic spindle of the mouse oocyte *Hum Reprod* **3**(8), 960-7

Vergun O, Keelan J, Khodorov BI and Duchen MR (1999) Glutamate-induced mitochondrial depolarisation and perturbation of calcium homeostasis in cultured rat hippocampal neurones *J Physiol* **519**, 451-466

Voisine C, Craig EA, Zufall N, von Ahsen O, Pfanner N and Voos W (1999) The protein import motor of mitochondria: unfolding and trapping of preproteins are distinct and separable functions of matrix Hsp70 *Cell* **97**, 565-574

Wallace RA and Selman K (1981) Cellular and dynamic aspects of oocyte growth in Teleosts *American Zoology* **21**, 325-343

Wallace RA and Selman K (1990) Ultrastructural aspects of oogenesis and oocyte growth in fish and amphibians *J Electron Microsc Tech* **16**, 175 - 201

Wang Y and Ge W (2003) Gonadotropin regulation of follistatin expression in the cultured ovarian follicle cells of zebrafish, *Danio rerio* *Gen Comp Endocrinol* **134**, 308-15

Wang Y and Ge W (2005) Involvement of Cyclic Adenosine 3',5'-Monophosphate in the Differential Regulation of Activin β A and β B Expression by Gonadotrophin in the Zebrafish Ovarian Follicle Cells. *Endocrinology* **144**, 491-499

Watson Pf and Fuller B (2001) Principles of cryopreservation of gametes and embryos In: Watson PF and Holt WV (eds.) Cryobanking the genetic resource: Wildlife conservation for the future? T&F, London, pp.156-170

Wei YH (1998) Oxidative stress and mitochondrial DNA mutations in human aging *Proc Soc Exp Biol Med* **217**, 53-63

Wendling NC, Bencic DC, Nagler JJ, Cloud JG and Ingermann RL (2004) Adenosine triphosphate levels in steelhead (*Oncorhynchus mykiss*) eggs: an examination of turnover, localization and role *Comp Biochem Physiol A Mol Integr Physiol* **137(4)**, 739-48

Wessel MT and Ball BA (2004) Step-wise dilution for removal of glycerol from fresh and cryopreserved equine spermatozoa *Anim Reprod Sci* **84(1-2)**, 147-56

Westerfield M (2000) The zebrafish book. A guide for the laboratory use of zebrafish (*Danio rerio*) Eugene: Univ. of Oregon Press.

White IG (1993) Lipids and calcium uptake of sperm in relation to cold shock and preservation: a review. *Reprod Fertil Dev* **5**,639-658

Widholm JM (1972) The use of fluorescein diacetate and phenosafranine for determining viability of cultured plant cells *Stain Technol* **47**,189-94

Wikstrom JD, Katzman SM, Mohamed H, Twig G, Graf SA, Heart E, Molina AJA, Corkey BE, Moitoso de Vargas L, Danial NN, Collins S and Shirihai OS (2007) β -Cell Mitochondria Exhibit Membrane Potential Heterogeneity That Can Be Altered by Stimulatory or Toxic Fuel Levels *Diabetes* **56**, 2569-2578

Wilding M, Carotenuto R, Infante V, Dale B, Marino M, Di Matteo L and Campanella C (2001a) Confocal microscopy analysis of the activity of mitochondria contained within the 'mitochondrial cloud' during oogenesis in *Xenopus laevis* Zygote **9**, 347-352

Wilding M, Dale B, Marino M, di Matteo L, Alviggi C, Pisaturo ML, Lombardi L and De Placido G (2001b) Mitochondrial aggregation patterns and activity in human oocytes and preimplantation embryos *Hum Reprod* **16(5)**, 909-917

Wood KA. and Youle RJ (1995) The role of free radicals and p53 in neuron apoptosis in vivo *J Neurosci* **15(8)**, 5851-5857

Woods E, Zieger M, Gao DY and Critser JK (1999) Equations for obtaining melting points for the ternary system ethylene glycol/sodium chloride/water and their application to cryopreservation *Cryobiology* **38**, 403-407

Wourms JP (1976) Annual fish oogenesis I. Differentiation of the mature oocyte and formation of the primary envelope *Dev Biol* **50**, 338-354

Wourms JP and Sheldon H (1976) Annual fish oogenesis II. Formation of the secondary egg envelope *Dev Biol* **50**, 355-366

Wu C, Rui R, Dai J, Zhang C, Ju S, Xie B, Lu X and Zheng X (2006) Effects of cryopreservation on the developmental competence, ultrastructure and cytoskeletal structure of porcine oocytes *Mol Reprod Dev* **73(11)**, 1454-62

Yakes F M and Van Houten B (1997) Mitochondrial DNA damage is more extensive and persists longer than nuclear DNA damage in human cells following oxidative stress *Proc. Natl. Acad. Sci. USA Cell Biology* **94**, 514-51

Yokoyama H, Danjo T, Ogawa K and Wakabayashi H (1997) A vital staining technique with fluorescein diacetate (FDA) and propidium iodide (PI) for the determination of viability of myxosporean and actinosporean spores *Journal of Fish Diseases* **20**, 281-286

Yamamoto N (1989) Effect of dimethyl sulfoxide on cytosolic ionized calcium concentration and cytoskeletal organization of hepatocytes in a primary culture. *Cell Struct. Funct.*, **14**, 75-85

Zeron Y, Pearl M, Borochoy A and Arav A (1999) Kinetic and temporal factors influence chilling injury to germinal vesicle and mature bovine oocytes *Cryobiology* **38(1)** 35-42

Zhang T, Rawson DM and Morris GJ (1993) Cryopreservation of pre-hatch embryos of zebrafish (*Brachydanio rerio*) *Aquat Living Resour* **6**, 145-153

Zhang T and Rawson DM (1998) Permeability of dechorionated one-cell and six-somite stage zebrafish (*Brachydanio rerio*) embryos to water and methanol. *Cryobiology* **37(1)**, 13-21

Zhang T, Isayeva A, Adams SL and Rawson DM (2005) Studies on membrane permeability of zebrafish (*Danio rerio*) oocytes in the presence of different cryoprotectants *Cryobiology* **50(3)**, 285-93

Zhang XS, Zhao L, Hua LC, Zhu HY (1989) A study on the cryopreservation of common carp *Cyprinus carpio* embryo *CryoLetters*, **10**, 271-278

Zhang YZ, Ouyang YC, Hou Y, Schatten H, Chen DY and Sun QY (2008) Mitochondrial behavior during oogenesis in zebrafish: a confocal microscopy analysis *Dev Growth Differ* **50(3)**, 189-201

Zhong TP, Rosenberg M, Mohideen MA, Weinstein B and Fishman MC (1984) gridlock, an HLH Gene Required for Assembly of the Aorta in Zebrafish *Science* **287**(5459), 1820-4

Zon LI (1999) Zebrafish: A New Model for Human Disease *Genome Res* **9**, 99-100

Appendix A:

Mitochondrial distribution and nuclei localization in the granulosa cells of stage III ovarian follicles

This additional and preliminary investigation was prompted by a referee's comment to the publication of the results on the distribution of mitochondria in the granulosa cells (Zampolla et al. 2009), and on the recent availability of a Leica TCS SP5 in this laboratory. A study was carried out to investigate nuclear location and size in the granulosa cells of stage III zebrafish oocytes, to further confirm the mitochondrial distributional arrangement at the margin of the granulosa cell. In order to show mitochondria and nuclei localization, JC-1 stain and DAPI (4',6-diamidino-2-phenylindole) were used with confocal microscopy. DAPI is a DNA-specific probe which forms a blue fluorescent complex by attaching to the minor groove of A-T rich sequences of DNA. It is extensively used for the determination of nuclear DNA content and for cell cycle analysis (Kapusinski 1995).

Staining of Mitochondria

Stage III ovarian follicles were stained with JC-1 and DAPI. A 1.5 mM stock solution of the JC-1 was prepared in DMSO according to the manufacturer's instructions. The dyes were used at a concentration of 5 μ M for JC-1 and 12.5 ng/ml for DAPI in Hanks' solution for 30 min at room temperature. Subsequently the follicles were washed three times with Hanks' solution, transferred into a 35 mm glass bottom dish (WillCo Wells) and studied by confocal microscopy.

Confocal microscopy

Stained samples were examined using a Leica TCS SP5 (Leica, Microsystems (UK) Ltd, Milton Keynes, Bucks, UK) confocal microscope equipped with Ar/Kr laser. Active mitochondria distribution and nuclei location was assessed through a series of optical sections. Objectives (20X, 40X and 63X water immersion), pinhole, filters, gain and

offset were kept constant throughout the experiments. Laser excitation and emission filters for the different labelled dyes were as follows: JC-1 FM: λ_{ex} =488 nm (excitation), (green) λ_{em} =510/550 nm (emission), red) λ_{em} =580/610 nm (emission), DAPI λ_{ex} =405nm (excitation), λ_{em} =460 nm (emission). Digital images were obtained with Leica TCS software and stored in TIFF format.

Results

Preliminary results showed DAPI bright blue staining of the nuclei in the granulosa cell, surrounded by mitochondria fluorescing green and red on the basis of the membrane potential (Fig.1). The nuclei are shown to occupy a major proportion of the cytoplasmic volume and, in part, to determine the peripheral location of the mitochondria.

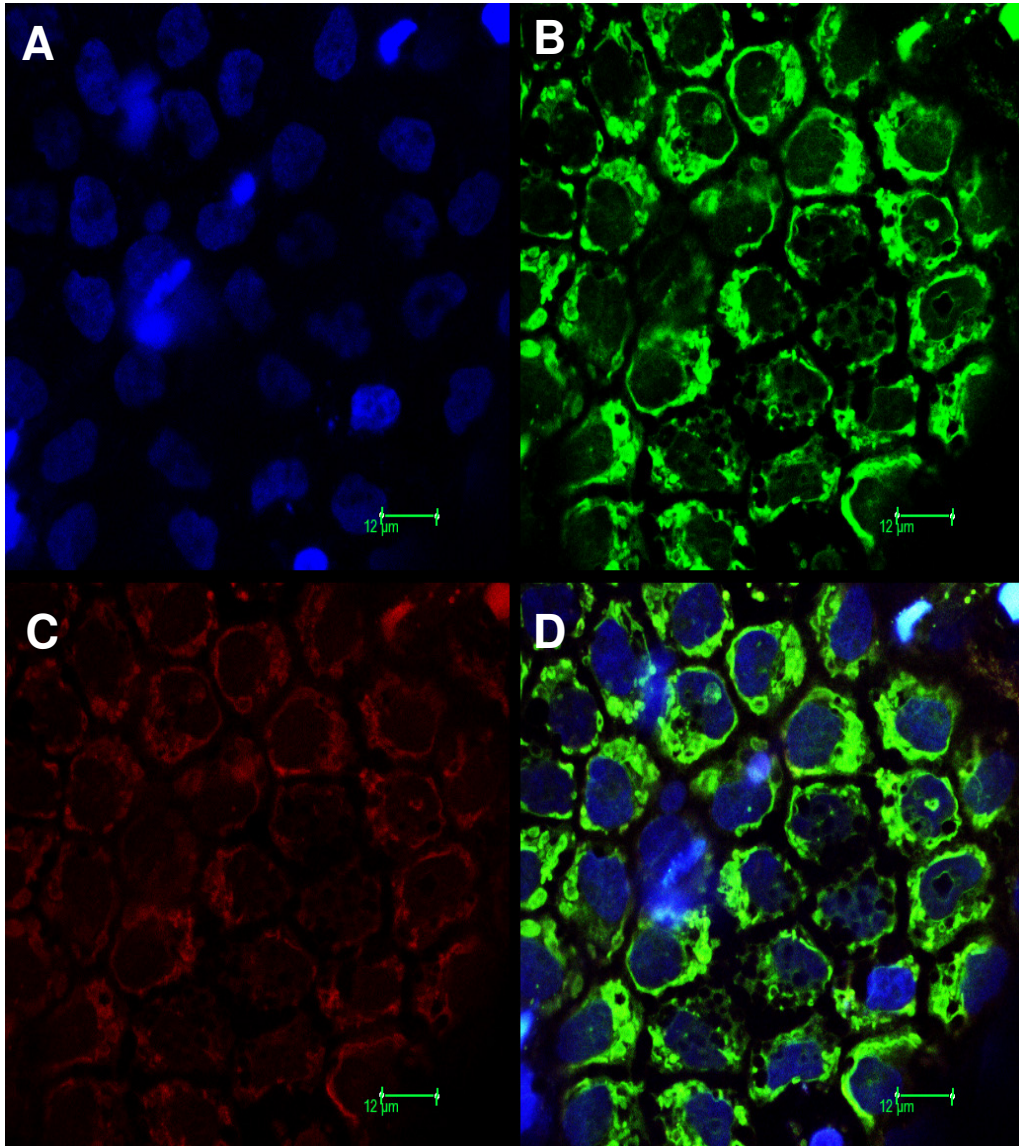


Fig. 1 Nuclei localisation and mitochondria distribution in granulosa cells surrounding stage III zebrafish oocyte. Blue (A) represents nuclei stained by DAPI, low polarised mitochondria stained by JC-1 fluoresce green (B), while high polarised mitochondria fluoresce red (C). Merged image showing nuclei and mitochondrial distributional arrangement at the margin of the cells (D).

Appendix B: Publications

Zampolla T., Zhang T. and Rawson D.M.(2008) Evaluation of Zebrafish (*Danio rerio*) Ovarian Follicle Viability by Simultaneous Staining with Fluorescein Diacetate and Propidium Iodide Cryolethers, 29(6), 463-475.

Zampolla T., Zhang T., Holt W.V. and Rawson D.M. (2009) Distributional arrangement of mitochondria in the granulosa cells surrounding stage III zebrafish (*Danio rerio*) oocytes. Theriogenology, in press XXX, 2009

Zampolla T., Spikings E., Zhang T. and Rawson D.M. Effect of cryoprotectants exposure on mitochondrial activity and mtDNA copy number. Abstract of poster presented at The Society for Low Temperature Biology (SLTB) Annual Meeting and AGM – Copenhagen 11th and 12th of September 2008.

Zampolla T., Rawson D.M. and Zhang T. Development of new viability assessment methods for zebrafish (*Danio rerio*) oocytes. Abstract of poster presented at Cryo 2006: 43rd Annual Meeting Of The Society For Cryobiology, Hamburg, Germany, July 24 –27, 2006, Abstracts Book, p.16.

EVALUATION OF ZEBRAFISH (*Danio rerio*) OVARIAN FOLLICLE VIABILITY BY SIMULTANEOUS STAINING WITH FLUORESCEIN DIACETATE AND PROPIDIUM IODIDE

T. Zampolla, T. Zhang and D.M. Rawson*

LIRANS Institute of Research in the Applied Natural Sciences, University of Bedfordshire, 250 Butterfield, Great Marlings, Luton, Bedfordshire, LU2 8DL, United Kingdom

*Correspondence author e-mail: david.rawson@beds.ac.uk

Abstract

Reliable fish oocyte quality assessment methods are essential in developing protocols for cryopreservation as well as their *in vitro* maturation and fertilisation. Current ovarian follicle viability assessment methods either lack sensitivity (e.g. Trypan Blue staining-TB) or are stage dependent (e.g. *in vitro* maturation and observation of germinal vesicle breakdown-GVBD). The aim of the present study was to develop a new viability assessment method for zebrafish ovarian follicles that is reliable, sensitive and not-stage specific. Fluorescein Diacetate (FDA) and Propidium Iodide (PI) were used for the first time to assess viability of zebrafish ovarian follicles. After preliminary studies to evaluate the efficacy of FDA and PI, a combination of these two fluorochromes was subsequently chosen and compared with TB staining and GVBD test in a series of cryoprotectant toxicity studies and following cryopreservation using stage III ovarian follicles. In all cases the FDA-PI test proved to be more sensitive than TB staining but less sensitive than the GVBD test. Ovarian follicle survivals after 4M Methanol treatment for 30 min at 22°C were $67.4 \pm 4.4\%$, $43.9 \pm 3.8\%$ and $19.6 \pm 1.9\%$ using TB, FDA-PI and GVBD test respectively. Survivals after cryopreservation procedure were $38.9 \pm 4.0\%$ and $28.9 \pm 2.5\%$ using TB and FDA-PI respectively when Hank's solution was used as medium and $45.2 \pm 4.3\%$ and $35.2 \pm 3.5\%$ when KCl buffer was used. The results showed the method to be promising, and it may offer a new approach for viability assessment of fish ovarian follicles.

Keywords: fluorescein diacetate, propidium iodide, ovarian follicles, zebrafish

INTRODUCTION

The development of zebrafish oocytes has been divided into five stages (26): stage I (primary growth stage); stage II (cortical alveoli stage); stage III (vitellogenic stage); stage IV (maturation stage); stage V (mature egg). A range of vital stains and other methods have been studied for assessing the viability of follicles at different stages, and among these TB staining and *in vitro* maturation followed by observation of germinal vesicle breakdown (GVBD) have been routinely used in our laboratories. The GVBD test is the most sensitive method, but this test can only be applied to stage III follicles as later stages have already undergone maturation

and germinal vesicle breakdown. Indeed, unlike maturation in mammals, where offspring have been produced using *in vitro* matured oocytes, in zebrafish there are few reports (16, 25) of offspring production derived by *in vitro* ovarian follicle maturation, and the stage used in these studies was late vitellogenic follicles with a diameter between 0.65-0.69 mm.

Whilst vital stains such as the TB are suitable for their applicability to all stages they do have several limitations. TB only assesses membrane integrity and it does not provide any information on the metabolic activity of the cells (20). The FDA test has been found to be suitable for assessing animal cells viability (27). Rotman and Papermaster (1965), in a detailed investigation, demonstrated the mode of action of this compound, providing evidence that indicated that the intracellular retention of fluorescein is dependent on the integrity of the cell membrane. The non-polar fluorescein-diacetate molecules enter the cell, are hydrolyzed by cellular esterases to produce the polar compound fluorescein. The resulting reaction, characterised by the appearance of bright-green fluorescence inside the cell, is termed *fluorochromasia*. In viable cells, the fluorescein is unable to pass through the intact membrane, accumulating in the cytoplasm of the cell, whilst damaged cells show a distinct loss of fluorescein through the cell membrane. The FDA test has been successfully employed to assess viability of pig oocytes (1, 6), mouse embryo (17), human cells (7) and ram spermatozoa (12). Staining of nonviable cells with propidium iodide (DNA-binding probe) has been performed on most cell types (23) as single or in combination with other fluorochromes (5, 8). Live cells with intact membranes are distinguished by their ability to exclude the dye that easily penetrates dead or damaged cells, intercalating with DNA and RNA to form bright red fluorescence. Since the dye is excluded by intact cell membranes, PI is an effective stain to identify non viable cells. The combination of FDA and PI has been used to determine viability of protozoa cyst (24), parasites spores (28) and mammalian cells (11, 14), it is used here for the first time to investigate zebrafish ovarian follicles.

MATERIALS AND METHODS

In this study stage III zebrafish ovarian follicles were used, during this stage the oocyte is surrounded by several cell layers and acellular structures (thecal layer, basement membrane, follicular layer and vitelline envelope). Following initial checks to test the efficacy of the FDA and PI methods, FDA-PI staining was compared with TB staining and GVBD test in a series of cryoprotectant (CPA) toxicity tests in different media commonly used with zebrafish follicles - Hank's solution, KCl buffer and Leibovitz L-15. The GVBD test was only carried out when the Leibovitz L-15 was used as it is the medium normally employed for zebrafish *in vitro* maturation. The FDA-PI test was also used, in comparison with TB, to assess ovarian follicle viability following cryopreservation. The GVBD test was not applicable after cryopreservation procedure as the follicles became transparent. This study used the optimum cryoprotective media and cooling rates for stage III zebrafish follicles that were previously identified in our laboratory (9, 20, 28).

Ovarian follicle collection

To collect follicles, adult female zebrafish (*Danio Rerio*) were anaesthetized with a lethal dose of tricaine (0.6mg/ml) for 5 min and decapitated before the ovaries were removed. The ovaries were immersed in 1.6mg/ml hyaluronidase (10) made up in either Hank's solution (137 mM NaCl, 5.4 mM KCl, 0.25 mM Na₂HPO₄, 0.44 mM KH₂PO₄, 1.3 mM CaCl₂, 1 mM MgSO₄, 4.2 mM NaHCO₃), KCl buffer (55 mM KCl, 55 mM K acetate, 1 mM MgCl₂, 2 mM CaCl₂, 10 mM M HEPES; pH 7.4) or 50% Leibovitz L-15 medium (1.3 mM CaCl₂* 2H₂O, 0.8 mM MgSO₄, 5.4 mM KCl, 0.4 mM KH₂PO₄, 138 mM NaCl, 1.3 mM Na₂HPO₄) for

10 min at room temperature. Follicles were separated by gentle pipetting, and then washed three times in Hank's, KCl buffer or 50% Leibovitz L-15 and stage III follicles selected.

Reliability of FDA-PI

In order to assess the reliability of FDA and PI stains and the combination of these two fluorochromes, a negative control was conducted exposing ovarian follicles to 99% methanol for 10 min at 22°C, while follicles for the control were held in Hank's solution or KCl buffer. Follicle viability of control and treated groups were assessed by FDA and PI alone and in combination (FDA-PI).

Ovarian follicle staining by FDA-PI

For FDA-PI staining, a stock solution of FDA was prepared by dissolving 5 mg FDA / 1 ml in acetone. The FDA working solution was freshly prepared before use by adding 0.04 ml of stock to 10 ml of PBS. The Propidium Iodide stock solution was made by dissolving 1 mg PI in 50 ml PBS. For FDA-PI staining, 0.1 ml (2 µg) of FDA working solution and 0.03 ml (0.6 µg) of PI stock solution were added directly to the follicles. The follicles were stained in the dark for 3 min (14). Follicles fluorescing bright green were considered to be viable, while nonviable cells stained bright red. FDA-PI stained follicles were examined with a fluorescence microscope (LEICA DM IL) with two filter cubes: I3 (excitation filter: bandpass (BP) 450-490 nm; dichromatic mirror: 510; suppression filter: longpass (LP) 515) and N.2.1 filter excitation filters: BP: 515-560 nm; dichromatic mirror: 580; suppression filter: LP: 590). This filter arrangement did not permit both green and red fluorescing follicles to be seen simultaneously.

Comparisons of FDA-PI with other viability assessment methods after follicle isolation

The FDA-PI test was subsequently compared with two other viability assessment methods routinely used in our laboratories, the TB and GVBD tests. The viability of ovarian follicles was assessed both immediately after follicle separation from the ovaries and after 30 min in L-15 medium at room temperature.

Comparisons of FDA-PI, TB and GVBD in cryoprotective agents (CPAs) toxicity tests

Follicles were exposed to 3 different CPAs, ethylene glycol (EG), methanol or dimethyl sulfoxide (DMSO) in the concentration range of 1 to 4M (made up in Hank's, KCl buffer or 50% Leibovitz L-15 medium) for 30 min at 22°C. Control follicles were incubated in the corresponding medium under the same conditions. For the assessment of follicle viability following CPA exposure, 15-40 follicles were held in bathing medium (10 min) followed by replacement of the medium with CPA supplemented medium. After incubation in CPAs for 30 min at 22°C, follicles were washed twice with bathing media and viability tests were conducted. The washing procedure was undertaken to remove the cryoprotectant prior to assessment. This step is required otherwise in the case of GVBD test, the ovarian follicles would be exposed to cryoprotectants for 24h. Furthermore, this procedure has been already described in previous works (see Plachinta et al. 2004). From our experience, washing does not affect the survival of the ovarian follicles. Hank's solution and KCl buffer were used for TB and FDA+PI tests, whilst 50% L-15 medium was used for TB, FDA+PI and GVBD tests.

Comparisons of FDA-PI and TB following cryopreservation procedure

4 M Methanol in combination with 0.2 M glucose was used in this study. Solutions of the CPAs were made up in KCl buffer or Hank's solution. After 30 min incubation in CPAs solution, follicles were loaded into 0.5 ml plastic straws and put into a programmable cooler (Planer KRYO 550). The following cooling protocol was used: cooling at 2°C/min from 20°C

to -12.5°C (seeding temperature), manual seeded and held for 5 min, freezing from -12.5°C to -40°C at 0.3°C / min, from -40°C to -80°C at 10°C/min and from -80 to -160°C at 50°C/ min, samples were then plunged in Liquid Nitrogen (LN₂) at -196°C and held in LN₂ for at least 10 in. Samples were thawed using a water bath at 27°C. Cryoprotectants were removed in 4 steps (2 M, 1 M and 0.5 M methanol in Hanks' solution or KCl buffer, 2.5 min for each step); the samples were then transferred to Hanks' solution or KCl buffer. Viability was assessed by FDA+PI and TB tests.

Ovarian follicle staining by Trypan Blue

TB was used to assess membrane integrity. Follicles were incubated in 0.2% of Trypan Blue for 3-5 min at room temperature and then washed in Hanks solution, KCl buffer or L15 medium. Unstained follicles were considered viable, while the follicles stained blue were considered non-viable.

Observation of Germinal Vesicle Breakdown (GVBD)

Examination of the physiological event of GVBD involved the incubation of stage III follicle in L15 medium supplemented with 0.1 µg/ml DHP (17α-Hydroxy-20βdihydroprogesterone) for 24h at 25°C. Prematurational follicles are opaque but become translucent following GVBD. Follicles that do not undergo maturation and germinal vesicle breakdown remained opaque.

Statistical Analysis of Data

Statistical analyses were performed using SPSS for Windows software (SPSS Inc., Version 12.0) and data are presented as mean ± SEM. For all experiments, three replicas were used for each treatment and experiments were repeated three times. Results were analyzed using a one-way ANOVA followed by least significant difference (LSD) post-hoc test ($P < 0.05$). When two groups were compared, results were analyzed using Student's t-tests ($P < 0.05$).

RESULTS

Reliability of FDA-PI

Simultaneous staining with FDA-PI showed distinctive differences between control and negative control. After exposure to 99% methanol for 10 min, dead follicles showed bright red colour due to propidium iodide penetration, while the same follicles were only faintly stained green by FDA. Living follicles produced fluorochromasia, represented by bright green and remain unstained by PI. Figure 1 shows the number of follicles of the control group and treated group indicating the proportion of follicles stained red by PI and stained green by FDA.

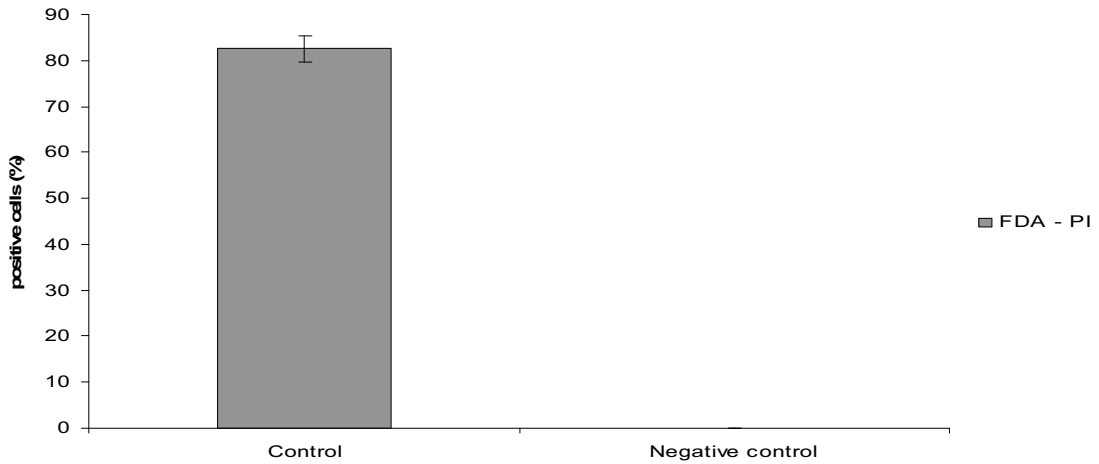


Figure 1. Viability of stage III ovarian follicles stained by PI and FDA. Control represents follicles in KCL buffer. Negative control represents follicles exposed to 99% Methanol for 10 min. Columns and error bars represent means \pm SEM of three experiments each with three replicates.

Comparisons of FDA-PI, TB and GVBD tests after follicles isolation

Viability assessment with FDA-PI, TB and GVBD was performed immediately after the separation of the follicles from the ovaries and after 30 min incubation in L-15 medium. The results showed that the percentage viability assessed by TB was always higher than the viability assessed by FDA-PI (Fig. 2). There were significant ($P < 0.05$) differences between the group obtained immediately after follicle separation and the group held at room temperature for 30 min in L-15 medium when the viability was assessed by TB, whilst there were no significant ($P > 0.05$) differences when the viability was assessed by FDA-PI and GVBD test (Fig 2).

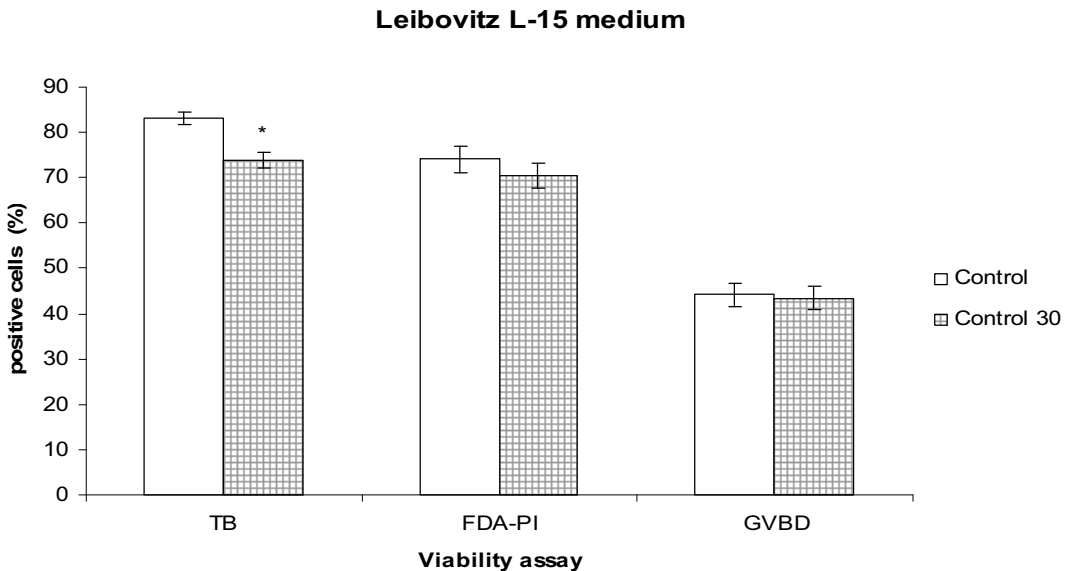


Figure 2. Comparisons of viability of stage III ovarian follicles using three viability assessment methods. Control: TB, FDA-PI and GVBD tests were performed immediately after follicle separation from the ovaries; control 30: follicles incubated at 22°C for 30 min in 50% Leibovitz L-15. Columns and error bars represent means \pm SEM of three experiments each with three replicates. *Significantly different from corresponding control value, $P < 0.05$.

Comparisons of FDA-PI, TB and GVBD in cryoprotective agents (CPAs) toxicity tests

Results showed that the FDA-PI staining is more sensitive than TB staining and the sensitivity appeared to increase with concentration of cryoprotectants. The study also showed that the toxicity of cryoprotectants generally increased with concentration using all three viability assessment methods (Fig. 3-4-5). There are difference in the TB, FDA-PI or GVBD control values at 1 M, 2 M, 3 M and 4 M CPA. These differences represent fish variability as the experiments were conducted on different days with new controls. However, the control groups were analyzed using a one-way ANOVA, which showed that there were no significant differences among control groups assessed by the same viability method. Methanol was the least toxic cryoprotectant to zebrafish ovarian follicles in all three different media. DMSO and EG were more toxic to stage III follicles and significantly reduced the viability of follicles when assessed by GVBD, FDA-PI or TB in all media (Fig. 3-4-5). The medium employed to make up the cryoprotectant solutions had no effects on follicle viability assessed after 30 min exposure to cryoprotectants at room temperature as similar results were obtained with all three different media (Fig. 3-4-5). Viabilities assessed by TB and FDA-PI were also compared when follicles were exposed to 4 M methanol with and without 0.2 M glucose in Hank's solution and KCl buffer as this cryoprotectant solution was identified as the optimum for zebrafish oocytes cryopreservation (9). Results showed that there were no significant differences ($P > 0.05$) between the control and treated groups when 4 M methanol + 0.2 M glucose was used and viability was assessed by FDA-PI and TB tests (Fig. 6).

Comparisons of FDA-P and TB following cryopreservation procedure

The percentage of viable follicles after cryopreservation assessed by FDA-PI was always lower than the viability evaluated by TB both with Hank's solution ($28.9 \pm 2.5\%$ and $38.9 \pm 4.0\%$) and KCl buffer ($35.2 \pm 3.5\%$ and $45.2 \pm 4.3\%$) (Fig. 7). Moreover, there were no significant ($P > 0.05$) differences between KCl buffer and Hank's solution after cryopreservation procedure when the viability was assessed by FDA-PI and TB (Fig. 7). The FDA-PI proved to be more sensitive than TB test as microscopic observation showed a decrease of green fluorescence in the follicles with intact membranes after cryopreservation compared to the control follicles.

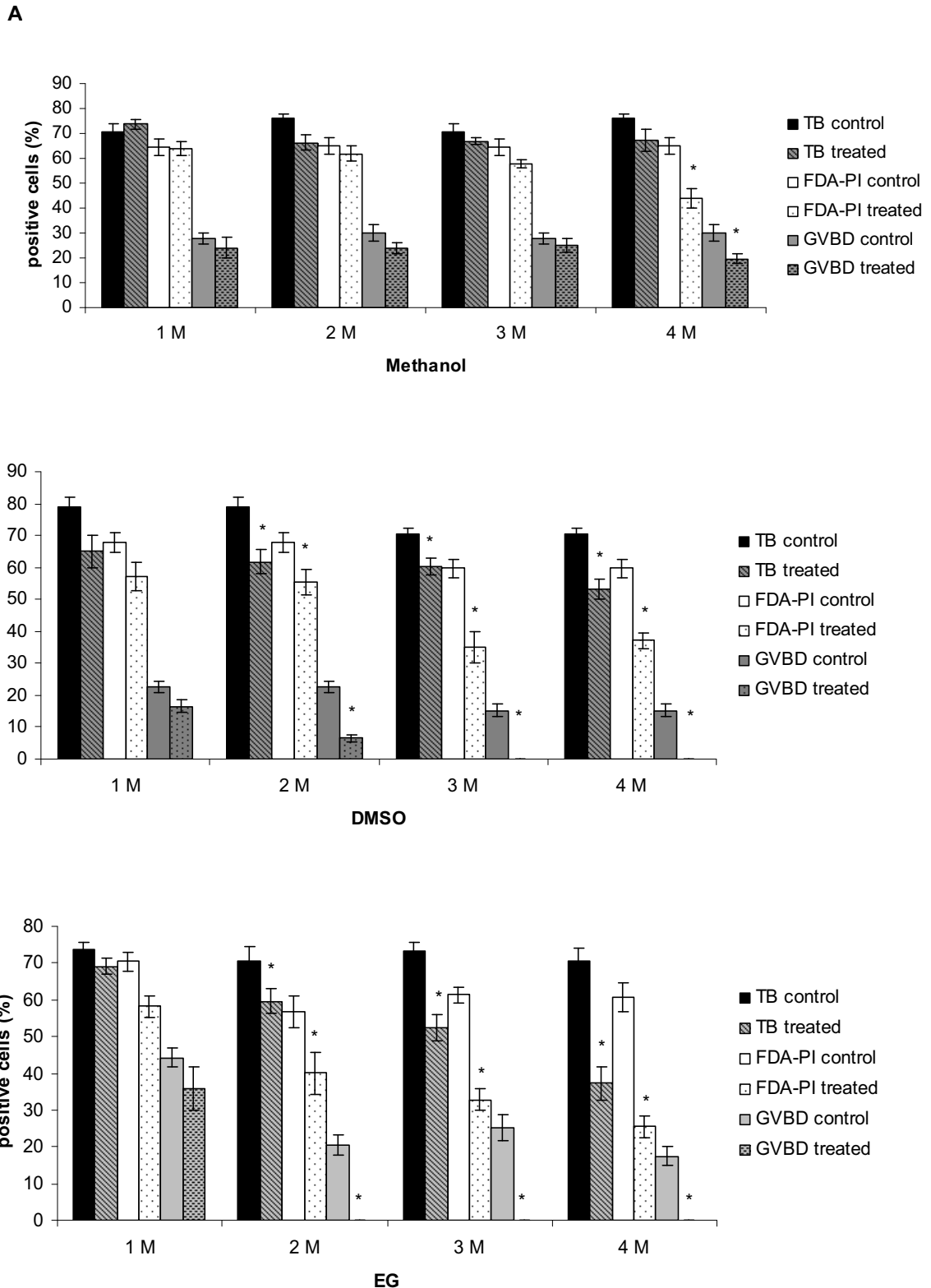


Figure 3. Comparisons of follicle viability assessed by TB, FDA-PI and GVBD tests following exposure to different concentrations of methanol (**A**), DMSO (**B**) and EG (**C**), in Leibovitz L-15 medium. Control: TB, FDA-PI and GVBD tests were performed after incubation of ovarian follicles at 22°C for 30 min in 50% Leibovitz L-15; treated: TB, FDA-PI and GVBD were conducted after ovarian follicles were exposed to 1-4 M methanol, DMSO or EG for 30 min at 22°C. Columns and error bars represent means \pm SEM of three experiments each with three replicates. *Significantly different from corresponding control value, $P < 0.05$.

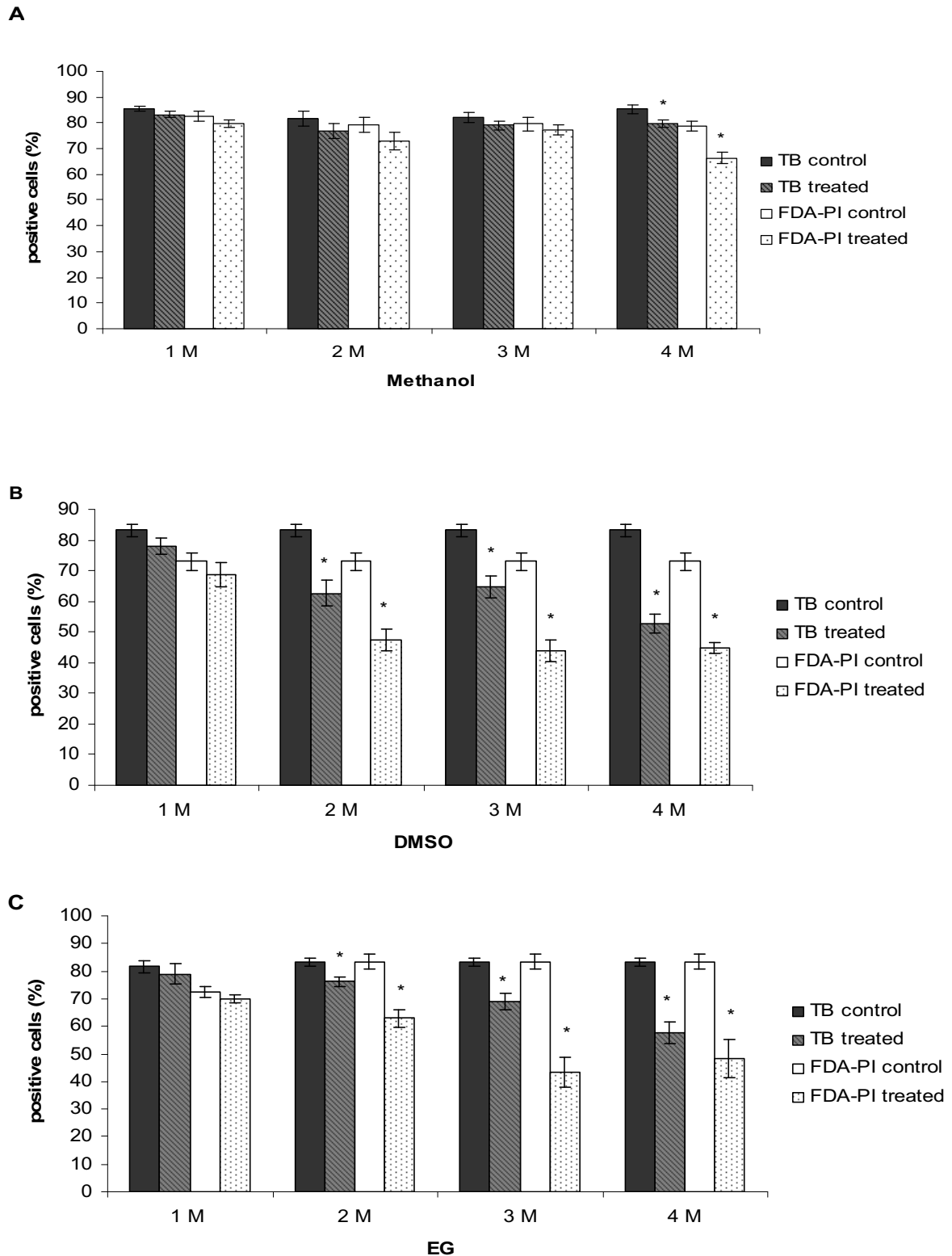


Figure 4. Comparisons of follicle viability assessed by TB and FDA-PI tests following exposure to different concentrations of methanol (A), DMSO (B) and EG (C), in Hank's solution. Control: TB and FDA-PI tests were performed after incubation of ovarian follicles at 22°C for 30 min in Hank's solution; treated: TB and FDA-PI were conducted after ovarian follicles were exposed to 1-4 M methanol, DMSO or EG for 30 min at 22°C. Columns and error bars represent means \pm SEM of three experiments each with three replicates. *Significantly different from corresponding control value, $P < 0.05$.

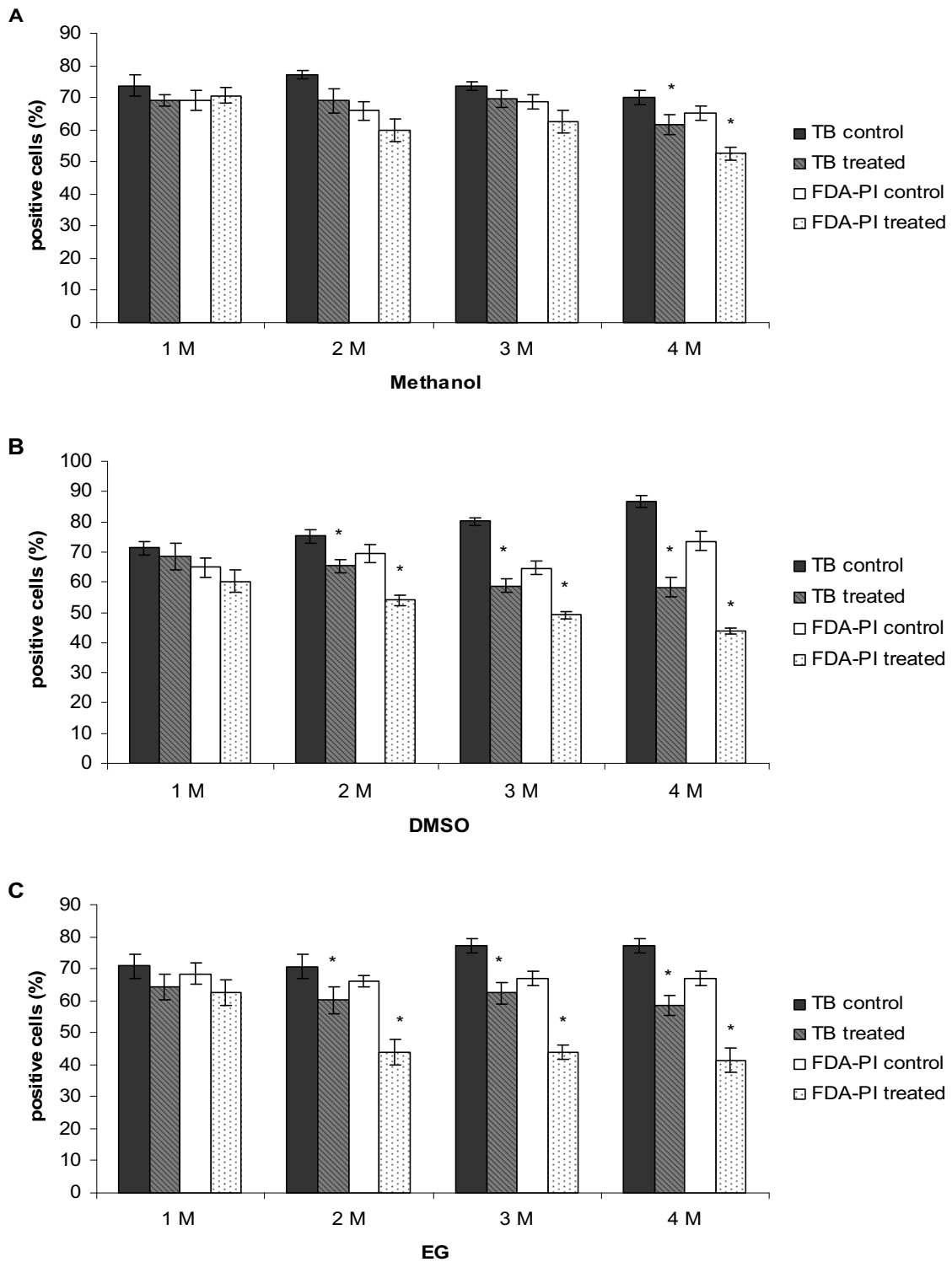


Figure 5. Comparisons of follicle viability assessed by TB and FDA-PI tests following exposure to different concentrations of methanol (**A**), DMSO (**B**) and EG (**C**), in KCl buffer. Control: TB and FDA-PI tests were performed after incubation of ovarian follicles at 22°C for 30 min in KCl buffer; treated: TB and FDA-PI were conducted after ovarian follicles were exposed to 1-4 M methanol, DMSO or EG for 30 min at 22°C. Columns and error bars represent means \pm SEM of three experiments each with three replicates. *Significantly different from corresponding control value, $P < 0.05$.

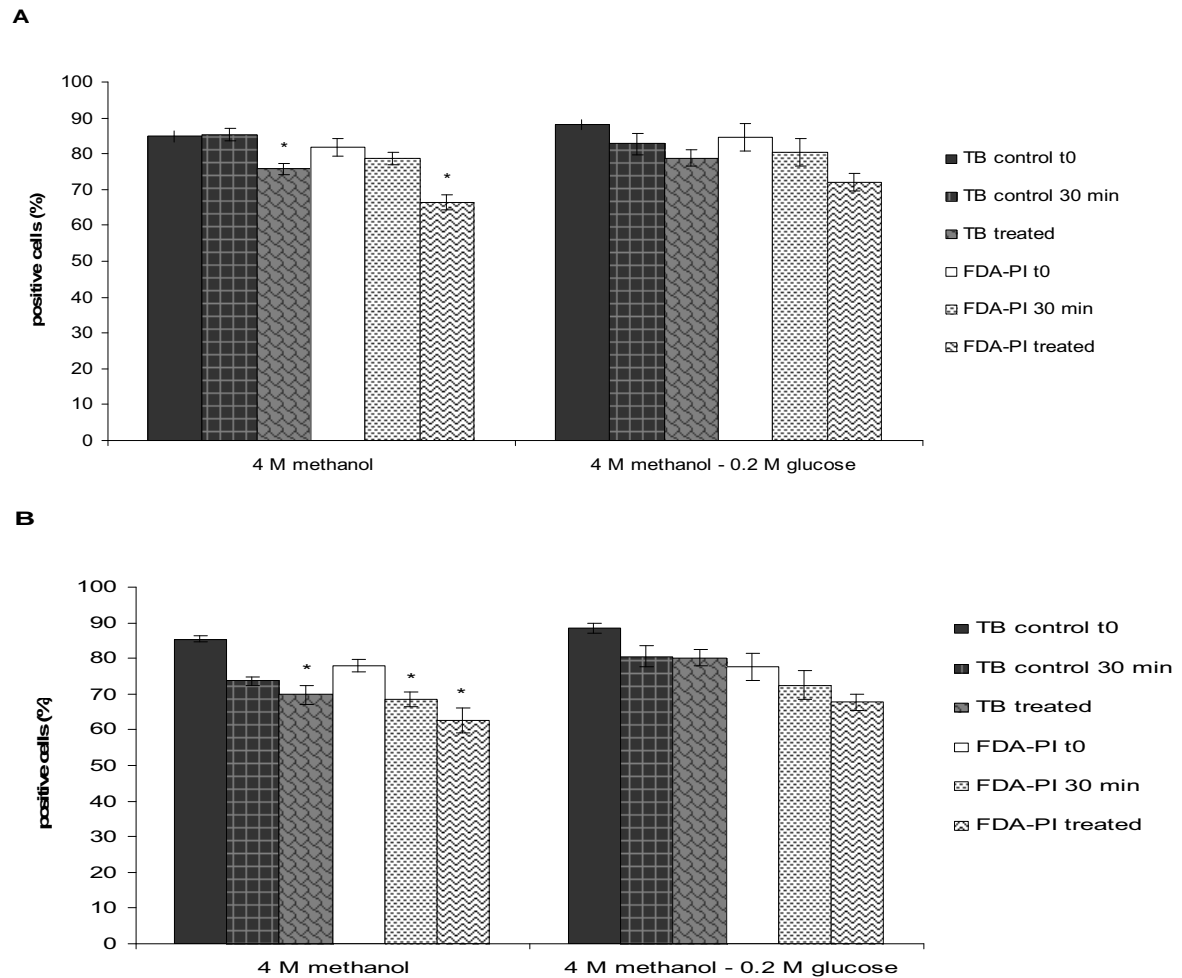


Figure 6. Comparisons of TB and FDA-PI tests on stage III follicles exposed to two cryoprotectant solutions – 4 M methanol or 4 M methanol + 0.2 M glucose - made up in Hank's solution (**A**) and KCl buffer (**B**). Control t0: viability was assessed after ovarian follicles separation. Control 30 min: ovarian follicles were incubated at 22°C for 30 min in KCl buffer. Treated: TB and FDA-PI were conducted after incubation of follicles in 4 M methanol or 4 M methanol + 0.2 M glucose. Columns and error bars represent means \pm SEM of three experiments each with three replicates. *Significantly different from corresponding control value, $P < 0.05$.

Optimal cryopreservation protocol

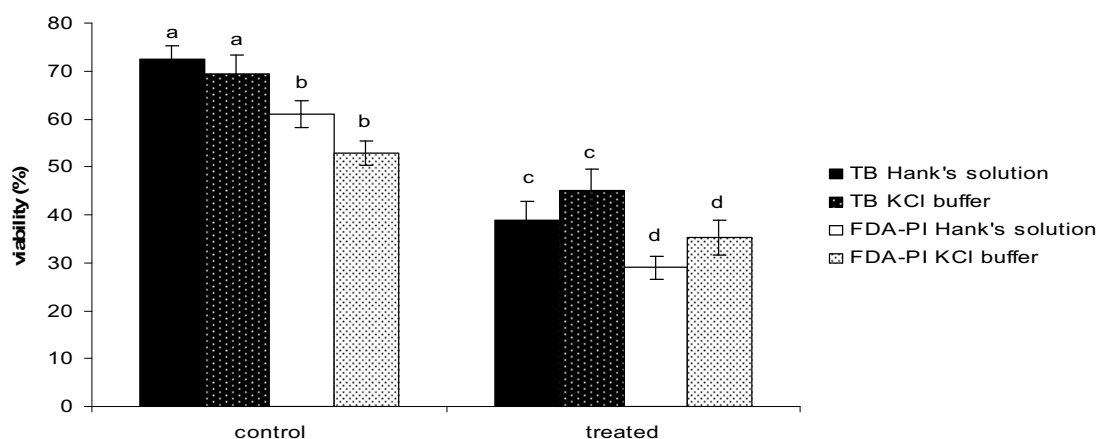


Figure 7. Comparisons of TB and FDA-PI viability tests of stage III follicles following cryopreservation, using 4 M methanol with 0.2 M glucose as cryoprotectants in either Hank's solution or KCl buffer. Control: TB, FDA+PI were performed on ovarian follicles held at 22°C; treated: TB and FDA-PI were conducted after cryopreservation of follicles in 4 M methanol and 0.2 M glucose. Columns and error bars represent means \pm SEM of three experiments each with three replicates; bars with different letter differ significantly ($P < 0.05$).

DISCUSSION

There are a limited number of studies in the literature on zebrafish ovarian follicle viability assessment. In these studies, carboxyfluorescein diacetate (19), Trypan Blue, thiazolyl blue (MTT) and GVBD (20) were used. The GVBD test is the most sensitive method for assessing follicles survival as it assesses oocytes developmental capability; however, it can only be applied to stage III follicles as later stages have already undergone maturation and germinal vesicle breakdown *in vivo*. Moreover, the GVBD test is not applicable in all experimental conditions. The TB test is one of the most common method to assess cell viability and it has been performed on many cell types (2, 18), but it assess only membrane integrity. TB is a vital dye, its reactivity is based on the fact that the chromophore is negatively charged and does not penetrate the cell unless the membrane is damaged. The results in this study showed that the FDA-PI test can be successfully employed to assay fish follicle integrity following exposure to different experimental conditions. This test proved to be more sensitive than TB but less sensitive than GVBD test.

The results from the present study also showed that L-15 medium is the most suitable medium for zebrafish follicles, when compared with two other solutions (Hank's solution and KCl buffer). This is thought to be because Leibovitz L-15 is bicarbonate free medium containing salts, which uses high level of amino acids in the free base form with buffering capacity, and has galactose as a carbohydrate source which produces lactic acid at a slower rate than glucose. It also contains pyruvate and alanine to generate bicarbonate for synthesis reaction. This medium has been designed for use in cell culture in free exchange with room air (3, 15).

The results from the present study showed that the toxicity of cryoprotectants generally increased with concentration using all three viability assessment methods. As previously reported (20), methanol is the least toxic cryoprotectant to stage III zebrafish follicles, followed by DMSO and EG. However, the results of this study showed that 4 M methanol had a toxic effect on zebrafish follicles since significant differences were observed between the

control and the treated follicles where the survival was assessed by FDA-PI and TB, these results are not in agreement with previous studies (20, 21). The use of high concentrations of CPA may induce osmotic damage and damage induced by the toxicity of the CPA itself. The use of 4 M methanol with 0.2 M glucose gave better results probably due to the combination of permeating and not-permeating cryoprotectants with their different mechanisms of action. The beneficial effect of the addition of low concentration of sugars to a freezing medium on zebrafish oocytes has already been reported (21). Plachinta et al. (2004) also reported that exposure of stage III zebrafish follicles to glucose concentrations <0.25 M have no toxic effect (20).

With both FDA-PI and TB assessment methods, there were no significant differences between KCl buffer and Hank's solution when these two solutions were used for cryopreservation procedure, this result is not in agreement with those previously reported (21).

The FDA-PI test proved to be more sensitive than Trypan Blue, after cryopreservation the follicles stained by FDA-PI showed a lower level of green fluorescence when compared to control follicles. Moreover, in the follicles following cryopreservation the green fluorescence seeped out of the follicles. The fluorescence decreasing could be due to the partial loss of esterase activity, while the damage of membrane could be the cause of the fluorescence seeping out of the cells. These results are in agreement with those from mammalian oocytes (4) where in heavily damaged oocytes with the esterase activity still intact, the fluorescein leaks through the cell membrane into the extracellular space. Follicles stained by PI showed the red fluorescence more delimited at the periphery of the follicles, probably involving the follicular layer.

The combined FDA-PI test showed that cryopreservation induced damage to the follicles, and the FDA-PI microscopic observations are supported by the fact that the follicle became translucent after thawing, making it difficult to use the GVBD test. This phenomenon has already been reported in previous studies (9, 13). Furthermore, the FDA-PI microscopic observation showed follicles leaking their content. Further studies to identify an optimal protocol for cryopreservation are needed considering the low percentage of survivals based on vital staining after cryopreservation. The results obtained from FDA-PI test showed a decrease of fluorescein production also evidences of a metabolic activity compromised even if the membrane could be still intact.

The FDA-PI method informs on both the physiological state and membrane integrity, as the FDA requires cellular esterase activity in addition to an intact membrane and PI, an intercalating dye, is known to pass only through the membranes of dead or dying cells. This approach can also be applied to oocytes at all stages. FDA-PI assay was chosen because it has been widely and successfully used in others cell studies. The main advantages of FDA-PI test are its speed, high sensitivity and simplicity.

In this study, FDA-PI staining was tested on fish follicles for the first time. The results show the method to be promising and offers a new test of the survival for fish follicles. Ultimately, for a full assessment of ovarian follicle survival further studies are needed. Additional biological markers need to be considered to allow a more detailed assessment of the effects of treatments such as cryopreservation on fish ovarian follicles.

REFERENCES

1. Albertini DF (1984) *Biol Reprod.* **30**,13-28.
2. Allison DC & Ridolpho P (1980) *J Histochem Cytochem.* **28**,700-3.
3. Barngrover JT & Thilly WG (1985) *J.Cell Sci.* **78**, 173-189.

4. Boender J (1884) *The Veterinary Quarterly*. **6**, 236-240.
5. Cai K, Yang J, Guan M, Ji W, Li Y & Rens W (2005) *Archives of Andrology*, **51**, 371-383 (13).
6. Didion BA, Pomp D, Martin MJ, Homanics GE & Markert CL (1990) *J Anim Sci*. **68**, 2803-10.
7. Frim J & Mazur P (1983) *Cryobiology*. **20**, 657-76.
8. Garner DL & Johnson LA (1995) *Biology of Reproduction* **53**, 276-284.
9. Guan M, Rawson DM & Zhang T (2008) *Theriogenology* **69**(3):269-75.
10. Guan M, Zhang T & Rawson DM (2008) *Cryobiology*
DOI:10.1016/j.cryobiol.2008.03.001.
11. Harrison RA & Vickers SE (1990) *J Reprod Fertil*. **88**, 343-52.
12. Holt WV & North RD (1994) *Biol Reprod*. **51**(3):414-24.
13. Isayeva A, Zhang T & Rawson DM (2004) *Cryobiology*. **49**,114-22.
14. Jones KH & Senft JA (1985) *J Histochem Cytochem*. **33**, 77-9.
15. Leibovitz A (1963) *Am. F. Hyg.* **78**, 173-180.
16. Li S, Mao Z, Han W, Yan W, Chen H & Yan S (1993) *Chinese Journal of Biotechnology* **9**, 247-255.
17. Mohr LR & Trounson AO (1980) *J Reprod Fertil*. **58**, 189-96.
18. Narayanan R, Kenney MC, Kamjoo S, Trinh TH, Seigel GM, Resende GP & Kuppermann BD (2005) *Invest Ophthalmol Vis Sci*. **46**,304-9.
19. Pearl M & Arav A (2000) *Cryo Letters*. **21**,171-178.
20. Plachinta M, Zhang T & Rawson DM (2004) *Cryo Letters*. **25**, 415-24.
21. Plachinta M, Zhang, T & Rawson DM *Cryo (2005)* 42nd Meeting of the Society for Cryobiology.
22. Rotman B & Papermaster BW (1966) *Proc Natl Acad Sci U S A*. **55**,134-41.
23. Sauch JF, Flanigan D, Galvin ML, Berman D & Jakubowski W (1991) *Appl Environ Microbiol*. **57**, 243-7.
24. Schupp DG & Erlandsen SL (1987) *Appl Environ Microbiol*.**53**,704-7.
25. Seki S, Kouya T, Tsuchiya R, Vldez Jr DM, Jin B, Hara T, Saida N, Kasai M & Edashige K (2008) *Reproduction* **135**(3): 285-92.
26. Selman K, Wallace RA, Sarka A & Qi X (1993) *Journal of morphology* **218**, 203-224.
27. Widholm JM (1972) *Stain Technol*. **47**,189-94.
28. Yokoyama H, Danjo T, Ogawa K & Wakabayashi H (1997) *Journal of Fish Diseases* **20**, 281-286.
29. Zhang T, Isayeva A, Adams SL & Rawson DM (2005). *Cryobiology*. **50** (3) **PPPP?**.

Accepted for publication 26/6/08

1 **Distributional arrangement of mitochondria in the granulosa cells**
2 **surrounding stage III zebrafish (*Danio rerio*) oocytes.**

3
4 Short title: Mitochondria in the zebrafish ovarian follicle

5
6 **T. Zampolla ^a, T. Zhang ^a, W. V. Holt ^b and D. M. Rawson ^{a*}**

7
8 *^a Institute of Research in the Applied Natural Sciences, University of Bedfordshire, 250*
9 *Butterfield, Great Marlings, Luton, Bedfordshire, LU2 8DL, UK*

10 *^b Institute of Zoology, Zoological Society of London, Regent's Park, London NW1 4RY,*
11 *UK*

12
13
14
15 **Corresponding author: David M. Rawson; Institute of Research in the Applied*
16 *Natural Sciences, University of Bedfordshire, 250 Butterfield, Great Marlings, Luton,*
17 *Bedfordshire, LU2 8DL, UK Tel: +44 (0) 1582 743743;*
18 *Fax: +44 (0) 1582 743741;*
19 *Email: david.rawson@beds.ac.uk*

23 **Abstract**

24

25 Mitochondria play a vital role during oocyte maturation, fertilization and embryo
26 development. In this study, confocal microscopy with the mitochondrial membrane
27 potential-sensitive dye JC-1 (5,5',6,6'-tetrachloro-1,1',3,3'-tetraethylbenzimidazolyl-
28 carbocyanine iodide) was used to investigate mitochondria distribution and activity of
29 stage III zebrafish ovarian follicles. To support the mitochondrial origin of the
30 fluorescence obtained by JC-1, a second mitochondrial probe, Mitotracker Green FM,
31 was used. Cryo-scanning and transmission electron microscopy were also used to validate
32 the distribution and localization of mitochondria obtained by mitochondrial staining. The
33 mitochondrial probes were unable to penetrate the oocyte, as a result it was not possible
34 to observe stained mitochondria in the oocyte cytoplasm. However, mitochondrial
35 staining of the granulosa cell layer surrounding the stage III zebrafish oocyte, exhibited a
36 hexagonal-polygonal distribution pattern of mitochondria. Cryo-scanning electron
37 microscopy studies also showed the oocyte surface to be covered by polygonal patterns of
38 ridges of the same dimensions as the mitochondria arrangement in the granulosa cells.
39 Whilst these results suggested the need for defolliculation to assess mitochondrial
40 distribution and activity in the stage III zebrafish oocyte cytoplasm, the findings will
41 contribute to our understanding of oogenesis and folliculogenesis processes in fish.

42

43 Key words: Mitochondria; Zebrafish (*Danio rerio*); Ovarian follicle; Granulosa cells;
44 Teleosts.

45

46

47 **1. Introduction**

48 Zebrafish belong to the multiple spawners class of fish with asynchronous-type ovaries,
49 where oocytes and follicles are found at different stages [1]. Each later stage III oocyte is
50 surrounded by an acellular structure, the vitelline envelope, a layer of granulosa cells, a
51 basement membrane, a further layer of thecal cells and by surface epithelium [2].

52 Several processes occurring in the stage III ovarian follicle strongly suggest the potential
53 involvement of mitochondria in supporting the growth phase of the oocyte, not only as
54 sources of energy in the form of ATP, but also in signal transduction pathways. In
55 zebrafish, it has already been reported that cAMP is the major second messenger that
56 mediates gonadotrophin actions in the ovary, and serves as intraovarian modulators [3].
57 Wang and Ge (2005) [4] reported the role of cAMP in the differential regulation of the
58 intraovarian mediators, activin β A and β B, expression in zebrafish ovarian follicle cells,
59 through cAMP-dependent signal transduction pathways.

60 Adequate ATP reserves in oocytes and embryos are required for normal nucleic acid and
61 protein synthesis, and the intracellular ATP concentration has been suggested as an
62 indicator of the developmental potential of mouse [5] and bovine [6] embryos.

63 Mitochondria are involved in other metabolic functions such as heme and non-heme iron
64 biogenesis [7], urea production and steroid biogenesis [8,9]. These organelles also control
65 the homeostasis of intracellular Ca^{2+} [10,11], and play an important role in the apoptotic -
66 signalling pathway [12].

67 However, few studies have addressed mitochondrial function in zebrafish ovarian
68 follicles. Studies have been carried out on mitochondrial DNA in zebrafish [13] and on

69 mitochondrial behaviour in early stage (stage I) of zebrafish oocyte [14], but little is
70 known about mitochondrial distribution and activity in later stage follicles/oocytes. Only
71 the study conducted by Selman et al. (1993) [1] identified aggregations of mitochondria
72 and endoplasmatic reticulum in the cortical ooplasm of early stage III zebrafish oocytes.

73 The aim of this study was to investigate mitochondrial distribution and activity in stage
74 III zebrafish ovarian follicle by confocal microscopy, using the fluorescent probe JC- 1
75 (5,5',6,6'-Tetrachloro-1,1',3,3'-tetraethyl-imidacarbocyanine iodide) to discriminate high
76 and low mitochondrial membrane potential. JC-1 fluorescence has two emission peaks,
77 with red fluorescence of j-aggregates indicating hyperpolarised mitochondria (high
78 membrane potential) and green fluorescence (JC-1 monomers) due to low membrane
79 potential [15,16]. JC-1 allows both mitochondrial metabolic status and distribution to be
80 determined. To validate the mitochondrial staining obtained by JC-1 a second
81 mitochondrial staining, MitoTracker Green FM, was used which also stains mitochondria
82 on the basis of mitochondrial membrane potential. Cryo-scanning and transmission-
83 electron microscopy techniques were also used to support the preliminary results obtained
84 by confocal microscopy, which showed a contiguous aggregation of mitochondria. The
85 use of this combined approach allowed the identification of mitochondria in the granulosa
86 layer of the ovarian follicles. Whilst both JC-1 and MitoTracker Green FM were able to
87 stain mitochondria in the granulosa cell layer, no mitochondria staining in the oocyte
88 cytoplasm was found indicating the inability of the two fluorescent probes to penetrate
89 the oocyte.

90

91

92

93 **2. Materials and methods**

94

95 *2.1 Follicle collection*

96 Adult female zebrafish (*Danio Rerio*) were maintained, handled and sacrificed in line
97 with protocols agreed by the Home Office and the University Ethics Committee as
98 meeting all current regulations. Follicles were collected from females anaesthetised with
99 a lethal dose of tricaine (0.6mg/ml) for 5 min and decapitated before ovary removal. The
100 ovaries were immersed in 1.6mg/ml hyaluronidase [17] made up in Hanks' solution
101 (137mM NaCl, 5.4 mM KCl, 0.25mM Na₂HPO₄, 0.44mM KH₂PO₄, 1.3mM CaCl₂, 1mM
102 MgSO₄, 4.2mM NaHCO₃) for 10 min at room temperature. Follicles were separated by
103 gentle pipetting, washed three times in Hanks' solution, and stage III follicles selected
104 according to Selman et al. (1993) [1].

105

106 *2.2 Staining of Mitochondria*

107 Stage III ovarian follicles, obtained by the enzymatic method, were stained with JC-1
108 (Sigma). A 1.5 mM stock solution of the dye was prepared in DMSO. The dye was used
109 at a concentration of 5µM in Hanks' solution for 30 min at room temperature.
110 Subsequently the follicles were washed three times with Hanks' solution, transferred to a
111 35 mm glass bottom dish (WillCo Dish, INTRACEL, Shepreth, Royston, UK) and
112 observed by confocal microscopy. For MitoTracker Green FM (M-7514, Invitrogen-
113 Molecular Probes, Paisley, UK) staining, a 1 mM stock solution of the dye was prepared
114 in DMSO. The dye was used at a concentration of 5µM in Hanks' solution for 30 min at

115 room temperature. Subsequently the follicles were washed three times with Hanks'
116 solution, transferred into a 35 mm glass bottom dish and viewed by confocal microscopy.

117 *2.3 Confocal microscopy*

118 Stained samples were examined using a Leica TCS-SP/DM IRBE (Leica, Microsystems
119 (UK) Ltd, Milton Keynes, Bucks, UK) confocal microscope equipped with Ar/Kr laser.
120 Active mitochondria distribution was assessed through a series of optical sections.
121 Objectives (20X, 40X and 63X water immersion), pinhole, filters, gain and offset were
122 kept constant throughout the experiments. Laser excitation and emission filters for the
123 different labelled dyes were as follows: JC-1 $\lambda_{\text{ex}} = 488$ nm (excitation), (green)
124 $\lambda_{\text{em}} = 510/50$ nm (emission), (red), $\lambda_{\text{em}} = 580/610$ nm (emission), MitoTracker Green
125 $\lambda_{\text{ex}} = 488$ nm (excitation), $\lambda_{\text{em}} = 500/60$ nm (emission). Digital images were obtained
126 with Leica TCS software and stored in TIFF format. The TIFF images represented in Fig
127 1 and Fig 2 (A, B) were enhanced with Adobe PhotoShop (V7); the brightness and
128 contrast were adjusted to enhance low GSV intensities in the oocyte. At least 30 ovarian
129 follicles in each group were assessed in three repeated experiments.

130

131 *2.4 Transmission Electron Microscopy (TEM)*

132 Follicles were held in Hanks' solution before specimen preparation for electron
133 microscopy. Follicles were fixed for 2 hours in a combination of 2% glutaraldehyde and
134 1% formaldehyde, 10X Hanks' solution was used as vehicle. The primary fixation was
135 followed by three washings each of 10 min (the first washing with Hanks' solution, the
136 second with Hanks' solution and distilled water with a ratio of 1:1, and the third one only
137 with distilled water) to remove all unreacted fixative. Follicles were then postfixed for 1

138 hour in 1% osmium tetroxide in distilled water, dehydrated in acetone, washed three
139 times in distilled water and then dehydrated in an acetone series of 10% increments in
140 distilled water for 30 minutes at each concentration. Once the concentration of acetone
141 reached 100%, the follicles were left for one hour and the 100% acetone was exchanged
142 three times. The follicles were then infiltrated with Spurr's resin (TAAB Laboratories
143 Equipment Ltd, Aldermaston, Berks, UK) by passing through a sequence of solution until
144 the dehydrating agent has been completely replaced by the final embedding mixture
145 (25%, 50%, 75% and 100% for 1 hour at each concentration). The 100% resin was
146 exchanged three times and the follicles were then embedded in resin in truncated pyramid
147 style BEEM capsules (TAAB Laboratories).

148

149 Ultrathin resin sections (90-100 nm thickness) were cut with a Reichert-Jung Ultracut
150 microtome (Leica, Microsystems (UK) Ltd, Milton Keynes, Bucks, UK), mounted on
151 mesh copper grids coated with Formvar. The sections were stained with 2% uranyl
152 acetate in 50% EtOH:ddH₂O and Reynold's lead citrate (Reynolds, 1963) and
153 examined in a JEOL 2011 (Jeol, Tokyo, Japan) transmission electron microscope and
154 imaged using an Ultrascan CCD camera (Gatan UK, Abingdon, UK)
155 Measurements were made on digital electron micrographs of fixed specimens using
156 Digital Micrograph (Gatan UK).

157

158 *2.5 Cryo-Scanning Electron Microscopy (Cryo-SEM)*

159 Follicles, obtained by separation from the ovaries, were held in Hanks' solution before
160 specimen preparation. Ovarian follicles were mounted onto a cryo stub smeared with

161 Tissue-Tek OCT Compound (Sakura Finetechnical Co. Ltd, Tokyo, Japan) and plunged
162 into pre-slushed LN₂. The sample was then transferred under vacuum to the Gatan (Gatan
163 UK, Abingdon, UK) Alto 2500 cryo chamber and fitted onto the cold stage where the
164 temperature was maintained at -180°C. Here it was fractured using the cold knife blade to
165 allow visualisation of the inner structures. The specimen was then etched by warming the
166 stage to -95°C for 1min to remove any contaminating ice. The stage temperature was then
167 returned to -150°C or colder and the specimen was coated with AuPd for 90secs. The
168 sample was then transferred to the Jeol FEG 6700 (Jeol (UK) Ltd, Welwyn Garden City,
169 UK.) Scanning Electron Microscope chamber for imaging. Images were recorded using
170 the on-board software system.

171

172

173 *2.6 Experimental designs*

174 *2.6.1 Mitochondrial distribution and activity investigation by confocal microscopy*

175 Mitochondrial distribution and activity in stage III ovarian follicle (follicle diameter:
176 0.34-0.69 mm), were evaluated by confocal microscopy using mitochondrial probe JC-1.
177 A second mitochondrial probe, MitoTracker Green FM, which also stains mitochondria
178 on the basis of mitochondrial membrane potential, was used to validate the mitochondrial
179 origin of fluorescence obtained with JC-1.

180

181 *2.6.2 Ovarian follicle structure and mitochondria distribution observation by electron* 182 *microscopy*

183 Stage III ovarian follicles were also examined by Cryo-Scanning Electron Microscopy
184 (Cryo-SEM) and Transmission Electron Microscopy (TEM) to investigate our hypothesis
185 that the layer around the outer margin of the oocyte that was stained by the mitochondrial
186 probes was the granulosa cell layer and also to show that the mitochondrial probes were
187 unable to penetrate the oocyte, as the TEM allowed the identification of mitochondria in
188 the oocytes which were not stained by mitochondrial probes.

189

190 **3. Results**

191

192 *3.1 Mitochondrial distribution and activity investigation by confocal microscopy*

193 More than 150 good quality, live ovarian follicles were screened by confocal microscopy
194 after exposure to JC-1 or MitoTracker Green FM; all the ovarian follicles examined
195 presented a contiguous peripheral aggregation of mitochondria in the granulosa cells
196 which surround the oocytes. A series of optical sections were undertaken of 40-50 intact
197 ovarian follicles. The photomicrographs shown in this paper are representative examples
198 of ovarian follicles obtained by confocal microscopy.

199 Both the JC-1 and the MitoTracker Green FM were consistently unable to penetrate the
200 oocytes, and no mitochondrial staining in the ooplasm was found (Fig. 1 and 2 B).

201 The fluorescence pattern shown by the mitochondria distribution was consistent in every
202 normal follicle and represented a well organised distributional arrangement, with each
203 fluorescence pattern having a diameter of 10-15 μm . The fluorescence was concentrated
204 at the margins of the each granulosa cell (Fig. 1).

205

206

207 Individual mitochondria consistently exhibited either green or red fluorescence,
208 suggesting the possibility that these could be functionally distinct subsets or that
209 metabolic turnover of activity (Fig. 1 A, B, C) is a normal feature of the oocyte-follicle
210 complex.

211 The exposure of ovarian follicles to a second mitochondrial probe MitoTracker Green
212 FM supported the results from the JC-1 staining, showing the same fluorescent patterns
213 of mitochondria in the granulosa cells layer (Fig. 2 A).

214

215 *3.2 Electron microscopic observations of ovarian follicle structure and mitochondria*
216 *distribution*

217 Cryo-SEM and TEM analyses of stage III ovarian follicles were undertaken to identify
218 the mitochondrial probe stained layer obtained in the confocal microscopy studies.
219 Preliminary results obtained by Cryo-SEM did not allow the layer to be identified, but the
220 fracture surface inside the ovarian follicle, obtained by Cryo-SEM, showed a polygonal
221 structure, surrounding the oocyte. Each polygonal structure had a diameter of 10-15 μm
222 (Fig. 2 C). TEM results showed that the enzymatic method of follicle separation from the
223 ovaries resulted in the removal of the surface epithelium and may have induced the
224 removal of the thecal layer or at least damaged the thecal layer (Fig. 3 A-B). TEM results
225 for the follicle layer showed characteristics of steroid secreting cells, with abundant

226 round, oval and elongate mitochondria with tubular cristae. (Fig. 3 C). TEM micrographs
227 also showed a gap of about 4 μm between the follicular layer and the vitelline envelope
228 (Fig. 3 A).

229 The stage III oocyte surface displayed endocytic activity during vitellogenesis; numerous
230 vesicles were found (Fig. 3 A). The surface of the oocyte presented numerous microvilli
231 that penetrate the pore canals of the vitelline envelope (Fig 3 D).

232

233 **4. Discussion**

234 This study has shown the inability of mitochondrial probes, JC-1 and MitoTracker Green
235 FM, to penetrate the oocyte. This is probably due to the low permeability of the thick
236 vitelline envelope which surrounds the zebrafish oocyte. However, the mitochondrial
237 staining involved the granulosa cell layer surrounding the oocytes in stage III zebrafish
238 ovarian follicles and suggests a location-dependent function at this stage to support
239 oocyte maturation.

240 The selective probes, JC-1 and MitoTracker Green FM allowed mitochondrial
241 distribution and activity to be determined. JC-1 staining showed a more definite pattern
242 probably due to the characteristics of the dye. JC-1 responds differentially to high or low
243 membrane potential. In cells with intact mitochondria, JC-1 accumulates in the
244 mitochondria as aggregates resulting in red fluorescence (600 nm) (high membrane
245 potential) and it can also accumulate in the monomeric form (525 nm) (low membrane
246 potential) and exhibits green fluorescence [15-16-19-20,21]. JC-1 has been used in
247 somatic cells, amphibian oocytes [22], mammalian oocytes and embryos [23-24,25].

248 Images from confocal microscopy showed the presence of both mitochondria, with high
249 and low membrane potential, this is in accordance with what has been reported by Zhang
250 et al. (2008) [14] in early stage zebrafish oocyte, where the green and red fluorescence
251 intensity were almost the same in the oocyte. This phenomenon could be due to a
252 metabolic turnover, as mitochondria have different roles at this stage of folliculogenesis,
253 as sources of ATP, of cAMP and in steroidogenesis. MitoTracker Green FM stains only
254 metabolically active mitochondria, as it accumulates in mitochondria regardless of
255 mitochondrial membrane potential.

256 The presence of abundant and active mitochondria in the granulosa cell layer, shown by
257 confocal microscopy, was also supported by electron micrographs confirming that the
258 layer stained by the mitochondria-specific probes was the granulosa cell layer. Moreover
259 this layer was rich in mitochondria, and showed features consistent with steroid secreting
260 cells; i.e. abundant round and oval mitochondria with tubular cristae, elongate
261 mitochondria and smooth endoplasmic reticulum [26,27]. The granulosa cells and thecal
262 cells have previously been shown to be sites of steroid synthesis in the teleost ovary [2-
263 28-29,30]. One explanation for the abundant mitochondria in the granulosa cells could be
264 their role in the synthesis of steroids [8,9].

265 The first, and rate-determining step [31], in steroid biosynthesis is the transport of
266 cholesterol to the inner mitochondria membrane by the steroid acute regulatory protein
267 (StAR) [32-33,34], where it is converted by enzymes of the cytochrome P450
268 superfamily and auxiliary electron transferring proteins into pregnenolone [35,31].
269 Papadopoulos et al. (2007) [36] also reported, in a detailed review, the possible

270 involvement of a larger multimeric mitochondrial complex of proteins assembled to
271 facilitate the import of the cholesterol into mitochondria.

272

273 The granulosa cells layer surrounding the oocyte, from which it is separated by the
274 vitelline envelope, showed a “polygonal” structure. The well organised distribution of
275 mitochondria shown by confocal microscopy analysis leads us to consider that the
276 cytoskeleton could be involved in holding the mitochondria in such a pattern. The
277 association of mitochondria with cytoskeleton fibrillar elements has been described
278 previously. Mitochondrial distribution is established by movement along the cytoskeletal
279 elements and by anchoring at the site where their function is required. They are
280 concentrated in areas of increased energy consumption, where they provide ATP.
281 Furthermore, Hall and Almahbobi (1997) [37] reported the involvement of the
282 cytoskeleton in the steroidogenic process and the interactions among mitochondria and
283 microtubules, microfilaments and intermediate filaments in steroidogenic cells for the
284 intracellular transport of cholesterol.

285

286 The patterns could also be due to the presence of a hexagonally structured egg envelope
287 as reported for Sole (*Pleuronichthys coenosus*) [38,39], where ultrastructural evidence
288 has shown that a single granulosa cell is associated with each hexagonal chamber. In
289 support of this hypothesis, comparison of the granulosa cells from the confocal images
290 with the polygonal structure obtained by cryo-SEM, showed they had a similar dimension
291 of 10-15 μm . From cryo-SEM micrographs this polygonal structure seems to belong to
292 the vitelline envelope. These results showed that the granulosa cells are polygonally

293 shaped and the fact that the mitochondria are arranged in such pattern at the periphery of
294 the granulosa cells surrounding the nucleus could suggest the presence of nuclear-
295 mitochondria interactions and also the association of mitochondria with the plasma
296 membrane. These possible interactions need further investigation.

297 Other roles of mitochondria in the granulosa cells layer in supporting the growth phase of
298 the oocyte could be explained by considering ATP as an energy source. Oocytes need an
299 efficient source of energy in the form of ATP to support their development, and ATP is
300 probably delivered to the oocyte using the gap junctional pathway. ATP is also required
301 as a substrate in signal transduction pathways, and the close interaction between follicle
302 cells layer and the oocyte which communicate through microvilli which extend from both
303 follicle cells and oocytes [1], would need to involve mitochondria. These intracellular
304 communications have been reported previously in zebrafish [40,41]. They are mediated
305 by different cell-cell contact structures including heterologous gap-junctions that allow
306 the passage of molecules with a molecular weight of up to 1 kDa, including both the
307 second messenger (cAMP) and ions, by means of diffusion [42,43]. Gonadotrophin
308 (GtH) receptors are localised on the surface of the follicle cells, and are not present on the
309 oocyte, therefore GtH signals received by follicle cells are passed to oocytes via gap
310 junctions. Ge et al. (2005) [44] also suggested the existence of hypothetical regulatory
311 loops between the oocyte and the follicle cells in zebrafish, with the involvement of the
312 activin system in transducing the gonadotropic signal.

313

314 The inability of the mitochondrial stains to penetrate the oocyte cytoplasm represents a
315 limit to the investigation of the organelle distribution throughout the ovarian follicle, and

316 a defolliculation procedure would be required and possibly the permeabilization of the
317 oocyte membrane.

318

319 However, this study identifies the spatial organisation of mitochondria in the granulosa
320 cells of stage III zebrafish ovarian follicles using JC-1 and confocal microscopy. These
321 findings will contribute in a better understanding of oocyte/folliculogenesis processes in
322 fish. Furthermore, in cryopreservation of fish ovarian follicle, changes in mitochondrial
323 activity could be used as indicator of cryo-impact and assist in the development of
324 optimal cryo-protocols.

325

326 **Acknowledgements**

327 This research was founded by the LIRANS strategic research fund.

328 We thank Dr. Allison van de Meene and Mrs Jean Devonshire, Centre for Bioimaging,
329 Plant Pathogen and Microbiology Department, Rothamsted Research, Harpenden, for
330 expert help and assistance with electron microscopy techniques and confocal microscopy
331 data acquisition and for the use of the equipments.

332

333 **References**

334 [1] Selman K, Wallace AR, Sarka A, Qi X. Stage of oocyte development in the Zebrafish,
335 *Brachydanio rerio*. J Morphol 1993, 218: 203-224.

- 336 [2] Nagahama Y. Endocrine regulation of gametogenesis in fish. *Int. J. Dev. Biol.* 1994,
337 38: 217-229.
- 338 [3] Wang Y, Ge W. Gonadotropin regulation of follistatin expression in the cultured
339 ovarian follicle cells of zebrafish, *Danio rerio*. *Gen Comp Endocrinol.* 2003, 134: 308-
340 15.
- 341 [4] Wang Y, Ge W. Involvement of Cyclic Adenosine 3',5'-Monophosphate in the
342 Differential Regulation of Activin β A and β B Expression by Gonadotrophin in the
343 Zebrafish Ovarian Follicle Cells. *Endocrinology* 2005, 144: 491-499.
- 344 [5] Calarco PG. Polarization of mitochondria in the unfertilized mouse oocytes.
345 *Developmental Genetics* 1995, 16: 36-43.
- 346 [6] Stojkovic SA, Zakhartchenko PV, Hutzler P, Goncalves PB, Wolf E. Mitochondrial
347 distribution and adenosine triphosphate content of bovine oocytes before and after in
348 vitro maturation: correlation with morphological criteria and developmental capacity after
349 in vitro fertilization and culture. *Biol Reprod.* 2001, 64: 904-9.
- 350 [7] Lill R, Kispal G. Maturation of cellular Fe-S proteins: an essential function of
351 mitochondria. *Trends Biochem Sci.* 2000 Aug;25(8):352-6.
- 352 [8] Crivello JF, Jefcoate CR. Intracellular movement of cholesterol in rat adrenal cells.
353 Kinetics and effects of inhibitors. *J Biol Chem.* 1980, 255: 8144–8151.
- 354 [9] Privalle CT, Crivello JF, Jefcoate CR. Regulation of intramitochondrial cholesterol
355 transfer to side-chain cleavage cytochrome P-450 in rat adrenal gland. *Proc Natl Acad Sci*
356 U S A. 1983, 80: 702–706.

357 [10] Nicholls D, Akerman K. Mitochondrial calcium transport. *Biochim Biophys Acta*.
358 1982; 683: 57-88.

359 [11] Miller WL. Steroidogenic acute regulatory protein (StAR), a novel mitochondrial
360 cholesterol transporter. *Biochim Biophys Acta*. 2007, 1771: 663-76.

361 [12] Green DR, Reed JC. Mitochondria and apoptosis. *Science*. 1998, 281:1309-12.

362 [13] Broughton RE, Milam JE, Roe BA. The complete sequence of the zebrafish (*Danio*
363 *rerio*) mitochondrial genome and evolutionary patterns in vertebrate mitochondrial DNA.
364 *Genome Research* 2001, 11: 1958-67.

365 [14] Zhang YZ, Ouyang YC, Hou Y, Schatten H, Chen DY, Sun QY. Mitochondrial
366 behavior during oogenesis in zebrafish: a confocal microscopy analysis. *Dev Growth* [15]
367 Reers M, Smith TW, Chen LB. J-aggregate formation of a carbocyanine as a quantitative
368 fluorescent indicator of membrane potential. *Biochemistry* 1991, 30: 4480–4486.

369 [16] Reers M, Smiley ST, Mottola-Hartshorn C, Chen A, Lin M, Chen LB. Mitochondrial
370 membrane potential monitored by JC-1 dye. *Methods Enzymol*. 1995, 260: 406–417.

371 [17] Guan M, Rawson DM, Zhang T. Development of a new method for isolating
372 zebrafish oocytes (*Danio rerio*) from ovary tissue masses. *Theriogenology* 2008, 69:
373 269-75.

374 [18] Reynolds ES. Use of lead citrate at high pH as an electron-opaque stain in electron
375 microscopy. *Journal of Cell Biology* 1963, 17: 208-212.

376 [19] Smiley ST, Reers M, Mottola-Hartshorn C, Lin M, Chen A, Smith TW, Steele GD,
377 Chen LB. Intracellular heterogeneity in mitochondrial membrane potentials revealed by

378 a J-aggregate-forming lipophilic cation JC-1. Proc Natl Acad Sci U S A. 1991, 88: 3671–
379 3675.

380 [20] Chen LB, Smiley ST, Mason WT. ed. *Fluorescent and Luminescent Probes for*
381 *Biological Activity*. 1993, pp. 124.

382 [21] Plasek J, Sigler K. Slow fluorescent indicators of membrane potential: a survey of
383 different approaches to probe response analysis. J Photochem Photobiol B. 1996, 33:
384 101-24.

385 [22] Wilding M, Carotenuto R, Infante V, Dale B, Marino M, Di Matteo L & Campanella
386 C. Confocal microscopy analysis of the activity of mitochondria contained within the
387 ‘mitochondrial cloud’ during oogenesis in *Xenopus laevis*. Zygote 2001, 9: 347-352

388 [23] Wilding M, Dale B, Marino M, di Matteo L, Alviggi C, Pisaturo ML, Lombardi L,
389 De Placido G. Mitochondrial aggregation patterns and activity in human oocytes and
390 preimplantation embryos. Hum Reprod. 2001, 5: 909-917.

391 [24] Van Blerkom J, Davis P, Mathwing V & Alexander S. Domains of high-polarized
392 and low-polarized mitochondria may occur in mouse and human oocytes and early
393 embryos. Hum Reprod. 2002, 2: 393-406.

394 [25] Van Blerkom J. Mitochondria in human oogenesis and preimplantation
395 embryogenesis: engines of metabolism, ionic regulation and developmental competence.
396 Reproduction 2004, 128: 269-280.

397 [26] Prince FP. Lamellar and tubular association of the mitochondrial cristae: unique
398 forms of the cristae present in steroid-producing cells. Mitochondrion 2002, 1: 381-389.

399 [27] Srijunngam J, Kitana N, Callard IP, Wattanasirmkit K. Ultrastructural changes in the
400 ovarian follicular wall during oocytes growth in the Nile Tilapia, *Oreochromis niloticus*
401 Linn. The Natural History Journal of Chulalongkorn University 2005, 5: 21-30.

402 [28] Nakamura M, Nagahama Y. Steroid Producing Cells during Ovarian Differentiation
403 of the Tilapia, *Sarotherodon niloticus*. Growth Differ 1985, 27: 701–708

404 [29] Nakamura Y, Specker JL, Nagahama Y. Ultrastructural analysis of the developing
405 follicle during early vitellogenesis in tilapia, *Oreochromis niloticus*, with special
406 reference to the steroid-producing cells. Cell Tissue Res. 1993, 272: 33-39.

407 [30] Petrino TR, Greeley MS Jr, Selman K, Lin YW, Wallace RA. Steroidogenesis in
408 *Fundulus heteroclitus*. II. Production of 17 alpha-hydroxy-20 beta-dihydroprogesterone,
409 testosterone, and 17 beta-estradiol by various components of the ovarian follicle. Gen
410 Comp Endocrinol. 1989, 76: 230–240.

411 [31] Jefcoate CR. High-flux mitochondrial cholesterol trafficking, a specialized function
412 of the adrenal cortex. J Clin Invest. 2002, 110: 881-890.

413 [32] Stocco DM, Clark BJ. Role of the steroidogenic acute regulatory protein (StAR) in
414 steroidogenesis. Biochem Pharmacol. 1996, 51: 197–205.

415 [33] Stocco DM, Wang X, Jo Y, Manna PR. Multiple signaling pathways regulating
416 steroidogenesis and steroidogenic acute regulatory protein expression: more complicated
417 than we thought. Mol Endocrinol. 2005, 19: 2647–2659.

418 [34] Miller WL. 2007 Steroidogenic acute regulatory protein (StAR), a novel
419 mitochondrial cholesterol transporter. Biochim et Biophys Acta 2007, 1771: 663-676.

420 [35] Catt KJ, Hardwood JP, Clayton RN, Davies TF, Chan V, Katikineni M, Nozu K,
421 Dufau MI. Regulation of peptide hormone receptors and gonadal steroidogenesis. Recent
422 Prog Horm Res. 1980, 36: 557-662.

423 [36] Papadopoulos V, Liu J & Culty M. Is there a mitochondrial signaling complex
424 facilitating cholesterol import? Mol Cell Endocrinol. 2007, 256-266: 59-64.

425 [37] Hall PF & Almahbobi G. Roles of microfilaments and intermediate filaments in
426 adrenal steroidogenesis *Histology of the mammalian adrenal cortex*. Microscopy research
427 and technique Nussdorfer, G.G. (ed). 1997, vol. 36, Los Alamos, New Mexico. pp 463-
428 479.

429 [38] Stehr CM, Hawkes JW. The development of the hexagonally structured egg envelope
430 in the C-O Sole (*Pleuronichthys coenosus*). J Morphol. 1983, 178: 267-284.

431 [39] Wallace RA, Selman K. Ultrastructural aspects of oogenesis and oocyte growth in
432 fish and amphibians. J Electron Microsc Tech. 1990, 16: 175 – 201.

433 [40] Kessel RG, Roberts RL, Tung HN. Intercellular junctions in the follicular envelope
434 of the teleost, *Brachydanio rerio*. J Submicrosc Cytol. 1988, 20: 415–424.

435 [41] Cerdà J, Reidenbach S, Prätzel S, Franke WW. Cadherin-Catenin Complexes During
436 Zebrafish Oogenesis: Heterotypic Junctions Between Oocytes and Follicle Cells. Biol
437 Reprod. 1999, 61: 692-704.

438 [42] Kumar NM, Gilula NB. The gap junction communication channel. *Cell* 1996, 84:
439 381-8.

440 [43] Yamamoto Y, Yoshizaki G. Heterologous gap junctions between granulosa cells and
441 oocytes in ayu (*Plecoglossus altivelis*): formation and role during luteinizing hormone-
442 dependent acquisition of oocyte maturational competence. J Reprod Dev. 2008, 54: 1-5.

443 [44] Ge W. Intrafollicular paracrine communication in the zebrafish ovary: the state of
444 the art of an emerging model for the study of vertebrate folliculogenesis. *Mol Cell*
445 *Endocrinol.* 2005, 237: 1-10.

446

447

448 **Figure legends**

449 **FIG. 1.** Distributional arrangement of mitochondria stained by JC-1 in the granulosa cells
450 which surround the oocyte during the vitellogenesis stage. (A) Low polarized organelles
451 fluoresce green, while higher polarized organelles fluoresce red owing to
452 multimerization of JC-1 and formation of J-aggregates (B). (C) Merged image showing
453 mitochondria with both red and green fluorescence suggested a metabolic turnover of
454 activity. Bars, 40 μm .

455 **FIG. 2** Mitochondria distribution in stage III zebrafish ovarian follicle exposed to 5 μM
456 MitoTracker Green FM (A and B). (A) Mitochondria stained by MitoTracker Green FM
457 showing the same pattern obtained with JC-1. Bar, 40 μm . (B) Low magnification view
458 of the ovarian follicle optical section stained by MitoTracker Green FM showing the
459 inability by the mitochondrial probe to penetrate the oocyte. Bar, 200 μm . (C) Fracture
460 surface inside stage III ovarian follicle obtained by Cryo-SEM. Polygonal structure,
461 which surrounded the oocyte, is shown. Each polygonal structure showed a diameter of
462 10 – 15 μm (square). Bar, 10 μm .

463 **FIG. 3.** Electron micrographs of stage III ovarian follicle. (A and B) The ooplasm was
464 surrounded by the vitelline envelope, which shows pore canals. External to the granulosa
465 cells layer was a basal lamina which divides the granulosa cells layer from the thecal
466 layer. Bars, 2 μm (A), 1 μm (B). (C) Electron micrograph of granulosa cell of
467 vitellogenic follicle, which contains abundant free ribosome, elongate mitochondria and
468 rough endoplasmic reticulum. Bar, 0.5 μm . (D). High-power TEM showing microvilli
469 from the oocyte passing through are the pore canals of the vitelline envelope. Bar, 0.5
470 μm . Vitelline envelope (VE); ooplasm (O); pore canals (pc); granulosa cell layer (F);
471 basal lamina (*); thecal layer (T); mitochondria (m); RER (R); free ribosome (r).

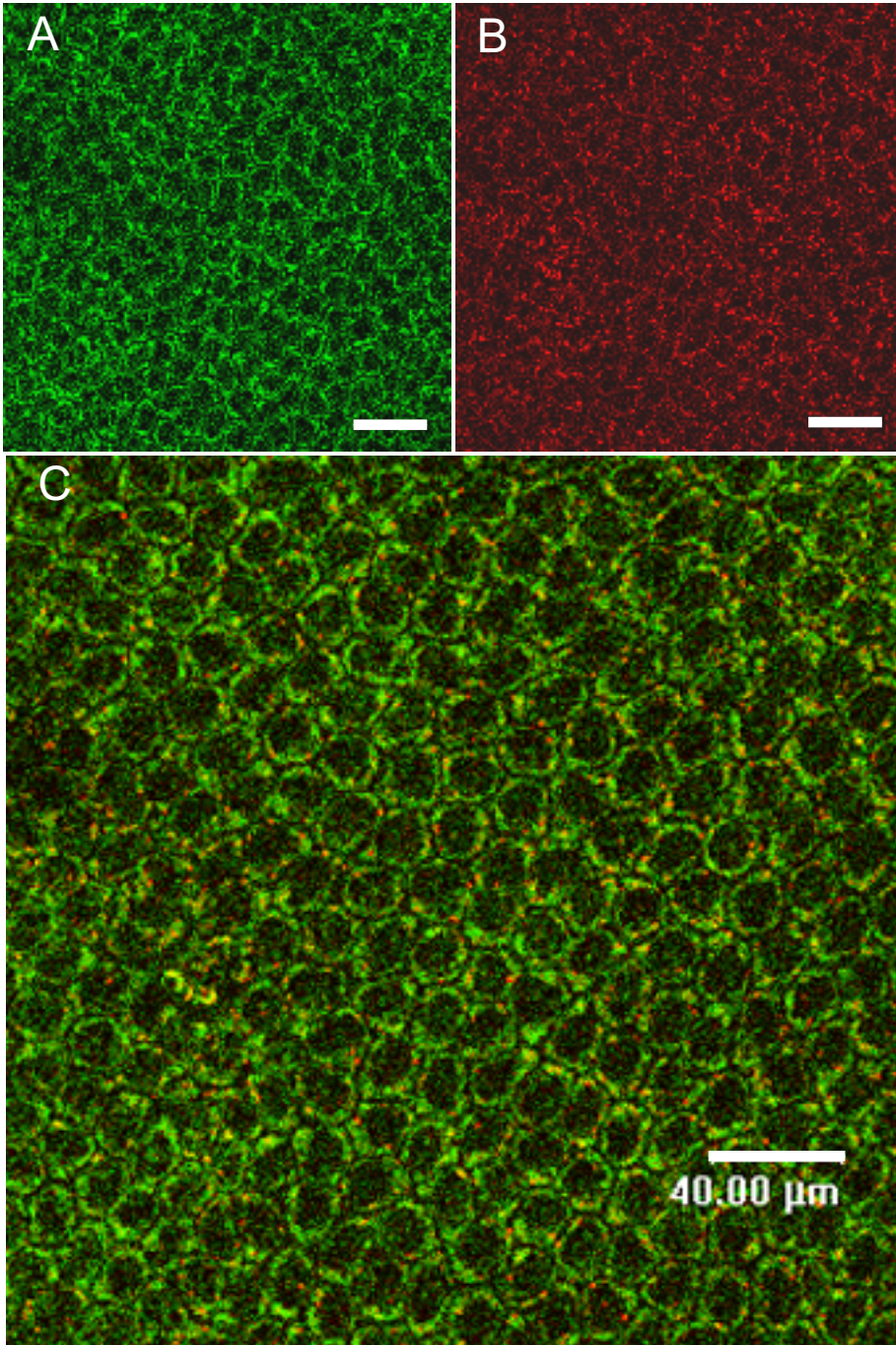


Fig. 1.

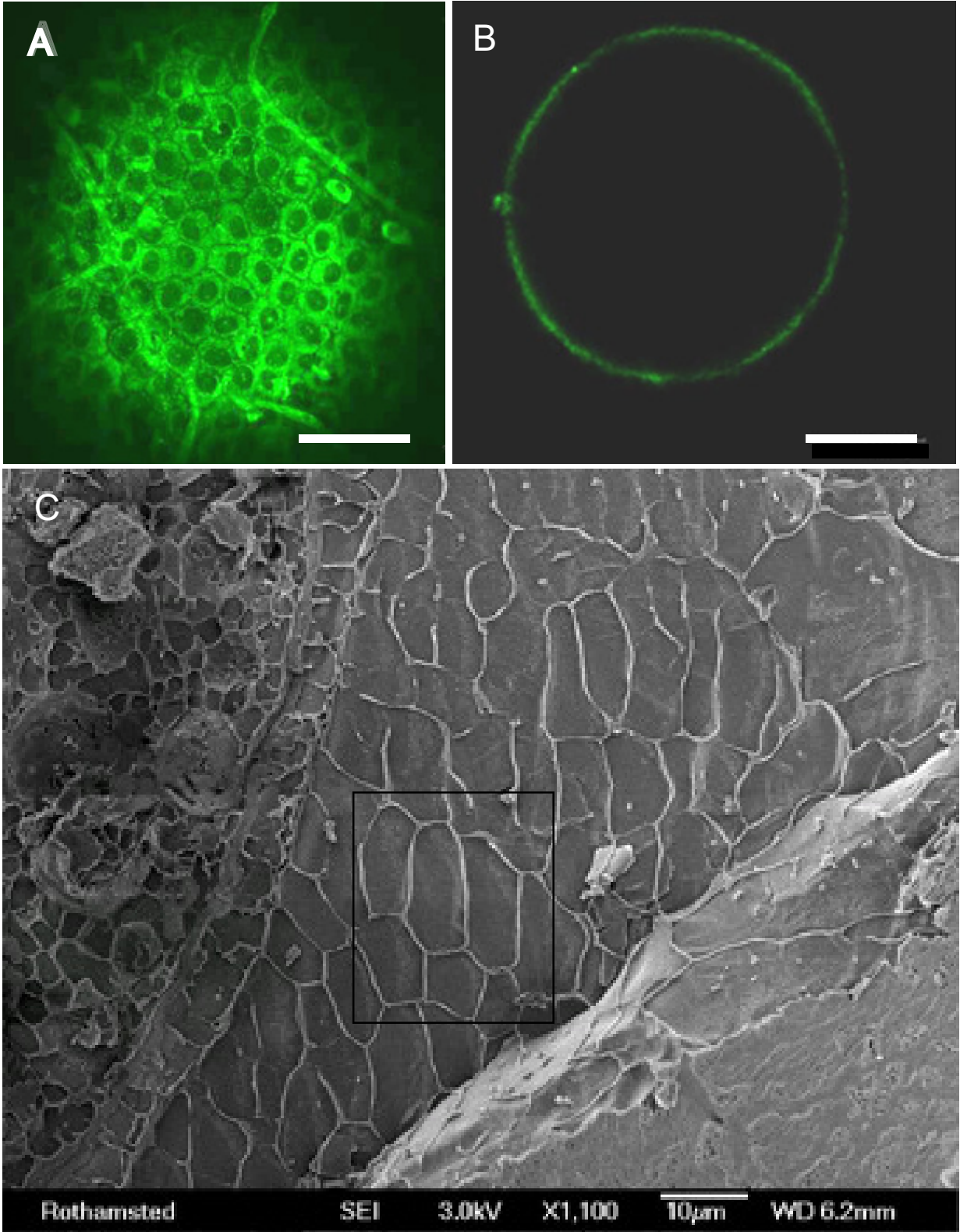


Fig. 2.

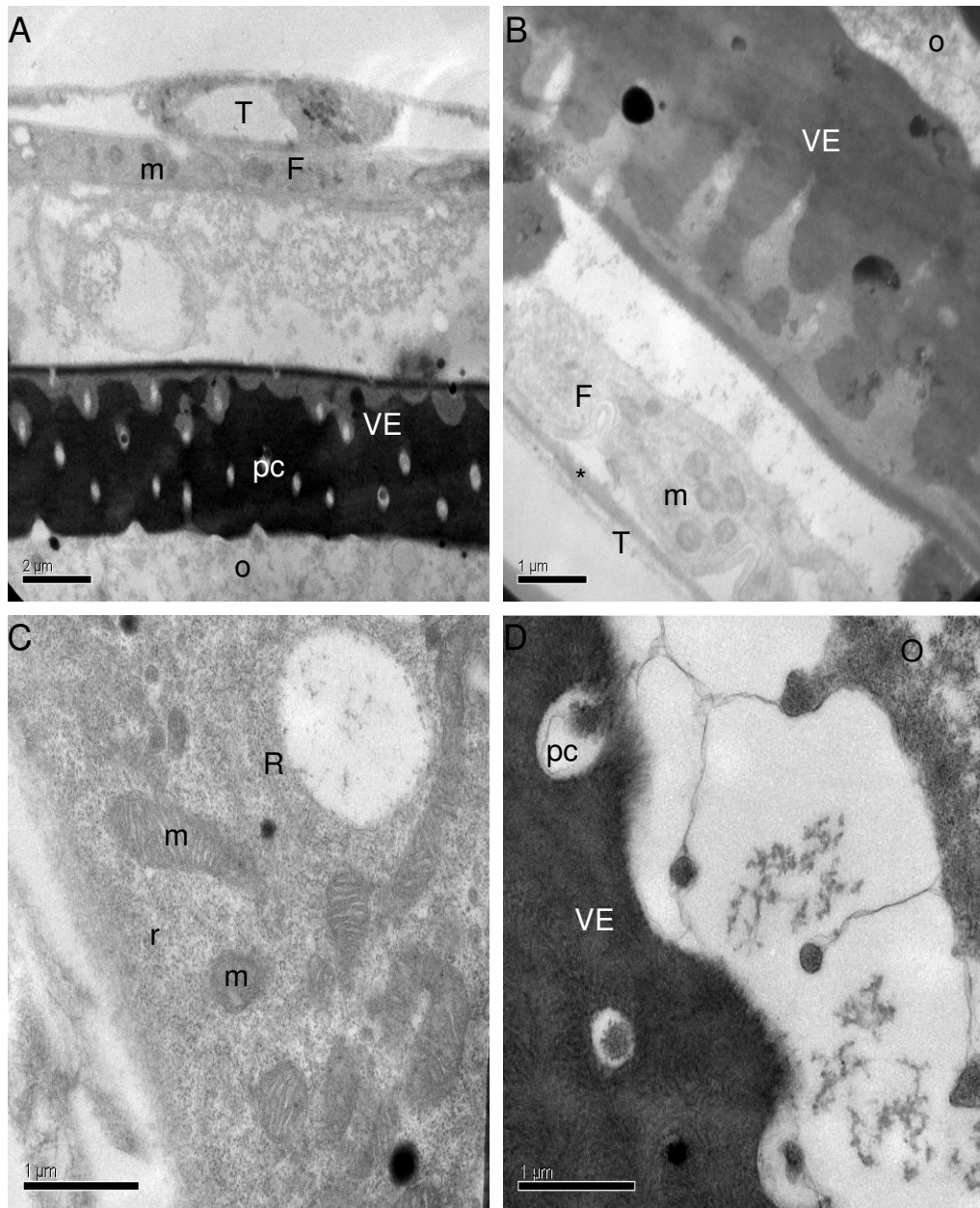
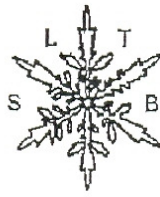


Fig. 3.



The 2008 Scientific Meeting and AGM
11-12 September

Faculty of Life Sciences
University of Copenhagen



Possible directions for low temperature biology in
the next five years

Faculty of Life Science, University of Copenhagen

Festauditoriet, Bulowsvej 17
1870 Frederiksberg C, Copenhagen

EFFECT OF CRYOPROTECTANTS EXPOSURE ON MITOCHONDRIAL ACTIVITY AND MTDNA COPY NUMBER

T. Zampolla, E. Spikings, T. Zhang, D. Rawson

LIRANS Institute of Research in the Applied Natural Sciences, 250 Butterfield, Great Marlings, Luton, LU2 8DL, UK

The late ovarian follicle of fish is a complex system of acellular and cellular structures surrounding the developing oocyte. The large size of fish oocytes and their high yolk content have been a barrier to their successful cryopreservation. Previous studies have investigated the use of cryoprotectants to reduce chilling injury and intra-cellular ice formation. However, there are other possible subtle impacts of cryopreservation which might not result in cell death, but can compromise future development.

Mitochondria have many functions that affect metabolism and reproduction. They are responsible for the production of most cellular ATP and are also implicated in cell aging and death. Quantitative variation in mitochondrial DNA (mtDNA) has been associated with gamete quality and reproductive success in other animals, including humans.

We aimed to investigate the effect of relatively non-toxic cryoprotectants (methanol and DMSO) on mitochondria of stage III zebrafish ovarian follicles. The determination of mtDNA copy number and the examination of mitochondrial activity using JC-1 were undertaken following exposure to cryoprotectants.

There were no significant differences in mtDNA copy number between control and treated follicles soon after the exposure to methanol. However, there were significant differences in mtDNA copy number between untreated follicles and those exposed to concentrations of 3 or 4 M methanol 5 hours following the exposure to the cryoprotectant. Exposure to DMSO caused an increase of mtDNA copy number and significant effects were found 5 hours after exposure to 3 or 4 M DMSO.

Confocal microscopy analysis of JC-1 staining patterns showed that even low concentrations of methanol induced changes in mitochondrial membrane potential in the follicle cells which surrounded the oocyte. At higher concentrations, 3 or 4 M, the cryoprotectant caused a loss of the mitochondrial distribution pattern.

This is the first report of an effect of cryoprotectant on zebrafish ovarian follicle mitochondria.

Development of new viability assessment methods for zebrafish (*Danio rerio*) oocytes

Tiziana Zampolla, David M. Rawson, Tiantian Zhang
University of Luton, Luton Institute of Research in the Applied Natural Sciences, LU1 5DU Luton, England

Reliable fish oocytes quality assessment methods are essential in developing protocols for their cryopreservation as well as their *in vitro* maturation and fertilization. Although some methods have been used to assessing fish oocytes viability, including trypan blue (TB) staining, thiazolyn blue (MTT) staining and *in vitro* maturation of oocytes followed by observation of germinal vesicle breakdown (GVBD), these methods have limitations relating to their low sensitivity and their applicability for specific development stages. New oocyte viability assessment methods are urgently needed. The aim of the present study is to develop new viability assessment methods for zebrafish (*Danio rerio*) oocytes. Fluorescence Diacetate (FDA) staining, Propidium Iodide (PI) staining and simultaneous staining with Fluorescence Diacetate + Propidium Iodide (FDA+PI), primarily used to determine viability of mammalian cells, were investigated using zebrafish oocytes. Stage III oocytes obtained from zebrafish ovaries were held in Hanks solution. Oocytes used both for positive and negative controls were exposed to FDA (5µg/ml, 10min), PI (5 or 50µg/ml, 5min) and FDA+PI (20µg/ml + 20µg/ml, 3min), all made up in PBS. Oocytes used for negative controls were obtained after exposure to 99% methanol for 10 min at 22°C. The results showed that both FDA and PI staining provided some ambiguous results. However, simultaneous staining with FDA+PI showed good results from both positive and negative controls. The FDA+PI staining was therefore used subsequently to compare with TB staining (0.2%, 5min) and GVBD test (oocytes were incubated in 50% L-15 medium supplemented with 1 mg/ml 17α-Hydroxy-20βdihydroprogesterone for 24hrs at 25°C) in a series of cryoprotectant toxicity tests using stage III oocytes. In these experiments, oocytes were exposed to 1-4M ethylene glycol (EG), methanol or dimethyl sulfoxide (ME₂SO) (made up in Hanks, KCl buffer or 50% Leibovitz L-15) for 30 min at 22°C. Control oocytes were incubated in the corresponding medium under the same conditions. Preliminary results showed that the FDA+PI staining is more sensitive than TB staining and its sensitivity is comparable to GVBD test. Normalised oocyte survivals after 1M EG treatment were 93.6±2.3%, 82.7±2.9% and 81.0±5.9% using TB, FDA+PI and GVBD respectively. In this study, FDA+PI staining was tested on fish oocytes for the first time. The preliminary results showed the method is promising and may offer a new reliable way of assessing the viability of fish oocytes. It can also be applied to oocytes at all stages.

Conflict of interest: None declared
Source of funding: None declared

For Best Poster Award.